

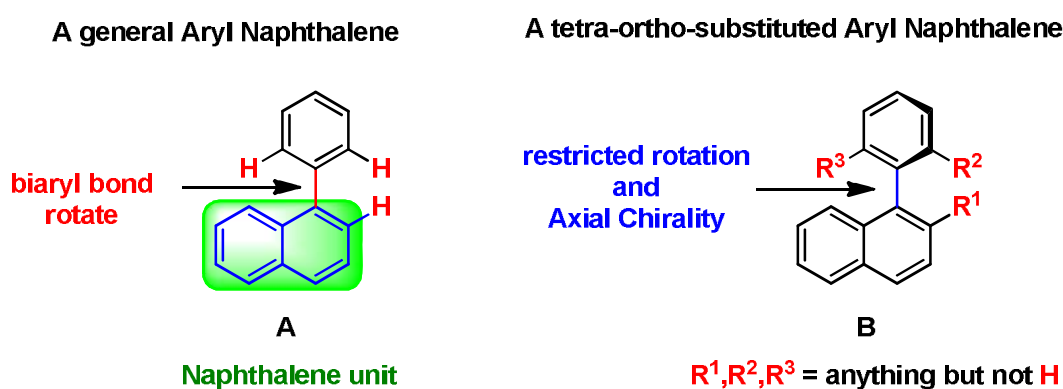
Chapter 3

Synthesis, resolution and application of hydroxylated binaphthalenes

- 3.1 *Introduction*
- 3.2 *Results and Discussion*
 - 3.2.1 Synthesis and resolution of novel hydroxylated binaphthalene compounds
 - 3.2.2 Synthesis of enantiomerically pure helicene like oxazines from atropisomeric 7, 7'-dihydroxy or 7-hydroxy BINOL. Study of their circularly polarized luminescence
 - 3.2.3 Synthesis of helical molecules from atropisomeric binaphthyl derivatives
- 3.3 *Conclusion*
- 3.4 *Experimental Procedures*
- 3.5 *Spectral data*
- 3.6 *X-ray Crystal Data*
- 3.7 *References*

3.1 Introduction

Naphthalene's structure consists of a fused pair of benzene rings. As shown in Scheme 1, there are two sets of equivalent hydrogen atoms at the 'alpha' positions (1, 4, 5, and 8) and the 'beta' positions (2, 3, 6, and 7). A substitution on the naphthalene ring makes the compound more active and gives rise to the derivatives of organic compounds. The aromatic ring present on naphthalene at C1 position show biaryl system, Without substitution at *ortho* position, the biaryl [C1(Ph)–C1(Ph)] axis rotates easily, as the substitution attached on the *ortho* position of biphenyl increases the rotation of the bond between C1(Ph)–C1(Ph) becomes difficult, and generate atropisomers.



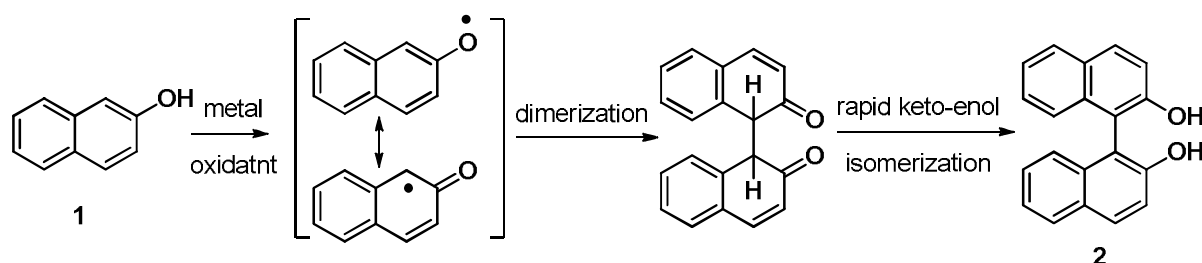
Scheme 1: A general example of naphthalene **A** and *ortho* substituted naphthalene **B**.

The substituted naphthalene containing biaryl compounds are of great importance, being present in a variety of useful chemical entities.¹ Many biologically active natural products² contain the binaphthalene moiety, with their potential use as anticancer,³ antifungal,⁴ antibacterial,⁵ as birth control agents,⁶ among others.⁷ These compounds also play a predominant role in the development and continued success of asymmetric transformations due to their unique axial chirality.⁹ In most cases these substituted binaphthalenes act as transition metal ligands, where they can give enantioselectivity during the catalytic cycle.¹⁰ This naphthalene unit also has shown to be effective in materials applications such as optoelectronics,¹¹ molecular switches,¹² and ligands in metal organic frameworks (MOF).¹³

A History of Binaphthalene Derivatives

Few binaphthalene compounds were reported before 21st century. In 1873 for first time, von Richter¹⁴ prepared it as a racemate. Since this pioneering work was initiated, the oxidative coupling reactions to afford BINOL has been extensively studied from 2-

naphthol using copper complexes,¹⁵ TiCl₄,¹⁶ and iron¹⁷ as shown in Scheme 3.¹⁸ Subsequently the next effort was focused on the separation of enantiomers of BINOL (*S* or *R*). The synthesis of optically pure (*R*)- or (*S*)-BINOL was achieved by separating the enantiomers of BINOL by using enzymatic or chemical resolution and direct stoichiometric or catalytic oxidative coupling of 2-naphthol.¹⁹ One of the earliest examples of chemical resolution was through separation of phosphoric acids and Cinchonine salt.²⁰ Resolution of racemic BINOL by separation of its complexes with naturally occurring (*S*)-proline was first attempted by Periasamy²¹ and recently reinvestigated by Hu.²² Enantioenriched BINOL has been made through a variety of methods and substitutions of the hydroxyl moiety have been accomplished.



Scheme 2

However, in 1979 Noyori first recognized it as a ligand for metal-mediated catalysis in the reduction of aromatic ketones and aldehydes.²³ Since then enantiomeric BINOL has become the most widely used ligands with various metal ions for both stoichiometric and catalytic asymmetric reactions.²⁴

BINOL occupied a prominent position in the chemical field and its ability to form highly enantioselective catalysts with main group elements,²⁵ transition metals²⁶ and rare earth elements.²⁷ Modifications of the BINOL skeleton aimed at changing its steric and electronic properties which were proven to be necessary and effective and thereby affecting the reaction environment by influencing the properties of the metal centre in several catalytic asymmetric reactions. Due to the easy manipulation of BINOL skeleton, it has been extensively studied in various metal catalyzed asymmetric transformations.

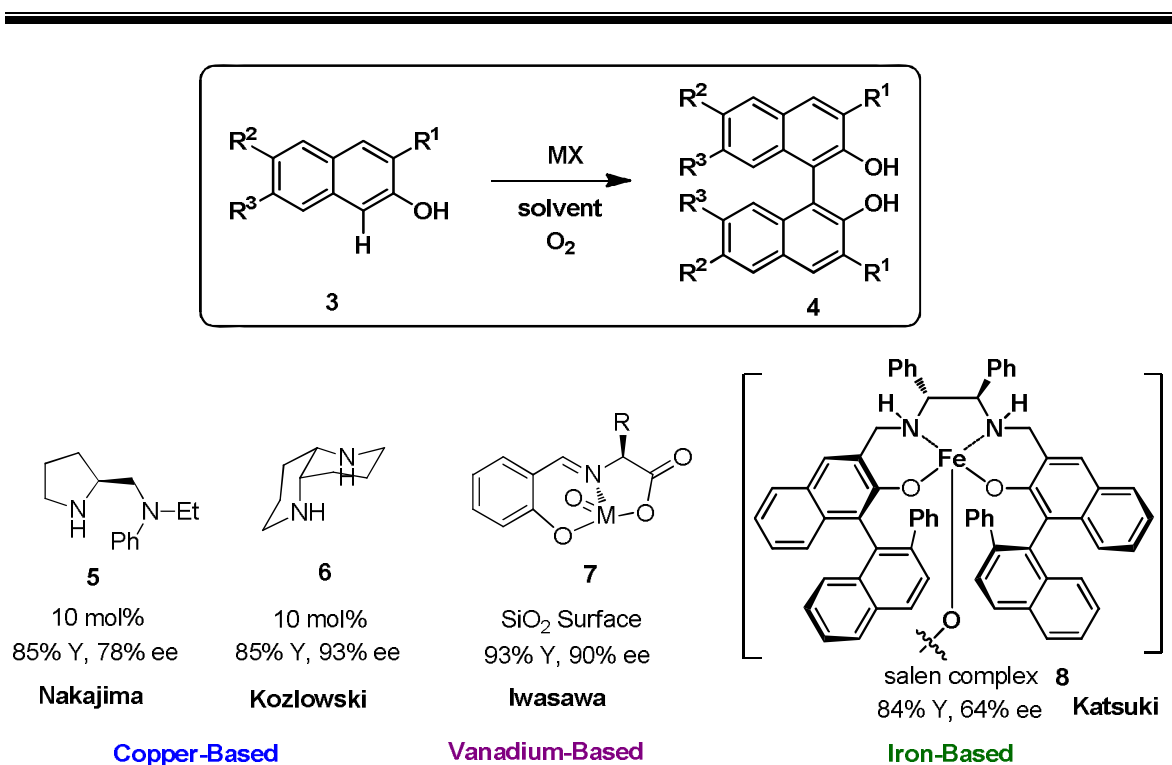
This initial synthesis of substituted binaphthalenes and their further unfunctionalization played a key role in understanding axial chirality originating from the restricted rotation around the biaryl bond (atropisomerism). By taking this as a starting point many routes

evolved to focus on the next generation of these unique motifs. In this chapter, our discussion mainly focused on oxidative coupling of naphthols.

Synthesis of substituted binaphthalens by oxidative coupling

Substituted naphthalene compounds are widely used in the field of chemical synthesis. Therefore many modern methods for the synthesis of substituted binaphthalenes have been reported in the last decade. Among which the most common methods are the metal-mediated coupling reactions. Oxidative coupling has been one of predominant methods for the synthesis of substituted binaphthalenes. In the last decade a lot of optimizing methodology was employed in this area to obtain synthetically challenging enantioenriched substituted binaphthalenes, especially with a focus on natural products.²⁸ Oxidative coupling is very effective in generating highly enantioenriched substituted binaphthalens directly from naphthols. The salient feature of oxidative coupling is the mild reaction conditions that are employed via a one-electron phenolic oxidation process (Scheme-2), differentiating them from other cross-coupling processes as they are extremely tolerant of many functional groups.²⁹ However, regioselectivity can be a problem with oxidative coupling due to lack of pre-functionalization which acts as a chemoselector in other methods.^{29b} Many unwanted side products are reported, especially when the chemical positions on the naphthols are electronically similar.^{29c}

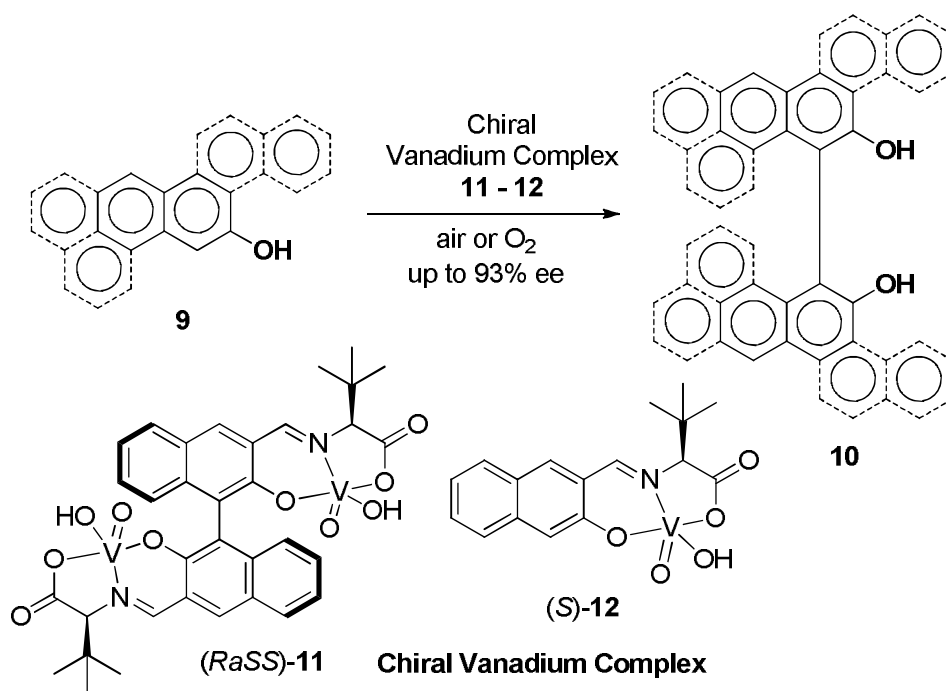
As previously discussed in chapter 1, there are many metals that can facilitate this coupling reactions (Scheme-3), such as copper catalysts. Similar work in this area was done by Wynberg,³⁰ Brussee,³¹ Yamamoto,³² and Kocovsky³³ who used chiral copper(II) amine oxidants to generate chiral BINOL derivatives. Additional work was performed by Nakajima³⁴ who pioneered the catalytic asymmetric coupling of naphthol with chiral amine ligand **5**. The Kozlowski group made further modifications and has shown excellent yields and enantioselectivities using copper with chiral amine ligand **6** and oxygen as the stoichiometric oxidant.³⁵ Currently, vanadium-based catalysts have been found to be quite effective at facilitating this coupling. The Iwasawa group have shown that they can provide BINOL derivative **4** in 93% yield and 90% ee using silica supported **7** and vanadium catalyst.³⁶ Iron-catalyzed coupling **8** has also been demonstrated by the Katsuki group, although the observed enantioselectivity is lower.³⁷ The iron-mediated coupling was catalyzed by salen complexes. There have also been many examples of total synthesis of natural products utilizing the oxidative coupling method as a key step.



Scheme 3: Multiple routes to asymmetric substituted binaphthalenes substrates through oxidative coupling

Overall, oxidative coupling is an effective procedure for the coupling of naphthols. However, this method is severely restricted as it works well, solely with naphthol-based precursors. Large sterically demanding *ortho* substituted naphthols have not been demonstrated *via* this method.

Recently, in 2014 Sasai and co-authors developed a vanadium-mediated enantioselective catalytic oxidative-coupling of polycyclic phenols. In this work various phenols of type **9** were successfully employed with 5 or 10 mol % of the catalyst to give the corresponding biphenols **10** in good to excellent yields; and with 93% ee (Scheme 4).³⁸



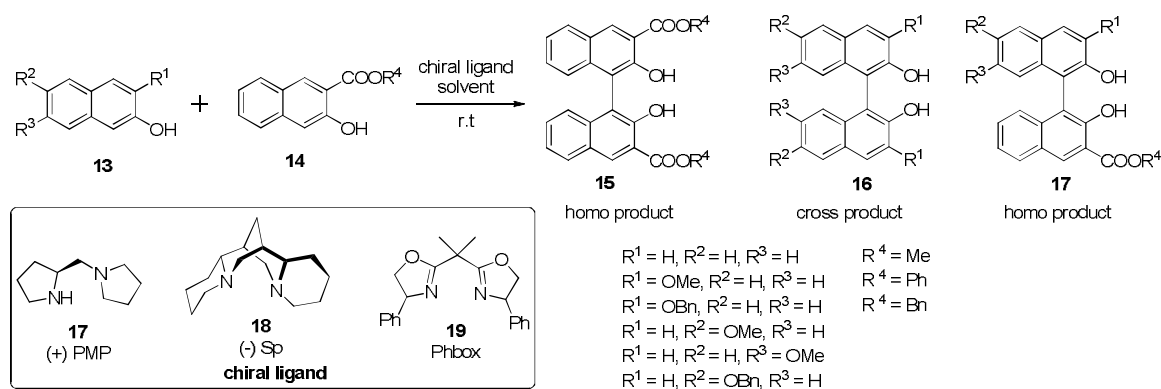
Scheme 4

Synthesis of substituted binaphthalens by cross-coupling

Besides the homo coupling of naphthol derivatives, the copper-mediated oxidative cross coupling of 2-naphthol has been investigated since the first report involving the coupling of 9-phenanthrol and 3-methoxy-2-naphthol. Hovorka and co-workers generalized the cross-coupling by investigating the reactivity of combinations of relatively electron-rich-2-naphthol and electron-deficient naphthoate and obtained cross-coupling products with selectivity more than 80%, while combinations of electron-rich or electron-deficient substrates led to decreased pair selectivity (around 30%).

There are few reports on the catalytic cross-coupling reaction leading to a binaphthol having an unsymmetrical structure, although several reactions using a stoichiometric amount of a metal complex were reported.³⁹ Only the report by Kozlowski and co-workers, on the catalytic asymmetric oxidative cross-coupling reaction between 2-naphthol and methyl 3-hydroxy-2-naphthoate with the CuBF₄-(*S,S*)-1,5-diaza-cis-decalin catalyst has recently appeared,⁴⁰ in which the cross-coupling product was obtained in a poor yield (8%) with a moderate enantioselectivity (72% ee in favour of *R* isomer). Habaue and co-authors reported the first synthesis of the poly(1,10-bi-2-naphthol) derivative, poly(2,3-dihydroxy-1,4-naphthylene), through the asymmetric oxidative coupling polymerization of the commercially available monomer, 2,3-dihydroxynaphthalene, with a novel

copper(I)catalyst system, $\text{CuCl}\cdot(S)\text{-}(-)\text{-}2,20\text{-isopropylidenebis(4-phenyl-2-oxazoline)}$ [(*S*)Phbox], at room temperature under an O_2 atmosphere, although the diamines, such as (+)-1-(2-pyrrolidinylmethyl)pyrrolidine [(+)-PMP] and (-)-sparteine [(-)-Sp]. During the course of study, they found that this catalyst system was also effective for the cross-coupling reaction between 2-naphthol derivatives **13** and 3-hydroxy-2-naphthoates **14** (Scheme 5).⁴¹



Scheme 5

Importance of binaphthalene derivatives

Substituted naphthalene containing compounds have a multitude of biological active natural products and many beneficial pharmacological properties (Figure 1). Gossypol⁴² **20** has shown antimalarial, proapoptotic, and antioxidant properties, while Ancistrobrevine **22** and Korupensamine⁴³ **23** have shown anti-HIV potential. Dioncophylline⁴⁴ **21** has demonstrated to be an effective insecticide.

Substituted binaphthalenes have also shown quite useful applications as chiral ligands in number of reactions (Figure 1). Two of the most well known chiral ligands are BINAP **24** and BINOL **2**, the former ligand is much investigated by Prof. Noyori in his landmark asymmetric hydrogenation. Both the ligands have demonstrated their ability in effective selectivity in a variety of asymmetric transformations.⁴⁵ In a review by Lemaire it was even stated that BINAP appears to be both the most used and the most useful ligand for asymmetric catalysis.^{45d} Additionally, monodentate phosphine (MOP) **25** was shown to be quite effective as a ligand in metal-catalyzed asymmetric transformations, where bisphosphines were shown to be ineffective.

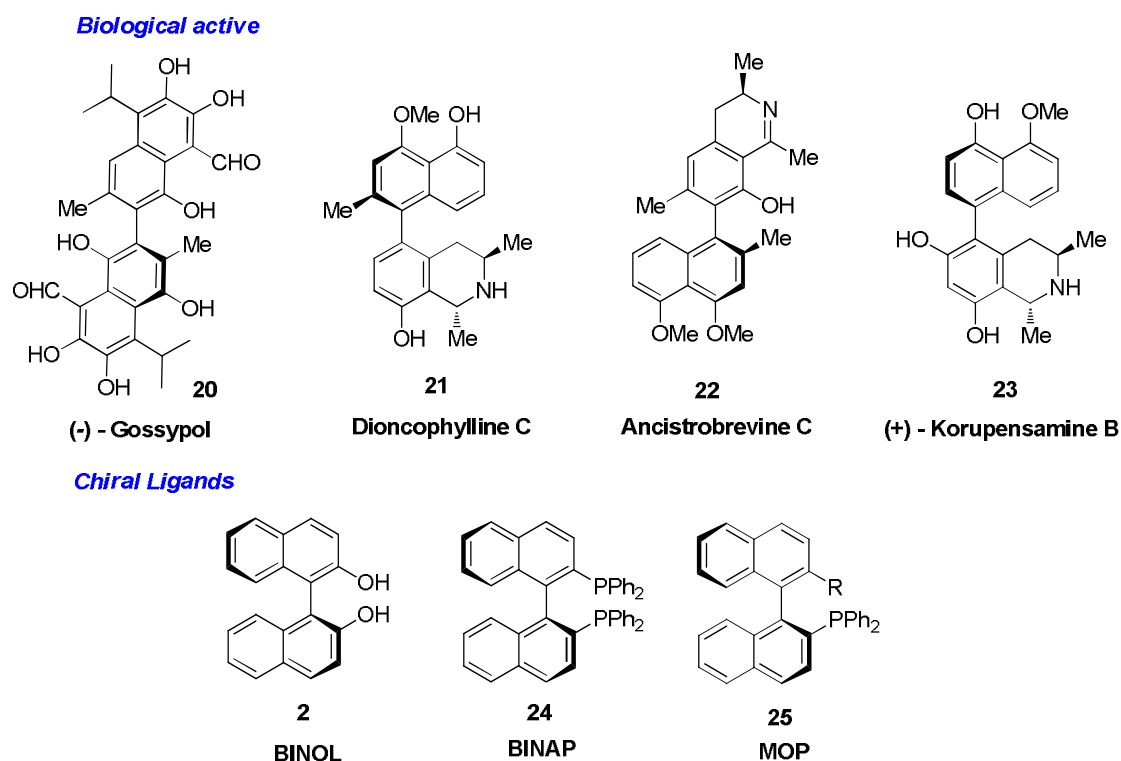
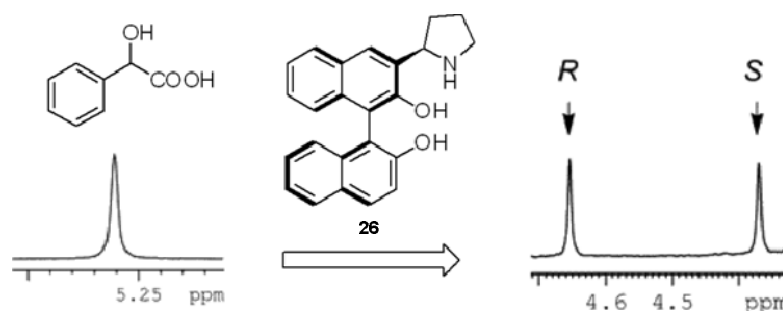


Figure 1: selected examples of substituted binaphthalenes

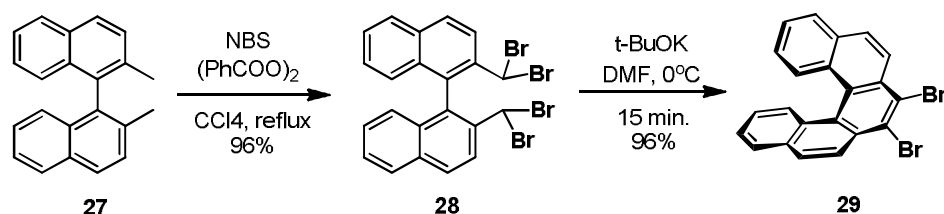
Binol is an important chiral building block and has been widely used in asymmetric catalysis and for enantioselective fluorescence sensors bearing a variety of recognition elements. This is due to the unique chiral and aromatic structure of the 1,1'-binaphthyl scaffold could provide both excellent chiral recognition capability and a large ring-current effect. Lei and co-authors designed and synthesized a novel chiral receptor of 3-(2''-pyrrolidinyl)-BINOL (Py-Binol) **26**, which has a 1,1'-binaphthyl chiral scaffold and a pyrrolidinyl group acting as the binding site for carboxylic acids. Therefore, they reported that the bifunctional receptor of (*R,R*)-Py-Binol **26** functions was a highly effective chiral shift reagent for determination of enantiomeric excess of a series of chiral carboxylic acids by $^1\text{H-NMR}$ (Scheme 6).⁴⁶



Scheme 6: Chiral shift reagent for enantiomeric excess determination for a series of chiral carboxylic acids by $^1\text{H-NMR}$

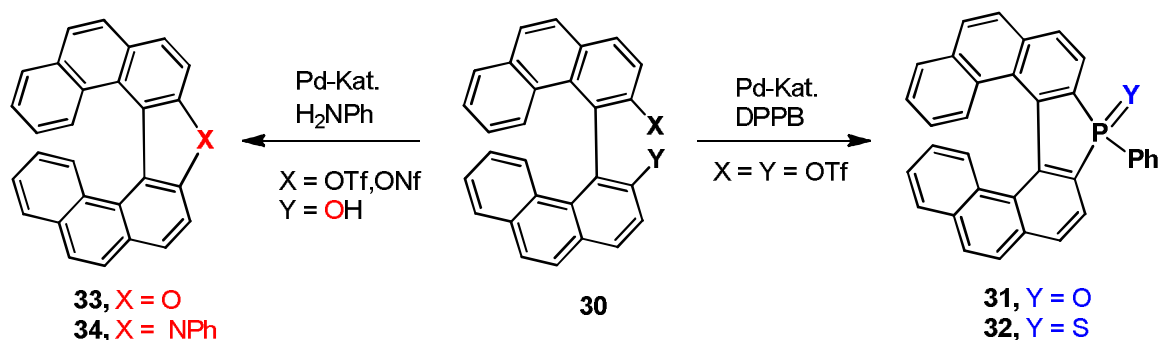
On the other hand, binaphthyl derivatives emerged as a suitable precursor for the construction helical shape as the 2,2'-position allows a facial bridging or cyclisation to helicene or helicene-like molecules, fan-shape molecules and butterfly shape molecules. Helical extension of π -conjugated systems is of great interest for the production of novel molecules and materials with unusual properties and applications.

Gingras and co-authors reported that functionalized pentahelicenes, which was synthesized from 2,2'-Bis(bromomethyl)-1,1'-naphthalene **28** precursor, which was synthesized from 2,2'-dimethyl-1,1'-binaphthalene **27** by an efficient radical tetrabromination with benzoyl peroxide and an excess of NBS. Finally, a mild and spontaneous ring closing step of benzylic dibromomethine coupling using of t -BuOK in DMF smoothly provided 7,8-dibromo[5]helicene **29** in excellent yield (Scheme 7).⁴⁷



Scheme 7: Expeditive Route to Functionalized Helicenes via a Benzylic Gem(dibromo)methine Coupling

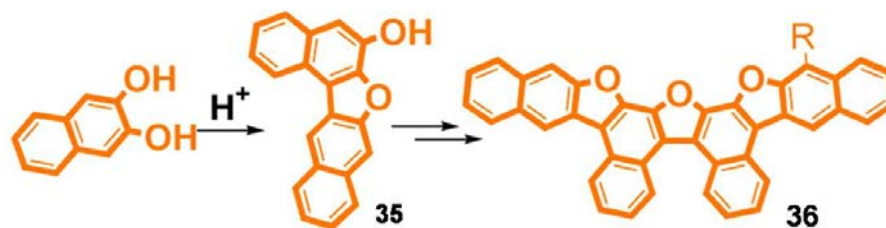
Nozaki *et al.*, reported the synthesis of oxa[7]helicenes **30**, aza[7]helicenes **31** and 15-phospha[7]helicenes **28**, **29** using palladium-catalyzed reactions from 4,4'-biphenanthryl-3,3'-diyl bis(trifluoromethanesulfonate) **27** (Scheme 8).⁴⁸



Scheme 8: Enantioenriched 15-phospha[7]helicenes, aza- and oxa[7]helicenes are synthesized from an enantiopure biphenanthryldiol in a highly stereoselective manner.

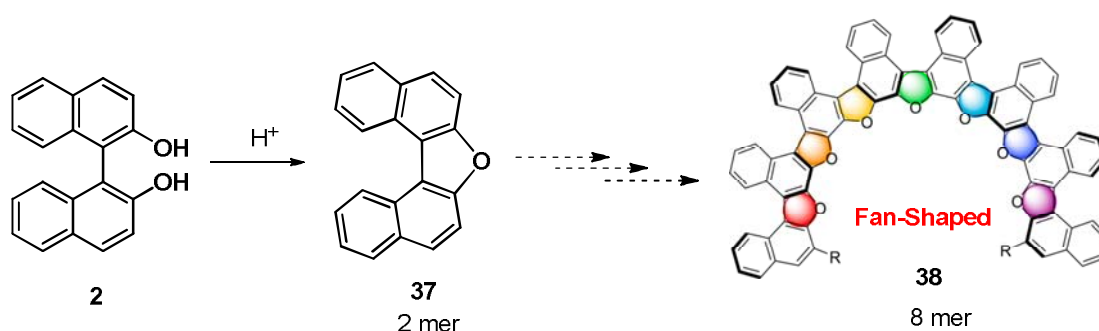
Tsubaki *et al.*, reported the construction of dinaphtho[2,1-b;2,3-d]furan-6-ol **35**, developed via a dehydration reaction involving two molecules of 2,3-dihydroxy naphthalene in the

presence of a strong acid. Starting from the dinaphthofuran, a variety of butterfly shaped derivatives **36** was synthesized (Scheme 9).⁴⁹



Scheme 9

Tsubaki and co-authors prepared a series of oligonaphthofurans composed of alternating naphthalene rings and furan rings using a bottom-up method. They selected naphthofuran 2mer **37** as a suitable synthon, which was obtained from the dehydration of binaphthol **2** under acidic conditions.⁵⁰ The Scheme 10 depicts the synthetic route for the fan-shaped oligonaphthofurans **38** (up to an 8mer) by repeating a bottom-up method from **37**. As the number of units increased, the construction of the furan ring by dehydration became more difficult.



Scheme 10: Synthesis fan-shaped oligonaphthofurans from binaphthol

There are also examples of substituted binaphthalenes in materials science, especially in the area of optoelectronics. Substituted binaphthalenes have also shown potential as ligands in homochiral metal organic frameworks. Oligonaphthalene **39** (Figure 2) demonstrate unique asymmetric optical properties that can be easily tuned⁵¹ and HMOFs **40** have shown usage as chiral chemoselectors.⁵²

The term optical rotation describes the angle through which linearly polarized light is rotated when exposed to the test sample. Optical rotation comes from the interaction of chiral materials with a linearly polarized light.

The optical rotation happens with a particular angle which depends upon particular molecular properties of the enantiomer in the medium and is proportional to the path length of the sample. In the medium of the other enantiomer under the same conditions, the angle of rotation is reversed but remains in same magnitude.

For a molecule whose mirror image is not super imposable on itself, left- and right-circularly polarized light have different refractive indices (n) and correspondingly different absorption coefficients (ϵ). This may happen for any molecule having only proper rotation elements of symmetry. A molecule possessing any improper rotation axis, a mirror plane, or centre of symmetry cannot be optically active. However, a substance can also be optically active due to a symmetrical arrangement of molecules; these molecules themselves need not necessarily be chiral. Arranging *achiral* molecules on a helix, results for instance in an optically active molecular assembly.

Determination of optical rotation is carried out by measurement of the amount of the angle of rotation - observed optical rotation, ' α ' - using an apparatus referred to as a polarimeter. The enantiomer that rotates the plane of polarization of a linearly polarized light in an anticlockwise direction, to the left, is named laevorotatory and given the symbol ($-$ or l), while the enantiomer that rotates the plane of polarization of a linearly polarized light in a clockwise direction, to the right, is named dextrorotatory and given the symbol ($+$ or d).

The extent of the rotation is characterized using an index called specific rotation $[\alpha]_D$ and its direction is determined by the sign ($+$) or ($-$). A closely related phenomenon is the formation of elliptically polarized light from plane-polarized light produced by an optically active medium in the area of its absorption bands. These effects can be understood in terms of the differences in refractive index (n) and absorbency index (ϵ) for left- and right-circularly polarized light.

The *specific rotation* $[\alpha]_D^t$ is defined as the observed angle of optical rotation when plane-polarized light is passed through a sample with a path length of 1 decimeter and a sample concentration of 1 gram per 1 deciliter. Since the optical rotation depends on the wavelength of the used light and on the temperature, both have to be specified with

experimental data. The *molar rotation* (or *molecular rotation*) is best suited to compare the optical activity of different substances. The specific and the molar rotation are obtained from the following equations.⁵⁵

$$\text{The specific rotation } [\alpha]_{\text{D}}^t = 100\alpha / (l \times c)$$

$$\text{The molar rotation } [\Phi]_{\text{D}}^t = \{[\alpha]_{\text{D}}^t \times \text{M.W}\} / 100$$

In equations: α (alpha) = observed rotation in degrees. l = the length of the polarimeter cell in decimetres. c = the concentration of the sample in g per 100 mL. t = the temperature in °C at which the measurement takes place. D = the D line of a sodium lamp with a wavelength of 589.6 nm.

Each molecule absorbs light at characteristic wavelengths according to the electronic nature of the molecule. The absorptions that are sensitive to the molecular electronic structure generally arise in the ultraviolet-visible (UV-Vis) wavelength region. These absorptions are named *electronic transitions* and happen as a result of excitation of the molecular electrons by light of the corresponding wavelength from a lower level of energy which is named *ground state* to a higher level of energy which is named *excited state*. The strength of any absorption is measured by the absorption coefficient (ϵ). Inside the absorption bands, the absorption coefficient for left and right polarized light is different ($\epsilon_L - \epsilon_R = \Delta\epsilon \neq 0$) due to its relationship to the refractive index for left and right circularly polarized light which are primarily different.

The optical properties most commonly used to study chirality are differences, either in absorption or refraction, between left- and right-circular polarized light interacting with molecules of a specific chirality. The difference between the optical absorption coefficients for left- and right-polarized light is called *circular dichroism* (CD); it is a function of the frequency of the light and may have either sign. It arises from the anisotropic absorption of polarized light by chiral solution containing an excess of one enantiomer. The other property is the difference between the refractive indices for left-circular and right-circular polarized light. It is still sometimes called *optical activity*, but a more recent meaningful and precise name is *optical rotatory dispersion* (ORD), which is obtained by determination of the optical rotation at different wavelengths of light and can be used to investigate the stereochemistry of molecules. It denotes to the equal but opposite directions of rotation of polarized light by the two opposite enantiomers in the

solution. Each molecule has an individual absorption spectrum, and each chiral molecule shows a corresponding individual CD spectrum. At all wavelengths, the CD spectrum for enantiomers is equal in magnitude but opposite in sign.⁵⁴⁻⁵⁶

However, chirality is of interest because of its application to stereochemistry in organic chemistry, inorganic chemistry, physical chemistry, biochemistry and supramolecular chemistry.

Chirality is a characteristic feature of molecular systems and plays an important role in the relationship between structure and function. Synthesis of chiral molecules represents one of the most fascinating aspects of modern synthetic organic chemistry in spite of the relative difficulties in studying complicated spectrum of new chiral compounds.

Optically active molecules with chiral axis are categorized as atropisomeric,⁵⁷ helical⁵⁸ or allene.⁵⁹ These well studied molecules have some of the unique optical properties linked with their structural architecture. It would be useful if methods are made available for the precise synthesis of optically pure helical or atropisomeric molecules and will be helpful for further evaluation of their specific chiroptical properties.

In this chapter we present the synthesis, resolution and determination of configuration of atropisomeric hydroxylated binaphthalene derivatives. These atropisomeric (axially chiral) molecules were then transformed to helicene and helicene like molecules. This chapter mainly describes the synthesis of atropisomeric binaphthalene based oxazine, which were prepared from hydroxylated binaphthalene compounds. Intermediate atropisomeric molecules converted into helicene-like oxazine derivatives and their optical properties were studied.

The chapter is mainly divided into three sections.

3.2 Results and Discussion

3.2.1 Synthesis and resolution of novel hydroxylated binaphthalene compounds

Structurally similar 2,2'-dihydroxy-1,1'-binaphthyl **2** (BINOL) possessing a C_2 -symmetric axis and its derivatives are widely utilized in asymmetric chemistry.⁶⁰ In comparison to BINOL, the chemistry of 2,2',7,7'-tetrahydroxy-1,1'-binaphthyl **41** is relatively less investigated, although its synthesis is known.^{61,62} However, its [1,1'-binaphthalene]-2,2',7,7'-tetrol derivative has received less attention and [1,1'-binaphthalene]-2,2',7-triol **44** is not known in the literature. In this section our focus is mainly on the synthesis and resolution of atropisomeric binaphthalene derivatives (Figure 4). Initially a series of hydroxy binaphthalenes **41-43** were synthesized by oxidative homo coupling (Scheme 11). Then compound **44-46** were synthesised by oxidative cross coupling reactions (Scheme 12). In the next part we have altered the ring size on chiral axis of binaphthyl unit. First, we have increased aromatic rings on chiral axis of binaphthylene. For this purpose we have synthesized compound **43** and converted it to compounds **52** and **53** by sequence of Mizoroki-Heck and photodehydrocyclization (Scheme 14). Secondly, we have built heterocyclic moiety 'oxazine' on chiral axis of binaphthyl. This oxazine consists of a six member ring with O and N fused with naphthalene. Having synthesized such molecules, **41** and **44**; they were converted to atropisomeric mono oxazines **47-49** (Scheme 18) and bis oxazines **50** and **51** (Scheme 19) by aromatic Mannich reactions respectively.

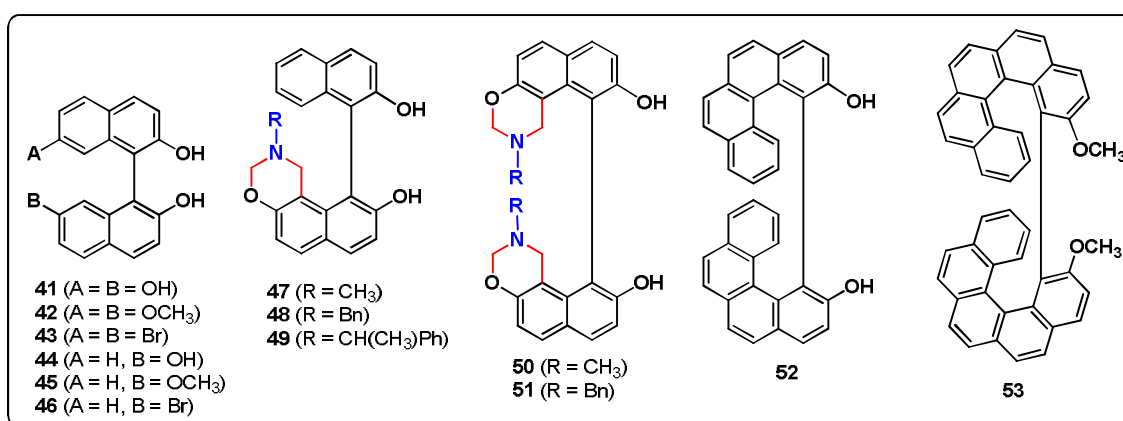
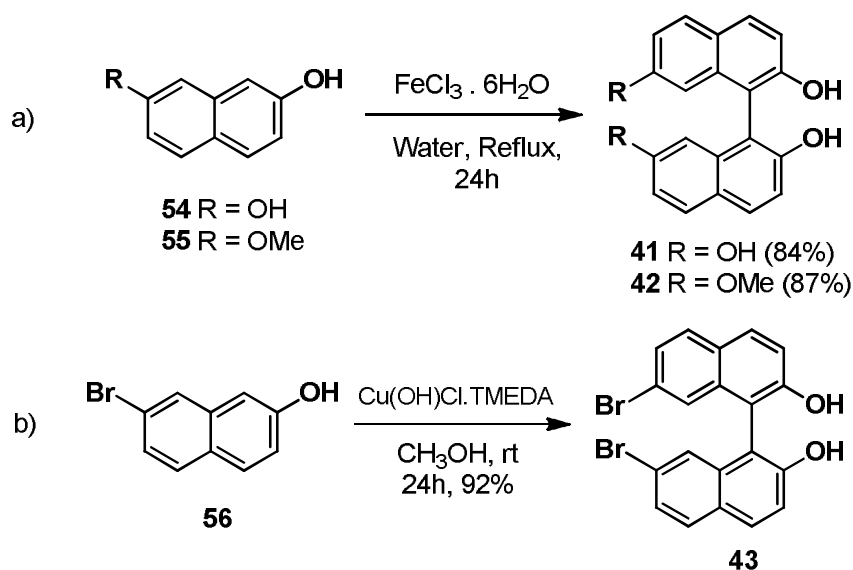


Figure 4: Summary of different types of atropisomeric BINOL derivatives synthesised

Synthesis of hydroxylated binaphthyl derivatives

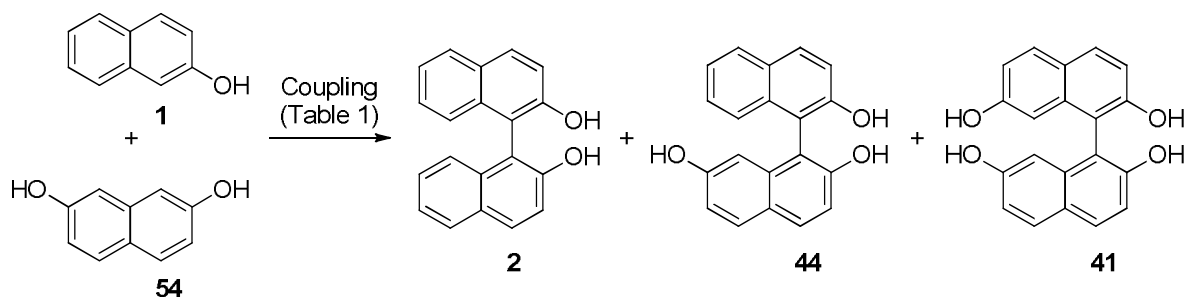
Racemic tetrol **41**, **42** and 7,7'-dibromo-[1,1'-binaphthalene]-2,2'-diol **43** was prepared by oxidative homo-coupling using routinely employed catalyst system of FeCl₃ and

Cu(OH)Cl·TMEDA from 2,7-dihydroxy naphthalene **54** (Scheme 11a) and 7-bromonaphthalen-2-ol **56** (Scheme 11b) respectively.



Scheme 11: synthesis of binaphthalene derivatives by oxidative homo coupling

The cross coupling of 2-naphthol **1** with other substituted naphthol derivatives is a well studied reaction.⁶³ However, cross coupling reaction between two naphthol units, both possessing electron releasing substituents tends to be less selective and the desired cross coupling products are accompanied by the formation of two other homo-coupling compounds. A good selectivity is achieved in a cross coupling reaction between the two coupling partners possessing considerable difference in the electron density.^{63a} However, in the present case we intend to couple two electron rich naphthol derivatives, **1** and **54**, and thus expect formation of the corresponding homo coupled products **2** and **41** (Scheme 12). Different reagent combinations were screened to test most suitable conditions favouring the desired product **44** and the details are summarized in Table 1.



Scheme 12: Oxidative cross coupling of naphthols.

Different combinations of **1** and **54** were chosen with FeCl₃ as the reagent for coupling reaction. The reactions were conducted in water at reflux temperature. In most of the reactions undesirable homo-coupling products **2** and **41** were obtained in considerable quantities along with unreacted 2-naphthol. The cross coupling product **44** was obtained in moderate yield in almost all conditions investigated. However, it was possible to separate all products with careful column chromatography on silica gel. Decreasing the amount of FeCl₃ favored the formation of tetrol **41** while suppressed homo-coupling of 2-naphthol (entry 5). The conditions in entry 2 and 3 of Table 1 appear more suitable for the desired cross coupling product and were followed to access the required triol **44** in gram quantity. We also investigated copper catalyst for the reaction, but the results were almost similar.⁶⁴

Table 1: Conditions screened for cross-coupling reaction of **1** and **54**.

No	Conditions ^a	Isolated yield ^b /%			
		1 ^c	2	44	41
1	1 (1.0 eq.) + 54 (0.8 eq.) + FeCl ₃ (2.5 eq.)	--	31	33	50
2	1 (1.25 eq.) + 54 (1.0 eq.) + FeCl ₃ (2.5 eq.)	24	30	38	59
3	1 (1.50 eq.) + 54 (1.0 eq.) + FeCl ₃ (2.5 eq.)	24	34	38	51
4	1 (2.00 eq.) + 54 (1.0 eq.) + FeCl ₃ (2.5 eq.)	33	30	35	49
5	1 (1.50 eq.) + 54 (1.0 eq.) + FeCl ₃ (1.5 eq.)	60	12	27	64
6	1 (1.50 eq.) + 54 (1.0 eq.) + CuCl ₂ (1.5 eq.) ^d	--	46	33	30

^aAll reactions were run in H₂O at reflux for 24 h. ^bYield of **44** & **2** was calculated based on **1** and yield of **44** & **41** was calculated based on **54**. ^cRecovered from reaction mixture. ^dWith benzyl amine (0.5 eq.) and piperidine (0.5 eq.).

The H-NMR of compound **44** showed three –OH signals at 5.13, 5.05 and 4.83, which disappeared when spectra was recorded in D₂O (Figure 4). The high resolution mass spectrum of **44** showed the molecular mass of the product and its isotope pattern were consistent with the calculated value for C₂₀H₁₄O₃ [M+1] 303.1021, found 303.1022 m/z. In IR spectrum the –OH stretching was confirmed as peaks at 3492, 3391 cm.⁻¹

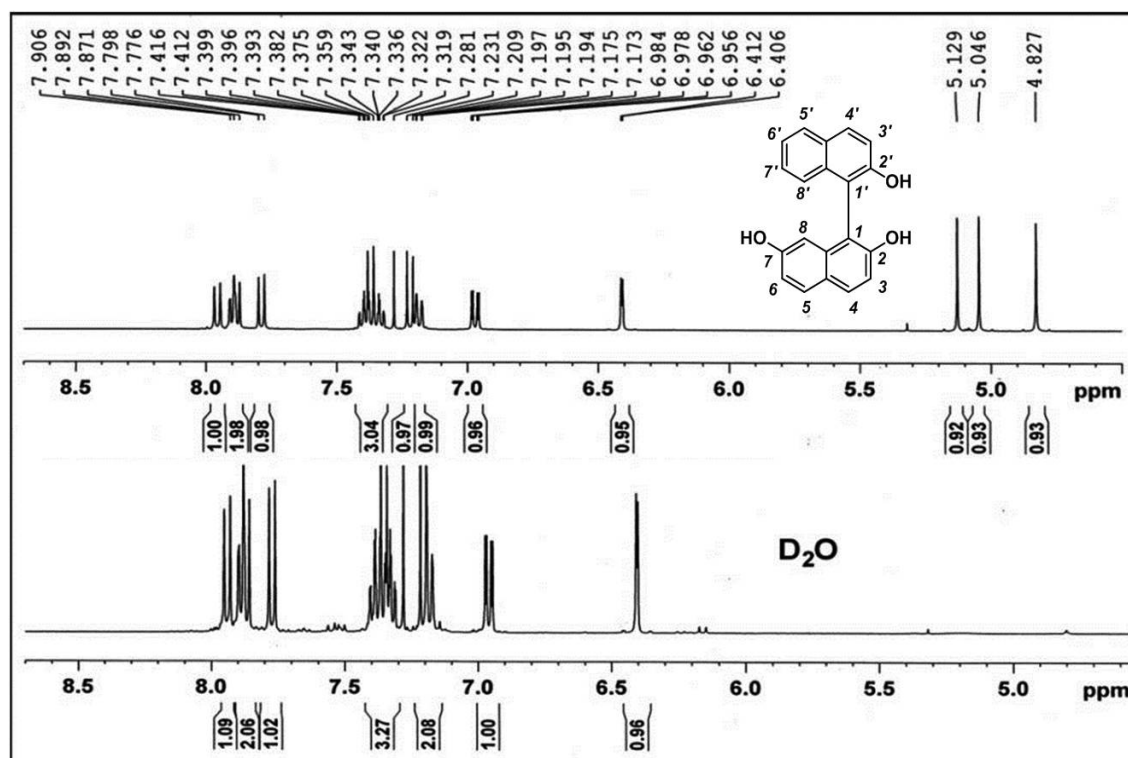
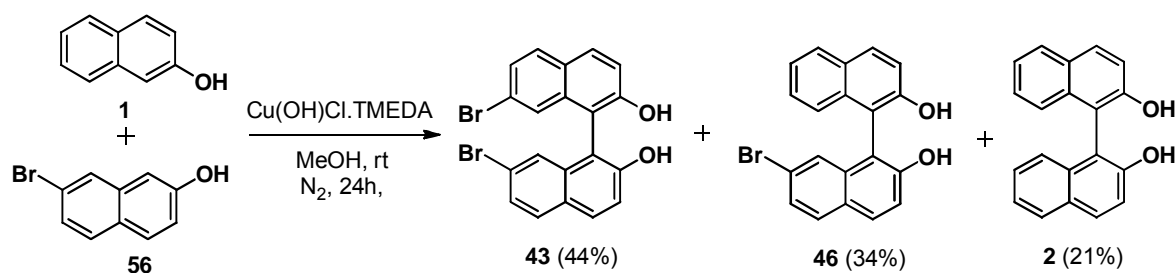


Figure 4

Similarly combinations of 7-bromonaphthalen-2-ol **56** and naphthalen-2-ol **1** were chosen with $\text{Cu}(\text{OH})\text{Cl}\cdot\text{TMEDA}$ as the reagent for cross-coupling reaction (Scheme 13). The reaction was conducted in methanol at room temperature (N_2 atmosphere). In this reaction undesirable homo-coupling products 7,7'-dibromo-[1,1'-binaphthalene]-2,2'-diol **43** and [1,1'-binaphthalene]-2,2'-diol **1** were obtained in considerable quantities. The cross coupling product 7-bromo-[1,1'-binaphthalene]-2,2'-diol **46** was obtained in moderate yield. However, it was possible to separate all products with careful column chromatography on silica gel. All products were characterised by spectral analysis.

The H-NMR of crossed product **46** showed broad signal for $-\text{OH}$ at δ 5.09. The high resolution mass spectrum of **46** showed the molecular mass of the product and its isotope pattern were consistent with the calculated value for $\text{C}_{20}\text{H}_{13}\text{BrO}_2$ [$\text{M}+\text{Na}$] 388.9976, found 388.9967 m/z . In IR spectrum showed $-\text{OH}$ stretching peaks at 3473, 3414 cm^{-1} .



Scheme 13: Oxidative cross coupling of naphthol and bromo naphthol

Search for new chiral molecules with different shape, size and functional group is an extremely crucial aspect of modern organic chemistry. This is particularly vital in the field of molecular recognition, supramolecular and medicinal chemistry, asymmetric synthesis and enantioselective catalysis, material chemistry etc. Amongst chiral class of compounds atropisomeric chiral molecules have acquired a unique place in the field of chemistry due to atropisomeric binaphthalene skeletons with a chiral environment around the space have been extensively studied for asymmetric catalysis, molecular recognition, and as a chiral auxiliary. In the most cases, the dihedral angle between the two aromatic systems plays an important role for the construction of suitable chiral environment. Therefore, binaphthalene based unit with a substantial dihedral angle have made significant contributions in this area. Among this class BINOL and BINAP represent most widely studied compounds, where much focus has been devoted to study their derivatives. Few compounds were reported on polycyclic biphenol derivatives in literature, such as bianthracenol **57**, biphenanthrols **58**, **59**, and bichrysenol **60** are also useful as chiral BINOL derivatives (Figure 5).⁶⁵⁻⁶⁷

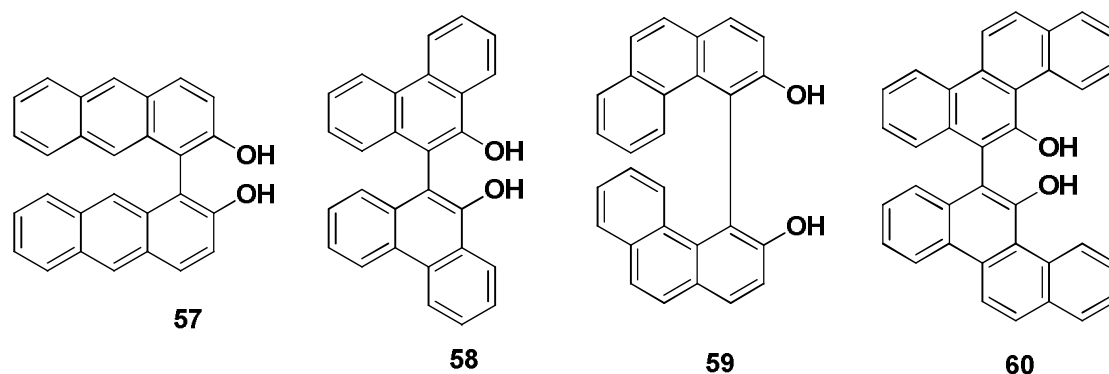


Figure 5: Chiral polycyclic biphenol derivatives.

In view of the successes achieved with substituted BINOLs and polycyclic biphenol derivatives (Figure 5), we designed molecules by introducing additional aromatic rings or

oxazine rings at the ends of the binaphthyl axis (Figure 6). The heterocyclic moiety ‘oxazine’ consists of six member ring with O and N fused with naphthalene.

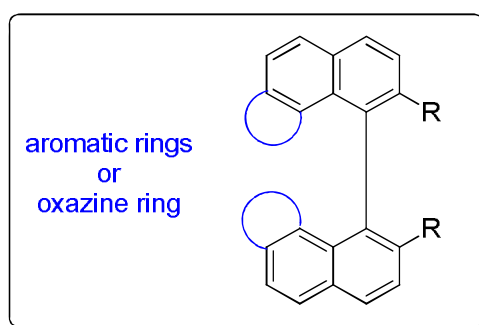
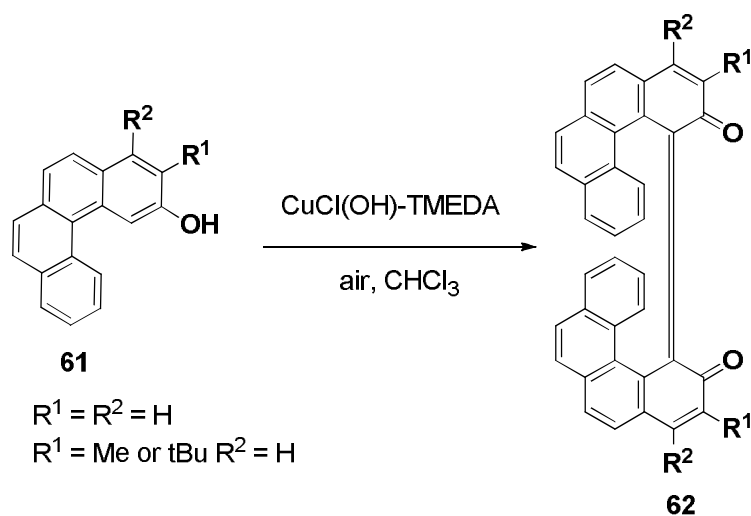


Figure 6

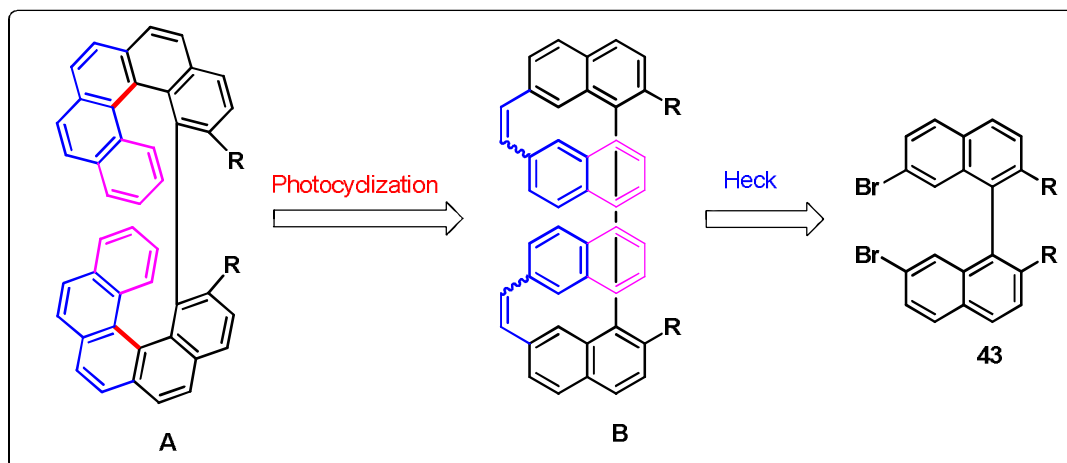
Synthesis of aromatic moiety contains atropisomeric binaphthyl derivatives

First we synthesised vaulted binaphthyl derivatives such as [1,1'-bibenzo[*c*]phenanthrene]-2,2'-diol **52**. Recently, Karikomi and co-workers reported the synthesis of helical quinone **62** derived from 2-hydroxybenzo[*c*]phenanthrene **61**. The oxidative coupling reaction of **61** using CuCl(OH)•TMEDA proceeded region- and stereoselectively at C1 position to produce helical quinone as the sole product (Scheme 14).⁶⁸



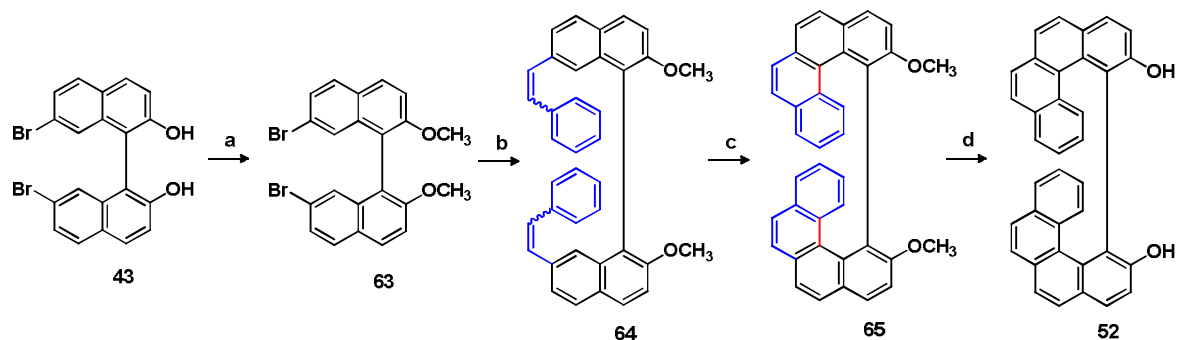
Scheme 13

To overcome this problem we applied Wittig-Heck and photocyclization methods for synthesis of compound **52** and **53**. According to the above mentioned points, the retrosynthetic scheme of preparation of target bis-helicenes **A** is presented in Scheme 14, where the first disconnection will lead to the cyclized precursor a olefin derivative **B**,⁶⁹ which can easily be built from **43** by Heck reaction.⁷⁰



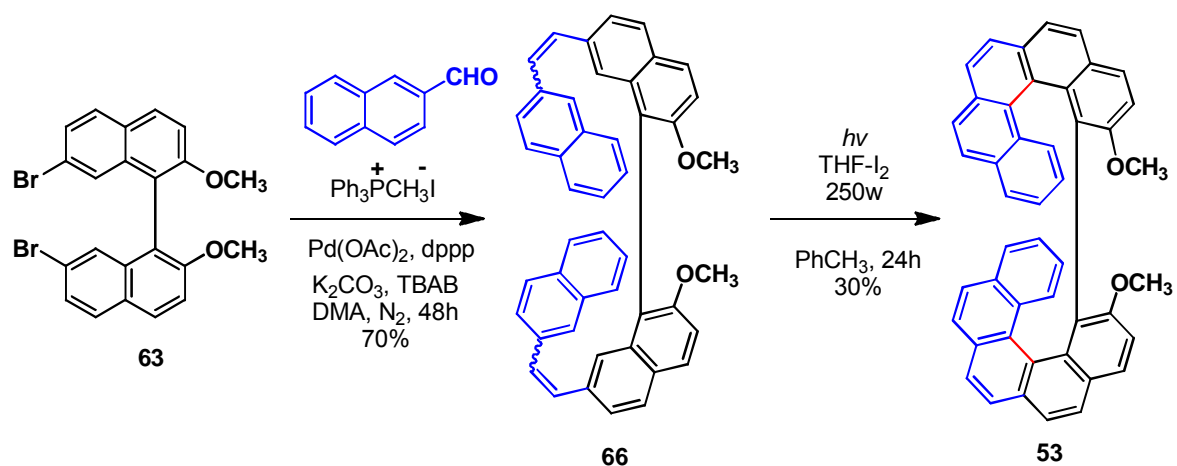
Scheme 14

First we synthesized [1,1'-bibenzo[*c*]phenanthrene]-2,2'-diol **52** by oxidative photocyclization of suitable styryl derivative of methoxy binaphthyl moiety (Scheme 15). We have chosen to convert 7,7'-dibromo-[1,1'-binaphthalene]-2,2'-diol **43** to the 7,7'-dibromo-2,2'-dimethoxy-1,1'-binaphthalene **63** by using MeI in the presence of base, which provided white solid with 98% yield. The product **63** was characterized by usual spectral analysis. Then compound **63** was converted to the olefin derivative **64** by double Mizoroki-Heck reaction using styrene and Pd-dppp to furnish white solid with 85% yield, the product **64** was confirmed by H-NMR and HRMS. In the H-NMR olefin protons showed doublet at δ 6.94, 7.05 ($J = 16.0$ Hz), and the high resolution mass spectrum of **64** showed the molecular mass of the product which was consistent with the calculated value for $C_{38}H_{30}O_2$ [$M+1$] 519.2324, found 519.2303 m/z . Then compound **64** was subjected to photodehydrocyclization with I_2 -THF with high pressure mercury vapour lamp furnished product **65** in 82% yield. The product **65** was characterized by H-NMR and HRMS. The H-NMR clearly showed disappearance of olefin signals. The high resolution mass reveal the molecular mass of the product and its isotope pattern were consistent with the calculated value for $C_{38}H_{26}O_2$ [$M+1$] 515.2011, found 515.1998 m/z . The compound **65** was treated with BBr_3 to furnish the target molecule [1,1'-bibenzo[*c*]phenanthrene]-2,2'-diol **43** with 98% yield. The product was characterized by spectral analysis. In the H-NMR, the $-OCH_3$ signal disappeared and $-OH$ signal was appeared at δ 10.27 in $DMSO-d_6$. And the high resolution mass spectrum of **66** showed the molecular mass of the product and its isotope pattern were consistent with the calculated value for $C_{36}H_{22}O_2$ [$M+1$] 487.1698, found 487.1676 m/z .



Scheme 15: Conditions, a) MeI, K₂CO₃, CH₃CN, 98%, b). Styrene, Pd(OAc)₂, dppp, K₂CO₃, TBAB, DMA, N₂, 48h, 89%, c). hv, THF-I₂, PhCH₃, 24h, 68%, d). BBr₃, MDC, °0 C- r.t. 3h, 98%.

For synthesis of [10,10'-bidibenzo[*c,g*]phenanthrene]-9,9'-diol **53** we followed the synthetic protocol of **52**. In this scheme olefin formation and photocyclization reactions are the key intermediate steps and synthetic scheme is outlined in Scheme 16. First the compound **63** was converted to the olefin derivative **66** by one pot Wittig -Heck reaction furnished 85% yield. In this reaction the olefin was generated *in-situ* by using 2-naphthaldehyde and one carbon Wittig salt (Ph₃PCH₃I). The product **66** was confirmed by spectral analysis. In the H-NMR the olefin protons showed doublet at δ 6.94, 7.05 (*J* = 16.0 Hz). The high resolution mass showed the molecular mass of the product and its isotope pattern were consistent with the calculated value for C₄₆H₃₄O₂ [M+Na] 641.2456, found 641.2452 *m/z*. Then compound **66** subjected to photodehydrocyclization with I₂-THF in presence of HPMV lamp yielded cyclised (angular-angular) product **67** as a light yellow solid (30%), along with angular-linear product **68** isolated from the reaction mixture. However, this reaction resulted in complex products. The isolated products were characterized by spectral analysis.



Scheme 16

In the H-NMR of compound **67** clearly indicated disappearance of olefin protons and all protons were shifted to upfield. The high resolution mass showed the molecular mass of the product and its isotope pattern were consistent with the calculated value for $C_{46}H_{30}O_2$ [M^+] 614.2246, found 614.2257 m/z . The H-NMR of **68** showed unsymmetrical pattern, whereas two $-OCH_3$ proton signals showed singlet at δ 3.67 and 2.72 ppm. The high resolution mass showed the molecular mass of the product and its isotope pattern were consistent with the calculated value for $C_{46}H_{30}O_2$ [$M+1$] 615.2324, found 615.2313 m/z .

The photocyclization of 2,2'-dimethoxy-7,7'-bis(2-(naphthalen-2-yl)vinyl)-1,1'-binaphthalene **66** may possibly follow three different pathways (Figure 7). Photocyclization by path-I will give angular-angular product, path-II will give linear-linear product and path-III gives angular-linear or linear-angular product.

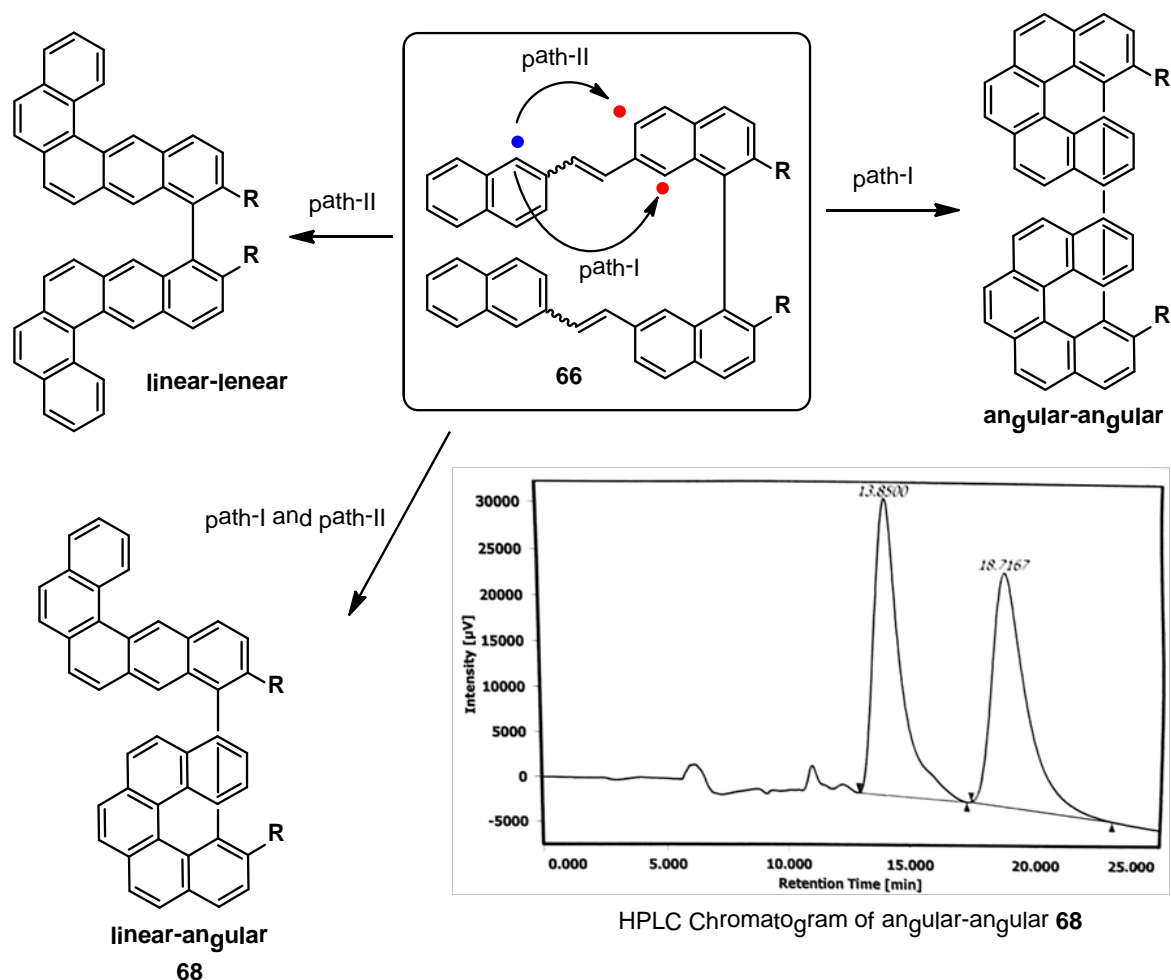


Figure 7

In angular-angular product formation it may possibly follow four orientations (Figure 8). Out of these orientations, modes outer-axis (I) and inner-axis (II) will lead to same orientation and outer-inner-axis (III) and inner-outer-axis (IV) also give one orientation. Hence, the cyclised product is expected to follow the two orientations (A and B).

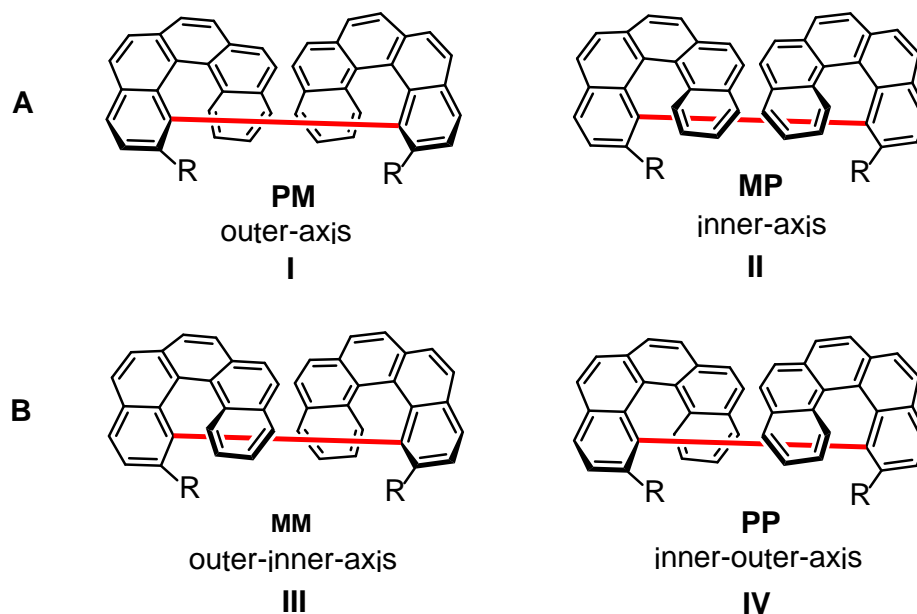


Figure 8

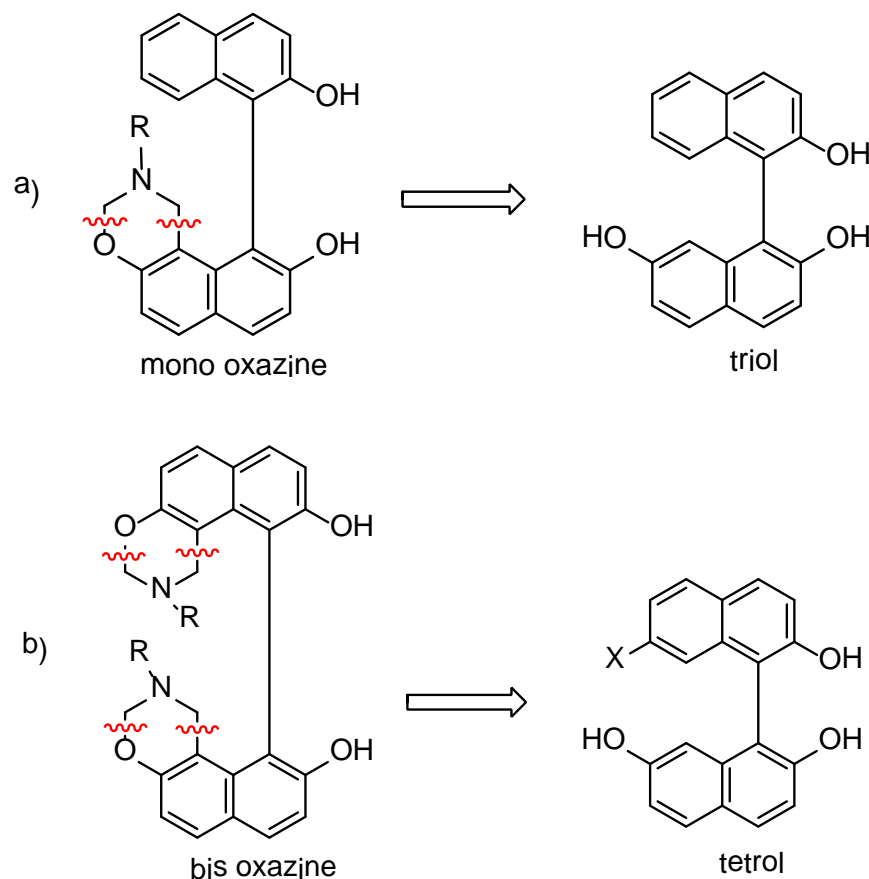
The HPLC analysis of **68** (angular-angular) on Chiralce OD-H column showed presence of two well resolved peaks at 13.85 and 18.72 mins (30 % hexane in isopropanol; 0.5 mL/min.) probably for outer-inner-axis orientation(III)/inner-outer-axis(IV) (**B**) product isomers (Figure 7), and expected to outer-axis(I)/inner-axis(II) (**A**) will give single peak due to meso nature of the compound.

This orientation requires interaction between the two almost perpendicularly oriented binaphthyl groups and may also pose a considerable challenge.

Synthesis of oxazine moiety contains atropisomeric binaphthyl derivatives

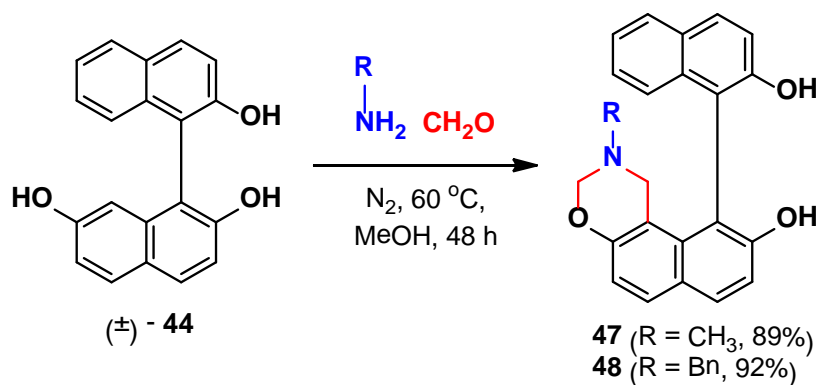
The oxazine containing compounds are a useful class of compounds in chemistry. The oxazine consists of a six member ring with O and N as heteroatoms. The oxazine moiety can be easily introduced in its framework. In the present work we intend to introduce an additional oxazine ring on binaphthyl axis (axially chiral molecules) which gives atropisomeric oxazine ring contain binaphthalene derivatives.

The retrosynthetic scheme of preparation of target atropisomeric mono oxazine is presented in Scheme 17a, where the disconnection will lead to the oxazine precursor of triol, which can easily be built from triol **44** by aromatic Mannich reaction⁷¹ with appropriate 1° amine and formaldehyde. Similarly, bis oxazines were presented in Scheme 17b, where the disconnection will lead to the oxazine precursor of tetrol, which can easily be built from tetrol **41** by double aromatic Mannich reaction with appropriate 1° amine and formaldehyde.



Scheme 17: Retrosynthesis of atropisomeric oxazine a) for mono oxazine b) for bis oxazine

Initially we have designed mono 1,3-oxazine ring on atropisomeric triol compound **44**. The preparation of triol **44** is already discussed in above section (Scheme 12). Atropisomeric mono oxazine compounds **47**, **48** were prepared from racemic triol **44** by aromatic Mannich reaction with methyl amine or benzyl amine, and formaldehyde respectively (Scheme 18). All prepared compounds were fully characterized by usual spectral and analytical techniques.

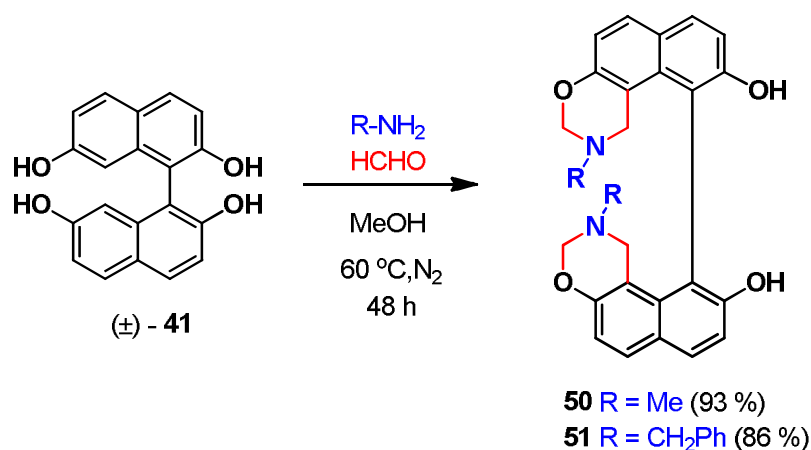


Scheme 18. Synthesis of atropisomeric mono-oxazine

The ¹H-NMR analysis of compound **47** showed a broad singlet at δ 5.06 and 5.22 for the two hydroxyl protons (-OH), a doublet at δ 4.63 (*J* = 9.2 Hz, 1H) and another doublet at δ 4.52 (*J* = 9.2 Hz, 1H) for the -N-CH₂-O methylene protons. At the same time the hydrogens of the -CH₂ group of Ar-CH₂-N- of the oxazine ring appear as doublet at δ 3.45 (*J* = 16.4 Hz, 1H) and another doublet at δ 3.86 (*J* = 16.4 Hz, 1H). The high resolution mass spectrum of **47** showed the molecular mass of the product and its isotope pattern were consistent with the calculated value for C₂₃H₁₉NO₃ [M⁺] 357.1365, found 357.1354 *m/z*. In the IR spectrum of compound **47** the peak observed at 3496 cm⁻¹ for -OH group, 1613, 1509 cm⁻¹ for aromatic -C=C- stretching.

The ¹H-NMR analysis of compound **48** showed broad two singlets at δ 5.09, 5.03 for the two hydroxyl protons (-OH). The -CH₂ protons of -N-CH₂-O observed as a doublet at δ 4.69 (*J* = 9.6 Hz, 1H) and another doublet at δ 4.59 (*J* = 9.6 Hz, 1H). The two doublets at δ 3.59 was for benzylic protons (*J* = 13.2 Hz, 2H) and the two protons of -CH₂ group of Ar-CH₂-N- showed two doublets at δ 3.50 and 2.94 (*J* = 16.8 Hz) for the of the oxazine ring. The high resolution mass spectrum of **48** showed the molecular mass of the product and its isotope pattern was consistent with the calculated value for C₂₉H₂₃NO₃ [M + 1]⁺ 434.1756, found 434.1750. The IR spectrum of **48** showed broad peak at 3469 cm⁻¹ for -OH group and 1668, 1620 cm⁻¹ for aromatic -C=C- stretching.

We have further designed bis-1,3-oxazine ring on atropisomeric tetrol **41**. The preparation of tetrol **41** has been discussed in above section (Scheme 11a). Similarly we have carried out the procedure standardized for the mono oxazine (Scheme 18) for synthesis of bis-oxazines. For which we started with tetrol **41** using double aromatic Mannich reaction to furnished racemic atropisomeric bis-oxazine compounds **50** and **51** in good yield (Scheme 19).



Scheme 19

The ¹H-NMR analysis of compound **50** showed symmetrical pattern, whereas a singlet at δ 5.06 for the two hydroxyl protons (-OH), the -CH₂ protons of -N-CH₂-O oxazine group observed as a two doublets at δ 4.74 and 4.61 ($J = 9.2$ 4H), At the same time the hydrogens of the -CH₂ group of Ar-CH₂-N- of the oxazine ring appear as two doublets at δ 3.63 and 3.19 ($J = 16.8$ Hz, 4H). The EI-mass spectrum of **50** agreed with the $[M+1]^+$ 429 m/z and $[M]^+$ 428 m/z peaks and the further continuous stable fragmentations of $[-CH_3]^+$ at m/z 398, $[(-CH_3-N)_2]^+$ at m/z 370. The IR spectrum of compound **50** showed 3464 cm^{-1} stretching frequency for -OH, and 1613, 1519 cm^{-1} for aromatic -C=C- stretching vibrations.

The ¹H-NMR analysis of compound **51** showed symmetrical pattern, whereas a singlet at δ 4.95 for the two hydroxyl protons (-OH). The -CH₂ protons of -N-CH₂-O observed as two doublets at δ 4.62 and 4.48 ($J = 9.6$ Hz for 4H). For benzylic protons showed broad singlet at δ 3.53 ppm and the two protons of -CH₂ group of Ar-CH₂-N- showed two doublets at δ 3.46 and 3.20 ($J = 16.8$ Hz). The EI-mass spectrum of the molecule **51** agreed with molecular ion $[M]^+$ peak at 580 m/z . The IR spectrum of compound **51** showed 3511 cm^{-1} for -OH group, 1611 cm^{-1} for aromatic -C=C- stretching vibrations.

Resolution of hydroxylated binaphthyl derivatives

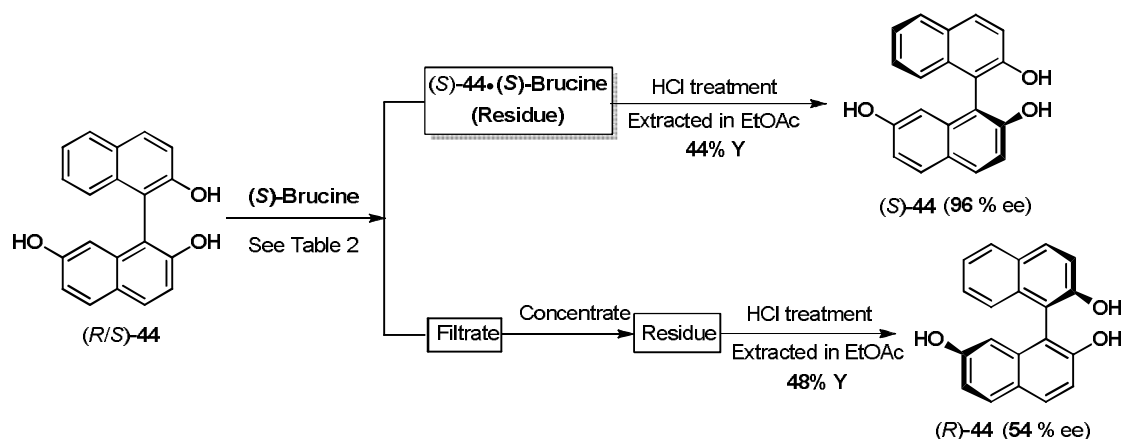
Several methods are reported for resolution of BINOL, such as optical resolutions through formation of diastereomers,⁷² enzymatic resolution,⁷³ resolution through inclusion complexes and asymmetric synthesis from 2-naphthol to obtain BINOL in enantiopure form.

The most widely used method for synthesis of optically pure BINOL involves optical resolution through formation of diastereomeric complexes using a chiral source. Resolution of racemic BINOL by separation of its complexes with naturally occurring (*S*)-proline was first attempted by Periasamy⁷⁴ and recently reinvestigated by Hu.⁷⁵ The recent work⁷⁵ also established the formation of inclusion complex of two molecules of BINOL with one molecule of (*S*)-proline, by the single crystal X-ray analysis.

Although several new resolution procedures have been reported in recent years, the most widely used method involves the preparation of the diastereomeric salt. Following this method, the resolution can be readily carried out on a large scale to get both enantiomers of high optical purity.

Resolution of racemic triol Using (*S*)-Brucine

The hydroxyl derivatives of binaphthyl system are known to form diastereomeric complexes and can be separated by fractional crystallization. Efforts were concentrated to search a suitable material which can form a complex with appropriate solubility to be able to separate the diastereomers by fractional crystallization. Different chiral basic materials were screened (Table 2) while the alkaloid (*S*)-Brucine was found effective in separating the two axial isomers of **44** by a single crystallization (Scheme 20). The salt of one isomer of **44** was separated as solid residue when refluxed with (*S*)-Brucine in methyl alcohol.⁷⁶ The free phenol was separated by treatment with aqueous mineral acid and simple extraction in organic solvent. The sample of triol **44** from the (*S*)-Brucine salt was analyzed by chiral phase HPLC analysis to be 96 % ee (Figure 9), while that from the solution showed moderate optical purity.



Scheme 20: Resolution of 2,2',7,7'-trihydroxy-1,1'-binaphthyl (*R/S*)-**44** by fractional crystallization with (*S*)-Brucine.

However, our initial efforts to use this and other amino acids or other alkaloids like Cinchonine and Quinine did not yield any resolution.

Table 2 Optimization of conditions for resolution of (*R/S*)-**44**

No	Chiral Resolving Agent	Solvent	Condition	Results			
				Precipitate		Filtrate	
				Yield (%)	% ee	Yield (%)	% ee
1	L-Proline	CH ₃ CN ^a	Reflux	No precipitates observed			
2	L-Phenyl glycine	CH ₃ CN	Reflux, 12h	-do-			
3	(+)-Cinchonine	CH ₃ CN	Reflux, 6h	-do-			
4	(-)-Quinine	CH ₃ OH	Reflux, 6h	-do-			
5	(<i>S</i>)-Brucine	Acetone ^a	Reflux, 6h	-do-			
6	(<i>S</i>)-Brucine	CH ₃ OH	Reflux, 4h	44	96.2	48	53.8
7	(<i>S</i>)-Brucine	Isopropanol	Reflux, 4h	46	50.0	50	50.0
8	(<i>S</i>)-Brucine	CH ₃ CN	Reflux, 4h	46	18.0	49	62.3

^aAlso investigated: CH₃OH, CH₂Cl₂, EtOAc, PhCH₃ and EtOH; Refluxed for 12 to 30 hours.

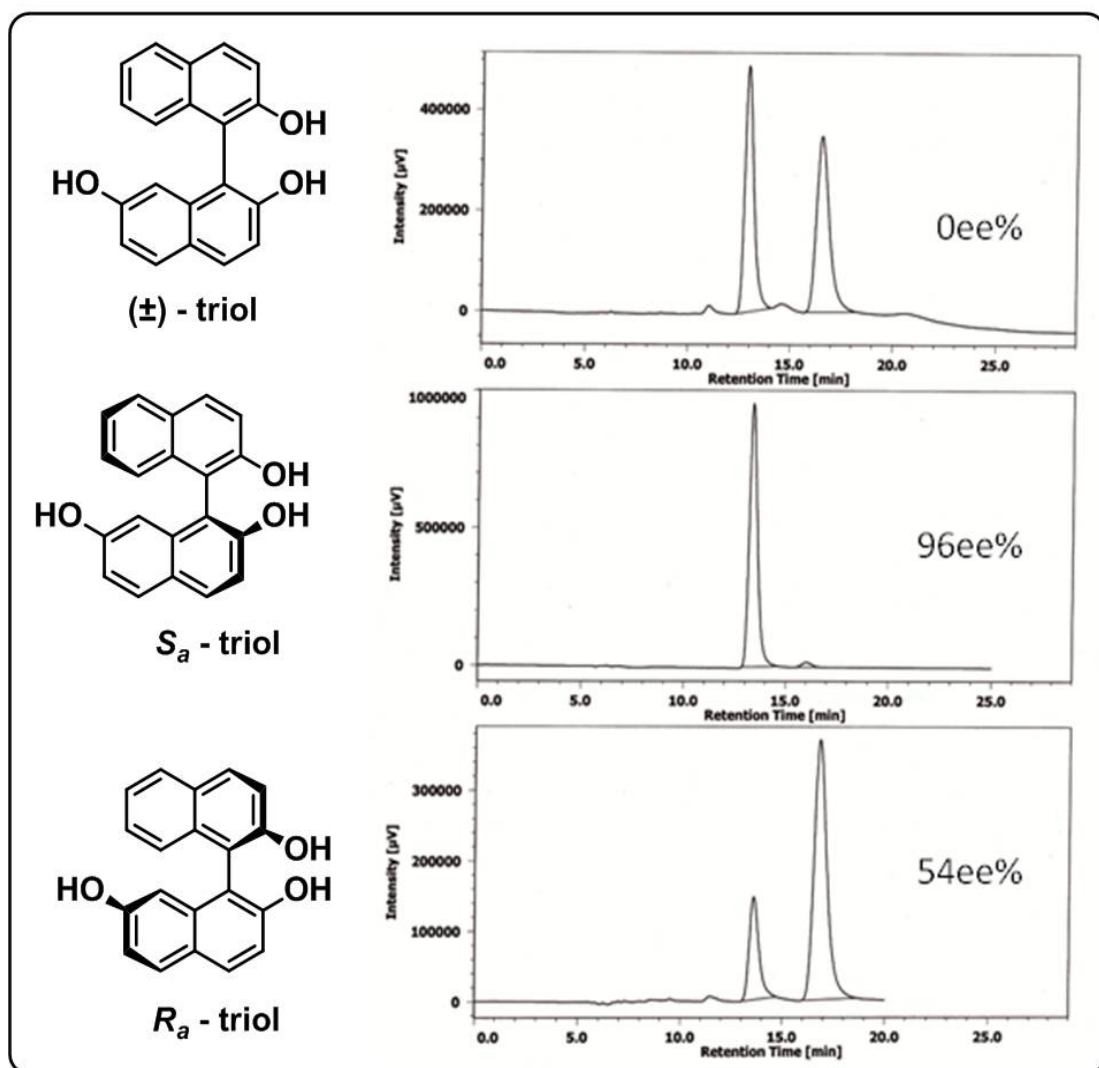


Figure 9: HPLC chromatograms of triol 44

The triol **44** was not known in the literature. The absolute configuration of the sample obtained from the residue as salt with (*S*)-Brucine was crystallized from methyl alcohol to get single crystal, while its X-ray diffraction analysis revealed it to be in S_a -form (Figure 10). Two molecules of (*S*)-Brucine formed two H-bonds with the two hydroxyl groups of **44**. The Brucine-N \cdots H-O-Ar bond and Brucine-C=O \cdots H-O-Ar bond were seen to be 1.889 and 1.875 Å, growing linearly in the crystal lattice which was crystallized in P1 space group. Such supramolecular assemblies for resolution of chiral molecules by (*S*)-Brucine are known in the literature (Figure 11), although not for separation of isomers of chiral phenols.⁷⁷

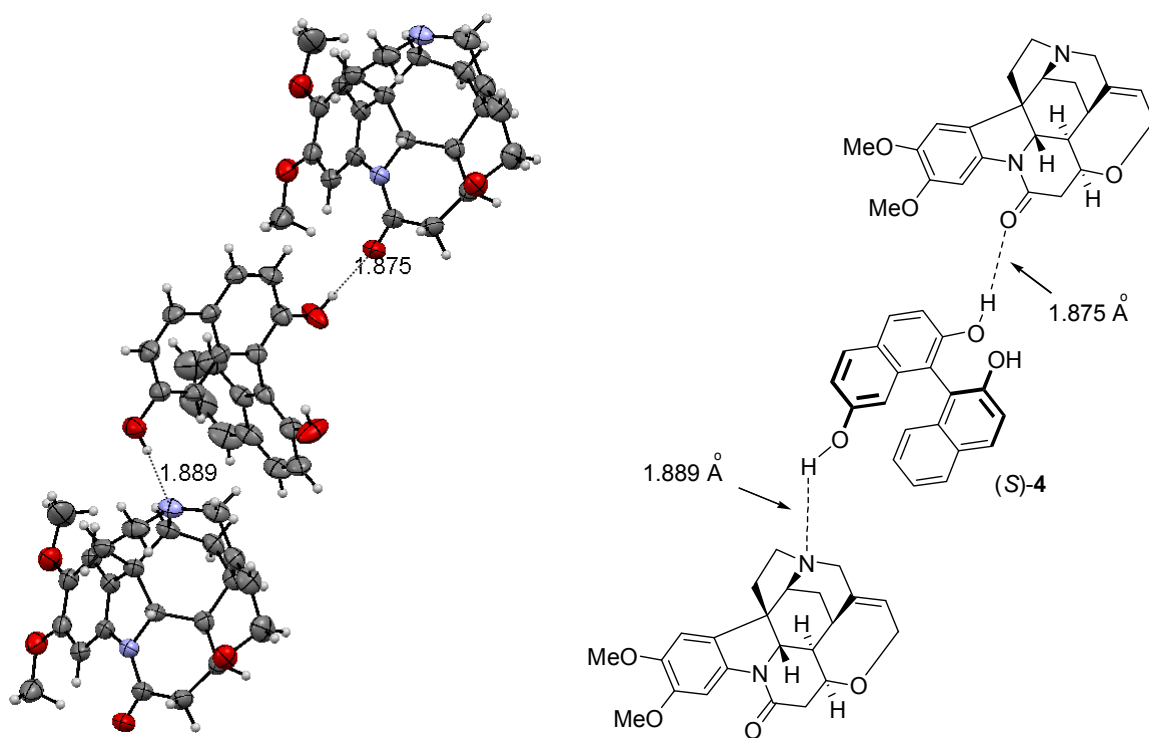


Figure 10: ORTEP diagram of the salt of (*S_a*)-44 and (*S*)-Brucine (CCDC 1023827)

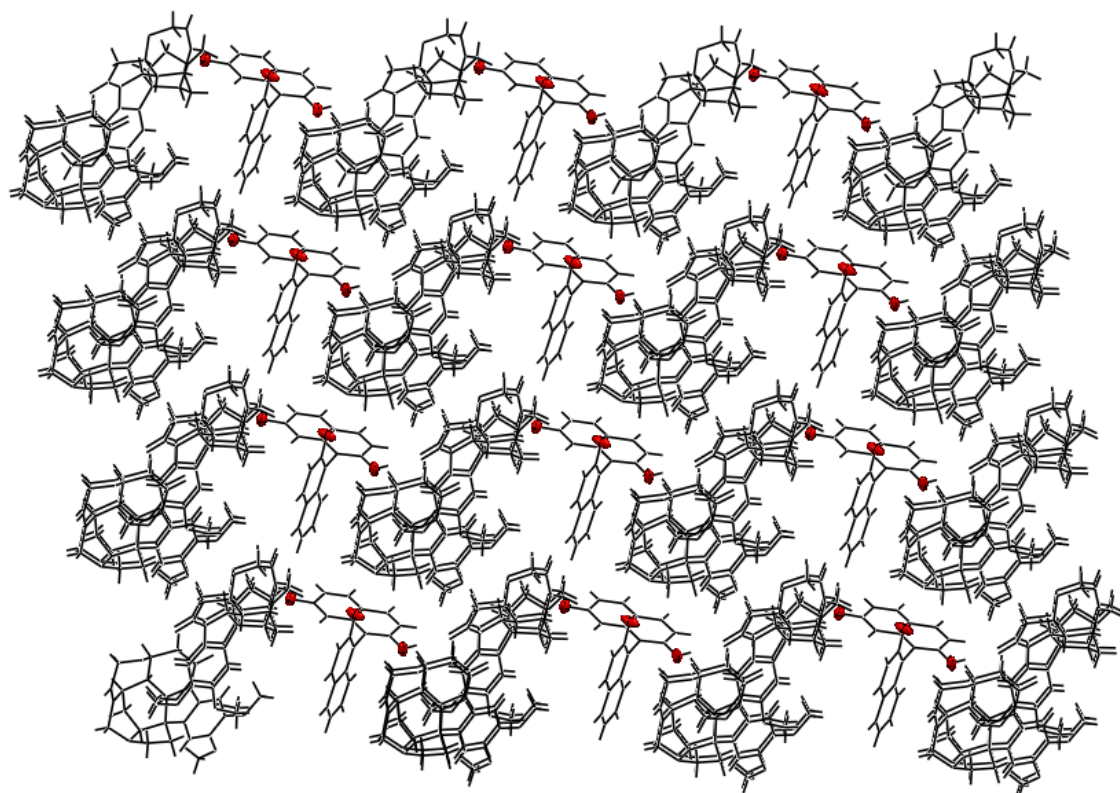


Figure 11: Crystal packing of the salt of (*S*)-Brucine and (*S_a*)-44

In the X-ray diffraction analysis the angle between the planes passing through the two naphthalene rings and angle between the axis of the molecules was established. The dihedral angle of the binaphthyl unit is 87.8° . The stereochemistry of the axis clearly show the S_a -configuration by considering the known chirality in the molecule from the chiral (*S*)-Brucine (Figure 12).

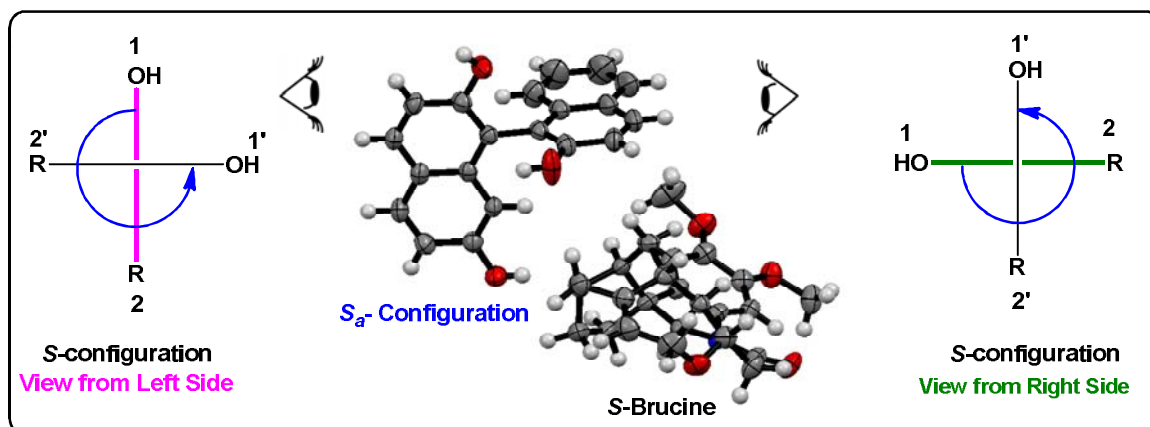
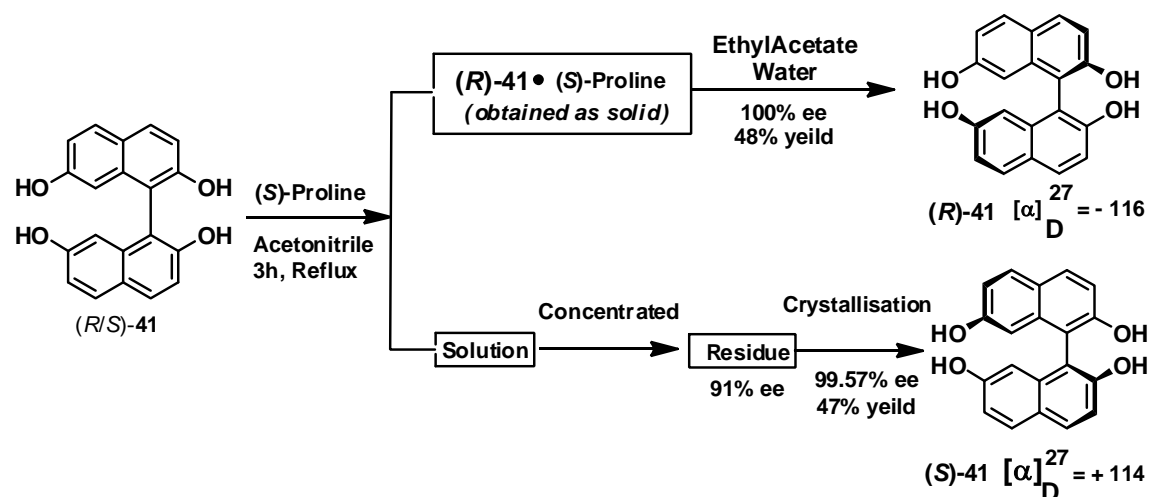


Figure 12: ORTEP diagram of the salt of (*R*)-Triol•(*S*)-Brucine. Configuration of the triol compound from the single crystal structure

Resolution of racemic tetrol Using (*S*)-Proline

The (\pm)-tetrol **41** was resolved by making its complex with (*S*)-Proline in acetonitrile (Scheme 21) and the resulting white precipitate was recrystallized in methanol to afford colourless crystals consisting of (*R*)-tetrol and (*S*)-Proline, which was established by single crystal X-ray analysis (Figure 13). Essentially enantiopure (*R*)-**41** was obtained in high yields after decomposition of the colorless crystalline complex by water and ethyl acetate mixture. The ethyl acetate was concentrated to give (*R*)-2,2',7,7'-tetrahydroxy-1,1'-binaphthyl {(*R*)-**41**} in 99.8 % ee based on HPLC analysis on chiralel OD-H (Figure 13).

The mother liquor acetonitrile was evaporated under reduced pressure to get (*S*)-2,2',7,7'-tetrahydroxy-1,1'-binaphthyl {(*S*)-**41**} as off white powder (Scheme 21). This sample was 91.0 % optically pure, which was enhanced by a single crystallization (MeOH:toluene, 1:1) to 99.6 % ee (Figure 13).



Scheme 21: Resolution of 2,2',7,7'-tetrahydroxy-1,1'-binaphthyl by fractional crystallization with (S)-Proline.

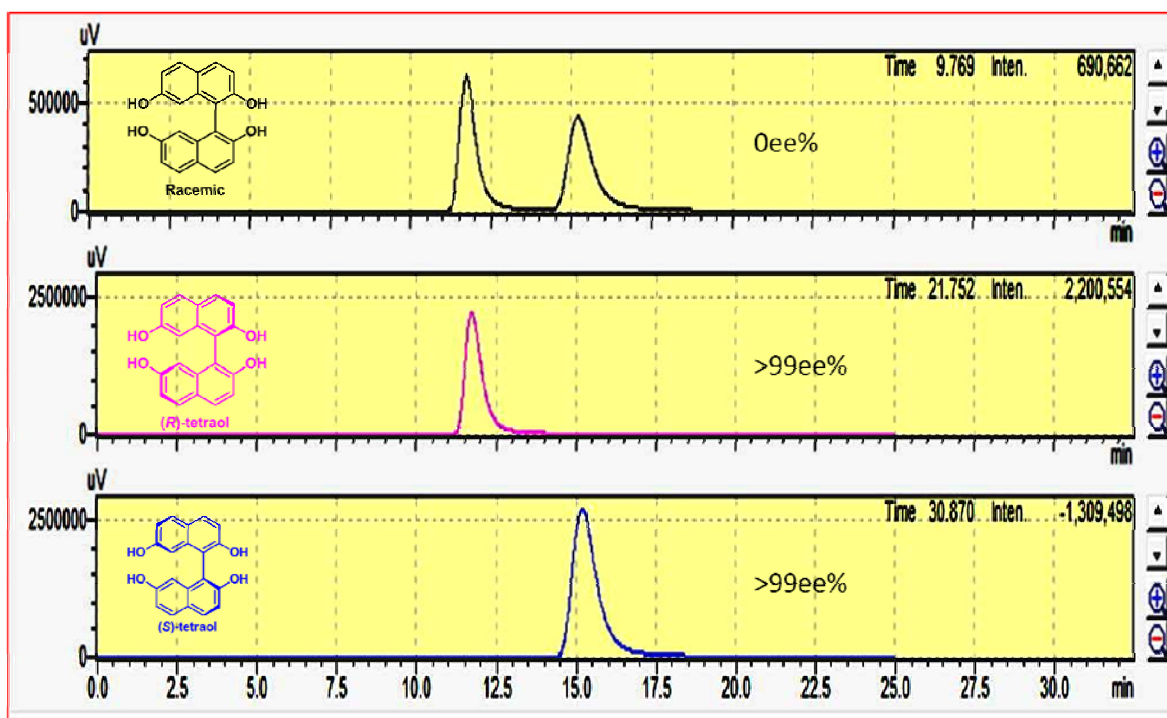


Figure 13: HPLC Chromatogram of tetrol 41

The optical rotations of the (R)-41 and (S)-41 were recorded in acetonitrile solution. The pure enantiomers of the (R)-41 and (S)-41 have opposite sign of optical rotation – 124 and + 109 respectively (Scheme 21). The CD spectrum of these compounds was run in acetonitrile. The isomers, (R)-41 showed negative cotton effect and (S)-41 showed positive cotton effect (Figure 14).

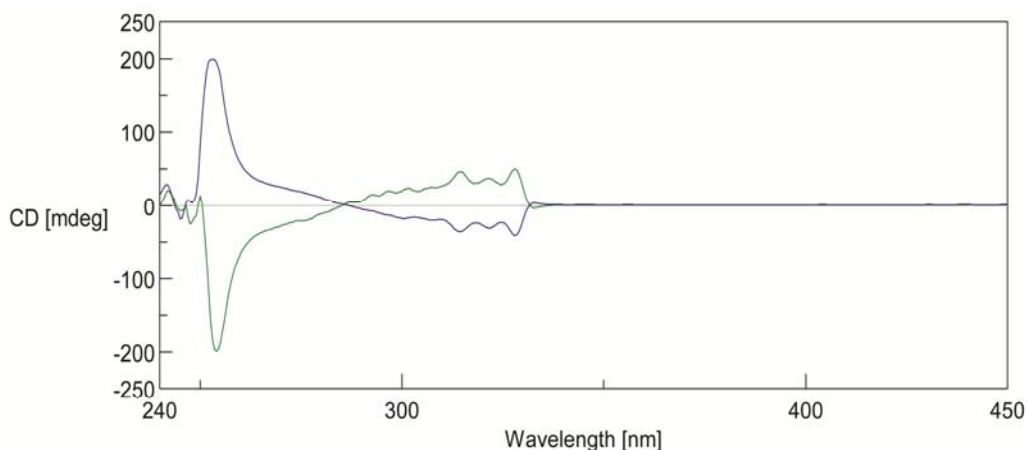


Figure 14: Circular dichroism spectra of resolved Tetraol : (Blue line) *R*-**41** and (Green line) *S*-**41** (*c* 8.44×10^{-4} M in acetonitrile, 25 °C).

Thus, a new and practical resolution of tetrol has been successfully achieved. In order to elucidate the molecular recognition pattern between host and guest molecules in the solid state, the structure of the molecular complex of (*R*)-**41** and (*S*)-Proline was determined by X-ray crystallography.

The single crystal of molecular complex (*R*)-**41** and (*S*)-Proline was obtained by slow evaporation from methanol solvent. The intermolecular organization and association in the molecular complex are shown in Figure 15. The structure of the molecular complex consisting of (*S*)-proline and (*R*)-tetrol. It can be seen in Figure 15 that (*S*)-proline exists in the form of the zwitterions in the crystal. The structural parameters exhibited for the host and guest molecules are in good agreement with standard values.⁷⁸

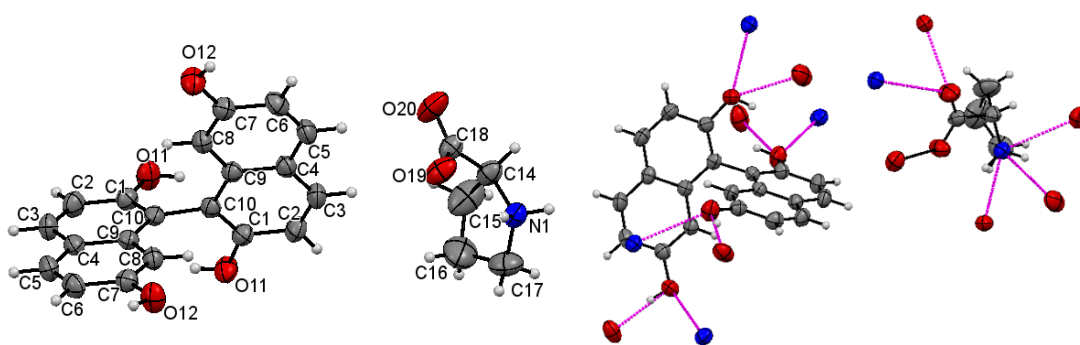


Figure 15: Perspective view of the molecular complex of (*R*)-tetrol and (*S*)-Proline, and hydrogen bonding in the molecular complex consisting of (*R*)-tetrol and (*S*)-Proline. Hydrogen bonds are shown as violet colour.

As shown in Figure 16 and 17, the structure of the molecular complex network between (*R*)-**41** and (*S*)-proline can be described as infinite chains of interlinked species that are

aligned in an alternating manner through hydrogen bonds. The hydrogen bonding pattern includes the four OH groups of tetrol as the proton donors and the carboxylate (-COO) and NH group of (*S*)-Proline as the proton acceptors, where the carboxylate O atoms and the N-H of (*S*)-proline, as well as the hydroxylic -H atoms of (*R*)-tetrol are all in a hydrogen-bonding environment. Each -OH group of the tetrol acts as the proton donor and (*S*)-proline serves as the proton accepters. Four (*S*)-Proline molecules interacted with two molecules of tetrol. Whereas 2,2' hydroxylic protons forms hydrogen bonding at O(11)-H(11) ---- O(20) of 2.653, O(11)-H(11) ---- N(1) 2.847, and terminal 7,7' hydroxylic protons forms hydrogen bonding at O(12)-H(12) ---- O(19) of 2.614, O(12)-H(12) ---- N(1) of 2.994. Simultaneously, hydrogen bonding interactions also occur between the carbonyl-O atom and N-H of (*S*)-proline (N(1) ---- O(20) of 2.870. The dihedral angle of the binaphthyl unit is 70.02° and its absolute configuration was unambiguously established to be *R*, through relation with the absolute configuration of (*S*)-Proline. The molecular complex network between (*R*)-tetrol and (*S*)-Proline can be described as infinite chains of interlinked species, which are aligned in an alternating manner through hydrogen bonds (Figure 17).

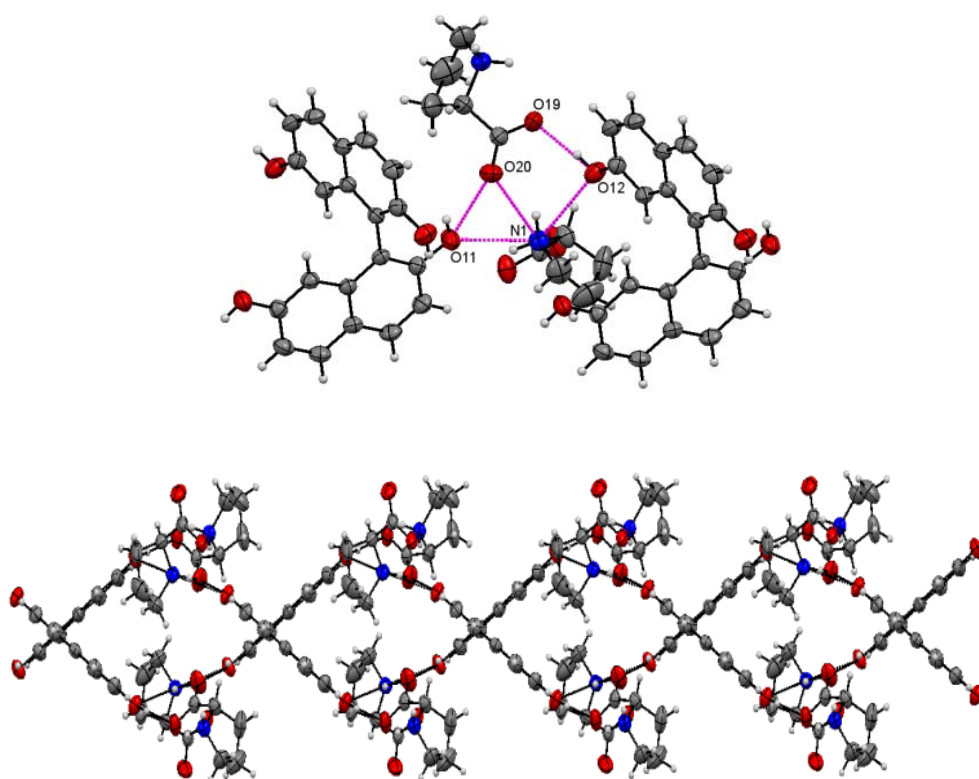


Figure 16: (*S*)-Proline molecules interacted with two molecules of (*R*)-tetrol through hydrogen bonding in the molecular complex consisting of (*R*)-tetrol and (*S*)-Proline chains of interlinked species

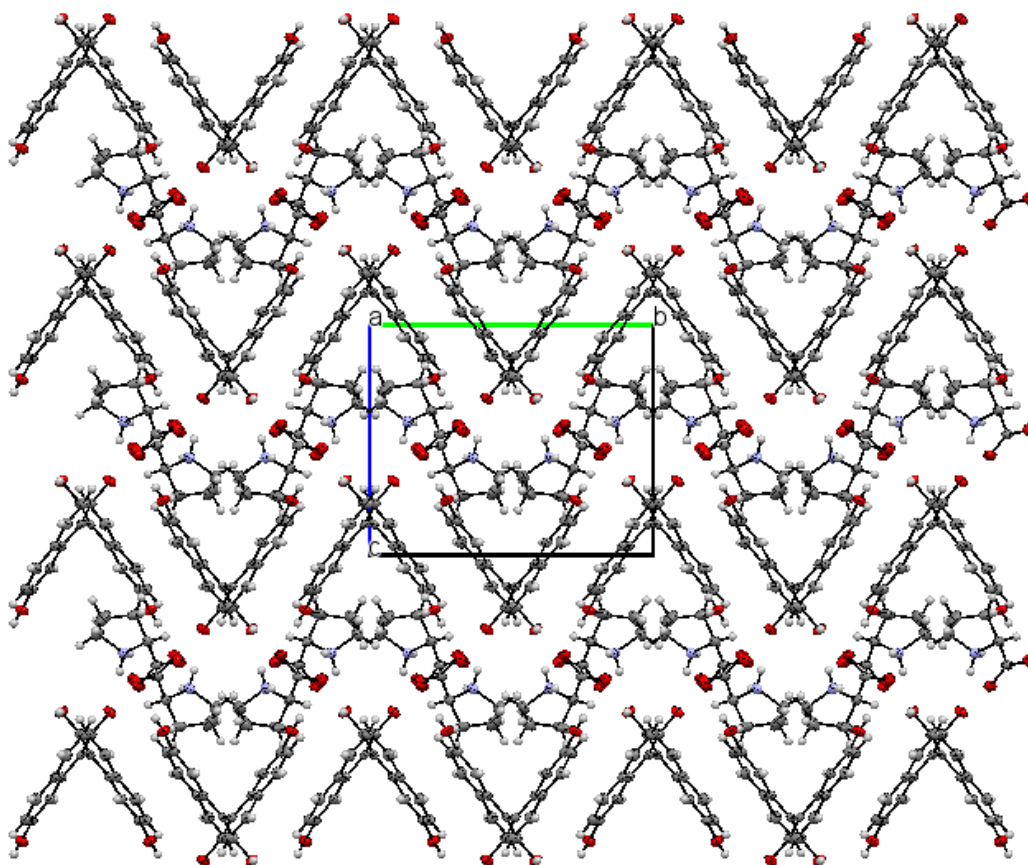


Figure 17: Packing diagram of the molecular complex of (*R*)-tetrol and (*S*)-Proline

In the X-ray diffraction analysis the angle between the planes passing through the two naphthalene rings and angle between the axis of the molecules was established. The stereochemistry of the axis clearly show the *R*-configuration by considering the known chirality in the molecule from the chiral (*S*)-Proline.

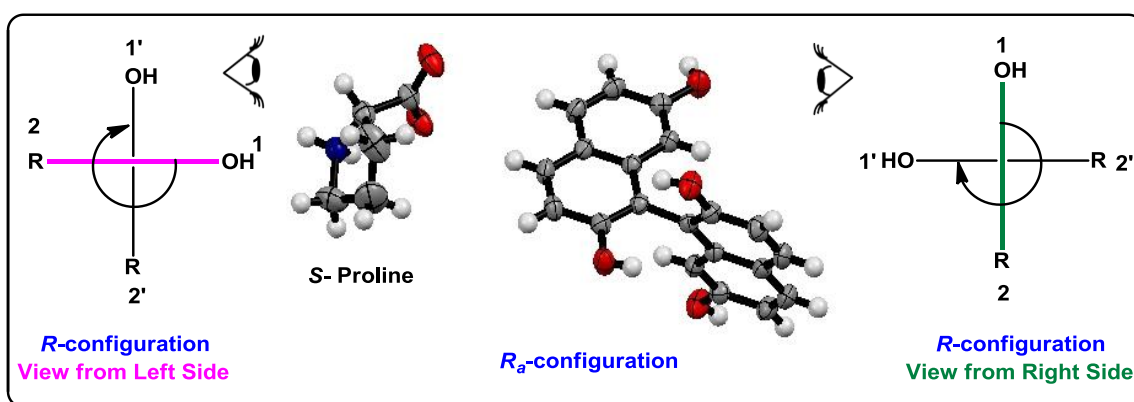
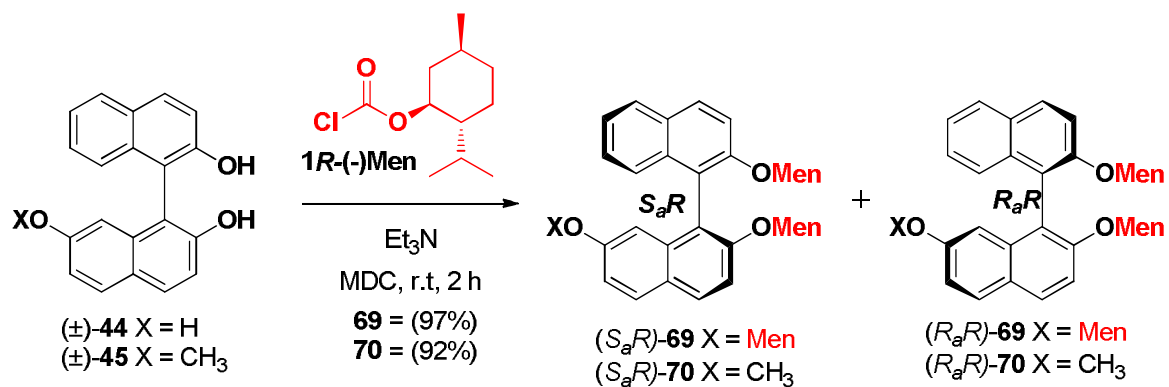


Figure 18: ORTEP diagram of the salt of (*R*)-Tetraol•(*S*)-Proline. Configuration of the tetraol compound from the single crystal structure

Attempted resolution via making diastereomers

In the previous section we have discussed the resolution of (\pm)-triol **44** was partially resolved via formation of the diastereomeric salt with bruicine (Scheme 20). In order to try to increase the optical purity (ee%) of the triol compound was converted to diastereomers according to the general procedure introduced by De Lucchi.⁷⁹ Thus, (\pm)-triol **44** was treated with the (1*R*,2*S*,5*R*)-(-)-menthyl chloroformate in the presence of triethylamine, and the resulting diastereoisomeric mixture of the bis(menthyl) carbonates (*S_aR*)-**69** and (*R_aR*)-**69** was isolated as a mixture in good yield. The diastereomers could not be isolated on column chromatography. The subsequent recrystallization from different solvent/conditions did not afford the pure diastereoisomers; not even enrichment was not observed (Scheme 22). The triol was converted to 7-methoxy-[1,1'-binaphthalene]-2,2'-diol **45** according to the procedure developed by Thongpanchang⁸⁰ (Scheme 27). Then treated with the (1*R*, 2*S*, 5*R*)-(-)-menthyl chloroformate and the resulting diastereoisomeric mixture of the bis(menthyl) carbonates (*S_aR*)-**70** and (*R_aR*)-**70** was isolated as a mixture on column chromatography with good yield (Scheme 22). The recrystallization in different solvent conditions could not furnished pure or enriched diastereomers.

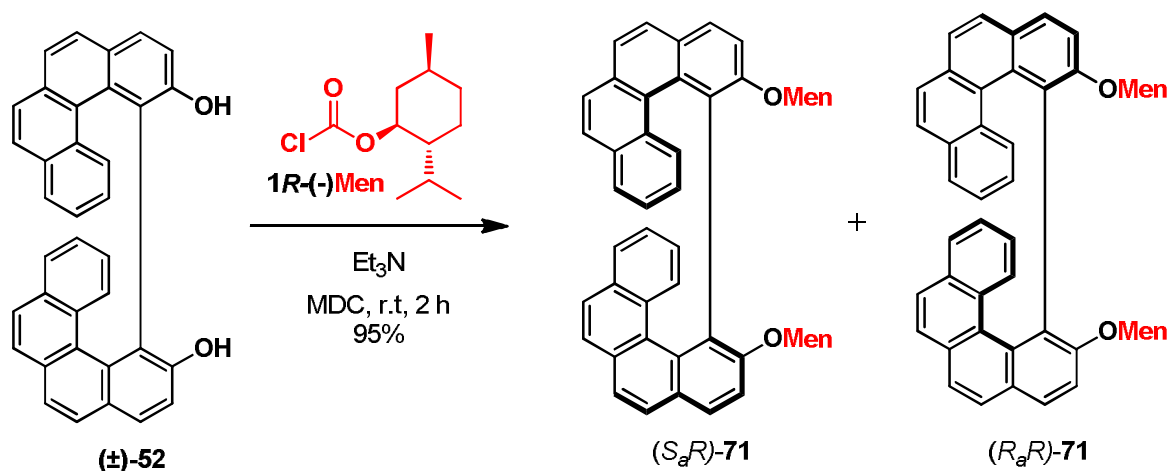


Scheme 22: Resolution of BINOL derivatives using Menthyl chloroformate

Resolution of [1,1'-bibenzo[*c*]phenanthrene]-2,2'-diol

The resolution of (\pm)-**52** was attempted by treatment with (1*R*,2*S*,5*R*)-(-)-menthyl chloroformate in the presence of triethylamine, and the resulting diastereoisomeric mixture of the bis(menthyl) carbonates (*S_aR*)-**71** and (*R_aR*)-**71** was isolated as a mixture in good yield (Scheme 23). This diastereomers could not be isolated on column chromatography.

The subsequent recrystallization from different solvent/ conditions did not afford the pure diastereoisomers.



Scheme 23

Thus in this work we have synthesized and resolved few hydroxylated binaphthyl systems and would be further used for synthesis of useful compounds.

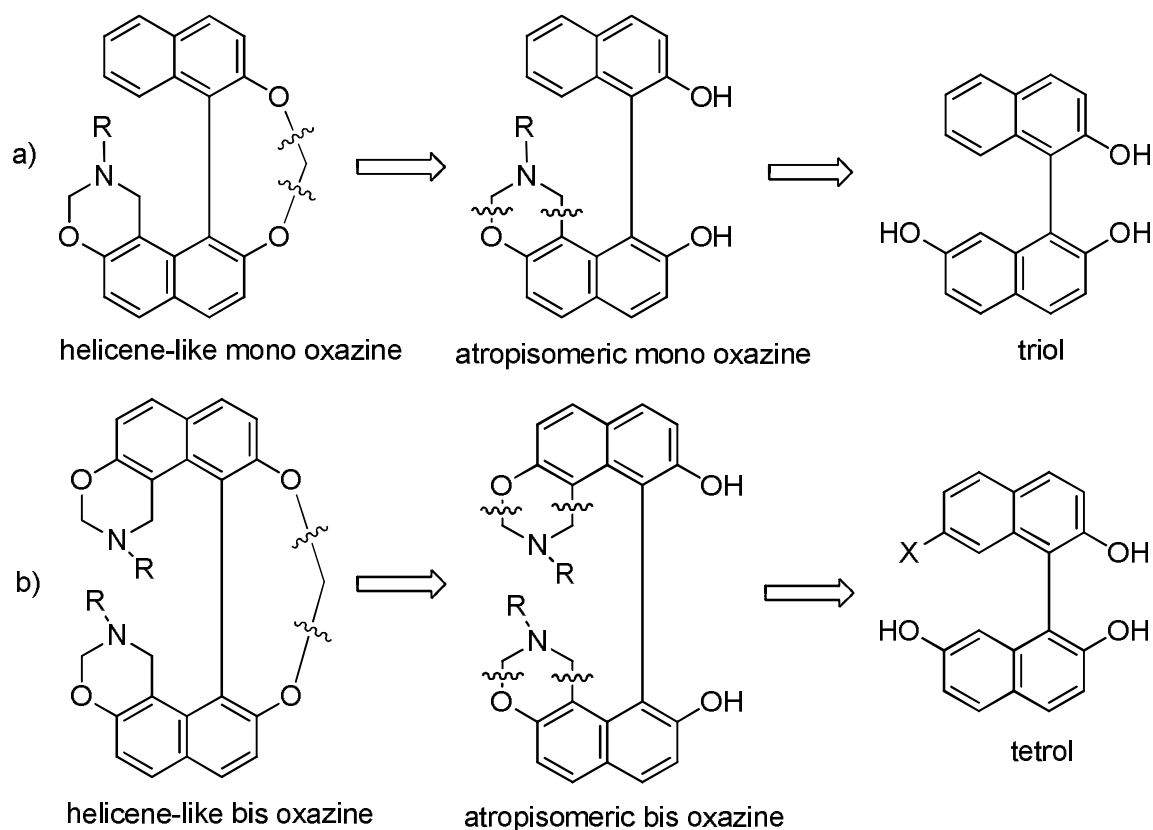
3.2.2 Synthesis of enantiomerically pure helicene like oxazines from atropisomeric 7, 7'-dihydroxy or 7-hydroxy BINOL, Study of their circularly polarized luminescence

Basically, there are two types of helical molecules such as helicene with continuous delocalization of π -electrons (carbahelicenes and heterohelicenes) and helicene-like molecules with possibly discontinuation of delocalization of π -electrons. The synthesis of new helical molecules with different shape, size and functional group is quite challenging in modern organic chemistry. This is particularly vital in the field of molecular recognition, supramolecular and medicinal chemistry, asymmetric synthesis and enantioselective catalysis, material chemistry etc. Amongst this class of compounds helically chiral molecules find a unique place due to some special chiroptical properties. Since the pioneering work on helicene by Newman in 1956,⁸¹ the area has presented a number of new helical molecules with a wide range of applications.⁸²

In the previous section we have synthesized atropisomeric binaphthylene derivatives with different shape, size and functional group. These atropisomeric binaphthylene derivatives were good precursor for synthesis of helicenes or helicene like molecules. In this section we present our efforts to synthesize helicene-like molecules from atropisomeric

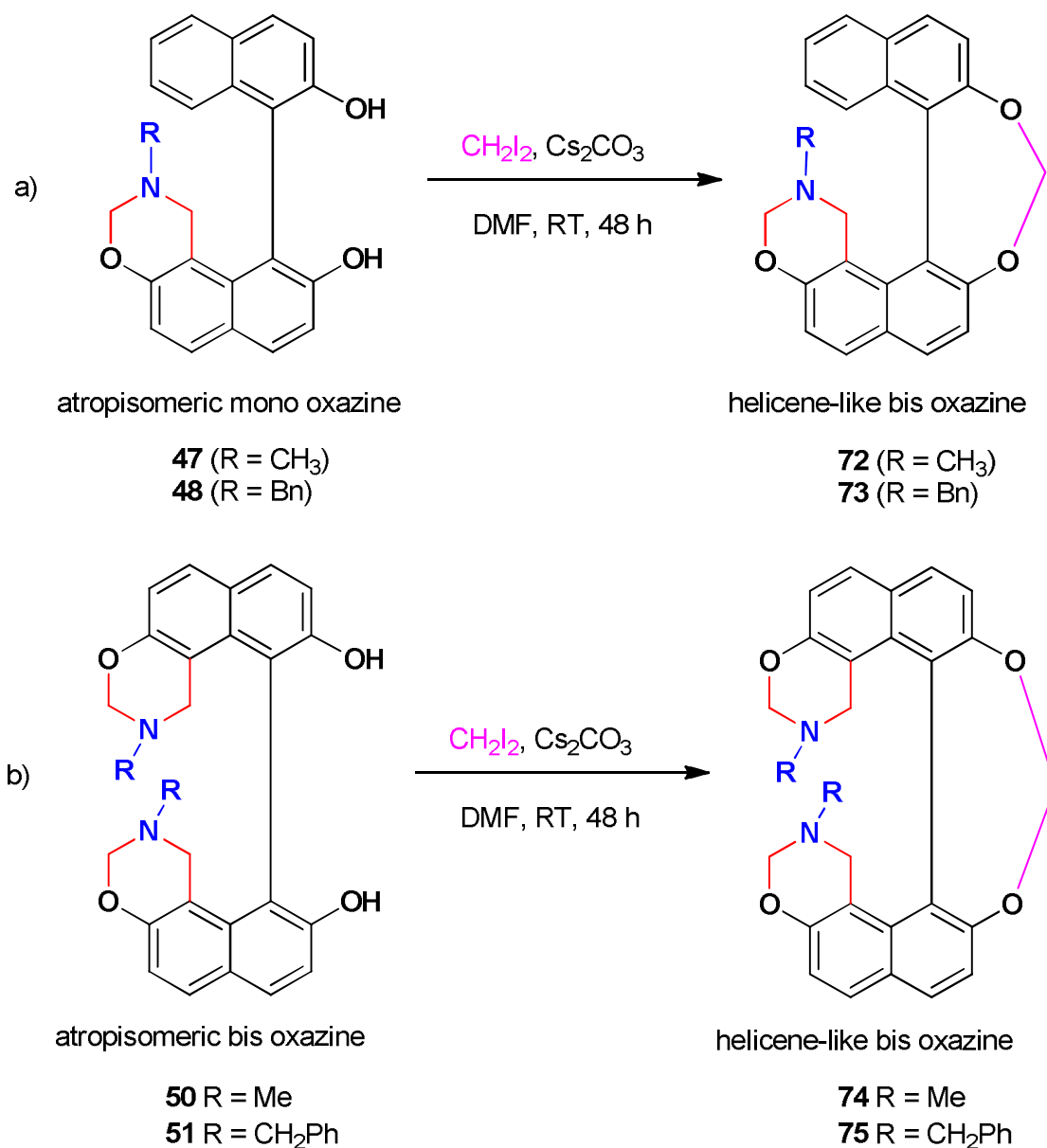
binaphthylene derivatives. In short we have attempted to transfer axial chirality to helicene-like chirality.

The retrosynthetic schemes of preparation of target helicene-like mono/bis oxazines is presented in Scheme 24, where the first disconnection will lead to the precursor atropisomeric mono/bis oxazines, which can easily be built from triol/tetrol by aromatic Mannich reaction with appropriate 1° amine and formaldehyde.



Scheme 24: Retrosynthesis of helicene-like mono/bis oxazine

Initially we have synthesized racemic helicene-like mono/bis oxazines derivatives from atropisomeric hydroxylated binaphthylene compounds by building an ether bridge with diiodomethane in the presence of Cs_2CO_3 (Scheme 25). All compounds were well characterized by usual spectral analysis.



Scheme 25: Synthesis of helicene-like oxazine derivatives a) for mono oxazine b) for bis oxazine

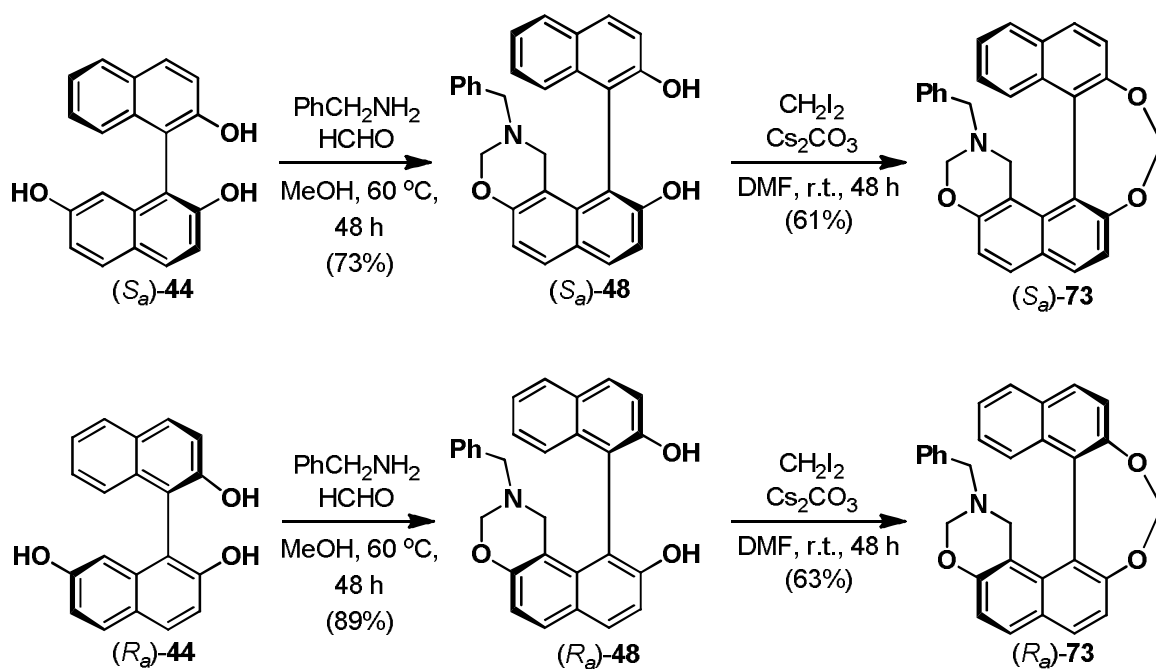
The ¹H-NMR spectrum of helicene-like mono oxazine compound **72** showed a broad singlet at δ 5.71 for the ether bridge methylene protons (-CH₂), a broad signal at δ 4.54 for the -N-CH₂-O methylene protons. At the same time the hydrogens of the -CH₂ group of Ar-CH₂-N of the oxazine ring appear as two doublets at δ 2.98 and 2.88 (J = 16.8 Hz, 2H), and sharp singlet appeared at δ 2.16 for methyl protons (-NCH₃). The ¹H-NMR spectrum of helicene-like mono-oxazine compound **73** showed two doublets at δ 5.70 and 5.67 (J = 10 Hz, 2H) for the ether bridge methylene protons (-CH₂), a broad singlet at δ 4.51 for the -N-CH₂-O methylene protons. At the same time the hydrogens of the -CH₂ group of Ar-CH₂-N- of the oxazine ring appear as two doublets at δ 3.47 and 3.32 (J = 12.8 Hz, 2H),

and broad singlet appeared at 3.05 for benzylic protons (-CH₂Ph). The high resolution mass spectrum of **73** showed the molecular mass of the product and its isotope pattern were consistent with the calculated value for C₃₀H₂₃NO₃ [M + 1]⁺ 446.1756, found 446.1750 *m/z*.

The ¹H-NMR spectra of the helicene-like molecule **74** shows a singlet at δ 5.64 for methylene protons of ether bridge of -O-CH₂-O and the two doublets at δ 4.53 and 4.50 (*J* = 9.2 Hz, 2H) of the -CH₂ group of -N-CH₂-O. The internal -CH₂ group proton of Ar-CH₂-N- are observed as the two doublets at δ 2.66 and 2.39 (*J* = 16.4 Hz, 2H). The EI-mass spectrum of the molecule **74** show the molecular ion peak at 440 *m/z* [M]⁺ and the base peak at *m/z* 439. The molecule was also analysed by MALDI-TOF-MS showed the (M+1) 441.1183 *m/z*. The ¹H-NMR of helicene-like bis-oxazine **75** showed a singlet at δ 5.59 for methylene bridge of -O-CH₂-O. The two doublets at δ 4.59 and 4.50 (*J* = 9.6 Hz, 2H) for the protons of the -CH₂ group of -N-CH₂-O. The benzylic -CH₂ protons observed as two doublets at δ 3.37 and 3.24 (*J* = 12.8 Hz, 4H). The internal -CH₂ group protons of Ar-CH₂-N- observed as two doublets at δ 2.71 and 2.53 (*J* = 16.4 Hz, 4H). The EI-mass spectrum of the molecule **75** showed the molecular ion peak [M]⁺ 592 *m/z*.

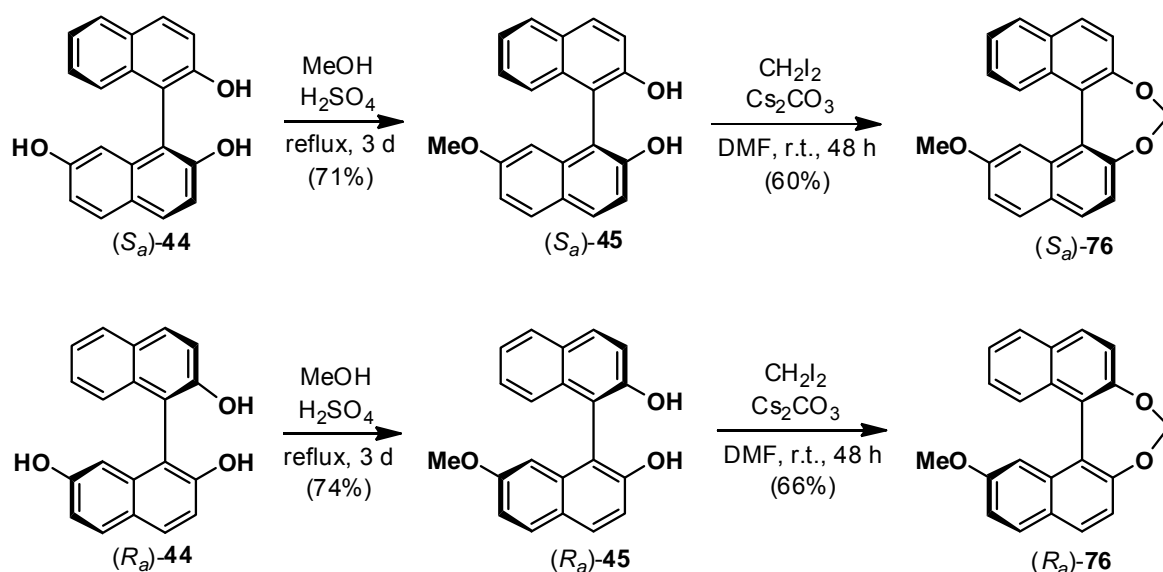
Synthesis of optically pure helicene like mono oxazines from atropisomeric 7-hydroxy BINOL

In the next set of such derivatives we have synthesized optically pure atropisomeric mono 1,3-oxazines. Optically pure (*S_a*)-**44** was subjected to aromatic Mannich reaction with benzyl amine and aqueous solution of formaldehyde to furnish (*S_a*)-**48**, which was further converted to helicene-like mono oxazine derivative (*S_a*)-**73** (>99 % ee). Same procedure was followed to access the other enantiomer (*R_a*)-**73**, but with lower optical purity (Scheme 26). All derivatives were characterized by usual spectroscopic and analytical techniques. The present derivatives of methylene bridge containing helicene-like mono oxazine molecules have only one element of chirality.



Scheme 26: Synthesis of enantiomers (*S_a*)-73 and (*R_a*)-73

Apart from the 1,3-oxazine derivatives, we have synthesized helicene-like molecules (*S_a*)-76 and (*R_a*)-76. Having obtained the optically pure isomer of triol **44**, we next embarked upon its conversion to mono methyl ether (*S_a*)-45, where the hydroxyl at C7 was selectively methylated⁸³ (Scheme 27). Further a methylene bridge was introduced between the remaining two free hydroxyl groups by standard procedure using diiodomethane in presence of cesium carbonate to afford (*S_a*)-76, which was characterized by usual spectroscopic and analytical techniques. On crystallization this compound was obtained as a single enantiomer (>99 % ee) and characterized by single crystal X-ray diffraction analysis (Figure 19). The analysis clearly indicate presence of two molecules in the unit cell both of *P*-helical description, crystallized in $P 2_1$ space group while the dihedral angle of 55.0° was observed. The other isomer (*R_a*)-44 was similarly converted to (*R_a*)-76, but in lower optical purity (~62 % ee). Our attempts to enrich this isomer by repeated crystallizations did not improve the optical purity. The present derivatives of methylene bridge containing helicene-like molecules have only one element of chirality.



Scheme 27: Synthesis of enantiomers (*S_a*)-76 and (*R_a*)-76

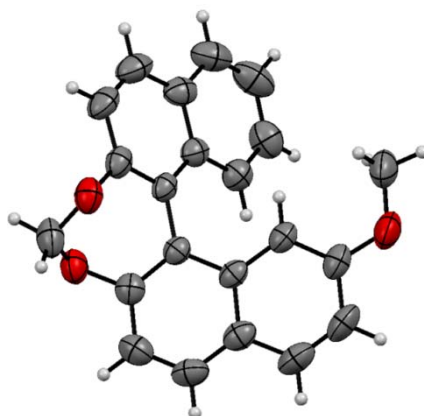
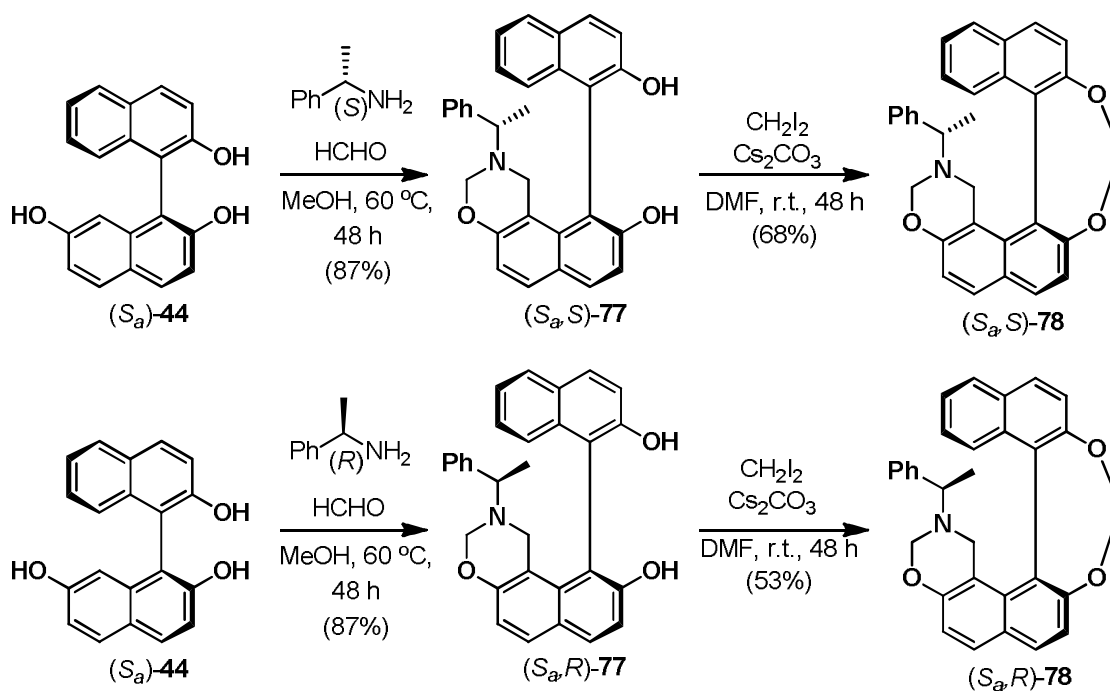


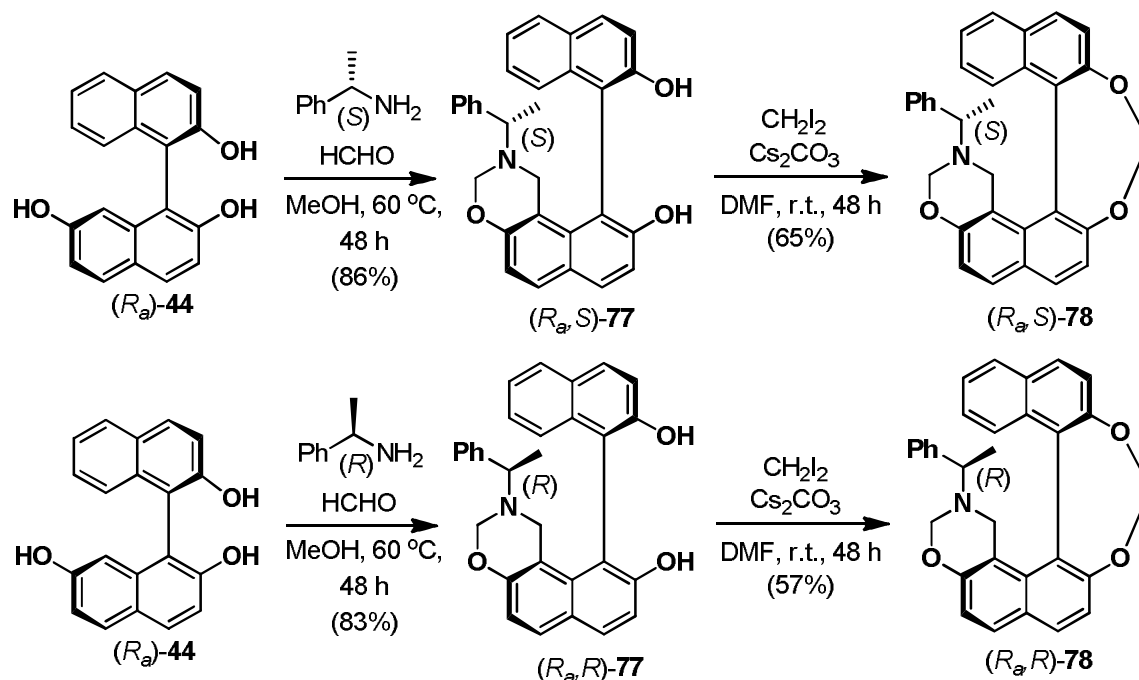
Figure 19: ORTEP of (*S_a*)-76 (CCDC 1453552)

In the above series further modification was introduced by adding another element of chirality where the oxazine ring was attached with chiral group. For this purpose optically pure 1-phenyl ethyl amine was chosen as the primary amine during aromatic Mannich reaction. First we carried out the reaction with racemic triol **44** furnished mixtures of diastereomers, which was converted into helicene-like oxazines, whereas this mixture of diastereomers could not be separated by column chromatography or crystallization. In next part we prepared optically pure helicene-like 1,3-oxazine from optically pure 1-phenyl ethyl amine. Accordingly optically pure triol (*S_a*)-**44** was treated with formaldehyde and separately with both isomers of 1-phenyl ethyl amine followed by bridge formation to afford (*S_{a,S}*)-**78** and (*S_{a,R}*)-**78** (Scheme 28). Both these diastereomers were obtained in high chiral purity (>99 % de).



Scheme 28: Synthesis of diastereomeric (S_a,S)-**78** and (S_a,R)-**78**

Identical reaction sequence was adopted to access other two diastereomers of (R_a,S)-**78** and (R_a,R)-**78** starting from (R_a)-**44** (Scheme 29). These diastereomers were initially obtained with moderate optical purity at the axial chirality, but eventually improved by single crystallization from ethyl acetate and hexane (up to 86 % de).



Scheme 29: Synthesis of diastereomeric (R_a,S)-**78** and (R_a,R)-**78**

The structure of a representative example of (*S_a*,*S*)-**78** was studied by its single crystal X-ray diffraction analysis (Figure 20). The analysis clearly indicate presence of four molecules in the unit cell all with *P*-helical description, crystallized in $P 2_1 2_1 2_1$ space group while the dihedral angle of 65.74° was observed. This mono oxazine derivative showed slightly higher dihedral angle compared to mono-methoxy derivative (*S_a*)-**76**, probably due to extended helical like structure as a result of additional heterocyclic ring.

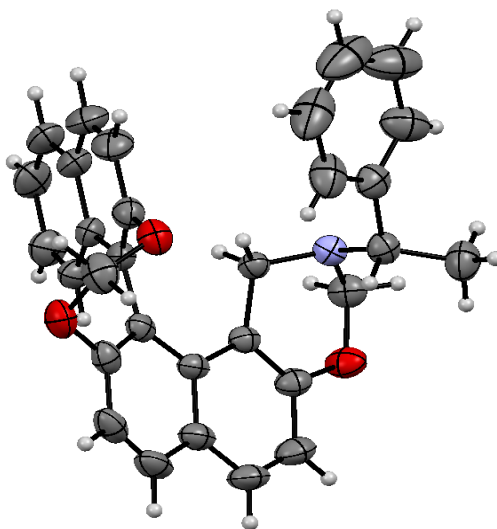


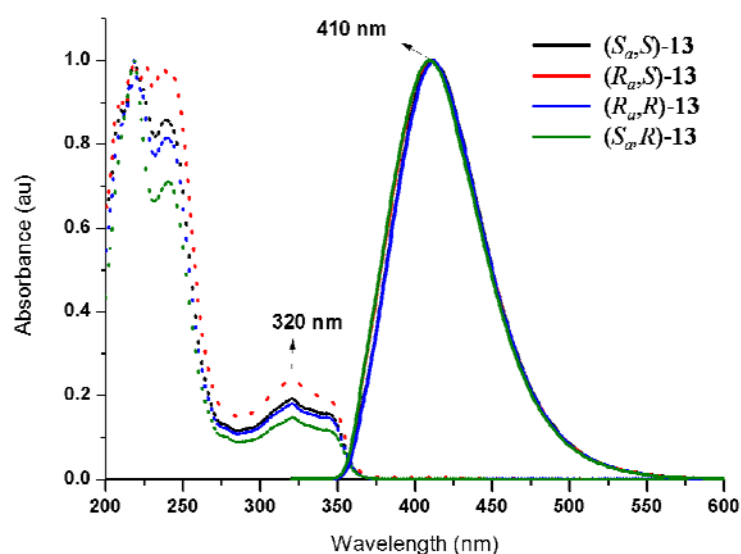
Figure 20: ORTEP of (*S_a*,*S*)-**78** (CCDC 1041059)

Having obtained optically pure samples of these four types of compounds we examined their chiroptical properties. The triol (*S_a*)-**44** with axial chirality showed specific optical rotation, OR, of about +30° (Table 3). This compound was converted to helicene-like molecule (*S_a*)-**76**, as expected there was a considerable enhancement in the value of specific OR.⁸⁴ This is in accordance with the characteristic observation for helical or helicene-like molecules.⁸⁵ The third type of molecules studied contained an additional oxazine ring fused to one of the naphthalene moieties. Optically pure sample of (*S_a*)-**73** with only a single chiral element in the helicene-like structure showed no significant enhancement in the OR value. In the next set of molecules we examined a combination of helicene-like basic framework and molecules with oxazine containing a stereogenic center. In this part we have prepared all four possible diastereomers of **78** and compared their OR values. In this set the two enantiomers (*S_a*,*S*)-**78** and (*R_a*,*R*)-**78** demonstrated slightly higher degree of OR as compared to the other set of enantiomers (*S_a*,*R*)-**78** and (*R_a*,*S*)-**78**. These two sets being diastereomeric to each other, we establish the match-mismatch effect of the two chiral elements in these helicene-like mono oxazines towards the plane polarized light.

Table 3 Correlation of the chiroptical properties of synthesized compounds

No	Compound	% ee	Specific OR ($[\alpha]_D$)	Molecular OR ($[\Phi]_D$)
1	(<i>S_a</i>)- 44	96	+30	+90.6
2	(<i>S_a</i>)- 76	>99	+1090	+3576
3	(<i>S_a</i>)- 73	98	+801	+3565
4	(<i>S_a</i> , <i>S</i>)- 78	98:2	+742	+3407
5	(<i>S_a</i> , <i>R</i>)- 78	90:10	+638	+2929
6	(<i>R_a</i> , <i>S</i>)- 78	86:14	-402	-1845
7	(<i>R_a</i> , <i>R</i>)- 78	99:1	-828	-3802

The four diastereomeric derivatives of helicene-like mono oxazines **78** showed typical UV and CD spectral features (Figure 21 and 22).⁸⁶ The UV-Vis spectra of all isomers of **78** in acetonitrile exhibit absorption bands in around 320 nm. The isomers showed blue emission in the range of 410 nm with a Stokes shift of about 90 nm. Presence of two opposite bisignate couplets, one at around 214 nm and another positive one at 237 nm were attributed to the *P*-helical-like configuration of (*S_a*,*S*)-**78**. As expected the two pairs of enantiomers show identical but opposite CD curves.

**Figure 21:** Normalized UV-Vis and fluorescence spectra of (*S_a*,*S*)-**78**, (*R_a*,*R*)-**78** and (*S_a*,*R*)-**78**, (*R_a*,*S*)-**78** (ext. at 318 nm)

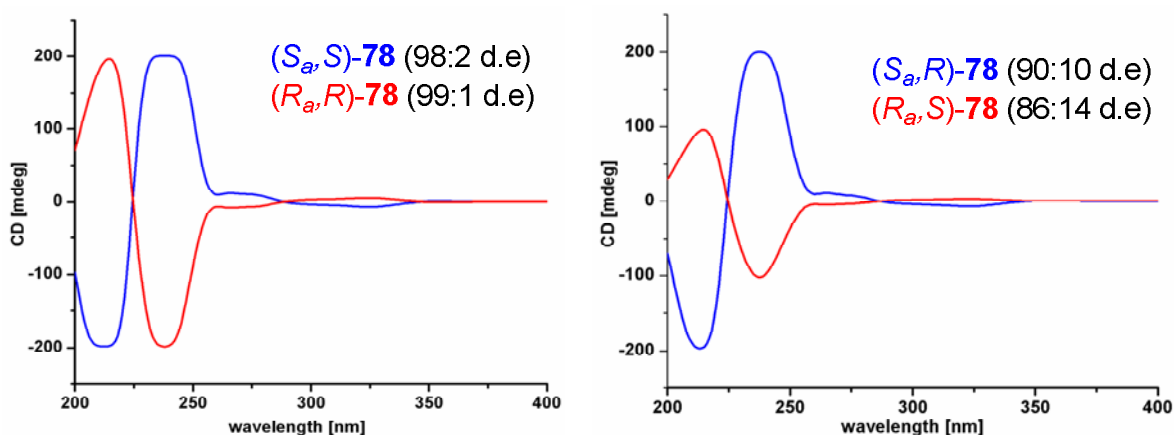
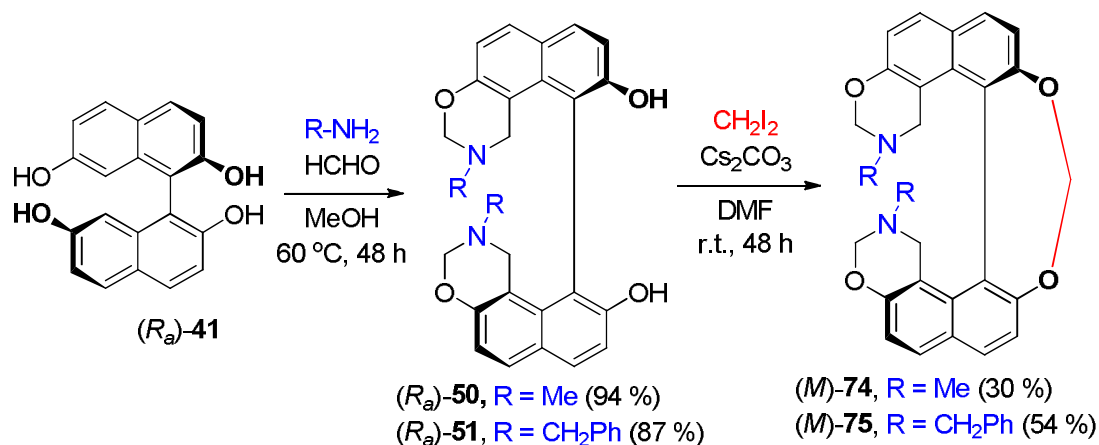


Figure 22: Circular dichroism spectra of enantiomer pairs (S_a,S)-**78**, (R_a,R)-**78** (left) and (S_a,R)-**78**, (R_a,S)-**78** (right) (c 3.81×10^{-4} M in CH_3CN , 25°C).

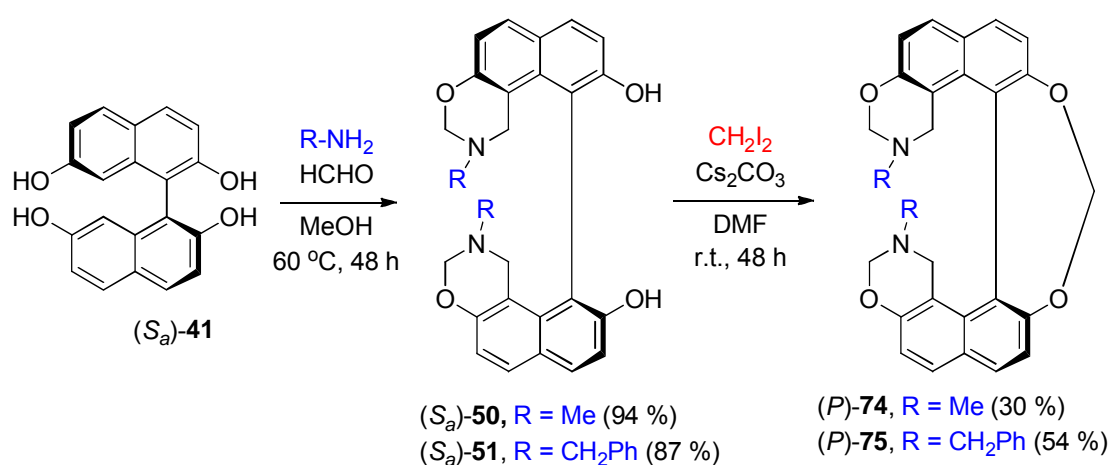
Thus the CD data corroborated with the absolute configuration of the helicene-like nmono-oxazines synthesized in this study.

Synthesis of optically pure helicene like bis-oxazines from atropisomeric 7,7' dihydroxy BINOL

After flourishing synthesized optically pure helicene-like mono oxazines derivatives, we focussed on synthesis of optically pure helicene-like bis-oxazines. Accordingly, optically pure isomer of (R_a)-**41** tetrol was converted to the aromatic Mannich reaction with methyl amine and formaldehyde furnished atropisomerically pure bis-oxazine dihydroxy compound (R_a)-**50**, which was then converted to the helicene like bis-oxazine (M)-**74** by building an ether bridge with diiodomethane and Cs_2CO_3 . Similarly the other set of compounds (R_a)-**51** and (M)-**75** were synthesized using benzyl amine as the primary amine in the aromatic Mannich reaction step (Scheme 30). Same strategy was then repeated with the other enantiomer of tetrol, (S_a)-**41** furnished optically pure atropisomeric bis-oxazines (S_a)-**50** and (S_a)-**51** which were cyclised render optically pure helicene-like derivatives (P)-**74** and (P)-**75** were synthesized (Scheme 31).



Scheme 30: Synthesis of optically pure isomers of helicene like bis-oxazines from $(R_a)\text{-41}$



Scheme 31: Synthesis of optically pure isomers of helicene like bis-oxazines from $(S_a)\text{-41}$

All synthesized derivatives were characterized by usual spectroscopic and analytical techniques. The optical rotations of the all these compounds were measured in chloroform solution. The pure enantiomers of the atropisomerically pure bis-oxazine dihydroxy compounds $(R_a)\text{-50}$, $(S_a)\text{-50}$ and $(R_a)\text{-51}$, $(S_a)\text{-51}$ have opposite sign of optical rotation with the similar specific rotation (Figure 23).

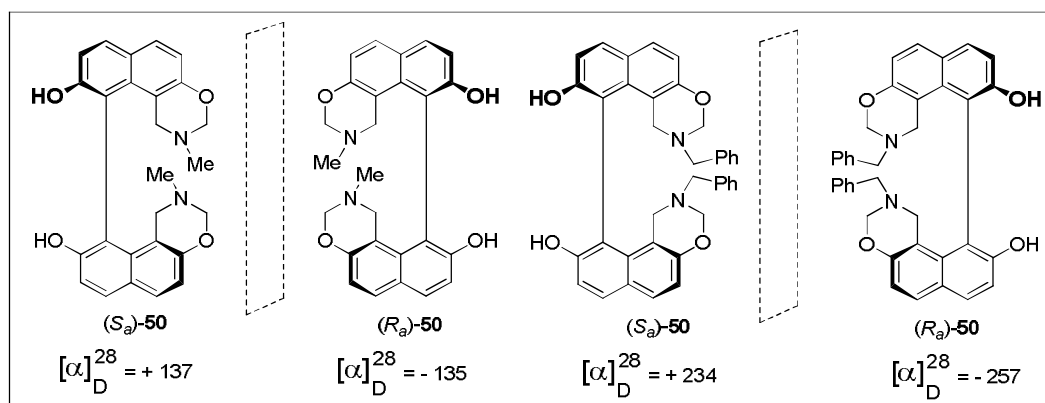


Figure 23: Optical rotations and enantiomer pairs of the atropisomerically pure bis-oxazine dihydroxy compounds $(R_a)\text{-50}$, $(S_a)\text{-50}$ and $(R_a)\text{-51}$, $(S_a)\text{-51}$

The CD spectrum of these compounds was run in acetonitrile. The isomers (R_a)-**50**, (S_a)-**50** (Figure 24a) and (R_a)-**51**, (S_a)-**51** (Figure 24b) have opposite CD spectrum.

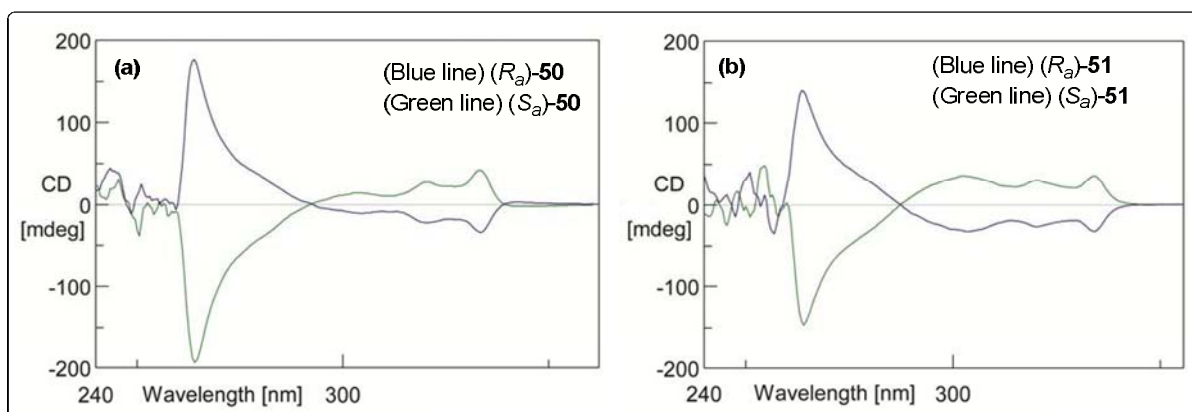


Figure 24: (a) Circular dichroism spectra of resolved I bis-oxazines with methyl: (Blue line) (R_a)-**50** and (Green line) (S_a)-**50** (c 8.44×10^{-4} M in acetonitrile, 25 °C) (b) Circular dichroism spectra of resolved bis-oxazines with benzyl: (Blue line) (R_a)-**51** and (Green line) (S_a)-**51** (c 8.44×10^{-4} M in acetonitrile, 25 °C).

The optical purity of the atropisomerically pure bis-oxazine dihydroxy compounds (R_a)-**50**, (S_a)-**50** (Figure 25) and (R_a)-**51**, (S_a)-**51** (Figure 26) were checked by chiral HPLC analysis.

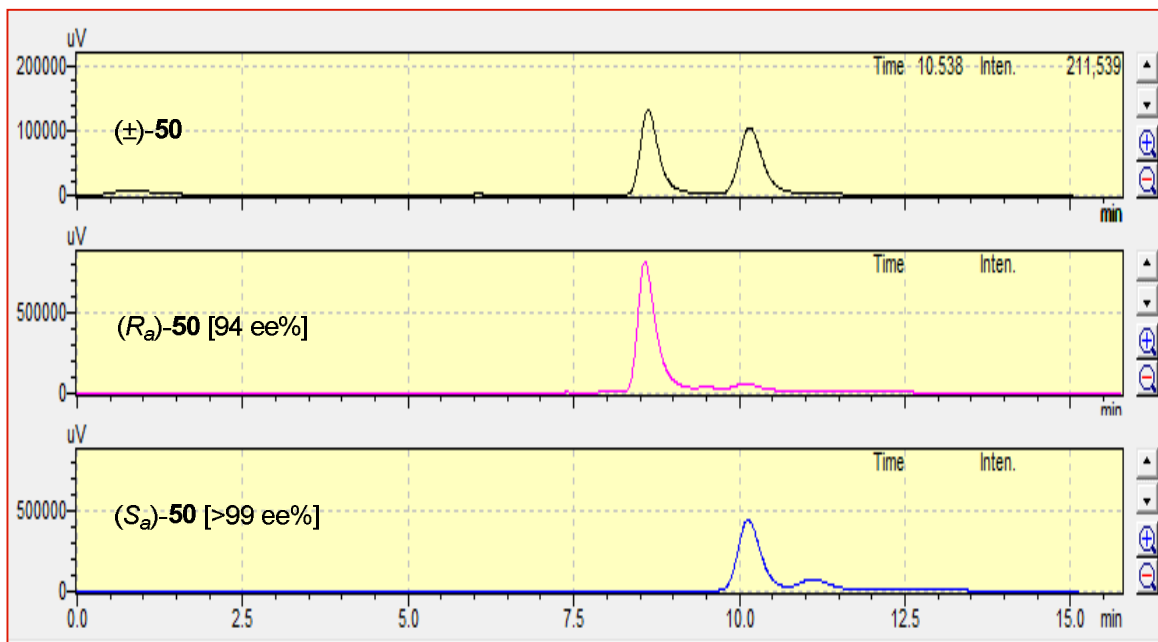


Figure 25: HPLC analysis of atropisomerically pure bis-oxazine dihydroxy compounds (R_a)-**50**, (S_a)-**50** R_t : 1) – 7.89 min 2) R_t – 10.69 min Solvent System: hexane: *iso*-propanol (70:30), Flow rate: 0.5 mL/min Chiral Column: Lux Amylose 2, UV: 254nm.

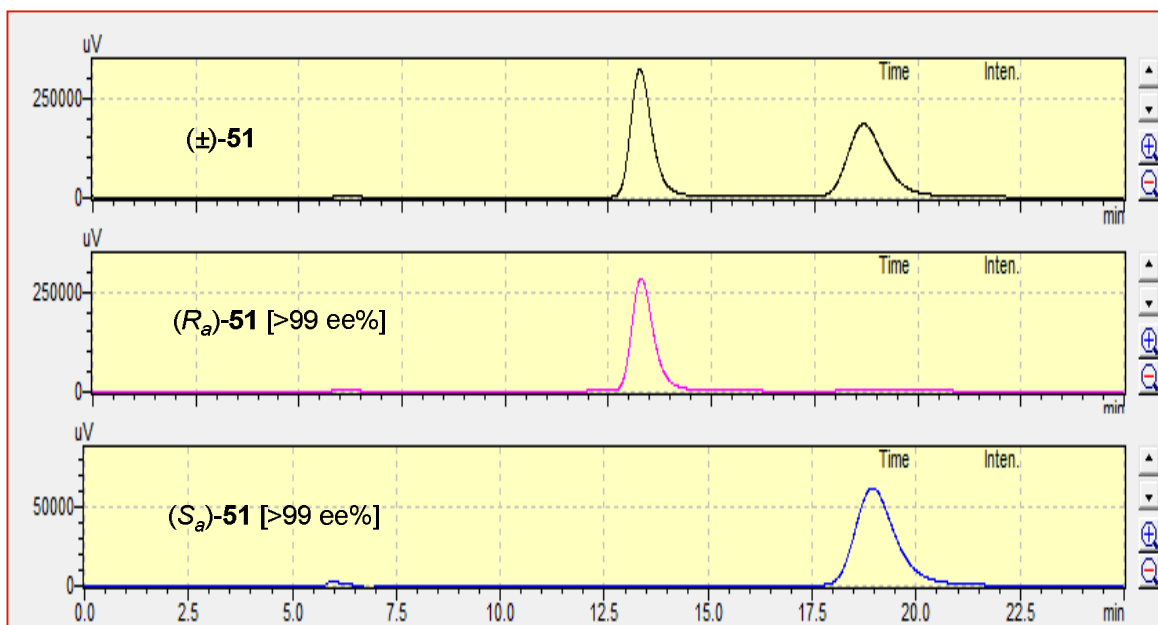


Figure 26: HPLC analysis of atropisomerically pure bis-oxazine dihydroxy compounds (R_a)-**51**, (S_a)-**51** R_t : 1) – 13.26 min 2) R_t – 18.68 min Solvent System: hexane: *iso*-propanol (70:30), Flow rate: 0.5 mL/min Chiral Column: OD-H, UV: 233 nm.

The optical rotations of the all helicene like bis-oxazine compounds were measured in chloroform solution. The pure enantiomers of the helicene like bis-oxazine compounds (P)-**74**, (M)-**74** and (P)-**75**, (M)-**75** have opposite sign of optical rotation with the similar specific rotation (Figure 27).

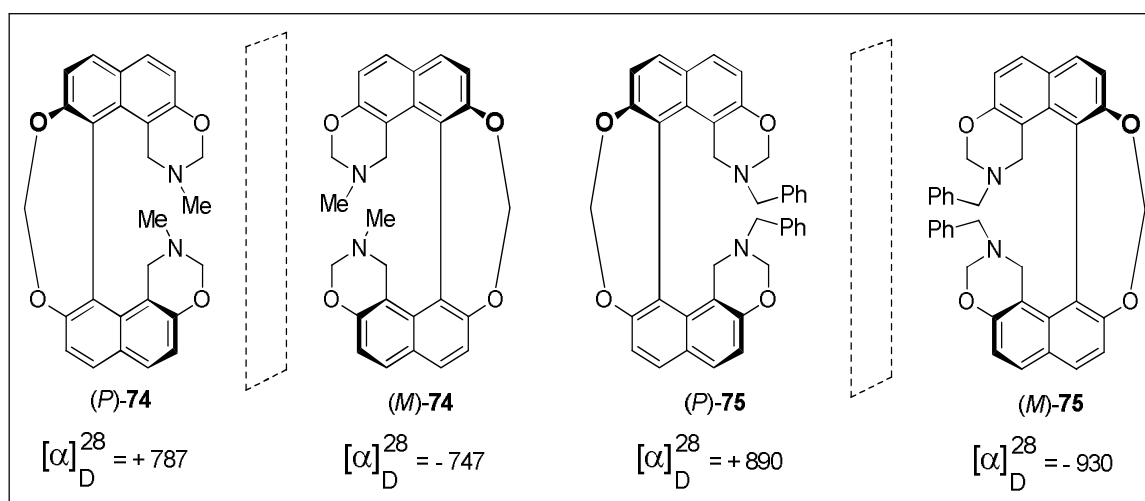


Figure 27: Optical rotations and enantiomer pairs of the helicene like bis-oxazine compounds (P)-**74**, (M)-**74** and (P)-**75**, (M)-**75**

The CD spectrum of these compounds was run in acetonitrile. The isomers (*P*)-**74**, (*M*)-**74** (Figure- 28a) and (*P*)-**75**, (*M*)-**75** (Figure 28b) have opposite CD spectrum.

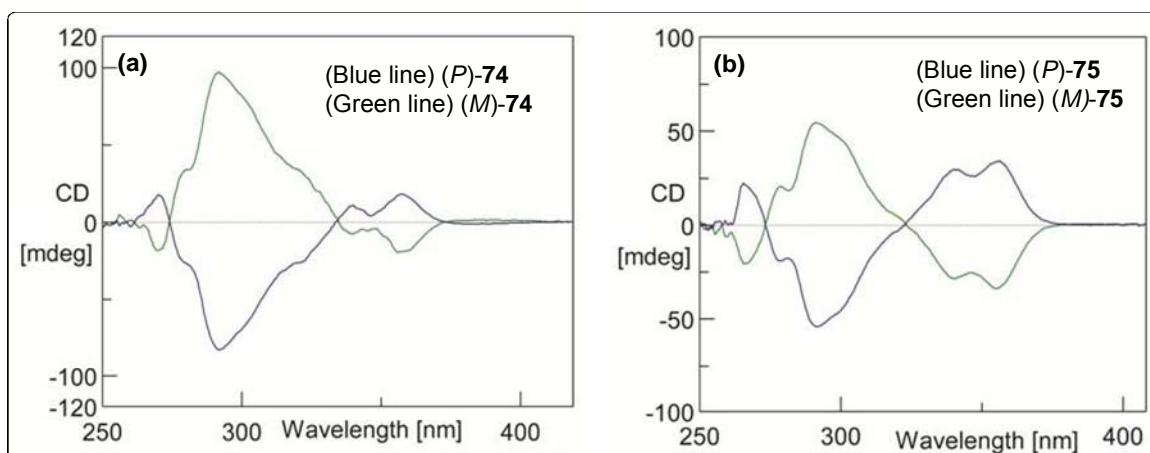


Figure 28: (a) Circular dichroism spectra of resolved helical bis-oxazines methyl: (Blue line) (*P*)-**74** and (Green line) (*M*)-**74** (c 1.13×10^{-3} M in acetonitrile, 25°C) (b) benzyl: (Blue line) (*P*)-**75** and (Green line) (*M*)-**75** (c 8.44×10^{-4} M in acetonitrile, 25°C).

The optical purity of the pure enantiomers of the helicene like bis-oxazine compounds (*P*)-**74**, (*M*)-**74** (Figure 29) and (*P*)-**75**, (*M*)-**75** (Figure 30) were checked by HPLC analysis.

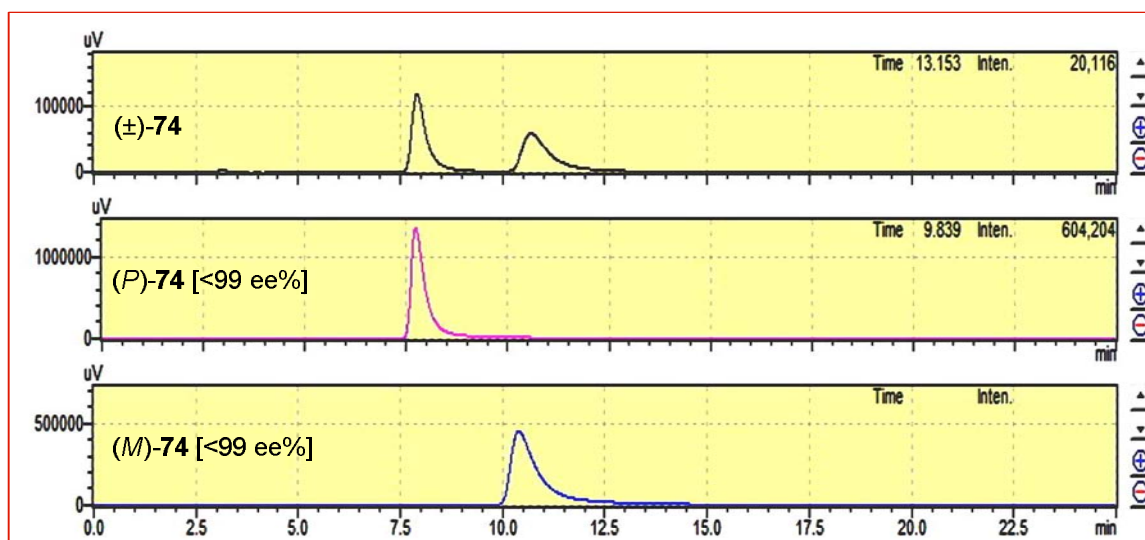


Figure 29: HPLC analysis of enantiomers of the helicene like bis-oxazine compounds (*P*)-**74**, (*M*)-**74** R_t : 1) – 7.89 min 2) R_t – 10.69 min Solvent System: hexane: *Is*o-propanol (70:30), Flow rate: 0.5 mL/min Chiral Column: Lux Amylose 2, UV: 254 nm

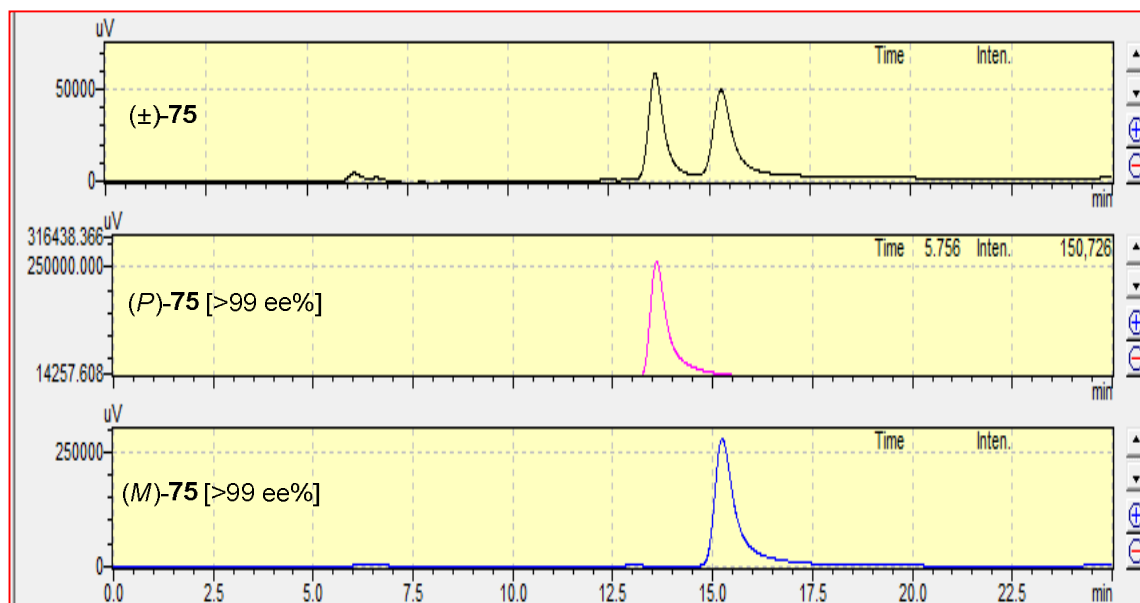


Figure 30: HPLC analysis of enantiomers of the helicene like bis-oxazine compounds (*P*)-**75**, (*M*)-**75** R_t : 1) – 13.64 min 2) R_t – 15.52 min Solvent System: hexane: *iso*-propanol (70:30), Flow rate: 0.5 mL/min Chiral Column: Lux Amylose 2, UV: 254 nm

The structure of helicene like bis-oxazine (*M*)-**75** was further established by its single crystal X-ray diffraction analysis (Figure 31).⁹¹ The dihedral angle between the two planes passing through flat naphthalene units was measured to be 66.13°, while the two oxazine rings assumed half chair like conformation⁹² flipping outside the helical axis. This enables the two benzyl groups to orient along with the helical axis of the structure.

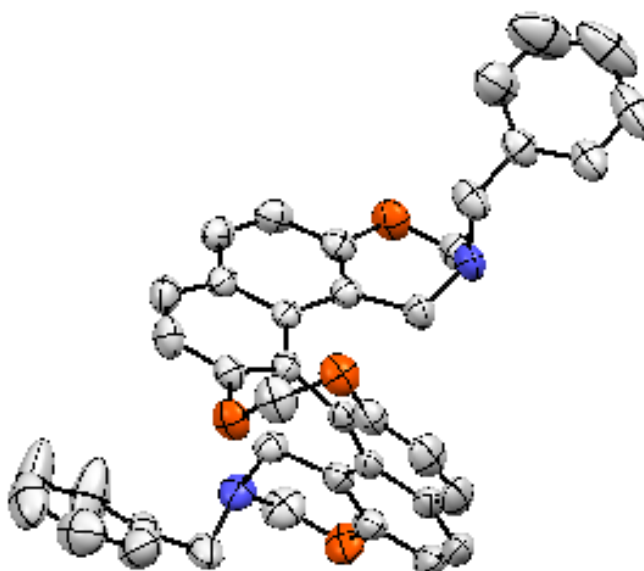


Figure 31: ORTEP diagram of (*M*)-**75**. Hydrogens are omitted for clarity (CCDC 948083)

The process involves conversion of axial chirality of open structure of **50** or **51** to helical chirality in the close structure of **74** or **75**. All the possible isomers of helicene like bis-oxazine were synthesized from (*R_a*)-**41** and (*S_a*)-**41** by the above scheme and their optical properties were studied. The observed optical rotation (OR) of the close helical like structure is expected to be much higher than the open atropisomeric structure.⁸⁷ This phenomena is due to the screw like arrangement of helical compounds and it is quite common for such types of molecules to have high OR values.^{58a,88-90} For example the OR of (*R_a*)-**50** was observed to be -135, which changed to -747 when it was converted to helicene like compound (*P*)-**74**. The comparison of the values of OR and molecular OR for the series of molecules under the present study is summarized in Table 4.

Table 4: Summary of OR and molecular OR of the atropisomeric and helicene like molecules.

Compound	OR [α]	Molecular OR [Φ]	Compound	OR [α]	Molecular OR [Φ]
(<i>R_a</i>)- 41	-116	-369			
(<i>R_a</i>)- 50	-135	-578	(<i>R_a</i>)- 51	-257	-1492
(<i>M</i>)- 74	-747	-3290	(<i>M</i>)- 75	-930	-5512
Compound	OR [α]	Molecular OR [Φ]	Compound	OR [α]	Molecular OR [Φ]
(<i>S_a</i>)- 41	+114	+362			
(<i>S_a</i>)- 50	+137	+587	(<i>S_a</i>)- 51	+234	+1359
(<i>P</i>)- 74	+787	+3467	(<i>P</i>)- 75	+890	+5275

Preliminary measurement of the Circularly Polarized Luminescence of bis oxazine compounds

We have resorted to Circularly Polarized Luminescence (CPL) measurements, the emission analog to CD to further investigate the influence of the helical like structure of the compounds of interest on the chiroptical properties. The circularly polarized luminescence (ΔI) and total luminescence (I) spectra measured for the helicene like bis-oxazine (*P*)-/(*M*)-**74** and (*P*)-/(*M*)-**75** in acetonitrile solutions at 295 K are shown in Figure 32.

The degree of circularly polarized luminescence is given by the luminescence dissymmetry ratio, $g_{\text{lum}}(\lambda) = 2\Delta I/I = 2(I_L - I_R)/(I_L + I_R)$, where I_L and I_R refer, respectively, to the intensity of left and right circularly polarized emissions.^{93,94,95} The solid lines in the CPL plot are presented to show the luminescence spectral line shape. As usual for most chiral organic chromophores and transition metal complexes,^{94,95,96,97} $|g_{\text{lum}}|$ that were obtained are small: +0.0015/+0.0009 and +0.0014/-0.0013 for (*P*)-/(*M*)-**74** and (*P*)-/(*M*)-**75**, as determined at the maximum emission wavelength, respectively. Although the g_{lum} values are very small (a value equal to ~ 0.001 corresponding to light that is only 0.1% circularly polarized), almost opposite CPL signals were measured for the two sets of pairs of helically pure bis-oxazine enantiomers. These results confirm that the helicene like bis-oxazine solutions in acetonitrile exhibit an active CPL signal and also that the emitted light is polarized in opposite directions for the two enantiomeric forms for each set of these helicene like structures. It must be pointed out that the CPL activity observed for the two sets of **74** and **75** corroborates the objective of this work that one can prepare the targeted helical-like molecules in optically pure form from the use of the achiral primary amines (active and opposite CPL response for each enantiomeric form of the two sets of **74** and **75**). It is worth noting that **74** and **75** give a relatively similar CPL response, which is in accordance with the slight structural differences between these two compounds. The only difference is the alkyl group attached to the *N* atom of oxazine (*N*-methyl and *N*-benzyl for **74** and **75**, respectively). Although it is well established that the CPL activity is dependent on the structural properties of the chiral compounds of interest,^{93,95} it can be concluded from the CPL results (i.e. similar g_{lum} magnitudes) that the structural changes are not sufficient to considerably influence in a different manner the chiroptical properties of these two compounds. The structural changes resulting from the replacement of the *N*-methyl by the *N*-benzyl substituent does not lead to a more pronounced interplanar or dihedral angle

of the helical compound, which would have resulted most likely on a more chiral system and, thus, a larger CPL signal. This is in line with the fact that the CPL response is more influenced by the chiral arrangement surrounding the luminescent/phosphorescent/fluorescent center than the contribution of chiral atoms present into the organic skeleton of a system of interest.^{93,95}

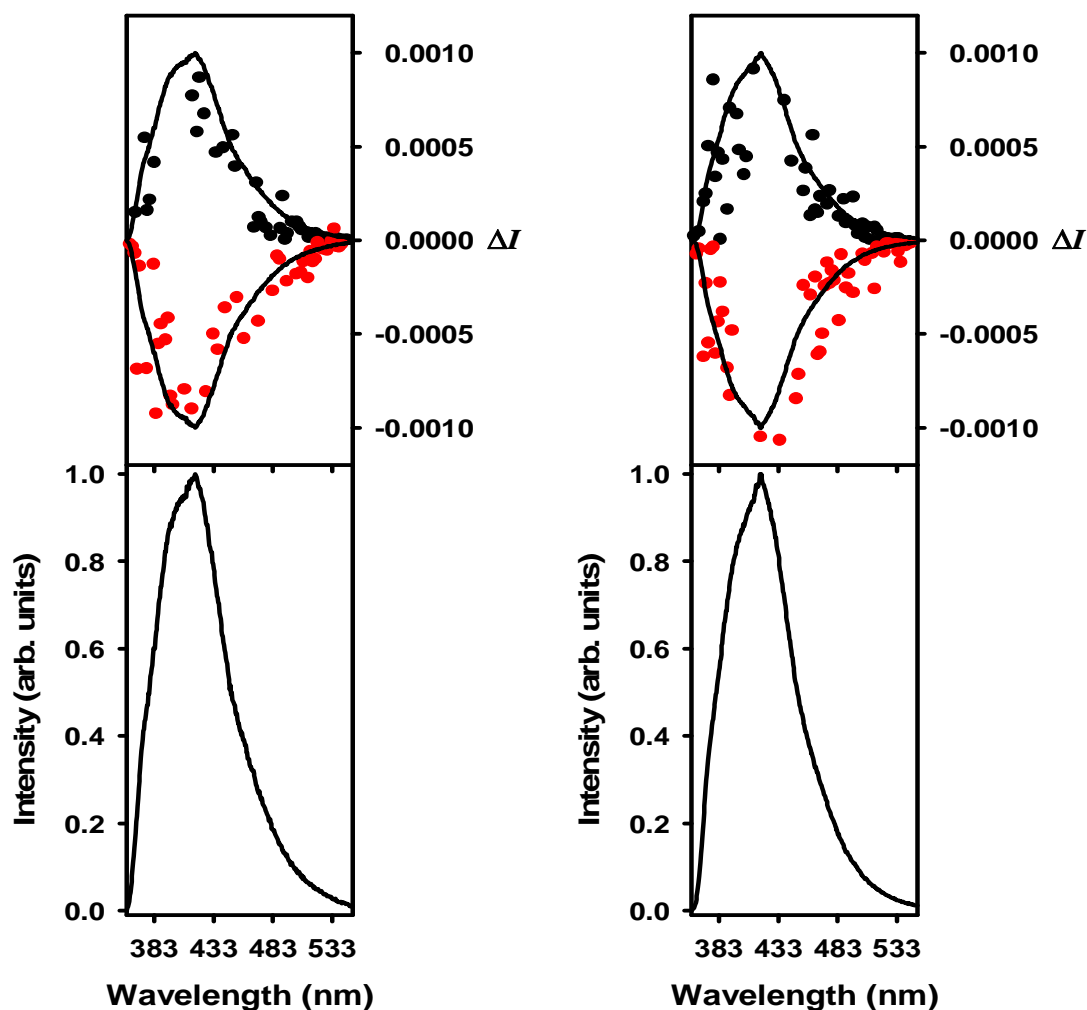


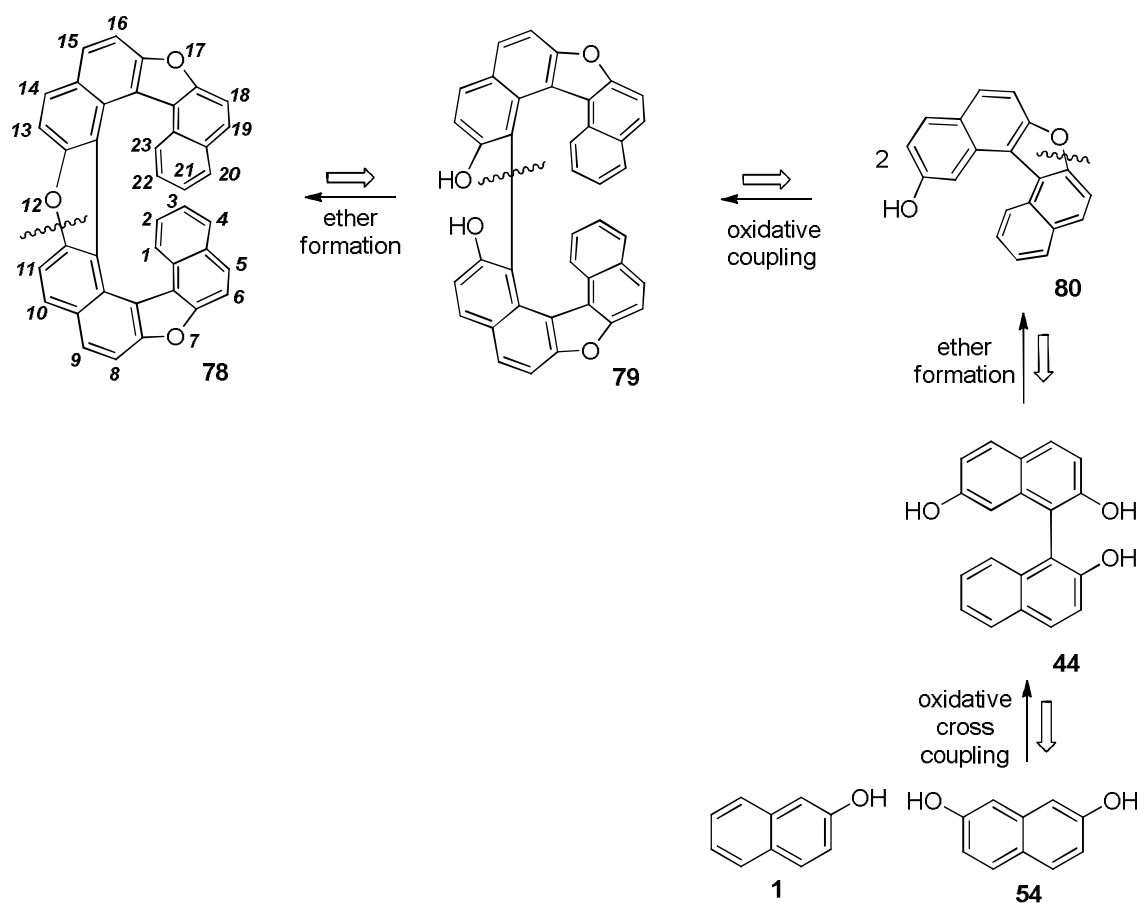
Figure 32: CPL (upper curves) and total luminescence (lower curves) spectra of the (*M*)-**74** (left red), (*P*)-**74** (left black), (*M*)-**75** (right red), and (*P*)-**75** (right black), compounds in 1 mM acetonitrile solutions at 295 K, upon excitation at 357 nm, respectively. The solid lines in the CPL plot are presented to show the luminescence spectral line shape.

3.2.3 Synthesis of helical molecules from atropisomeric binaphthyl derivatives

Screw shaped helical molecules comprising *ortho*-fused aromatic rings acquire a unique shape in order to release the internal strain. Such molecules have been widely studied in recent years due to some unique properties associated to its structure.⁹⁸ Basically there are two types of helical molecules, carbohelicenes and heterohelicenes. Although the early work was more focused on the former class, recently more interesting properties are observed for the latter type of helical molecules which may contain one or different heteroatoms. Polycyclic aromatic oxygen containing molecules, particularly fused furans are expected to provide relatively high HOMO levels⁹⁹ and are known to show interesting utility in electronic devices, as organic light-emitting diodes (OLEDs)¹⁰⁰ or organic field-effect transistors (OFETs).¹⁰¹ Synthesis and study of oligonaphthafurans has also been reported recently¹⁰² where the systematic correlation of the number of naphthafuran units and the physical properties is evaluated. The compounds belonging to the general class of oxahelicenes have been synthesized and their various properties have been studied.¹⁰³ The special properties of helical molecules are attributed to the extended conjugation of the π -electrons in the framework.

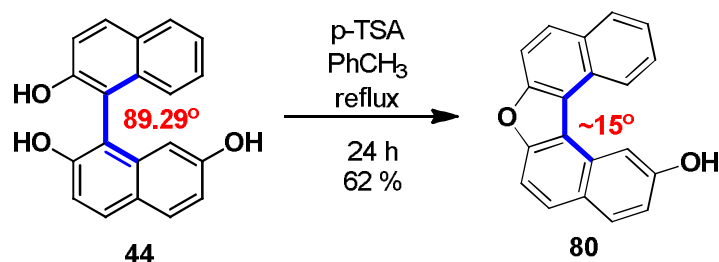
In this section we report the design and synthesis of one such large oxygen containing 7,12,17-trioxa[11]helicene, which is expected to form nearly one and half rotation of a helical twist involving a considerable delocalization of π electrons and also we synthesized small helicene molecules, and attempt their resolution.

The retrosynthesis for the target molecule 7,12,17-trioxa[11]helicene **78** is presented in Scheme 32. The central naphthofuran ring can be built by acid catalyzed ether formation from the corresponding binaphthol structure **79** according to the procedure developed by Thongpanchang.^{6d} The diol **79** can be synthesized by oxidative coupling of 2-hydroxy-7-oxa[5]helicene **80** by standard procedure. The desired molecule **80** can be prepared by acid promoted selective ether formation from 1,1'-binaphthalenyl-2,2',7-triol **44**, which can be obtained by oxidative cross coupling of 2-naphthol **1** and 2,7-dihydroxynaphthalene **54**. Proposed conversion of **80** to **79** by oxidative coupling is expected to be a difficult step, due to the steric considerations.



Scheme 32: Retrosynthesis of 7,12,17-trioxa[11]helicene **78**

The cross coupling of 2-naphthol **1** with **54** furnished triol **44** as discussed in previous section in Scheme 12. The pure sample of triol **44** was subjected to the acid catalyzed ether formation by the standard procedure developed earlier.⁸⁰ The desired product 2-hydroxy-7-oxa[5]helicene **80** was obtained in good yield from the reaction mixture by simple work up and column chromatography over silica gel (Scheme 33). The reaction involving dehydration of **44** is a difficult conversion of a perpendicular structure of binaphthyl framework to more planer oxa[5]helicene **80** unit. The calculated dihedral angle of dinaphthofuran system similar to **44**, was expected to be close to 85,^o which changes to merely about 15^o (in **80**) when such cyclization occurs.^{5a} Due to small dihedral angle the helical isomers of **80** are expected to possess low isomerisation barrier resulting in to fast interconversion.



Scheme 33: Synthesis of 2-hydroxy-7-oxa[5]helicene.

The oxidative homo-coupling of 2-hydroxy-7-oxa[5]helicene **80** may possibly follow four different pathways (Figure 32). Out of these orientations, the modes B, C and D will lead to the steric crowding and hence the coupling is expected to follow the more feasible mode A. The homo-coupling between two molecules of **80** should be the key step in the synthesis of the target molecule. The homo-coupled product **79** (in mode A) will be then subjected to acid catalyzed ether formation to obtain the final compound **78** (Figure 33). The above conversion requires interaction between the two nearly perpendicularly oriented hydroxyl groups and may again pose a considerable challenge.

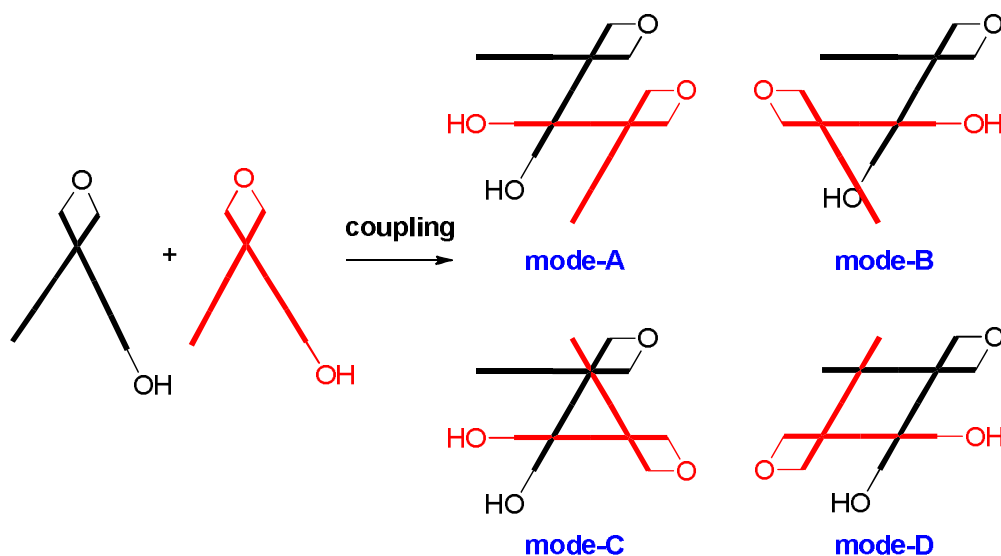


Figure 32: Possible modes of coupling of **80**.

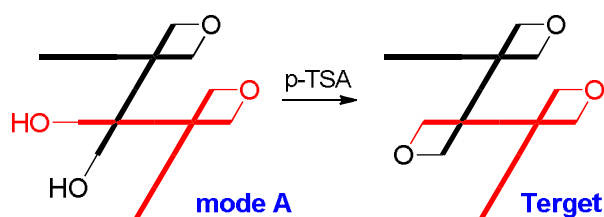
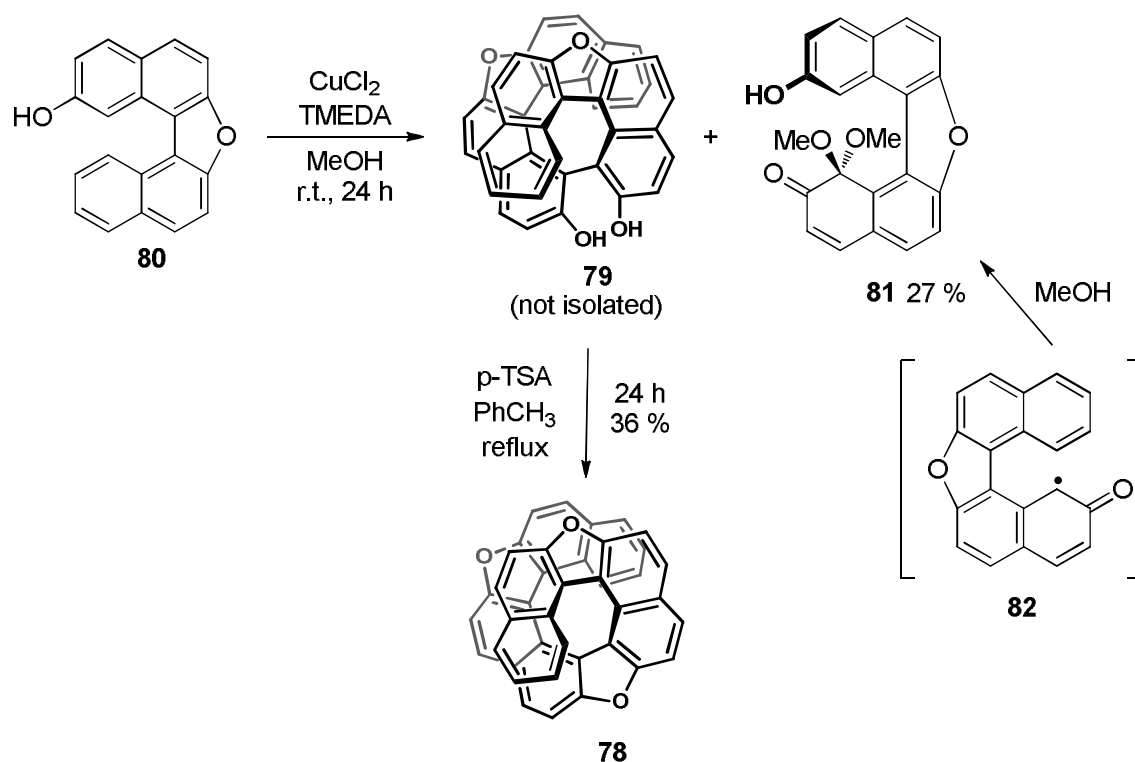


Figure 33: Possible modes of coupling of target **79**.

The homo-coupling of **80** was initially screened with aqueous FeCl₃, however, the reaction resulted in complex products and no significant compounds were isolated. Hence, other routinely used catalyst system of CuCl₂•TMEDA was screened in dry methyl alcohol at room temperature (Scheme 34). The coupling product **79** was found to be difficult to purify on silica gel column. However, another deep orange colored, less polar crystalline compound was isolated from the reaction mixture. The orange colored compound was characterized to be 1,1-dimethoxy-2-oxo-12-hydroxy-7-oxo[5]helicene **81**, isolated in low yield (27%). This unexpected compound was formed in several repeat experiments when performed in methyl alcohol. All the other fractions were collected presumably containing required homo-coupling product **79** and subjected to acid catalyzed ether formation. Repeated attempts to separate and access pure sample of **79** were not successful. The above coupling reaction also failed in other solvents such as ethyl alcohol, 2-propanol or 1,4-dioxane. The cyclization of crude **79** was performed with *p*-TSA in refluxing toluene and the desired oxa-helicene **78** was isolated in moderate yield (36%) as light yellow needles.



Scheme 34: Coupling of 2-hydroxy-7-oxo[5]helicene **80**

The structure of **81** was established by spectral analysis, and confirmed by single crystal X-ray diffraction study.¹⁰⁴ The ¹H NMR of **81** showed only one singlet at δ 3.22 for six

hydrogens of methoxy group, indicating rapid interconversion between the two isomers during the measurement at ambient conditions. The same was observed in ^{13}C NMR when the methoxy carbon showed a single peak at δ 51.87. The α,β -unsaturated ketone system was established by observing the resonance peaks of two doublets in ^1H NMR at δ 6.27 and 9.62. The formation of such an unexpected compound can be attributed to the trapping of a radical intermediate **82** by methyl alcohol during the coupling reaction. Formation of such keto-radical intermediate has been proposed earlier.¹⁰⁵ Such a product **81** was not observed when other alcohols were used as solvents, probably trapping of intermediate **82** was only feasible with smaller methyl alcohol. The structure of **81** was established by single crystal X-ray analysis (Figure 34).¹⁰⁴ The dihedral angle was observed to be 15.4° in this compound, which was crystallized in $Pn2_1$ space group.

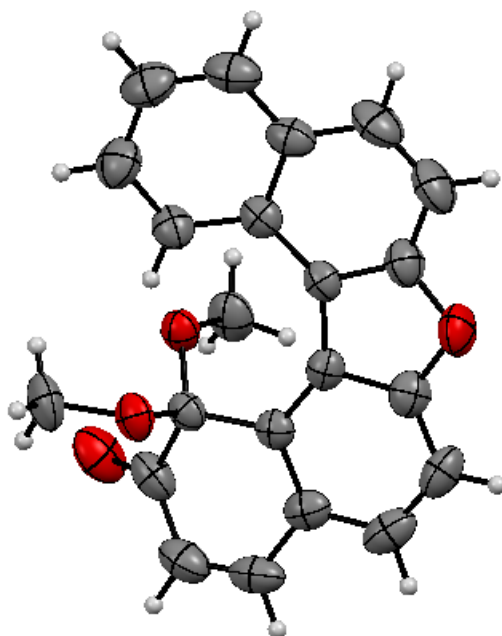


Figure 34: ORTEP diagram of **81** (CCDC999893)

After the less polar compound **81** was isolated the silica gel column, it was quickly eluted with ethyl acetate and the mixture of polar compounds, presumably containing **79**, was collected. The mixture was then subjected to acid catalyzed cyclization with *p*-TSA in refluxing toluene to obtain the desired target compound **78**, purified by careful chromatography over silica gel. The compound **78** was obtained as yellow crystals from ethyl acetate and characterized by spectral techniques and single crystal X-ray diffraction analysis.¹⁰⁴ The ^1H NMR show ten signals indicating the symmetrical nature of the molecule. Hydrogen attached to C2 (and C22) appear as typical triplet type multiplet at δ

6.26 due to the shielding effect of the terminal ring.¹⁰⁶ The proton attached to the next carbon C3 (and C21) appear to have shifted downfield and show similar multiplet at δ 6.95, as it is in the deshielding zone of the terminal ring. All other signals appear as doublets, confirming the symmetrical structure (Figure 35). Similarly ten signals for the aromatic carbons were seen in ^{13}C NMR due to the symmetrical nature, while molecular ion peak was observed at 548 m/z, which is also the base peak.

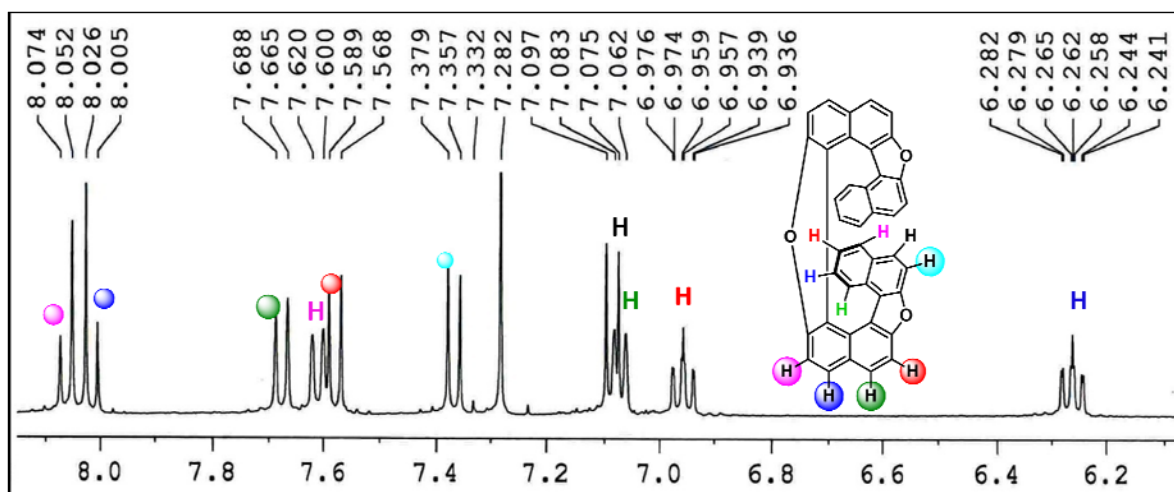


Figure 35: Aromatic region of the ^1H NMR of **78**.

The single crystal X-ray analysis of **78** further established the structure (Figure 36). The compound was crystallized in the $P 2_1/c$ space group; its unit cell consists of two molecules one in '*P*' conformation and the other in '*M*' conformation (Figure 37). This indicates the absence of any spontaneous resolution, a phenomenon occasionally observed in some helical molecules during crystallization.¹⁰⁷ The shape of the molecule is quite large, viewed from the side looks like a 'Z' shape, the diagonal length is about 10.1 Å, the width is about 9.9 Å, while the intramolecular pitch of the outer helicene is about 4.8 Å (Figure 36). The interplaner angle in **78** was found to be 24.37° and agrees well in the established observation for larger helicenes where it tends to decrease for elongated structures.¹⁰⁸ The torsional angle between the inner carbon atoms of **78** was found to be 4.39° (C23-C23a-C23b-C23c), 10.95° (C23a-C23b-C23c-23Cd), 23.71° (C23b-C23c-C23d-C23e), 19.30° (C23c-C23d-C23e-C23f) and 2.66° (C23d-C23e-C23f-C23g) suggesting different degree of distortion in the aromatic rings. As a consequence of torsional strain generated due to the helical shape the bond lengths in the skeleton are different. In comparison of the standard bond length of benzene (1.393 Å),¹⁰⁹ the range of carbon-carbon bond lengths of the inner helix was observed to be 1.429 - 1.437 Å, while

the same on the outer periphery was shorter as seen in the range of 1.347 - 1.360 Å. It was also interesting to see difference between the bond lengths of the two fused furan rings. The bond length of the side furan rings C23b-C23c (and C23h-C23i) was 1.461 Å, while the same for inside furan ring C23e-C23f was found to be slightly elongated to be 1.471 Å, clearly due to much greater strain exerted in the central section.

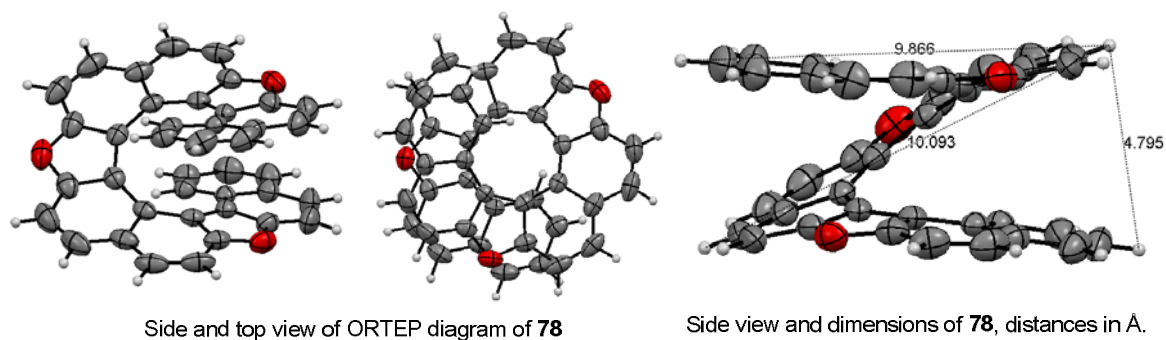


Figure 36: Stereoview of compound **78** (CCDC 999892)

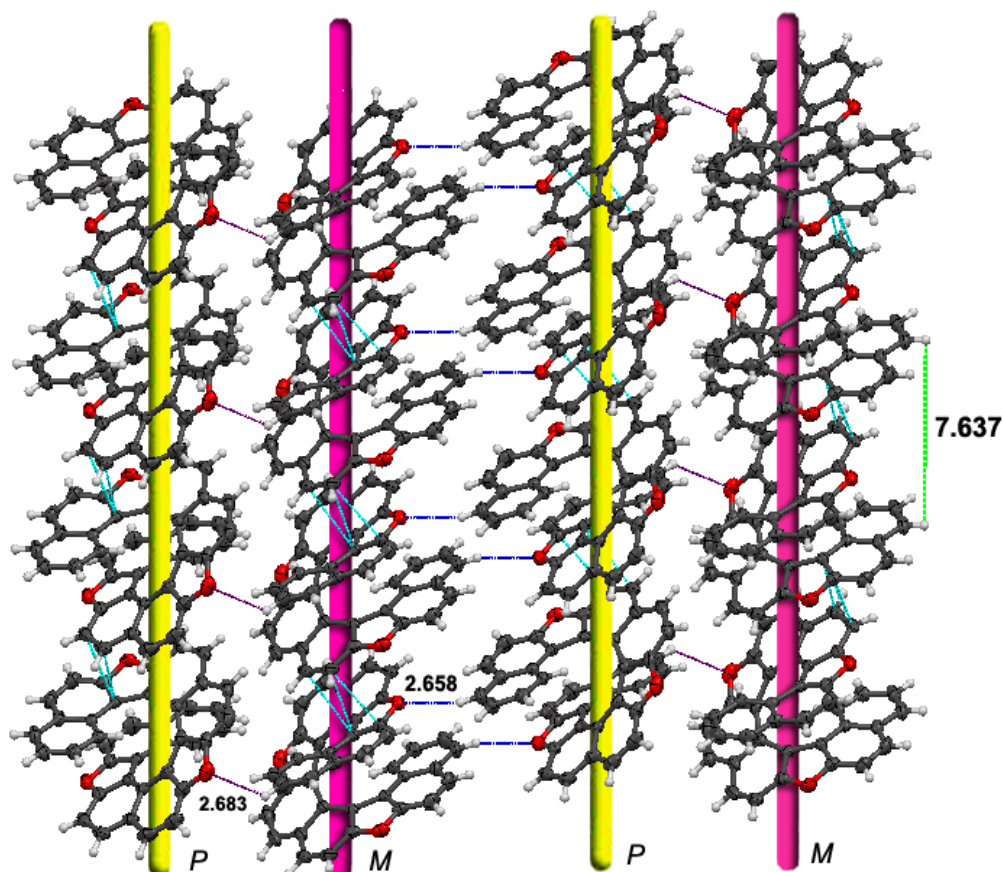


Figure 37: Stacking of **78** in the crystal, with a helical pitch of 7.637 Å. The rods represent the position of helical axis, yellow for '*P*' and purple for '*M*' isomer

The optical and thermal properties of highly conjugated helicene **78** were measured. The UV-Vis and fluorescence spectra indicated an absorption maxima at 352 nm and emission at 432 nm, with a shoulder peak at 450 nm (Figure 38), indicating Stokes shift of 80 nm. The observed λ_{em} values and the nature of the peaks are in the range observed for similar oligonaphthofurans (364–486 nm).¹¹⁰ The fluorescence quantum yield (Φ) of **78** was observed to be 0.191, as determined using a standard solution of quinine sulfate (0.1 M H₂SO₄, measured at an excitation wavelength of 350 nm).

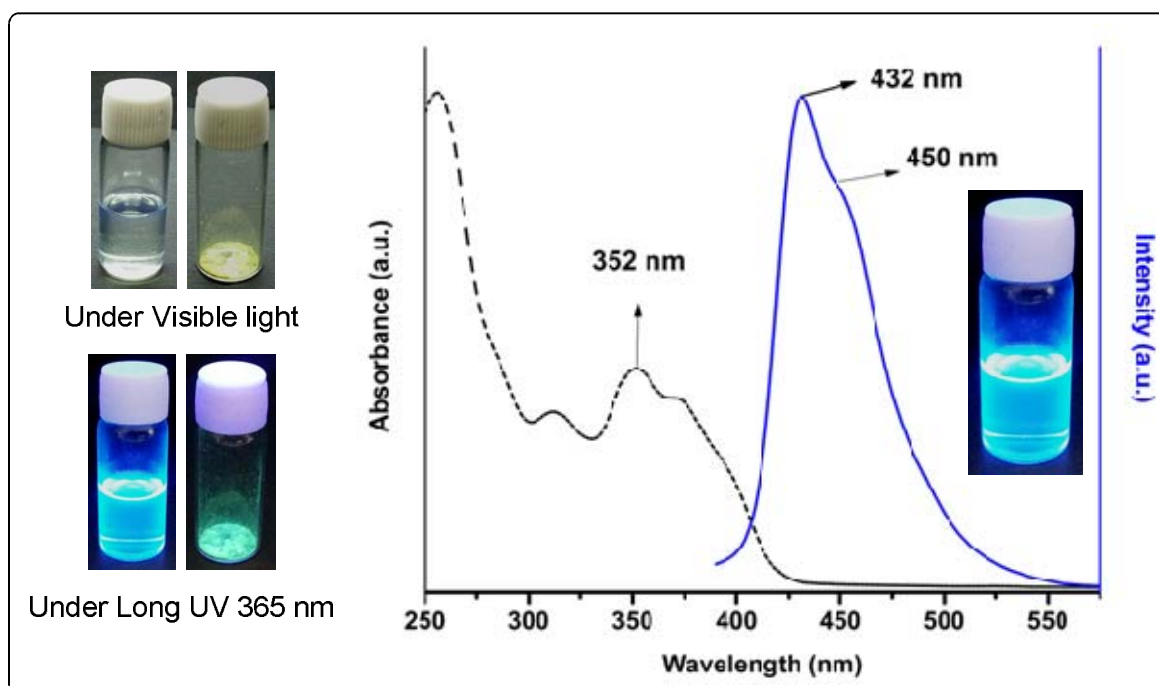


Figure 38: UV-Vis and fluorescence spectra of **78**

Thermal behavior of **78** was investigated by differential scanning calorimetry (DSC) where the sample was heated at 10 °C/min from 35 to 385 °C under inert atmosphere (Figure 39). Analysis indicated the melting point 345.5 °C and the glass transition temperature (T_g) at 245.5 °C, indicating the high thermal stability, expected of such helicenes.^{111, 112}

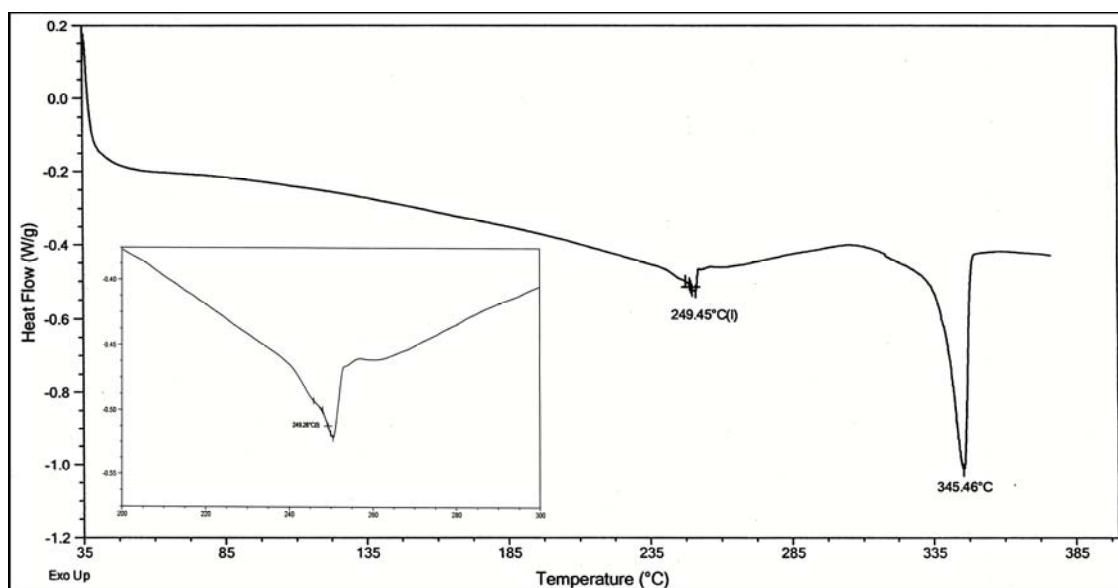


Figure 39: DSC thermogram of 7, 12, 17-trioxa[11]helicene **78** flow rate 10°C/min to 385°C

The HPLC analysis of **78** on Chiralpak IC column showed presence of well resolved peaks at 11.15 and 12.95 mins (10 % hexane in isopropanol; 0.5 mL/min.) indicating the two helical isomers (Figure 40).

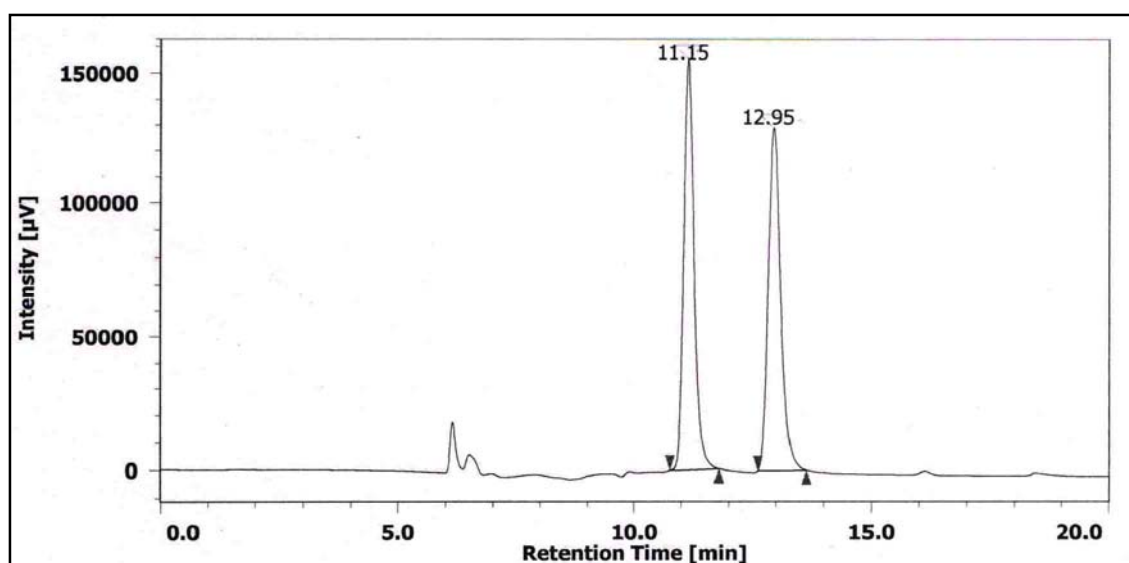


Figure 40: HPLC analysis for 7,12,17-trioxa[11]helicene **78**

After success of large helicene molecule **78**, we focused on the synthesis of hetero atom (N, O, S) containing helical molecules and its resolution. Introduction of hetero atoms revealed that they are especially beneficial to the electronic, optical, or photorefractive properties of the heterohelicene-based material.¹¹³ Although considerable attention has been devoted to the thia-helicenes,¹¹⁴ the azahelicenes¹¹⁵ and compared aza- and thia-

helicenes, the oxa-helicenes are less explored (Figure 41). Oxa-helicene can be classified as oxygen-containing heteroaromatic system with a unique structure. Despite its helical structure, the molecule does not exhibit optical activity probably due to the rapid racemization at ambient temperature.

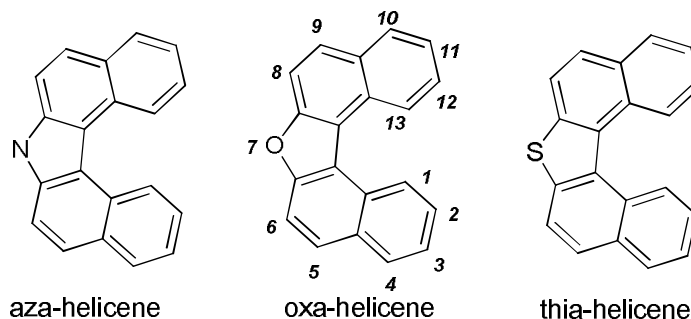
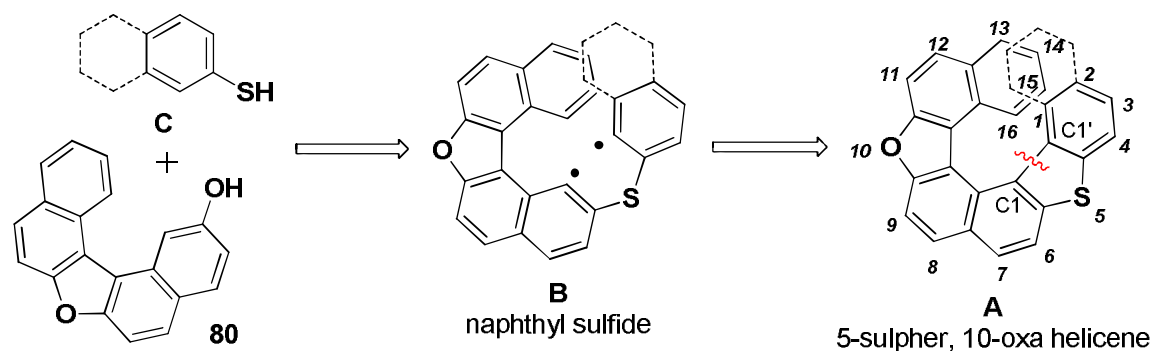


Figure 41: Examples of hetero[5]helicenes

Interestingly, Thongpanchang reported the synthesis of dinaphthothiophene by the oxidative photocyclization of dinaphthyl sulphide.¹¹⁶ It was envisioned that such an approach could be applied for the direct synthesis of our target 5-thia-10-oxa helicene **A**.

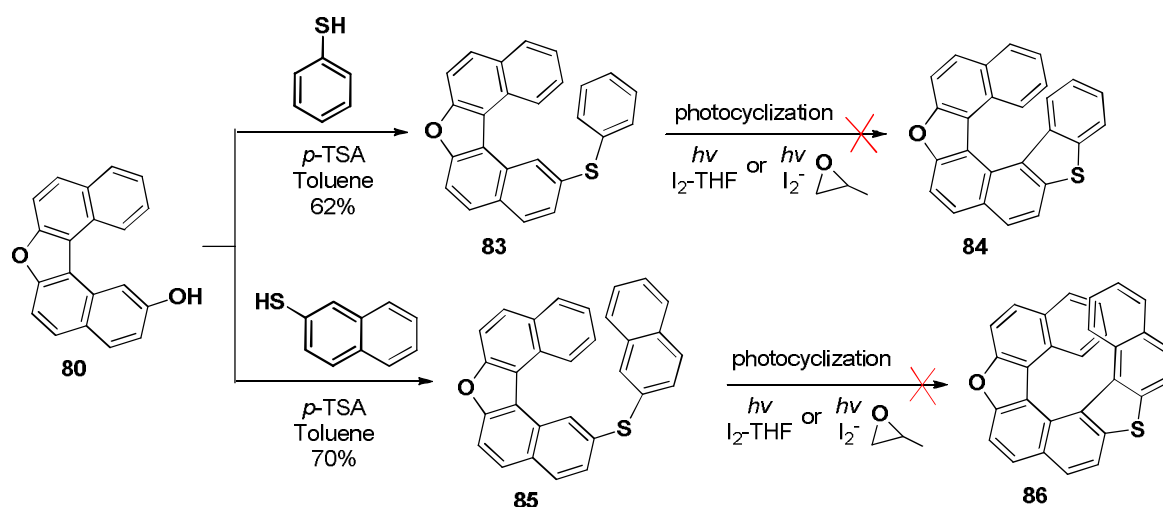
Retrosynthetic disconnection at the C1–C1' bond of 5-thia-10-oxa helicene **A** suggests that the precursor for photochemical reaction could be naphthyl sulfide **B** which could be derived straight forwardly from the acid-mediated nucleophilic aromatic substitution between 2-hydroxy-7-oxa[5]helicene **80** and benzenethiol or 2-naphthalene thiol **C** (Scheme 35).



Scheme 35

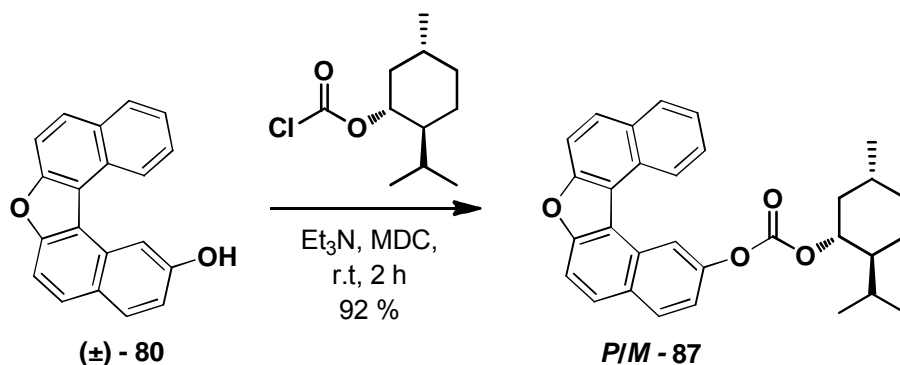
The reaction of 2-hydroxy-7-oxa[5]helicene **80** and 2- benzenethiol was thus carried out in the presence of *p*-TsOH in refluxing toluene for 2 h to provide the desired naphthyl sulfide **88** in 62 % yield. The sulfide was then subjected to oxidative photocyclization in the presence of I₂-THF or I₂ and propylene oxide (Scheme 36). In both cases formation product **89** not detected, as the starting material was recovered. Similar reaction was

carried out with 2-naphthalenethiol furnished **90** 70% yield (Scheme 36), which upon oxidative photocyclization did not yield **91** in the both case and starting material was recovered.



Scheme 36

Focus was then shifted on resolution of 2-hydroxy-7-oxa[5]helicene **80**, which showed a single peak on chiral stationary phase HPLC at room temperature. The possible enantiomers of **80** could not be separated from the rapidly interconverting unresolvable helical structures owing to ineffective overlap of the terminal rings, due to small dihedral angle the helical framework of oxa[5]helicene. In order to effect a change the dihedral angle and possibly increasing the barrier of isomerization we envisioned to prepare its carbonate derivative with optically active (-)-menthyl chloroformate. This derivative may provide an opportunity to resolve the isomers of this helical molecule. Accordingly the compound **80** was treated with the (1*R*,2*S*,5*R*)-(-)-menthyl chloroformate in the presence of triethylamine at room temperature to afford the diastereomeric carbonate **87** in good yield (Scheme 37).



Scheme 37: Preparation of (-)-menthyl carbonate of 2-hydroxy-7-oxa[5]helicene

The diastereomers of carbonate **87** could not be isolated by careful column chromatography and several crystallizations. This was further confirmed when a racemic sample of **80** was obtained after the removal of the carbonate auxiliary using standard conditions (aqueous KOH/MeOH, r.t.).

The compound **87** was characterized by ^1H NMR spectroscopy for further structural information (Figure 42). In this spectrum, the terminal aromatic protons (C11H and C12H) were observed as multiplet at δ 7.78 and 7.62 ppm, respectively, and the signal of C1H gave a doublet at δ 9.04 with a *meta* coupling with C3H proton ($J = 2.4$ Hz). Comparison of C1H proton for compounds **80** (δ 8.51) and **87** (δ 9.04), indicated an up field shift in **87**. The hydrogen of C3H appeared as a doublet of doublet in **7** (δ 7.20), which shifted down field in **87** (δ 7.44). This splitting is due to its coupling with *ortho* C4H proton and *meta* C1H ($J = 8.8$ and 2.4 Hz). Interestingly the inside C13H proton showed doublet at most down field region δ 9.12 for **7** and δ 9.15 for **87**, indicating its position in the ring current of the other aromatic ring, rather than below as usually seen in case of helical molecules.

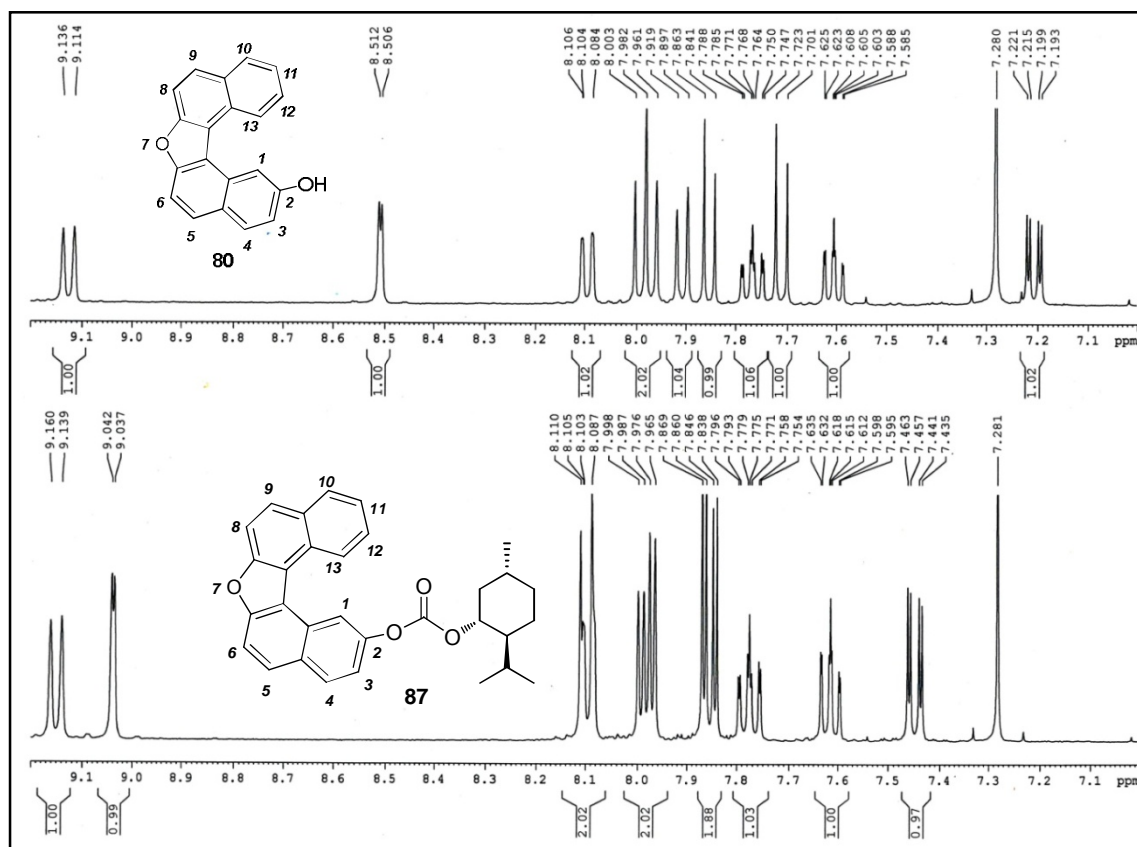


Figure 42: ^1H NMR of compound **80** and **87** in CDCl_3

To analyse the helical structure of **87**, a suitable single crystal of **87** was developed by the slow evaporation from hexane solution. Compound **87** crystallizes in the monoclinic chiral space group $P2_1$ with the asymmetric unit composed of two heterochiral helical molecules P -**87** and M -**87** in crystal packing in the solid state.¹¹⁷ Select bond lengths, distances of non-bonded atoms, and torsion angles are presented in Table 5. Some of the bonds of the outer side C-C bonds were of the order of 1.315 - 1.371 Å, slightly shorter compared to the average bond of benzene (1.39 Å). For helicene structure, as expected the inside bond lengths were found to be bit elongated in the range of 1.394 - 1.470 Å (Figure 43).

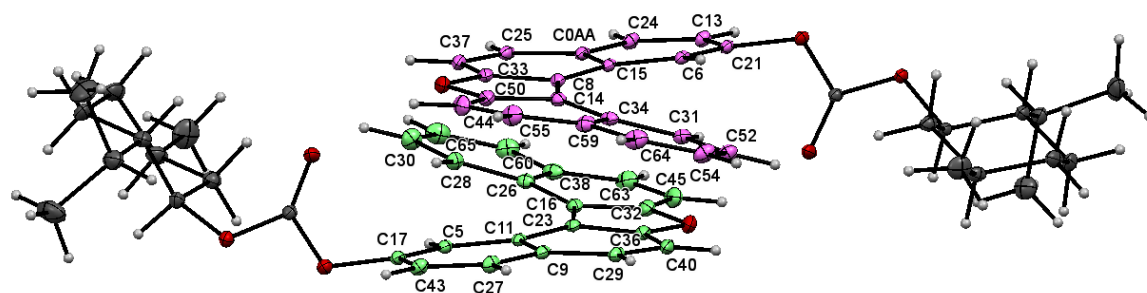


Figure 43 ORTEP diagram of **87** (CCDC1019988)

Table 5: Structural parameters of 7 oxa [5]helicene **87**

<i>P</i> -Helix		<i>M</i> - Helix	
C–C bonds at inner helix (Å)	C–C bonds at outer helix (Å)	C–C bonds at inner helix (Å)	C–C bonds at outer helix (Å)
C5-C11 (1.394)	C43-C27 (1.365)	C6-C15 (1.414)	C13-C24 (1.371)
C11-C23 (1.432)	C29-C40 (1.348)	C15-C8 (1.441)	C25-C37 (1.372)
C23-C16 (1.470)		C8-C14 (1.464)	
C16-C26 (1.428)	C45-C63 (1.358)	C14-C34 (1.427)	C44-C55 (1.315)
C26-C28 (1.424)	C60-C65 (1.334)	C34-C31 (1.399)	C64-C54 (1.353)
Average 1.429	1.351	1.429	1.353
Torsion angle (°) (<i>P</i>)		Torsion angle (°) (<i>M</i>)	
C5-C11-C23-C16 (ϕ_1)	9.27	C6-C15-C8-C14 (ϕ_1)	6.97
C11-C23-C16-C26 (ϕ_2)	12.02	C15-C8-C14-C34 (ϕ_2)	9.00
C23-C16-C26-C28 (ϕ_3)	7.39	C8-C14-C34-C31 (ϕ_3)	10.84
$\phi_1+\phi_2+\phi_3$	28.68	$\phi_1+\phi_2+\phi_3$	26.81

The internuclear distance between the C1 and C13 carbon atoms for (*P*) helical is 3.312 Å, and for (*M*) is 3.341 Å which is just adequate to accommodate two aryl C–H bonds (for (*P*) 0.929 Å, for (*M*) 0.931 Å) in the same plane, as seen in the space-filling model (Figure 44). This distance confirms that there is slight steric repulsion between the hydrogen atoms attached to the C1 and C13 carbon atoms, which thus offers a very low energy to the racemization barrier. Molecule **87** exists in dynamic equilibrium at room temperature in solution, and therefore the helical conformers are not separable.

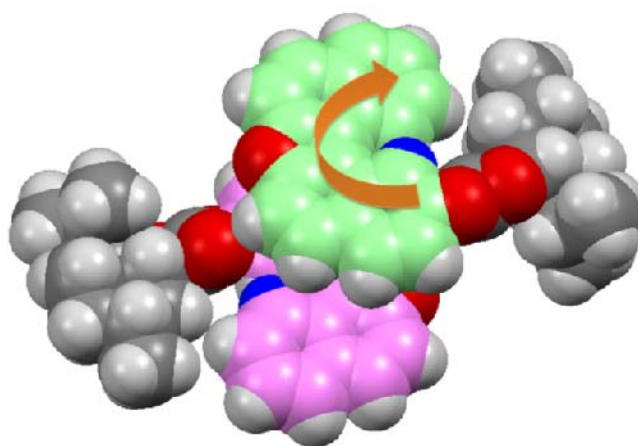


Figure 44: Space filling model representation of Single X-ray structure of **87**, light green (*P*), violet (*M*) (The close proximity and overlap of hydrogens at C-1 and C-13 positions, Hydrogen in blue colour)

The crystal lattice of compound **87** also shows there are no hydrogen bonds. All present short-range contacts are intermolecular (Figure 45). The majority of the short-range contacts are formed between oxa[5]helicene moieties of compound **87** in addition the menthyl carbonate keto oxygen contacts with oxa[5]helicene moiety hydrogen. The short-range interactions appeared in between *P* and *M* isomer at C8–C9 and C0AA–C23 short-range interactions 3.383 Å and 3.370 Å respectively, and O-H40, O19-H37 short-range interactions 2.602, 2.701 respectively. The dihedral angle of the binaphthyl unit is 19.93 and 17.93° and its absolute configuration was found to be *P* and *M* respectively, unambiguously through relation with the absolute configuration of (1*R*,2*S*,5*R*)-(-)-menthyl chloroformate. The molecular complex network between (*P*) and (*M*) can be described as infinite chains of interlinked species, which are associated in an alternating manner through short contacts (Figure 46).

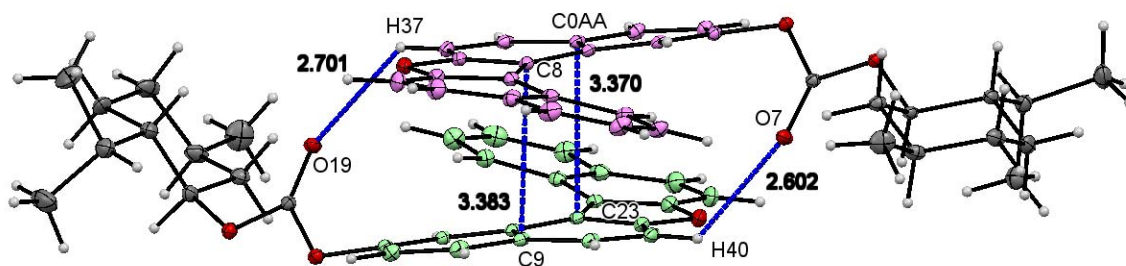


Figure 45: Short range contacts in crystal lattice of compound **87**.

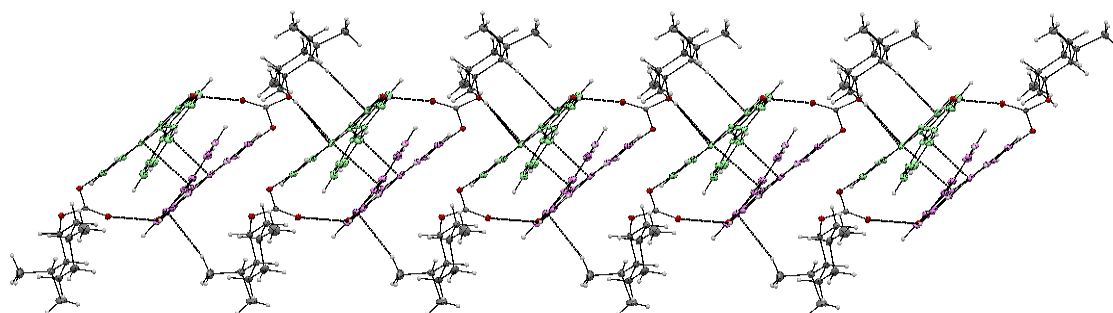


Figure 46: Short range contacts network between (*P*)-**87** and (*M*)-**87** can be described as infinite chains of interlinked species.

Thermal behavior of oxa[5]helicenes was investigated by means of differential scanning calorimetry (DSC) where the sample was heated at the rate of 10 °C/min from 25 to 300 °C, under the inert atmosphere of nitrogen. The analysis indicated the melting point of compound **80** to be 209 °C, and compound **87** 104 °C.

Thus in this work we have discussed the structure of (-)-menthyl carbonate derivative of 2-hydroxy oxa[5]helicene and explained its inability to show stable, separable helical conformations. The two units show small difference in the structural parameters probably due to the effects created by the diastereomeric pairs.

Therefore, in order to increase the crowding at inner helix of the oxa-helicene structures, which will be capable of exhibiting the structural twist and showing the helical isomers. With this aim synthesis of a list of oxa[5]helicene with a possibility of existing helical shape is attempted.

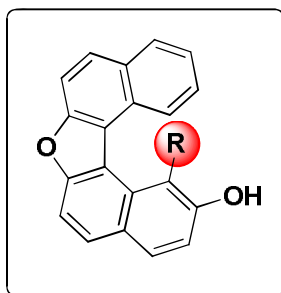
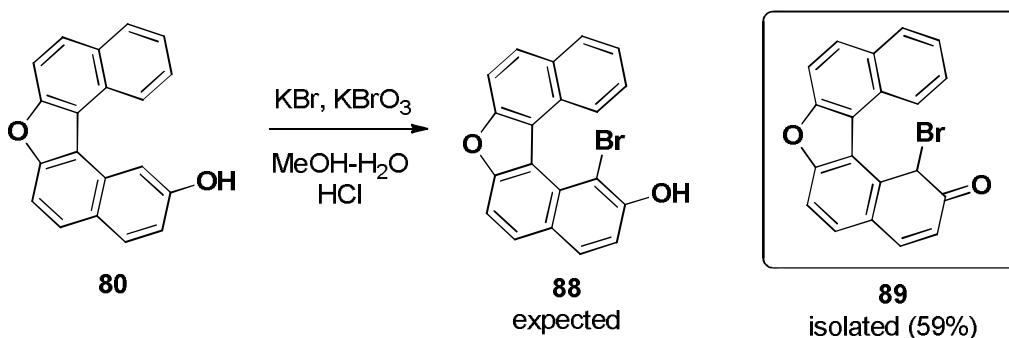


Figure 47

Structures of **80** will have a possibility to introduce an electrophile at the C-1 position, which will be inside the helical shape. Because of the introduction of the different substituent at the C-1 position of the **80** the required steric interaction will be achieved.

In order to increase the crowding at inner helix (C1 position) of compound **80** by bromination or nitration reactions have been carried out. The first attempt to introduce a substituent at C-1 position was done by bromination of the compound **80**. Reaction of **80** with KBr and KBrO₃ in presence of HCl-H₂O in methanol at room temperature for 18 h furnished the unexpected product **89** with 59% yield (Scheme 38). The isolated product **89** was characterized by single crystal analysis and spectroscopic methods.



Scheme 38

The structure of **89** was established by spectral analysis, and confirmed by single crystal X-ray diffraction study.¹¹⁵ The ¹H NMR of **89** showed only one singlet at δ 6.44 for CHBr hydrogen, indicating rapid interconversion between the two isomers during the measurement at ambient conditions. The α,β -unsaturated ketone system was established by observing the resonance peaks of two doublets in ¹H NMR at δ 6.37 and 9.09. The formation of such an unexpected compound can be attributed to the trapping of a radical intermediate at C1 position by bromine radical during the coupling reaction. Formation of such keto-radical intermediate has been proposed earlier.¹⁰⁵

The structure of **89** was established by single crystal X-ray analysis (Figure 48).¹¹⁵ CCDC The dihedral angle was observed to be 23.18° in this compound, which was crystallized in P 2₁/n space group.

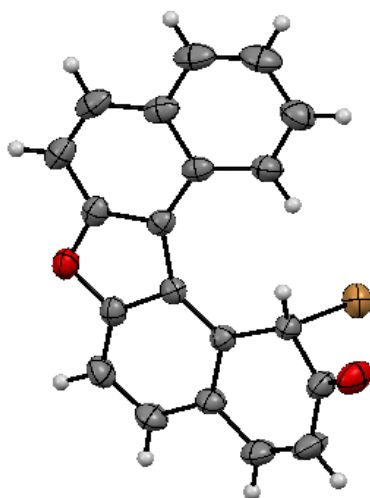
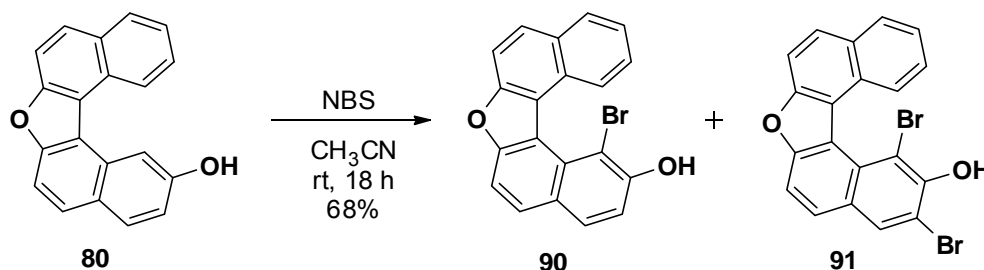


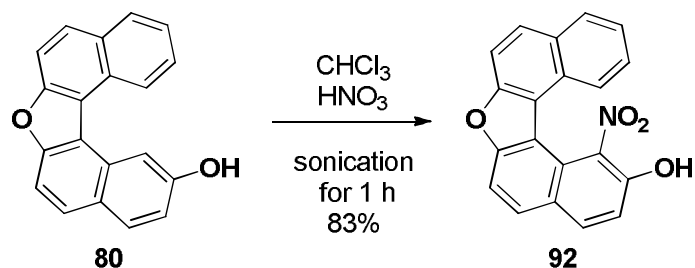
Figure 48 ORTEP diagram of **89** (CCDC1424317)

Since our attempts did not succeed, another strategy was followed for introducing the bromine atom at inner helix position by N-bromosuccinimide (NBS). Compound **80** was reacted with NBS in acetonitrile to give a mixture of mono and di brominated derivative **90** and **91** with 68% yield (Scheme 39). In proton NMR clearly showed 92:8 ratios respectively.



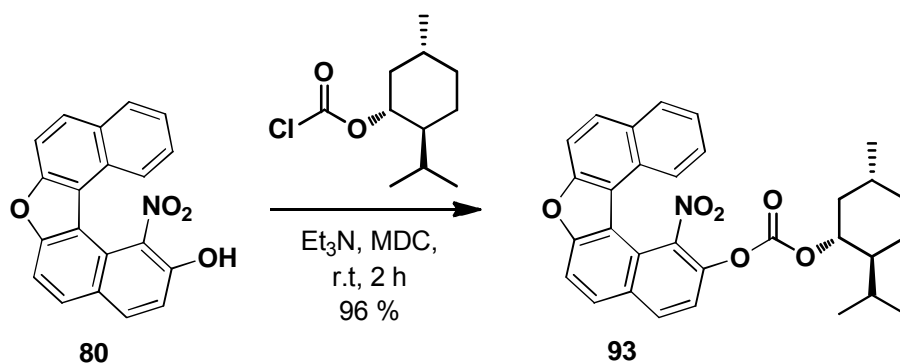
Scheme 39

Next we carried out nitration of compound **80** with concentrated HNO₃ by sonication for 2 h furnished **92** with 83% yield (Scheme 40). The structure of **92** was established by spectral analysis. The ¹H NMR of **92** showed disappearance of C1-H. The high resolution mass spectrum of **92** showed the molecular mass of the product and its isotope pattern were consistent with the calculated value for C₂₀H₁₁NO₄ [M+Na]⁺ 352.0586, found 352.0576 *m/z*.



Scheme 40

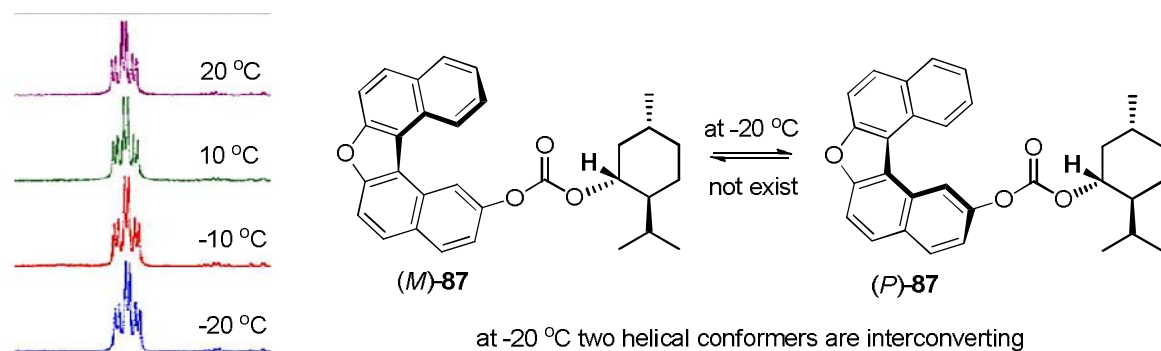
Then we attempted resolution of **92** with treatment of (1*R*,2*S*,5*R*)-(-)-menthyl chloroformate in the presence of triethylamine at room temperature in 96 % yield (Scheme 41). The enantiomers (*P/M*) of helicanyl carbonate **93** could not be isolated on column chromatography, or even with crystallizations.



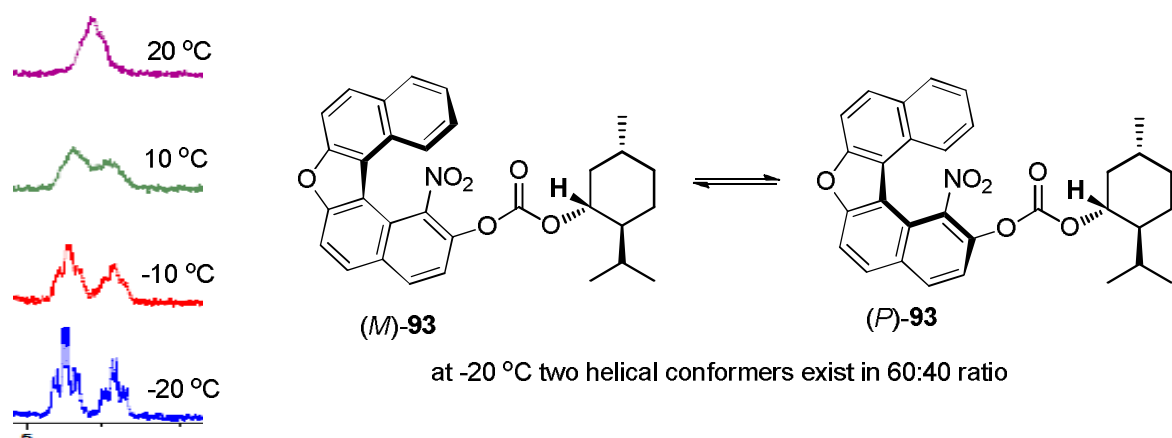
Scheme 41

Finally we performed HPLC analysis of **92** and **93** on chiral columns such as Chiralcel OD-H, Chiralpak IC, Chiralpak IE, Lux 5u Amylase-2 and Chiral Amide-1. In all these case separation of helical conformers were not detected, at ambient temperature.

However, we were able to study the dynamic behaviour of this molecule by recording its low temperature H-NMR spectra. The low temperature ¹H NMR analysis (-20 °C) of both compounds showed interesting results, establishing the presence of helical conformers on introduction of nitro group inside the helical cavity. Compound **87** showed no helical isomerism upto -20 °C (Scheme 42), but significantly compound **93** showed helical twist and forms helical conformers (*P*)-**93** or (*M*)-**93** with 60:40 ratio (Scheme 43). We believe the presence of nitro group at the C1 position created sufficient twist to show two diastereomers at the NMR scale at -20 °C, confirming the helical conformation.



Scheme 42: Low temperature ^1H NMR study of **87**



Scheme 42: Low temperature ^1H NMR study of **93**

At this stage we are unable to establish the helical isomers at ambient conditions, as well as the chiral description of the major isomer, but the results are encouraging for further research in this area.

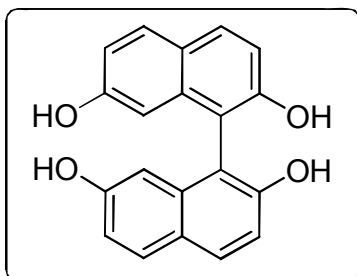
3.3 Conclusion

In this chapter we have described the preparation and resolution of triol, tertol by making its complex via diastereomeric salt formation. The configuration of resolved compounds was established by single crystal X-ray analysis. We present our efforts to synthesize optically pure helicene like mono-oxazines from chiral starting material. All the compounds were fully characterized and their optical properties were measured. We present our efforts to synthesize optically pure helicene like bis-oxazines from optically pure atropisomeric molecules. In effect we have converted axial chirality to helicene like chirality. We have fully characterized all the compounds and measured their optical properties. We have resorted to study the circularly polarized luminescence (CPL), the emission analogue to CD, to further investigate the influence of the helicene like structure on the chiroptical properties.

In particular we have succeeded to synthesised 7,12,17-trioxa[11]-helicene, a large helical molecule from 7-oxa-[5]-helicene, and characterized by NMR, HRMS, UV, fluorescent, HPLC and single crystal X-ray analysis. We achieved to synthesis of helical twisting of oxa[5]helicene by introducing nitro (-NO₂) group at inner helix, and its clearly showed helical isomers (*P* and *M*) on NMR time scale at low temperature (-20 °C).

3.4 Experimental Procedures

7,7'-dihydroxy-2,2'-binaphthol (41)



A solution of $\text{FeCl}_3 \cdot 6\text{H}_2\text{O}$ (24.290 g, 89.8 mmol) in water (200 mL) was added drop wise for 1 h at 100 °C to the solution of 2,7-dihydroxynaphthalene (12.00 g, 74.90 mmol) in 500 mL of water. After the addition the reaction mixture was refluxed for 24 h and then cooled to room temperature and extracted with ethyl acetate (2 x 500 mL)

the solvent was dried over sodium sulphate and concentrated under reduced pressure to obtain the crude black mass. Purification of compound by column chromatography on silica gel using gradient petroleum ether: ethyl acetate (100:00 to 80:20) as eluent to obtained an off white solid (10.10 g, 85%).

$^1\text{H NMR}$ (400 MHz, CDCl_3): δ 7.89 (d, $J = 8.8$ Hz, 2H), 7.80 (d, $J = 8.8$ Hz, 2H), 7.22 (d, $J = 9.2$ Hz, 2H), 6.99 (dd, $J = 2.4, 8.8$ Hz, 2H), 6.45 (d, $J = 2.4$ Hz, 2H), 5.11 (s, 2H for -OH group).

MS (EI): m/z , (%) 319 (22), 318 (100), 301 (09), 300 (38), 289 (07), 281 (06), 273 (11), 271 (09), 226 (06), 215 (08), 213 (11), 202 (07), 189 (06), 160 (07), 150 (10), 131 (09), 113 (16), 106 (12).

7,7'-dimethoxy-[1,1'-binaphthalene]-2,2'-diol (42)

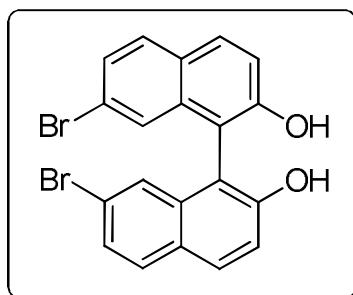
Compound **42** was prepared from 7-methoxynaphthalen-2-ol by same procedure as that of **41**.

M.p. 148-149 °C (Lit.⁴⁸ 144-146 °C).

$^1\text{H NMR}$ (400 MHz, CDCl_3): δ 7.90 (d, $J = 8.8$ Hz, 2H), 7.81 (d, $J = 8.8$ Hz, 2H), 7.24 (d, $J = 8.8$ Hz, 2H), 7.06 (dd, $J = 2.8, 9.2$ Hz, 2H), 6.50 (d, $J = 2.4$ Hz, 2H), 5.09 (s, 2H for -OH), 3.60 (s, 6H).

$^{13}\text{C NMR}$ (100.6 MHz, CDCl_3): δ 159.08 (Cq), 153.33 (Cq), 134.70 (Cq), 131.14 (CH), 130.02 (CH), 124.77 (Cq), 116.04 (CH), 115.11 (CH), 110.05 (Cq), 103.10 (CH), 55.16 (-OCH₃).

7,7'-dibromo-[1,1'-binaphthalene]-2,2'-diol (**43**)



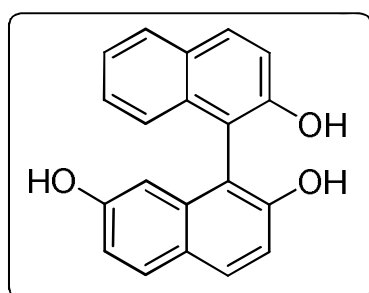
A solution of Cu(OH)Cl.TMEDA (6.24 g, 26.91 mmol) and 7-bromonaphthalen-2-ol (5.0 g, 22.42 mmol) in MeOH (25 mL) under a nitrogen atmosphere. After the solution had been purged with nitrogen for 5 min, and the mixture was stirred at room temperature for 24 h under nitrogen. The reaction mixture was poured into the mixed solvent of 1 M hydrochloric acid solution and ethyl acetate. The organic layer was separated, washed successively with water and brine, and dried over sodium sulfate, and the solvent was evaporated to give a residue. The residue was purified by column chromatography on silica gel using light petroleum ether:ethyl acetate (100:0 to 80:20) as eluent to obtain an orange solid **43** (9.20 g, 92%).

M.p. 194-196 °C.

¹H NMR (CDCl₃, 400 MHz) δ 7.98 (d, *J* = 9.2 Hz, 2H, ArH), 7.79 (d, *J* = 8.8 Hz, 2H, ArH), 7.59 (d, *J* = 8.8 & 2 Hz, 2H, ArH), 7.41 (d, *J* = 9.2 Hz, 2H, ArH), 7.27 (d, *J* = 8.4 Hz, 2H, ArH), 5.11 (s, 2H, OH).

MS (EI): *m/z*, (%) 446 (40), 445 (63), 444 (93), 443 (66), 442 (42), 441 (93), 284 (36), 283 (35), 256 (44), 255 (100).

[1,1'-binaphthalene]-2,2',7-triol (**44**)



A solution of FeCl₃·6H₂O (42.18 g, 156.08 mmol) in 200 mL water was added drop wise for 1 h at 100 °C to the solution of 2,7-dihydroxynaphthalene **54** (10 g, 62.43 mmol) and 2-naphthalene **1** (13.5 g, 93.65 mmol) in 500 mL of water. After the addition the reaction mixture was refluxed for 24 h, completion of the reaction the 2, 7-dihydroxynaphthalene reaction mixture was cooled to room temperature and extracted with ethyl acetate (2 X 500 mL) the solvent dried over sodium sulphate and concentrated under reduced pressure to obtain the crude black mass. Purification of compound by column chromatography on silica gel using gradient petroleum ether: ethyl acetate 100:00 to 70:30 as eluent to obtain binaphthol derivatives. Yield of **44** & **2** was calculated based on **1** and yield of **44** & **41** was calculated based on **54**.

2-Naphthalol (**1**): Yield = 3.20 g, 24% (recovered).

Binol (**2**): Yield = 3.60 g, 34% (M.p. = 216-218 °C).

Tetrol (**41**): Yield = 5.11 g, 51% (M.p. = 122-124 °C).

Triol (**44**): Yield = 7.15 g, 38% (M.p. = 172-174 °C).

¹H NMR (CDCl₃, 400 MHz) δ 7.96 (d, *J* = 9.2 Hz, 1H), 7.91-7.87 (d, *J* = 8.4 Hz, 2H merged), 7.78 (d, *J* = 8.8 Hz, 1H), 7.42-7.39 (m, 1H), 7.37 (d, *J* = 9.2 Hz, 1H), 7.34-7.28 (m, 1H), 7.22 (d, *J* = 8.8 Hz, 1H), 7.18 (d, *J* = 8.4 Hz, 1H), 6.97 (dd, *J* = 8.8, 2.4 Hz, 1H), 6.41 (d, *J* = 2.4 Hz, 1H), 5.13 (s, 1H), 5.05 (s, 1H), 4.83 (s, 1H).

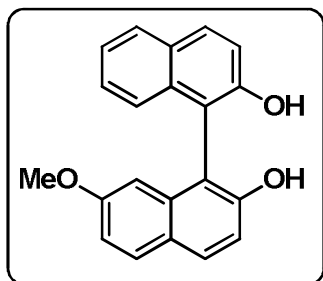
¹³C NMR (CDCl₃, 100.6 MHz): δ 154.9, 153.5, 152.7, 134.9, 133.3, 131.5, 131.3, 130.5, 129.5, 128.4, 127.6, 124.8, 124.2, 124.1, 117.7, 115.6, 115.3, 110.9, 109.4, 106.4.

IR (KBr): ν 3492 (OH), 3391 (OH), 1620, 1593, 1560, 1470, 1216, 1150, 838, 820.

Mass (EI) *m/z*, (%): 301.88 (100) and (ESI) [M+1] 303.4.

HRMS (ESI⁺) calcd for C₂₀H₁₄O₃ (M + 1)⁺ 303.1012, found 303.1022.

7-methoxy-[1,1'-binaphthalene]-2,2'-diol (**45**)



To a solution of triol (0.25 g, 0.83 mmol) in MeOH (10 mL) was added concentrated H₂SO₄ (0.04 mL, 0.83 mmol). The reaction mixture was allowed to gently reflux for 3 days. After quenching with saturated potassium carbonate solution, the crude product was extracted with ethyl acetate. The crude product was purified by column chromatography over silica

gel using light petroleum ether/ethyl acetate as eluent (100:00 to 90:20) furnishing a white solid (0.19 g, 74%).

M.p. 90-92 °C.

¹H NMR (CDCl₃, 400 MHz): δ 8.01-7.98 (d, *J* = 8.8 Hz, 1H), 7.93-7.90 (d, *J* = 8.8 Hz, 2H), 7.82-7.80 (d, *J* = 8.8 Hz, 1H), 7.42-7.40 (d, *J* = 8.8 Hz, 1H), 7.39-7.33 (m, 2H), 7.26-7.24 (d, *J* = 8.8 Hz, 1H), 7.23-7.21 (d, *J* = 8.8 Hz, 1H), 7.06-7.04 (dd, *J* = 2.8 & 8.8 Hz, 1H), 6.46-6.45 (d, *J* = 2.8 Hz, 1H), 3.57 (s, 3H).

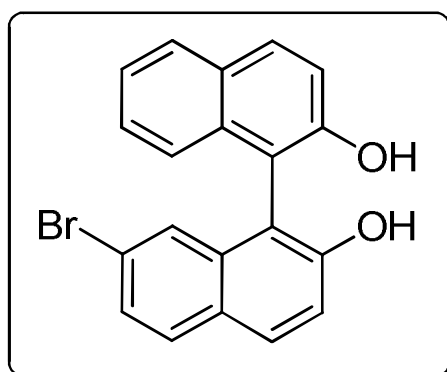
^{13}C NMR (CDCl_3 , 100.6 MHz): δ 159.08, 153.37, 152.70, 134.89, 133.22, 131.41, 131.12, 130.01, 129.48, 128.41, 127.49, 124.73, 124.23, 124.04, 117.76, 116.02, 115.14, 110.98, 109.99, 103.20, 55.13.

IR (KBr) ν 3470, 3058, 2951, 1657, 1620, 1512, 1466, 1374, 1273, 1222, 1178, 1031, 838, 749 cm^{-1} .

MS (EI): m/z , (%) 316 (100).

HRMS (ESI $^+$) calcd for $\text{C}_{21}\text{H}_{16}\text{O}_3$ $[\text{M} + 1]^+$ 317.1177, found 317.1171.

7-bromo-[1,1'-binaphthalene]-2,2'-diol (**46**)



A solution of $\text{Cu}(\text{OH})\text{Cl} \cdot \text{TMEDA}$ (1.56 g, 6.73 mmol), 7-bromonaphthalen-2-ol **56** (1 g, 4.48 mmol) and 2-naphthalol **1** (0.77 g, 5.38 mmol) in 30 mL MeOH. The solution had been purged with nitrogen for 5 min, and the mixture was stirred at room temperature for 24 h under nitrogen. The reaction mixture was poured into the mixed solvent of 1 M hydrochloric acid solution and ethyl acetate.

The organic layer was separated, washed successively with water and brine, and dried over sodium sulfate, and the solvent was evaporated to give a residue. The residue was purified by column chromatography on silica gel using light petroleum ether:ethyl acetate (100:0 to 80:20) as eluent to obtain binaphthol derivatives. Yield of **43** & **46** was calculated based on **56** and yield of **46** & **2** was calculated based on **1**.

2-Naphthalol (**1**): 15% (recovered).

Binol (**2**): 21% (M.p. = 216-218 $^{\circ}\text{C}$).

7,7'-dibromo-[1,1'-binaphthalene]-2,2'-diol (**43**): 44% (M.p. = 194-196 $^{\circ}\text{C}$).

7-bromo-[1,1'-binaphthalene]-2,2'-diol (**46**): 34%.

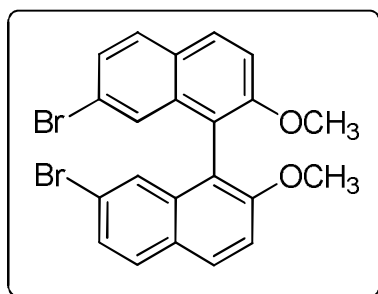
^1H NMR (CDCl_3 , 400 MHz): δ 8.00 (d, J = 8.8 Hz, 1H), 7.97- 7.92 (d, J = 9.2 Hz, 2H merged), 7.77 (d, J = 8.4 Hz, 1H), 7.47 (dd, J = 8.8, 2.0 Hz, 1H), 7.44-7.39 (m, 2H), 7.37-7.33 (m, 1H), 7.30 (d, J = 2.0 Hz, 1H), 7.12 (d, J = 8.4 Hz, 1H), 5.09 (broad signal for -OH, 2H).

^{13}C NMR (CDCl_3 , 100.6 MHz) δ 152.76, 133.40, 131.46, 129.45, 128.43, 127.52, 124.22, 124.07, 117.77, 110.81.

IR (KBr): ν 3473, 3414, 1613, 1499, 1381, 1353, 1325, 1210, 1166, 936, 839.

HRMS (ESI^+): calcd for $\text{C}_{20}\text{H}_{13}\text{BrO}_2$ [$\text{M}+\text{Na}$] 388.9976, found 388.9967 m/z .

7,7'-dibromo-2,2'-dimethoxy-1,1'-binaphthalene (**63**)



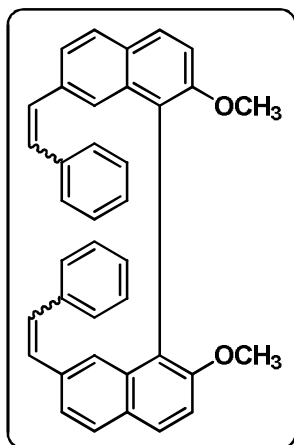
To a mixture of **43** (2 g, 4.50 mmol) and K_2CO_3 (6.22 g, 45.0 mmol) in acetonitril (50 mL), was added CH_3I (3.19 g, 22.5 mmol). The stirring mixture was refluxed for 18 h, then cooled to room temperature and filtered through a pad of celite. The celite was washed twice with ethyl acetate. The organic phases were collected, dried, and concentrated under reduced pressure to give a solid which was purified by column chromatography on silica gel using light petroleum ether:ethyl acetate (100:0 to 90:10) as eluent to obtained as a white solide **63**.

M.p. 201 - 205°C.

^1H NMR (CDCl_3 , 400 MHz): δ 7.97 (d, $J = 9.2$ & 3.6 Hz, 2H, ArH), 7.75 (d, $J = 8.8$ Hz, 2H, ArH), 7.47 (d, $J = 8.8$ Hz, 2H, ArH), 7.42 (d, $J = 8.8$ & 1.6 Hz, 2H, ArH), 7.23 (d, $J = 1.6$ Hz, 2H, ArH), 3.79 (s, 3H, OCH_3).

IR (KBr): ν 3045, 3021, 2991, 2832, 1615, 1581, 1497, 1461, 1344, 1320, 1255, 1168, 1148, 1099, 1070, 922, 821, 717.

2,2'-dimethoxy-7,7'-di((E)-styryl)-1,1'-binaphthalene (**64**)



In dry N_2 flushed two-necked r.b. flask a mixture of **63** (0.50 g, 1.13 mmol), styrene (0.35 g, 3.38 mmol), palladium acetate (2.53 mg, 0.011 mmol) and dppp (5.57 mg, 0.014 mmol), TBAB (0.145 g, 0.45 mmol), and K_2CO_3 (0.78 g, 5.63 mmol) in dry N,N -dimethylacetamide (20 mL) was taken and kept under N_2 atmosphere. The reaction mixture heated to 140°C for 40 h. The cooled mixture was then poured into water (50 mL) and extracted with ethyl acetate (3 X 50 mL). The combined organic layer was washed with water (2 X 50 mL), dried with anhydrous

sodium sulfate, concentrated in vacuum and purified by column chromatography using silica gel and petroleum ether as eluent to give **64** as white solid 0.520 g, 89%).

M.p. 150–152 °C.

¹H NMR (CDCl₃, 400 MHz): δ 8.00 (d, *J* = 8.8 Hz, 2H, ArH), 7.90 (d, *J* = 8.8 Hz, 2H, ArH), 7.68 (d, *J* = 8.8 & 1.6 Hz, 2H, ArH), 7.46 (d, *J* = 8.8 Hz, 2H, ArH), 7.42 (d, *J* = 8.4 Hz, 4H, ArH), 7.31 – 7.27 (m, 4H, ArH), 7.22 - 7.18 (m, 2H, ArH), 7.11 (s, 2H, ArH), 7.05 (d, *J* = 16.4 Hz, 2H, C=CH), 7.97 (d, *J* = 16.4 Hz, 2H, HC=C,), 3.79 (s, 3H, OCH₃).

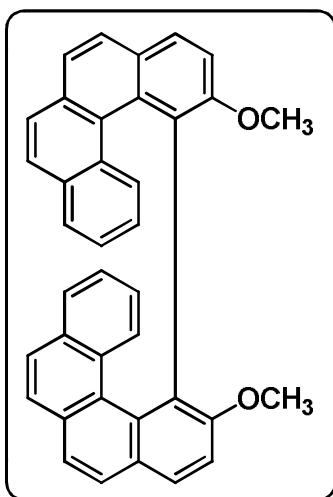
¹³C NMR (CDCl₃, 100.6 MHz): δ 155.46 (2 × Cq), 137.37 (2 × Cq), 135.28 (2 × Cq), 134.40 (2 × Cq), 129.49 (2 × CH), 129.27 (2 × CH), 128.83 (4 × CH, merged), 128.57 (6 × CH, merged), 128.53 (2 × CH), 127.46 (2 × CH), 126.47 (2 × CH), 124.99 (2 × CH), 120.56 (2 × CH), 119.66 (2 × Cq), 113.98 (2 × CH), 56.86 (2 × OCH₃).

IR (KBr): ν 3022, 2931, 2835, 1617, 1590, 1508, 1459, 1248, 1094, 1068, 959, 825.

MS (EI): *m/z*, (%) 518 (9), 452 (12), 450 (100), 415 (29).

HRMS (ESI⁺) calcd for C₃₈H₃₀O₂ [M+1] 519.2324, found 519.2303 *m/z*.

2,2'-dimethoxy-1,1'-bibenzo[*c*]phenanthrene (**65**)



To a solution of **64** (0.45 g, 0.87 mmol) in toluene (575 mL) was added iodine (0.485 g, 1.91 mmol) and tetrahydrofuran (14.1 mL, 173.75 mmol) in a standard immersion photo reactor. Then degassed for 15 minutes on sonication and irradiated with 250 W high pressure mercury vapor lamp for 24 h. The reaction mixture was washed with aqueous sodium thiosulfate (3 X 150 mL), dried over anhydrous sodium sulfate. The solvent was removed under reduced pressure. The residue was chromatographed on silica gel column by eluting with petroleum ether to afford **65** as white solid in a

yield of 0.302 g (68%).

M.p. >260 °C.

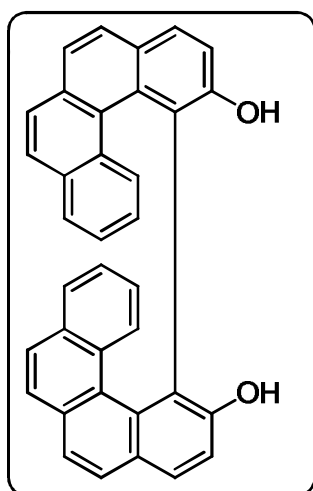
¹H NMR (CDCl₃, 400 MHz) δ 7.55 (d, *J* = 8.8 Hz, 2H, ArH), 7.51 (d, *J* = 9.2 Hz, 2H, ArH), 7.28 - 7.26 (merged, 2H, ArH), 7.23 (d, *J* = 8.4 Hz, 2H, ArH), 7.10 (d, *J* = 9.2 Hz, 2H, ArH), 7.08 (d, *J* = 8.8, 2H, ArH), 7.03 (d, *J* = 8.4, 2H, ArH), 6.94 – 6.90 (m, 4H, ArH), 6.50 (dt, *J* = 6.8 & 1.2 Hz, 2H, ArH), 4.37 (s, 3H, OCH₃).

¹³C NMR (CDCl₃, 100.6 MHz): δ 156.10 (2 × Cq), 130.50 (2 × Cq), 129.85 (2 × Cq), 129.17 (2 × Cq), 129.08 (2 × CH), 128.36 (2 × Cq), 127.84 (2 × Cq), 125.88 (2 × CH), 125.65 (2 × Cq), 125.49 (2 × CH), 125.46 (2 × CH), 124.98 (2 × CH), 124.61 (2 × CH), 123.38 (2 × Cq), 123.26 (2 × CH), 122.72 (2 × CH), 122.51 (2 × CH), 112.94 (2 × CH), 56.44 (2 × OCH₃).

IR (KBr): ν 3045, 2934, 2835, 1687, 1679, 1585, 1490, 1277, 1256, 1079, 1074, 829.

HRMS (ESI⁺): calcd for C₃₈H₂₆O₂ [M+1] 515.2011, found 515.1998 *m/z*.

[1,1'-bibenzo[*c*]phenanthrene]-2,2'-diol (**52**)



To a solution of **65** (0.27 g, 0.53 mmol) in CH₂Cl₂ (10 mL) at 0°C, BBr₃ (0.3 mL, 3.15 mmol) was added. The solution was allowed to warm to room temperature and stirred for 18 h. The excess of BBr₃ was decomposed by the dropwise addition of water. The resulting mixture was diluted with water and extracted with CH₂Cl₂ (3 X 25 mL). The organic phases were collected, dried and concentrated under reduced pressure to afford the crude product which was then purified by column chromatography using silica gel and petroleum ether as eluent to give **52** as white solid (0.25 g, 98%).

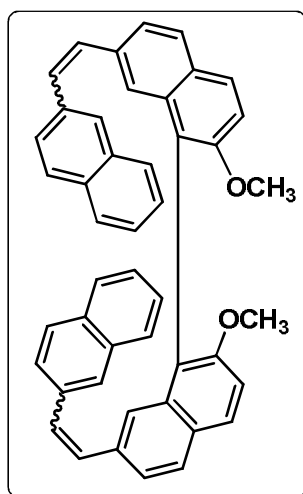
M.p. 240-242 °C.

¹H NMR (CDCl₃, 400 MHz): δ 10.27 (broad singlet, 2H, -OH) 7.42 (d, *J* = 8.8 Hz, 2H, ArH), 7.38 (d, *J* = 8.8 Hz, 2H, ArH), 7.29 (d, *J* = 7.6 Hz, 2H, ArH), 7.23 (d, *J* = 8.4 Hz, 2H, ArH), 7.08 (d, *J* = 8.4, 4H, ArH), 7.01 (d, *J* = 8.4, 2H, ArH), 6.97–6.93 (m, 2H, ArH), 6.90 (d, *J* = 8.4 Hz, 2H, ArH), 6.56-6.52 (m, 2H).

¹³C NMR (CDCl₃, 100.6 MHz): δ 154.69, 130.33, 129.95, 129.64, 128.80, 128.39, 127.69, 125.98, 125.74, 125.49, 125.20, 125.09, 124.95, 123.68, 123.15, 122.63, 122.20, 119.05.

HRMS (ESI⁺) calcd for C₃₆H₂₂O₂ [M+1] 487.1698, found 487.1676 *m/z*.

2,2'-dimethoxy-7,7'-bis(2-(naphthalen-2-yl)vinyl)-1,1'-binaphthalene (66)



In dry N₂ flushed two-necked r.b. flask a mixture of **63** (0.50 g, 1.06 mmol), 2-Naphthaldehyde (0.39 g, 2.54 mmol), triphenylmethyl phosphonium iodide (1.03 g, 2.54 mmol), palladium acetate (4.76 mg, 0.02 mmol) and dppp (17.47 mg, 0.04 mmol), TBAB (0.068 g, 0.21 mmol), and K₂CO₃ (0.73 g, 5.29 mmol) in dry N,N-dimethylacetamide (20 mL) was taken and kept under N₂ atmosphere. The reaction mixture heated to 140°C for 40 h. The cooled mixture was then poured into water (25 mL) and extracted with ethyl acetate (3 X 50 mL). The combined organic layer was washed with water (2 X 50 mL), dried with anhydrous sodium sulfate, concentrated in vacuum and purified by column chromatography using silica gel and petroleum ether as eluent to give **66** as white solid (0.46 g, 70%).

M.p. 198–200 °C.

¹H NMR (CDCl₃, 400 MHz): δ 8.03 (d, *J* = 8.8 Hz, 2H, ArH), 7.94 (d, *J* = 8.8 Hz, 2H, ArH), 7.79 – 7.74 (m, 10H, ArH), 7.63 (dd, *J* = 8.4 & 1.6 Hz, 2H, ArH), 7.49 (d, *J* = 9.2 Hz, 2H, ArH), 7.46 – 7.41 (m, 4H, ArH), 7.23 (d, *J* = 16.4 Hz, 2H, C=CH), 7.18 (s, 2H, ArH) 7.11 (d, *J* = 16.4 Hz, 2H, HC=C), 3.82 (s, 3H, OCH₃).

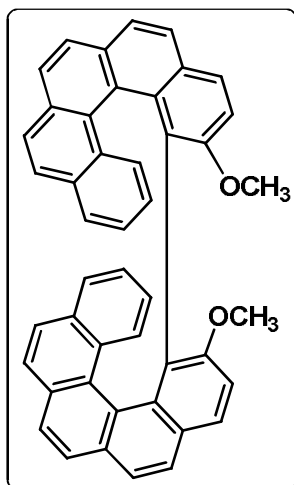
¹³C NMR (CDCl₃, 100.6 MHz): δ 155.51, 135.32, 134.89, 134.46, 133.65, 132.93, 129.85, 129.29, 128.88, 128.58, 128.16, 127.95, 127.64, 126.48, 126.23, 125.78, 125.10, 123.58, 120.54, 119.70, 114.03, 56.88.

IR (KBr): ν 3052, 3017, 2835, 1677, 1617, 1594, 1509, 1252, 1096, 958, 826

MS (EI) *m/z* (%): 618(8), 576 (15), 438 (38), 367 (50), 338 (57), 313 (84), 256 (52), 239 (100), 183 (99), 129 (74).

HRMS (ESI⁺) calcd for C₄₆H₃₄O₂ [M+Na] 641.2456, found 641.2452 *m/z*.

9,9'-dimethoxy-10,10'-bidibenzo[c,g]phenanthrene (**67**)



To a solution of **66** (0.40 g, 0.65 mmol) in toluene (575 mL) was added iodine (0.36 g, 1.42 mmol) and tetrahydrofuran (10.5 mL, 129.45 mmol) in a standard immersion photo reactor. Then degassed for 15 minutes on sonication and irradiated with 250 W high pressure mercury vapor lamp for 24 h. The reaction mixture was washed with aqueous sodium thiosulfate (3 X 150 mL), dried over anhydrous sodium sulfate. The solvent was removed under reduced pressure. The residue was chromatographed on silica gel column by eluting with petroleum ether to afford **67** as white solid in a yield of 0.120 g (30%).

M.p. >250 °C.

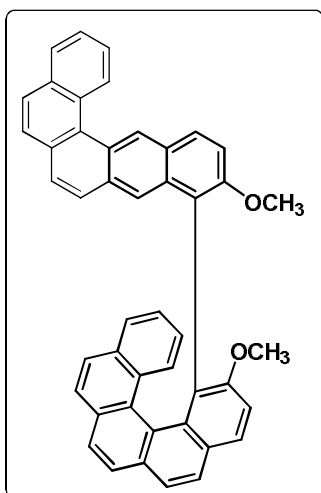
¹H NMR (CDCl₃, 400 MHz): δ 7.39 (d, *J* = 8 Hz, 2H, ArH), 7.34 (d, *J* = 8.4 Hz, 2H, ArH), 7.28 - 7.26 (d, merged, 4H, ArH), 7.18 - 7.14 (m, 14H, ArH), 6.85 - 6.81 (m, 2H, ArH), 6.60 (d, *J* = 8.8 Hz, 2H, ArH) 3.54 (s, 3H, OCH₃).

¹³C NMR (CDCl₃, 100.6 MHz): δ 154.51, 132.57, 130.19, 129.70, 128.58, 128.34, 128.11, 127.92, 127.21, 126.57, 126.48, 126.22, 126.02, 125.36, 124.64, 124.58, 123.78, 122.81, 122.49, 121.33, 111.35, 53.72.

IR (KBr): ν 3039, 2926, 2826, 1594, 1580, 1514, 1485, 1300, 1271, 1257, 1113, 1057, 827

HRMS (ESI⁺) calcd for C₄₆H₃₀O₂ [M⁺] 614.2246, found 614.2257 *m/z*.

11-methoxy-10-(9-methoxydibenzo[c,g]phenanthren-10-yl)benzo[a]tetraphene (**69**)



Yield = 17%.

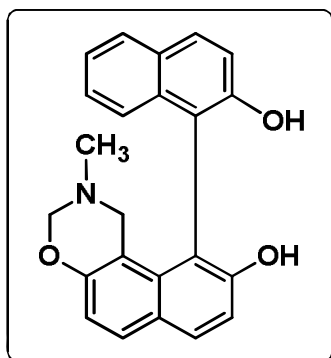
M.p. >230 °C.

¹H NMR (CDCl₃, 400 MHz): δ 9.30-9.21 (d, *J* = 8.8 Hz, 1H), 9.21 (s, 1H), 8.34-8.22 (d, *J* = 8.8 Hz, 1H), 8.17 (s, 1H), 8.09-7.94 (m, 3H), 7.89-7.86 (two doublets merged, *J* = 8.8 Hz, 2H), 7.81-7.77 (m, 2H), 7.73-6.66 (m, 4H), 7.61-7.59 (d, *J* = 9.2 Hz, 1H), 7.45-7.43 (d, *J* = 8.8 Hz, 1H), 7.19-7.17 (d, *J* = 8.4 Hz, 1H), 6.79-6.75 (m, 1H), 6.62-6.58 (m, 1H), 5.90-5.58 (m, 1H), 3.67 (s, 3H), 2.72 (s, 3H).

HRMS (ESI⁺) calcd for C₄₆H₃₀O₂ [M+1] 615.2324, found

615.2313 *m/z*.

(±) 10-(2-hydroxynaphthalen-1-yl)-2-methyl-2,3-dihydro-1H-naphtho[1,2-e][1,3]oxazin-9-ol (47)



A solution of formaldehyde (0.09 g, 37% w/v, 0.25 mL, 3.18 mmol) and methylamine (0.05 g, 1.59 mmol) in methanol (10 mL) was stirred for 30 min under nitrogen atmosphere, to this solution [1,1'-binaphthalene]-2,2',7-triol (0.40 g, 1.32 mmol) was added in one portion. The solution was stirred for 48 h at 60 °C. After the completion of the reaction the mixture was concentrated and the crude product was purified

by column chromatography on silica gel using light petroleum ether:ethyl acetate (100:0 to 70:30) as eluent to obtain a yellow solid which was dried in vacuum (0.420 g, 89 %).

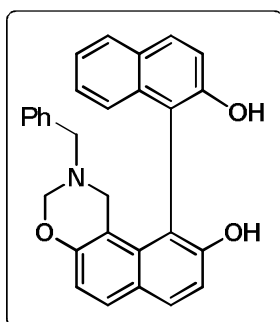
M.p. 102-104 °C.

¹H-NMR (CDCl₃, 400 MHz): δ 7.98-7.97 (d, *J* = 8.8 Hz, 1H, ArH), 7.89-7.86 (m, 2H, ArH), 7.71-7.69 (d, *J* = 8.8 Hz, 1H, ArH), 7.41-7.38 (m, 2H, ArH), 7.33-7.31 (d, *J* = 8.8 Hz, 1H, ArH), 7.24-7.21 (m, 2H, ArH) 6.96-6.94 (d, *J* = 8.8 Hz, 1H, ArH), 5.21 (broad singlet, 1H, OH), 5.09 (broad singlet, 1H, OH), 4.64 -4.62 (d, *J* = 9.2 Hz, 1H, N-CH₂-O), 4.54-4.51 (d, *J* = 9.2 Hz, 1H, N-CH₂-O), 3.47-3.43 (d, *J* = 16.4 Hz, 1H, Ar-CH₂-N), 2.88-2.85 (d, *J* = 16.4 Hz, 1H, Ar-CH₂-N), 2.18 (s, 3H, N-CH₃)

¹³C NMR (CDCl₃, 100.6 MHz): δ 154.10, 153.20, 152.65, 133.84, 133.21, 132.80, 131.89, 129.46, 129.13, 129.06, 128.60, 128.25, 127.97, 125.83, 124.24, 124.05, 117.42, 116.84, 114.67, 113.94, 111.49, 108.77, 82.24 (N-CH₂-O), 50.40 (N-CH₃), 39.11 (Ar-CH₂-N)

IR (KBr): ν 3496 (OH), 3055, 2954, 2904, 1613, 1509, 1435, 1343, 1271, 1236, 1163, 1137, 1105, 1070, 1023, 982, 859, 817, 784, 752.

(±) 2-benzyl-10-(2-hydroxynaphthalen-1-yl)-2,3-dihydro-1H-naphtho[1,2-e][1,3]oxazin-9-ol (48)



A solution of formaldehyde (0.24 g, 37% w/v, 0.79 mL, 7.95 mmol) and benzylamine (0.43 g, 3.97 mmol) in methanol (10 mL) was stirred for 30 min under nitrogen atmosphere, to this solution [1,1'-binaphthalene]-2,2',7-triol **41** (1 g, 3.31 mmol) was added in one portion. The solution was stirred for 48 h at 60 °C. After the completion of the reaction the mixture was concentrated and the crude product was purified by column chromatography on silica gel using light petroleum ether:ethyl acetate (100:0 to 70:30) as eluent to obtain a yellow solid **48** which was dried in vacuum (1.3 g, 92 %).

M.p. 92-94 °C.

¹H NMR (CDCl₃, 400 MHz) δ 7.89-7.86 (d, *J* = 8.8 Hz, 2H), 7.82-7.79 (d, *J* = 9.2 Hz, 1H), 7.73-7.71 (d, *J* = 9.2 Hz, 1H), 7.36-7.29 (m, 3H), 7.23-7.21 (d, *J* = 8.8 Hz, 1H), 7.20-7.15 (m, 4H) 6.99-6.97 (m, 3H), 5.09-5.03 (broad singlet, 2H, OH), 4.70 -4.68 (d, *J* = 9.6 Hz, 1H), 4.60-4.58 (d, *J* = 9.6 Hz, 1H), 3.62-3.59 (d, *J* = 13.2 Hz, 1H), 3.52-3.48 (d, *J* = 16.8 Hz, 1H), 3.49-3.46 (d, *J* = 13.2 Hz, 1H), 2.96-2.92 (d, *J* = 16.8 Hz, 1H).

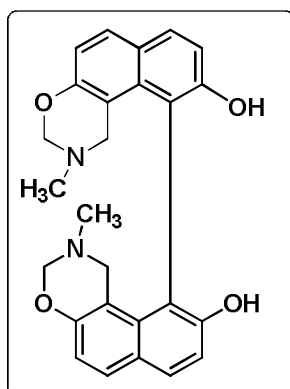
¹³C NMR (CDCl₃, 100.6 MHz): δ 154.08, 153.68, 152.49, 137.58, 133.64, 133.19, 132.76, 131.63, 129.46, 128.97, 128.59, 128.51, 128.26, 127.89, 127.06, 125.86, 124.21, 123.93, 117.35, 116.94, 114.68, 113.78, 111.92, 108.91, 80.67(NCH₂O), 55.26 (ArCH₂N), 48.13 (NCH₂Ph).

IR (KBr): ν 3469 (OH), 3052, 2951, 2897, 1668, 1620, 1522, 1515, 1456, 1374, 1273, 1219, 1169, 1031, 838, 749.

MS (ESI)⁺ [M+1]⁺ 434.2.

HRMS (ESI⁺) calcd for C₂₉H₂₃NO₃ [M + 1]⁺ 434.1756, found 434.1750.

(±) 2,2'-dimethyl-2,2',3,3'-tetrahydro-1H,1'-H-[10,10'-binaphtho[1,2-e][1,3]oxazine]-9,9'-diol (**50**)



A solution of formaldehyde (0.324 g, 0.87 mL, 37 % w/v, 10.8 mmol) and methylamine (0.167 g, 0.42 mL, 40 % w/v, 6.91 mmol) in methanol (10 mL) was stirred at room temperature (30 min) under nitrogen atmosphere. This solution was treated with 2,2',7,7'-tetrahydroxy-1,1'-binaphthyl **41** (0.715 g, 2.24 mmol) and the solution was stirred at 60 °C (48 h). After the completion of the reaction the mixture was concentrated and the crude product was purified by column chromatography on silica

gel using light petroleum ether:ethyl acetate (100:0 to 60:40) as eluent to obtain a white solid (0.89 g, 93%).

M.p. 209-210 °C.

¹H NMR (CDCl₃, 400 MHz): δ 7.84 (d, *J* = 8.4 Hz, 2H), 7.68 (d, *J* = 8.8 Hz, 2H), 7.14 (d, *J* = 8.8 Hz, 2H), 6.95 (d, *J* = 8.8 Hz, 2H), 5.06 (s, 2H, -OH), 4.74 (d, *J* = 9.2 Hz, 2H), 4.60 (d, *J* = 9.2 Hz, 2H), 3.63 (d, *J* = 16.8 Hz, 2H), 3.20 (d, *J* = 16.8 Hz, 2H), 2.82 (s, 6H).

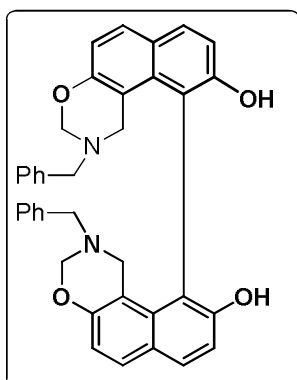
¹³C NMR (CDCl₃, 100.6 MHz): δ 153.97 (Cq), 153.60 (Cq), 133.16 (CH), 132.92 (Cq), 129.80 (CH), 125.82 (Cq), 117.03 (CH), 114.33 (CH), 111.88 (Cq), 111.32 (Cq), 82.36 (OCH₂N), 50.85 (ArCH₂N), 39.25 (NCH₃).

MS (EI): *m/z*, (%): 429 (15), 428 (53), 427 (13), 398 (11), 385 (13), 384 (13), 370 (13), 369 (17), 368 (31), 325 (22), 324 (13), 314 (14), 313 (34), 297 (24), 295 (14), 271 (14), 239 (27), 226 (21), 213 (19), 58 (100), 57 (34).

Anal. Calcd. for C₂₆H₂₄N₂O₄: C 72.88, H 5.64; N 6.54. Found: C 72.78, H 5.40, N 6.64.

IR (KBr): ν 3464, 2891, 1613, 1519, 1455, 1345, 1302, 1250, 1087, 1021, 938, 878, 861, 815, 756, 700, 598 cm⁻¹

(±)2,2'-dibenzyl-2,2',3,3'-tetrahydro-1H,1'H-[10,10'-binaphtho[1,2-e][1,3]oxazine]-9,9'-diol (51)



A solution of formaldehyde solution (0.27 g, 37% w/v, 0.734 mL, 9.04 mmol) and benzylamine (0.49 g, 4.52 mmol) in methanol was stirred for 30 min under nitrogen atmosphere, to this solution (*R*)-2,7,2',7'-tetrahydroxy-1,1'-binaphthyl (0.60 g, 1.88 mmol) was added in one portion. The solution was stirred for 48 h at 60 °C. After the completion of the reaction the mixture was concentrated and the crude product was purified by column chromatography on silica gel using light petroleum

ether:ethyl acetate (100:0 to 60:40) as eluent to obtain a white solid which was dried in vacuum (0.95 g, 86 %).

M.p. 190-192 °C.

¹H NMR (CDCl₃, 400 MHz): δ 7.73 (d, *J* = 8.8 Hz, 2H), 7.60 (d, *J* = 8.8 Hz, 2H), 7.16 (m, 6H), 6.95 (m, 6H), 6.89 (d, *J* = 8.8 Hz, 2H), 4.95 (s, 2H), 4.62 (d, *J* = 9.6 Hz, 2H), 4.48 (d, *J* = 9.2 Hz, 2H), 3.55 (m, 4H), 3.47 (d, *J* = 16.8 Hz, 2H), 3.20 (d, *J* = 16.8 Hz, 2H).

¹³C NMR (CDCl₃, 100.6 MHz): δ 153.91 (Cq), 153.81 (Cq), 137.45 (Cq), 132.95 (CH), 132.73 (Cq), 129.49 (CH), 128.32 (2 X CH), 128.25 (2 X CH), 127.01 (CH), 125.50 (Cq), 117.20 (CH), 114.11 (CH), 111.84 (Cq), 111.74 (Cq), 80.73 (OCH₂N), 55.34 (ArCH₂N), 48.56 (NCH₂Ph).

MS (EI): *m/z*, (%) 579 (21), 550 (06), 488 (11), 460 (12), 444 (08), 369 (28), 324 (36), 313 (48), 312 (52), 311 (62), 296 (24), 238 (48), 194 (78), 134 (32), 118 (94), 92 (12), 91 (100), 89 (08).

Anal. Calcd. for C₃₈H₃₂N₂O₄: C 78.60, H 5.55; N 4.82. Found: C 78.22, H 5.19, N 4.77.

IR (KBr): 3511, 2882, 1611, 1514, 1449, 1343, 1138, 1078, 1024, 932, 833, 734, 705, 608 cm.⁻¹

Resolution of 1,1'-binaphthyl-2,2',7-triol (**44**)

Racemic triol **44** (1 g, 3.31 mmol) and (*S*)-Brucine (0.76 g, 3.31 mmol) were taken in MeOH (30 mL). The mixture was refluxed for 4 h, and then cooled to room temperature to give white precipitates, which were filtered and crystallized in methanol to furnish colourless crystals of the molecular complex. The crystals were added to a mixture of ethyl acetate – HCl (1M, 1:1) and stirred at room temperature for 10 min. The solid crystals were completely dissolved, the organic layer was separated, and the water phase extracted with ethyl acetate (2 X 50 mL). The organic layer was dried over anhydrous Na₂SO₄, concentrated at reduced pressure, to give (*S_a*)-1,1'-binaphthyl-2,2',7-triol (0.440 g, 48 %), M.p.172-174°C, $[\alpha]_D^{28} = + 30$ (*c* = 0.30, acetonitrile). [96.2 % ee based on HPLC on chiralpak OD-H].

The mother liquor MeOH was evaporated under reduced pressure to get residue then treated with a mixture of ethyl acetate – HCl (1M, 1:1) and stirred at room temperature for 10 min. The residue was completely dissolved, the organic layer was separated, and the water phase extracted with ethyl acetate (2 X 50 mL). The organic layer was dried over anhydrous Na₂SO₄, concentrated at reduced pressure, to give (*R_a*)-1,1'-binaphthyl-2,2',7-triol as off white powder (0.480 g, 48 %), M.p.172-174°C. This sample was 54.0 % optically pure, $[\alpha]_D^{28} = -12$ (*c* = 0.30, acetonitrile).

Resolution of 2,2',7,7'-tetrahydroxy-1,1'-binaphthyl (**41**)

Racemic tetrol **41** (2.1 g, 6 mmol) and (*S*)-proline (0.76 g, 6 mmol) were taken in acetonitrile (30 mL). The mixture was refluxed for 3 h, and then cooled to room temperature to give white precipitates, which were filtered and crystallized in methanol to furnish colourless crystals of the molecular complex. The crystals were added to a mixture of ethyl acetate - water (3:2 v/v; 40 mL) and stirred at room temperature for 2 h. The solid crystals were completely dissolved, the organic layer was separated, and the water phase extracted with ethyl acetate (2 X 50 mL). The organic layer was dried over anhydrous Na₂SO₄, concentrated at reduced pressure, to give (*R_a*)-2,2',7,7'-tetrahydroxy-1,1'-binaphthyl (0.998 g, 48 %), M.p.122-124°C, $[\alpha]_D^{28} = - 116$ (*c* = 0.10, acetonitrile). [99.8 % ee based on HPLC on chiralpak OD-H.]

The mother liquor acetonitrile was evaporated under reduced pressure to get (*aS*)-2,2',7,7'-tetrahydroxy-1,1'-binaphthyl as off white powder (0.99 g, 47 %), M.p.122-124°C. This

sample was 91.0 % optically pure, which was enhanced by a single crystallization (MeOH:toluene, 1:1) to 99.6 % ee $[\alpha]_D^{28} = +114$ ($c = 0.10$, acetonitrile).

[1,1'-binaphthalene]-2,2',7-triyl tris((1R,2S,5R)-2-isopropyl-5-methylcyclohexyl) tricarbonate (69)

To the solution of **44** (0.30 g, 0.99 mmol) and triethylamine (0.11 g, 1.09 mmol) in dichloromethane was added (1R,2S,5R)-(-)-menthyl chloroformate (0.24 g, 1.09 mmol) drop wise at 0 °C under N₂ atmosphere. After the completion of the reaction (tlc) the reaction mixture was poured in ice cold water. The aqueous layer was extracted with dichloromethane (2 X 50 mL) combine the extract and washed with water (2 X 50 mL) and the organic layer was dried over Na₂SO₄ and evaporated to obtained crude solid. The crude product was purified by column chromatography over silica gel using petroleum ether/ethyl acetate as eluent (100:00 to 95:5) furnishing a semisolid **69** (0.820 g, 97%).

bis((1R,2S,5R)-2-isopropyl-5-methylcyclohexyl)(7-methoxy-[1,1'-binaphthalene]-2,2'-diyl) dicarbonate (70)

Compound **70** was prepared from 7-methoxy-[1,1'-binaphthalene]-2,2'-diol by same procedure as that of **69**.

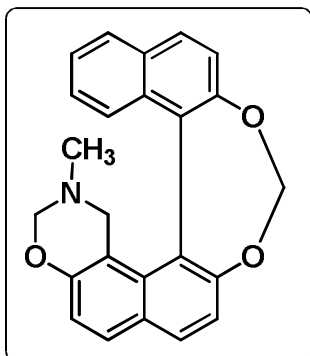
Yield = 0.486 (92%).

[1,1'-bibenzo[c]phenanthrene]-2,2'-diylbis((1R,2S,5R)-2-isopropyl-5-methylcyclohexyl) dicarbonate (71)

Compound **71** was prepared from [1,1'-bibenzo[c]phenanthrene]-2,2'-diol **52** by same procedure as that of **69**.

Yield = 0.399 (95%).

10-methyl-10,11-dihydro-9H-naphtho[1'',2'':6',7'] [1,3]dioxepino[4',5':7,8]naphtha [1,2-e][1,3]oxazine (72)



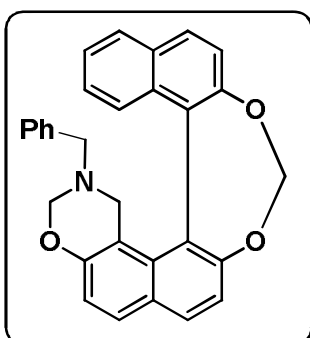
A solution of **47** (0.35 g, 0.98 mmol) and anhydrous Cs_2CO_3 (1.6 g, 4.90 mmol) in dry DMF (5 mL) and CH_2I_2 (0.39 g, 1.47 mmol) was added and the mixture was stirred 48 h at room temperature under nitrogen atmosphere. After the completion of the reaction (tlc) the reaction mixture was poured in ice cold water. The aqueous layer was extracted with chloroform (3 X 100 mL) combine the extract and washed with water (2 X 100 mL) and the organic layer was dried over Na_2SO_4 and evaporated to obtained crude solid. The crude product was purified by column chromatography over silica gel using petroleum ether/ethyl acetate as eluent (100:00 to 80:20) furnishing a white solid **72** (0.23 g, 63%).

M.p. 156-158 °C.

^1H NMR (CDCl_3 , 400 MHz): δ 7.97-7.94 (d, $J = 8.8$ Hz, 1H, ArH), 7.91-7.90 (d, $J = 8.4$ Hz, 1H, ArH), 7.90-7.88 (d, $J = 8.8$ Hz, 1H, ArH), 7.80-7.78 (d, $J = 8.8$ Hz, 1H, ArH), 7.49-7.47 (d, $J = 8.8$ Hz, 1H, ArH), 7.43-7.39 (m, 1H, ArH), 7.33-7.31 (d, $J = 8.4$ Hz, ArH), 7.28-7.24 (m, 1H, ArH), 7.19-7.18 (d, $J = 8.4$ Hz, 1H, ArH), 7.07-7.05 (d, $J = 8.8$ Hz, 1H, ArH), 5.72-5.71 (AB splitting, $J = 6.4$ Hz, 2H, O- $\underline{\text{CH}_2}$ -O), 4.55 -4.54 (broad signal, 2H, N- $\underline{\text{CH}_2}$ -O), 3.02-2.98 (d, $J = 16.8$ Hz, 1H, Ar- $\underline{\text{CH}_2}$ -N), 2.90-2.86 (d, $J = 16.8$ Hz, 1H, Ar- $\underline{\text{CH}_2}$ -N), 2.16(s,3H, N- $\underline{\text{CH}_3}$).

^{13}C NMR (CDCl_3 , 100.6 MHz): δ 152.75, 152.36, 149.69, 133.36, 132.69, 131.17, 130.13, 129.27, 128.81, 128.62, 127.92, 126.63, 125.06, 124.44, 123.45, 120.50, 118.10, 117.78, 112.19, 102.76, 82.69 (N- $\underline{\text{CH}_2}$ -O), 52.26 (N- $\underline{\text{CH}_3}$), 38.86 (Ar- $\underline{\text{CH}_2}$ -N).

10-benzyl-10,11-dihydro-9H-naphtho[1'',2'':6',7'] [1,3]dioxepino[4',5':7,8]naphtha [1,2-e][1,3]oxazine (73)



A solution of **78** (0.30 g, 0.69 mmol) and anhydrous Cs_2CO_3 (1.13 g, 3.46 mmol) in dry DMF (5 mL) and CH_2I_2 (0.28 g, 1.04 mmol) was added and the mixture was stirred 48 h at room temperature under nitrogen atmosphere. After the completion of the reaction (tlc) the reaction mixture was poured in ice cold water. The aqueous layer was extracted with

chloroform (3 X 100 mL) combine the extract and washed with water (2 X 100 mL) and the organic layer was dried over Na₂SO₄ and evaporated to obtained crude solid. The crude product was purified by column chromatography over silica gel using petroleum ether/ethyl acetate as eluent (100:00 to 80:20) furnishing a white solid (0.18 g, 61%).

M.p. 162-164°C.

¹H NMR (CDCl₃, 400 MHz) δ 7.93-7.91 (d, *J* = 8.8 Hz, 1H), 7.91-7.89 (d, *J* = 8.8 Hz, 1H), 7.89-7.87 (d, *J* = 8.4 Hz, 1H), 7.83-7.81 (d, *J* = 8.8 Hz, 1H), 7.42-7.40 (d, *J* = 8.8 Hz, 1H) 7.40-7.36 (dt, *J* = 8 & 1.2 Hz, 1H), 7.33-7.31 (d, *J* = 8.4 Hz, 1H), 7.26-7.18 (m, 5H), 7.10-7.08 (d, *J* = 8.8 Hz, 1H) 7.06-7.04 (m, 2H), 5.71-5.67 (two doublet, *J* = 10 Hz, 2H) 4.51 -4.50 (broad singlet, 2H), 3.48-3.45 (d, *J* = 12.8 Hz, 1H), 3.33-3.30 (d, *J* = 12.8 Hz, 1H), 3.05-2.99 (m, 2H).

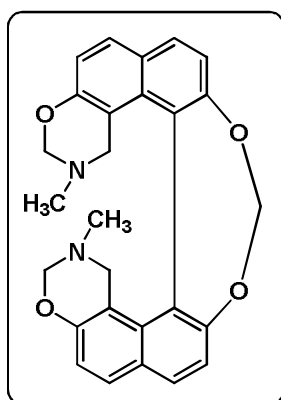
¹³C NMR (CDCl₃, 100.6 MHz): δ 153.16, 152.41, 149.70, 137.56, 133.34, 132.70, 131.16, 130.05, 129.37, 129.17, 128.84, 128.65, 128.30, 127.95, 127.23, 126.62, 125.04, 124.48, 123.50, 120.47, 118.18, 117.83, 112.54, 102.76 (O-CH₂-O), 79.71 (N-CH₂O), 54.64 (Ar-CH₂N), 51.16 (N-CH₂Ph).

IR (KBr) ν 3033, 2951, 2891, 2848, 1611, 1508, 1456, 1362, 1323, 1268, 1233, 1135, 1045, 996, 912, 830, 807, 746, 722.

MS (EI) *m/z*, (%): [M]⁺ 445.2 (100) and (ESI)⁺ [M+1]⁺ 446.2.

HRMS (ESI⁺) calcd for C₃₀H₂₃NO₃ [M + 1]⁺ 446.1756, found 446.1750.

Synthesis of compound Helical [1,3]-Bis-oxazine (74)



A solution of **50** (1.0 g, 2.33 mmol) in dry DMF (15 mL) was added CH₂I₂ (0.94 g, 0.43 mL, 3.49 mmol) and the mixture was stirred for 48 h at room temperature. After the completion of the reaction (monitored by tlc) the reaction mixture was poured in ice cold water. The aqueous was extracted with chloroform (3 X 100 mL) combine the extract and washed with water (2 X 100 mL) and the organic layer was dried over Na₂SO₄ and evaporated to obtain brown viscous oil. The crude product was purified by column chromatography over silica gel using a gradient of petroleum ether:ethyl acetate (100:00 to 70:30) as eluent to get a white solid **74** (0.57 g, 56 %).

M.p. 178-179 °C.

¹H NMR (CDCl₃, 400 MHz): δ 7.83 (d, *J* = 8.4 Hz, 2H), 7.70 (d, *J* = 8.8 Hz, 2H), 7.28 (d, *J* = 8.8 Hz, 2H), 6.96 (d, *J* = 8.8 Hz, 2H), 5.64 (s, 2H), 4.53 (d, *J* = 9.2 Hz, 2H), 4.50 (dd, *J* = 2.4, 9.6 Hz, 2H), 2.66 (d, *J* = 16.4 Hz, 2H), 2.39 (d, *J* = 16.4 Hz, 2H), 2.06 (s, 6H).

¹³C NMR (CDCl₃, 100.6 MHz): δ 152.65 (Cq), 151.03 (Cq), 133.92 (Cq), 131.17 (CH), 129.52 (CH), 127.89 (Cq), 126.23 (Cq), 118.05 (CH), 117.20 (CH), 111.84 (Cq), 102.17 (OCH₂O), 82.77 (OCH₂N), 51.30 (ArCH₂N), 38.59 (CH₃).

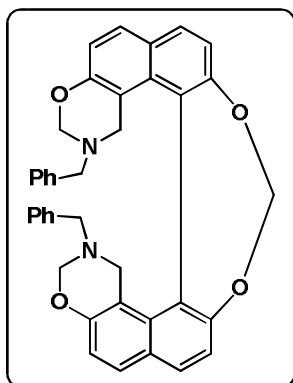
MALDI-TOF-MS: *m/z* = 441.1183 ([M+H]⁺).

MS (EI): *m/z*, (%) 440 (32), 439 (100), 410 (10), 396 (12), 382 (22), 381 (18), 380 (11), 354 (11), 353 (11), 352 (15), 323 (29), 312 (17), 311 (11), 295 (14), 239 (15), 238 (12), 69 (10).

Anal. Calcd. for C₂₇H₂₄N₂O₄: C 73.62, H 5.49, N 6.35. Found: C 73.28, H 5.74, N 6.35.

IR (KBr): 3070, 2951, 2890, 1610, 1509, 1450, 1362, 1321, 1296, 1236, 1195, 1162, 1127, 1083, 1050, 1000, 922, 839, 795, 721 cm⁻¹.

Synthesis of compound Helical [1,3]-Bis-oxazine (75)



A solution of pure 2,2'-bis-(1-phenyl-ethyl) 2,3,2',3'-tetrahydro-1H,1'H-[10,10']bi[naphtho[1,2-e][1,3]oxazinyl]-9,9'-diol (0.550 g, 0.95 mmol) and Cs₂CO₃ (1.543 g, 4.74 mmol) in dry DMF (10 mL) and CH₂I₂ (0.380 g, 0.114 mL, 1.42 mmol) was added and the mixture was stirred 48 h at room temperature. After the completion of the reaction (monitored by tlc) the reaction mixture was poured in ice cold water. The aqueous layer was extracted with chloroform (3 X 100 mL) combine the extract and washed with water (2 X 100 mL) and the organic layer was dried over Na₂SO₄ and evaporated to obtained crude solid. The crude product was purified by column chromatography over silica gel using a gradient of petroleum ether/ethyl acetate as eluent (100:00 to 80:20) giving a white solid **75** (0.330 g, 59%).

M.p. 222-224 °C.

¹H NMR (CDCl₃, 400 MHz): δ 7.76 (d, *J* = 8.4 Hz, 2H), 7.69 (d, *J* = 9.2 Hz, 2H), 7.23-7.20 (m, 6H), 7.13 (d, *J* = 8.4 Hz, 2H), 6.99-6.97 (m, 4H), 6.96 (d, *J* = 9.2 Hz, 2H), 4.57 (d, *J* = 9.6 Hz, 2H), 4.50 (dd, *J* = 2.0, 9.2 Hz, 2H), 3.37 (d, *J* = 12.8 Hz, 2H), 3.23 (d, *J* = 12.8 Hz, 2H), 2.71 (d, *J* = 16.4 Hz, 2H), 2.53 (d, *J* = 16.4 Hz, 2H).

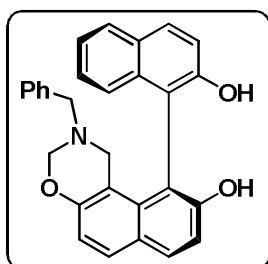
¹³C NMR (CDCl₃, 100.6 MHz): δ 152.85 (Cq), 150.84 (Cq), 137.45 (Cq), 133.74 (Cq), 130.90 (CH), 129.56 (CH), 129.04 (2 X CH), 128.23 (2 X CH), 127.79 (Cq), 127.11 (CH), 126.27 (Cq), 117.98 (CH), 117.13 (CH), 112.03 (Cq), 102.04 (O-CH₂-O), 80.34 (NCH₂O), 54.44 (ArCH₂N), 49.41 (NCH₂Ph).

MS (EI): *m/z*, (%) 592 (08), 536 (09), 439 (14), 382 (25), 298 (31), 256 (27), 255 (28), 236 (31), 182 (36), 127 (26), 119 (29), 111 (35), 97 (42), 95 (37), 91 (100), 85 (28), 84 (32), 83 (75), 81 (48), 71 (47).

Anal. Calcd. for C₃₉H₃₂N₂O₄: C 79.03, H 5.44, N 4.73. Found: C 78.64, H 5.30, N 4.65.

IR (KBr): 3026, 2990, 2929, 2885, 2858, 1610, 1509, 1453, 1363, 1323, 1244, 1199, 1155, 1132, 1068, 1036, 1009, 925, 839, 786., 745, 696 cm.⁻¹

(*S*_a) 2-benzyl-10-(2-hydroxynaphthalen-1-yl)-2,3-dihydro-1H-naphtho[1,2-*e*][1,3]oxazin-9-ol [(*S*_a)-48]

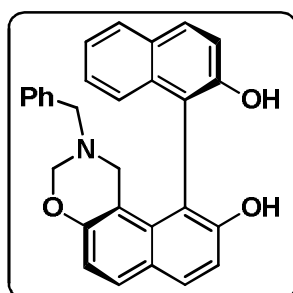


Compound (*S*_a)-48 was prepared by same procedure as that of (±)-48.

Yield = 73.2 %.

M.p. 90-92 °C.

(*R*_a) 2-benzyl-10-(2-hydroxynaphthalen-1-yl)-2,3-dihydro-1H-naphtho[1,2-*e*][1,3]oxazin-9-ol [(*R*_a)-48]

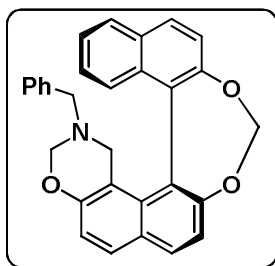


Compound (*R*_a)-48 was prepared by same procedure as that of (±)-48.

Yield = 89.4 %.

M.p. 92-94 °C.

(*S_a*)-10-benzyl-10,11-dihydro-9H-naphtho[1'',2'':6',7']-[1,3]dioxepino[4',5':7,8]naphtha[1,2-e][1,3]oxazine [(*S_a*)-73]



Compound (*S_a*)-73 was prepared by same procedure as that of (\pm)-73.

Yield = 60.9 %.

M.pt. 164-166 °C.

$[\alpha]_D^{28} = + 800$ ($c = 0.8$, CHCl_3).

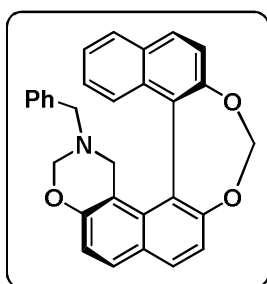
¹H-NMR (CDCl_3 , 400 MHz): δ 7.93-7.91 (d, $J = 8.8$ Hz, 1H), 7.92-7.90 (d, $J = 8.8$ Hz, 1H), 7.89-7.88 (d, $J = 8.4$ Hz, 1H), 7.83-7.81 (d, $J = 8.8$ Hz, 1H), 7.43-7.41 (d, $J = 8.8$ Hz, 1H) 7.40-7.36 (dt, $J = 8$ & 1.2 Hz, 1H), 7.34-7.32 (d, $J = 8.4$ Hz, 1H), 7.27-7.19 (m, 5H), 7.11-7.09 (d, $J = 8.8$ Hz, 1H) 7.06-7.04 (m, 2H), 5.71-5.68 (two doublet, $J = 10$ Hz, 2H) 4.54 -4.48 (broad singlet, 2H), 3.49-3.46 (d, $J = 12.8$ Hz, 1H), 3.34-3.31 (d, $J = 12.8$ Hz, 1H), 3.09-3.00 (AB splitting, $J = 16.8$ Hz, 2H).

MS (EI) m/z , (%): $[\text{M}]^+$ 445.2 (100), 354 (11), 327 (12), 326 (65), 325 (38), 296 (35), 295 (61), 278 (38), 238 (38).

MS (ESI⁺): $[\text{M}+1]$ 446 m/z .

IR (KBr) ν 3024, 2905, 2842, 1609, 1508, 1451, 1356, 1322, 1280, 1235, 1138, 1043, 1010, 909, 830, 806, 751, 722.

(*R_a*)-10-benzyl-10,11-dihydro-9H-naphtho[1'',2'':6',7']-[1,3]dioxepino[4',5':7,8]naphtha[1,2-e][1,3]oxazine [(*R_a*)-73]



Compound (*R_a*)-73 was prepared by same procedure as that of (\pm)-73.

Yield = 63.3 %.

M.p. 164-166°C.

$[\alpha]_D^{28} = - 195$ ($c = 0.8$, CHCl_3).

¹H NMR (CDCl_3 , 400 MHz) δ 7.93-7.91 (d, $J = 8.8$ Hz, 1H), 7.92-7.90 (d, $J = 8.8$ Hz, 1H), 7.89-7.88 (d, $J = 8.4$ Hz, 1H), 7.83-7.81 (d, $J = 8.8$ Hz, 1H), 7.43-7.41 (d, $J = 8.8$ Hz, 1H) 7.40-7.36 (dt, $J = 8$ & 1.2 Hz, 1H), 7.34-7.32 (d, $J = 8.4$ Hz, 1H), 7.27-7.19 (m, 5H), 7.11-7.09 (d, $J = 8.8$ Hz, 1H) 7.06-7.04 (m, 2H), 5.71-5.68 (two doublet, $J = 10$ Hz, 2H) 4.54 -4.48 (broad singlet, 2H), 3.49-3.46 (d, $J = 12.8$ Hz, 1H), 3.34-3.31 (d, $J = 12.8$ Hz, 1H), 3.09-3.00 (AB splitting, $J = 16.8$ Hz, 2H).

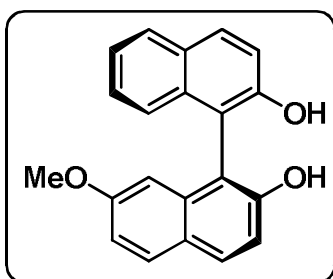
7.11-7.09 (d, $J = 8.8$ Hz, 1H) 7.06-7.04 (m, 2H), 5.71-5.68 (two doublet, $J = 10$ Hz, 2H) 4.54-4.48 (broad singlet, 2H), 3.49-3.46 (d, $J = 12.8$ Hz, 1H), 3.34-3.31 (d, $J = 12.8$ Hz, 1H), 3.09-3.00 (AB splitting, $J = 16.8$ Hz, 2H).

MS (EI) m/z , (%): $[M]^+$ 445.2 (100), 354 (11), 327 (12), 326 (65), 325 (38), 296 (35), 295 (61), 278 (38), 238 (38).

MS (ESI⁺): $[M+1]$ 446 m/z .

IR (KBr) ν 3033, 2951, 2891, 2848, 1611, 1508, 1456, 1362, 1323, 1268, 1233, 1200, 1135, 1045, 1009, 996, 912, 830, 807, 751, 722 cm^{-1} .

(*S_a*) 7-methoxy-[1,1'-binaphthalene]-2,2'-diol [(*S_a*)-45]

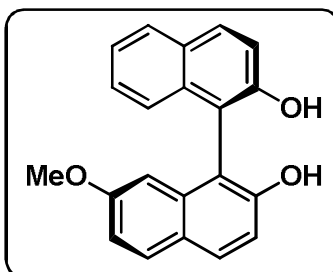


Compound (*S_a*)-45 was prepared by same procedure as that of (\pm)-45.

Yield = 71.2 %.

M.p. 92-94 °C.

(*R_a*) 7-methoxy-[1,1'-binaphthalene]-2,2'-diol [(*R_a*)-45]

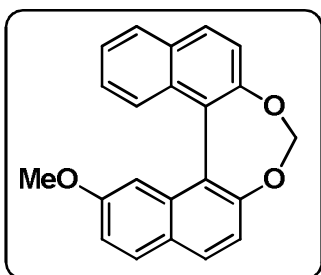


Compound (*R_a*)-45 was prepared by same procedure as that of (\pm)-45.

Yield = 74.2 %.

M.p. 90-92 °C.

(\pm) 10-methoxydinaphtho[2,1-d:1',2'-f][1,3]dioxepine (76)



A solution of pure 7-methoxy-[1,1'-binaphthalene]-2,2'-diol (0.10 g, 0.32 mmol) and anhydrous Cs_2CO_3 (0.52 g, 1.58 mmol) in dry DMF (5 mL) and CH_2I_2 (0.13 g, 0.47 mmol) was added and the mixture was stirred 48 h at room temperature under nitrogen atmosphere. After the completion of the reaction (tlc) the reaction mixture was poured in ice cold water. The aqueous layer was extracted with chloroform (3 X 100 mL) combine the extract and washed with water (2 X 100 mL) and the organic layer was dried over Na_2SO_4

and evaporated to obtain crude solid. The crude product was purified by column chromatography over silica gel using petroleum ether/ethyl acetate as eluent (100:00 to 90:10) furnishing a white solid (0.08 g, 83%).

M.p. 138 °C.

¹H NMR (CDCl₃, 400 MHz) δ 8.00 (d, *J* = 8.8 Hz, 1H), 7.96 (d, *J* = 8.4 Hz, 1H), 7.93 (d, *J* = 8.8 Hz, 1H), 7.85 (d, *J* = 8.8 Hz, 1H), 7.58 (d, *J* = 8.4 Hz, 1H) 7.52 (d, *J* = 8.4 Hz, 1H), 7.49-7.45 (m, 1H), 7.36 (d, *J* = 8.4 Hz, 2H), 7.13 (dd, *J* = 8.8 & 2.4 Hz, 1H) 6.80 (d, *J* = 2.4 Hz, 2H), 5.72 (s, 2H) 3.44 (s, 3H).

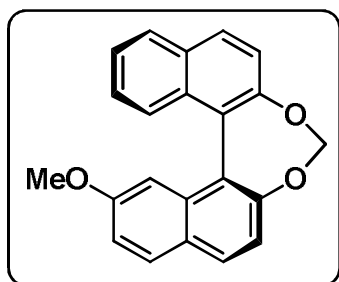
¹³C NMR (CDCl₃, 100.6 MHz): δ 157.85, 152.00, 151.23, 133.82, 131.68, 130.32, 129.96, 128.50, 127.30, 127.26, 126.30, 125.86, 125.05, 121.10, 118.43, 117.99, 105.48, 103.17, 55.00 (OCH₃)

IR (KBr) ν 3062, 3005, 2946, 2829, 1659, 1625, 1581, 1524, 1464, 1361, 1260, 1223, 1132, 1033, 828, 744 cm⁻¹.

MS (ESI)⁺ 329.2 m/z.

HRMS (ESI⁺) calcd for C₂₂H₁₆O₃ [M + 1]⁺ 329.1178, found 329.1172.

(*S*_a) 10-methoxydinaphtho[2,1-d:1',2'-f][1,3]dioxepine [(*S*_a)-76]



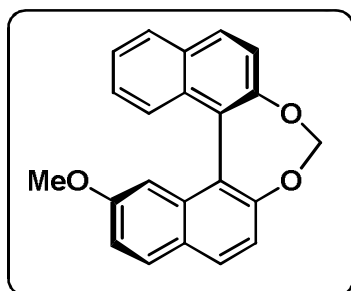
Compound (*S*_a)-76 was prepared by same procedure as that of (±)-76.

Yield = 60.2 %.

M.p. 136-138°C.

[α]_D²⁸ = +1090 (*c* = 0.65, CHCl₃).

(*R*_a) 10-methoxydinaphtho[2,1-d:1',2'-f][1,3]dioxepine [(*R*_a)-76]



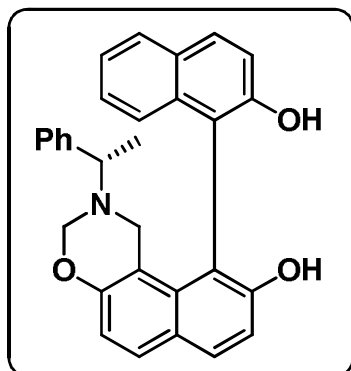
Compound (*R*_a)-76 was prepared by same procedure as that of (±)-76.

Yield = 66.3 %.

M.p. 137-138°C.

[α]_D²⁸ = - 319 (*c* = 0.65, CHCl₃).

(±) 10-(2-hydroxynaphthalen-1-yl)-2-((S)-1-phenylethyl)-2,3-dihydro-1H-naphtho [1,2-e][1,3]oxazin-9-ol (77)



A solution of formaldehyde (0.36 g, 37% w/v, 1.19 mL, 11.9 mmol) and (*S*)- α -phenyl ethyl amine (0.72 g, 5.96 mmol) in methanol (10 mL) was stirred for 30 min under nitrogen atmosphere, to this solution [1,1'-binaphthalene]-2,2',7-triol (1.5 g, 4.96 mmol) was added in one portion. The solution was stirred for 48 h at 60 °C. After the completion of the reaction the mixture was concentrated and the crude product was purified by column chromatography on silica gel using light petroleum ether:ethyl acetate (100:0 to 70:30) as eluent to obtain a mixture of diastereomers as a yellow solid which was dried in vacuum (1.92 g, 86 %).

¹H NMR (CDCl₃, 400 MHz) δ 7.88-7.84 (m, 3H), 7.79-7.77 (d, *J* = 8.8 Hz, 1H), 7.70-7.68 (d, *J* = 8.8 Hz, 2H), 7.37-7.28 (m, 5H), 7.26-7.19 (m, 9H) 7.08-7.01 (m, 7H), 6.96-6.94 (two doublets, *J* = 8.8 Hz, 2H), 6.91-6.88 (m, 1H) 4.79-4.71 (m, 2H), 4.57-4.45 (two doublets, *J* = 9.6 Hz, 2H), 3.69-3.56 (m, 2H), 3.45-3.41 (m, 2H), 3.07-2.82 (two doublets, *J* = 16.8 Hz, 2H), 0.91-0.89 (m, 6H).

MS (EI⁺): *m/z*, (%) 447 (21), 446 (13), 445 (13), 430 (7), 316 (27), 315 (30), 312 (33), 297 (98), 284 (14), 105 (100) and (ESI⁺): 448.3 *m/z* [M+2].

HRMS (ESI⁺) calcd for C₃₀ H₂₆ O₃ N [M + 1]⁺ 448.19127, found 448.19073.

(*S_a*) 10-(2-hydroxynaphthalen-1-yl)-2-((*S*)-1-phenylethyl)-2,3-dihydro-1H-naphtho [1,2-e][1,3]oxazin-9-ol [(*S_a*,*S*)-77]

Compound (*S_a*,*S*)-77 was prepared by same procedure as that of (±)-77.

Yield = 86.5 %.

(*S_a*) 10-(2-hydroxynaphthalen-1-yl)-2-((*R*)-1-phenylethyl)-2,3-dihydro-1H-naphtho[1,2-e][1,3]oxazin-9-ol [(*S_a*,*R*)-77]

Compound (*S_a*,*R*)-77 was prepared by same procedure as that of (±)-77.

Yield = 86.7 %.

(*R_a*) 10-(2-hydroxynaphthalen-1-yl)-2-((*S*)-1-phenylethyl)-2,3-dihydro-1H-naphtho[1,2-*e*][1,3]oxazin-9-ol [(*S_a*,*R*)-77]

Compound (*R_a*,*S*)-77 was prepared by same procedure as that of (±)-77.

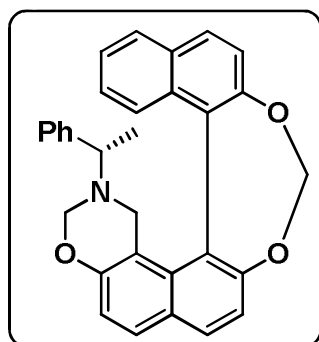
Yield = 85.6 %.

(*R_a*) 10-(2-hydroxynaphthalen-1-yl)-2-((*R*)-1-phenylethyl)-2,3-dihydro-1H-naphtho[1,2-*e*][1,3]oxazin-9-ol [(*R_a*,*R*)-77]

Compound (*R_a*,*R*)-77 was prepared by same procedure as that of (±)-77.

Yield = 83.2 %.

(±)-10-((*S*)-1-phenylethyl)-10,11-dihydro-9H-naphtho[1'',2'':6',7']-[1,3]dioxepino[4',5':7,8]naphtho[1,2-*e*][1,3]oxazine (78)



A solution of pure 2-benzyl-10-(2-hydroxynaphthalen-1-yl)-2,3-dihydro-1H-naphtho[1,2-*e*][1,3]oxazin-9-ol (0.7 g, 1.57 mmol) and anhydrous Cs₂CO₃ (2.55 g, 7.83 mmol) in dry DMF (5 mL) and CH₂I₂ (0.63 g, 2.35 mmol) was added and the mixture was stirred 48 h at room temperature under nitrogen atmosphere. After the completion of the reaction (tlc) the reaction mixture was poured in ice cold water. The

aqueous layer was extracted with chloroform (3 X 100 mL) combine the extract and washed with water (2 X 100 mL) and the organic layer was dried over Na₂SO₄ and evaporated to obtained crude solid. The crude product was purified by column chromatography over silica gel using petroleum ether/ethyl acetate as eluent (100:00 to 80:20) furnished mixture of diastereomers as a yellow solid (0.38 g, 53%).

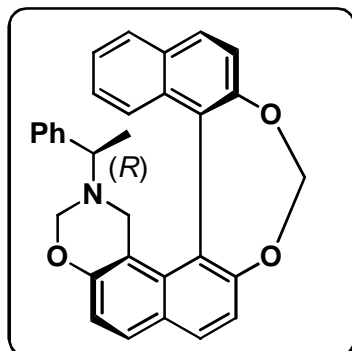
¹H NMR (CDCl₃, 400 MHz) δ 7.99-7.97 (d, *J* = 8.8 Hz, 1H), 7.94-7.77 (m, 7H), 7.49-7.47 (d, *J* = 8.8 Hz, 1H), 7.43-7.04 (m, 19H, including CDCl₃), 6.83-6.81 (m, 2H), 5.71-5.70 (m, 1.5H) 5.62 -5.56 (AB splitting, *J* = 20.8Hz, 2H), 4.94-4.91 (d, *J* = 9.6 Hz, 1H), 4.59-4.57 (dd, *J* = 9.6 & 0.8 Hz, 1H), 4.47-4.44 (d, *J* = 9.6 Hz, 0.6H), 4.36-4.33 (dd, *J* = 9.6 Hz, 1H), 3.52-3.37 (m, 3H), 2.96-2.92 (d, *J* = 16.8 Hz, 1H), 2.68-2.63 (d, *J* = 16.8 Hz, 1H), 2.33-2.30 (d, *J* = 9.6 Hz, 1H) 1.9-1.18 (d, *J* = 6.4 Hz, 3H), 0.98-0.96 (d, *J* = 6.4 Hz, 2H).

IR (KBr) ν 3058, 2968, 2894, 1611, 1509, 1463, 1449, 1326, 1268, 1233, 1200, 1155, 1129, 1104, 1039, 997, 927, 838, 807, 754, 700.

MS (ESI⁺): 460.2 m/z.

HRMS (ESI⁺) calcd for C₃₁ H₂₆ O₃ N [M + 1]⁺ 460.1913, found 460.1907.

(R_a)-10-((R)-1-phenylethyl)-10,11-dihydro-9H-naphtho[1'',2'':6',7']-[1,3]dioxepino[4',5':7,8]naphtho[1,2-e][1,3]oxazine [(R_a,R)-78]



Compound (R_a,R)-78 was prepared by same procedure as that of (±)-78.

Yield = 56.7 %.

M.p. 180-182 °C.

[α]_D²⁸ = - 828 (c = 0.1, CHCl₃).

¹H NMR (CDCl₃, 400 MHz): δ 7.87 (d, *J* = 8.8 Hz, 1H), 7.83 (d, *J* = 8.4 Hz, 1H), 7.76 (d, *J* = 8.8 Hz, 2H), 7.36-7.34 (m, 1H), 7.29-7.14 (m, 7H), 7.05 (d, *J* = 8.8 Hz, 1H), 6.82 (dd, *J* = 8.4 & 1.6 Hz, 2H), 5.62 (d, *J* = 3.6 Hz, 1H), 5.56 (d, *J* = 3.2 Hz, 1H), 4.92 (dd, *J* = 9.6 & 2.4 Hz, 1H), 4.57 (d, *J* = 9.6 Hz, 1H), 3.39 (q, *J* = 6.8 Hz, 1H), 2.85 (dd, *J* = 16.4 & 2 Hz, 1H), 2.66 (d, *J* = 16.4 Hz, 1H), 1.18 (d, *J* = 6.8 Hz, 3H).

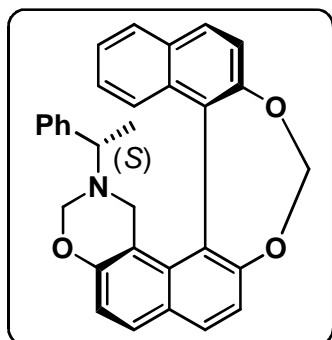
¹³C NMR (CDCl₃, 100.6 MHz): δ 153.68, 152.21, 149.36, 143.47, 133.26, 132.70, 131.00, 130.91, 129.54, 129.14, 128.63, 128.48, 128.22, 127.85, 126.92, 126.43, 124.85, 124.55, 123.47, 120.17, 117.97, 117.67, 113.09, 102.54 (O-CH₂-O), 78.70 (NCH₂O), 57.14 (ArCH₂N), 48.84 (NCH₂Ph), 20.25 (CH₃).

IR (KBr) ν 3054, 3019, 2973, 2909, 2851, 1610, 1509, 1454, 1323, 1274, 1140, 1007, 989, 890, 757, 700.

MS (ESI⁺): *m/z*, (%) 460 [M+1]

HRMS (ESI⁺) calcd for C₃₁H₂₆NO₃ [M + 1]⁺ 460.1913, found 460.1915.

(*R_a*)-10-((*S*)-1-phenylethyl)-10,11-dihydro-9H-naphtho[1'',2'':6',7']-[1,3]dioxepino [4',5':7,8] naphtho[1,2-e][1,3]oxazine [(*R_a,S*)-78]



Compound (*R_a,S*)-78 was prepared by same procedure as that of (\pm)-78.

Yield = 64.5 %.

M.p. 80-82 °C.

$[\alpha]_D^{28} = -402$ ($c = 0.4$, CHCl₃).

¹H NMR (CDCl₃, 400 MHz): δ 7.99 (d, $J = 8.8$ Hz, 1H), 7.92 (d, $J = 8.0$ Hz, 1H), 7.91 (d, $J = 8.8$ Hz, 1H), 7.82 (d, $J = 8.8$ Hz, 1H), 7.49 (d, $J = 8.8$ Hz, 1H), 7.43-7.39 (m, 1H), 7.32 (d, $J = 8.4$ Hz, 1H), 7.27-7.19 (m, 5H), 7.11-7.06 (m, 3H), 5.72-5.69 (broad singlet, 2H), 4.45 (d, $J = 9.6$ Hz, 1H), 4.35 (dd, $J = 9.6$ & 2.8 Hz, 1H), 3.53 (q, $J = 6.4$ Hz, 1H), 3.47 (dd, $J = 9.6$ & 2.8 Hz, 1H), 2.93 (d, $J = 16.8$ Hz, 1H), 0.95 (d, $J = 6.8$ Hz, 1H).

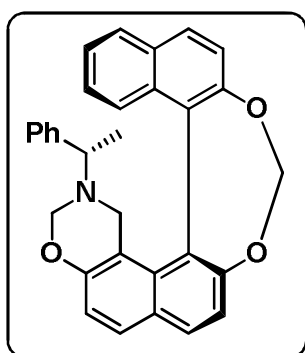
¹³C NMR (CDCl₃, 100.6 MHz): δ 153.53, 152.39, 149.65, 143.41, 133.20, 132.64, 131.29, 131.11, 130.08, 129.36, 129.06, 128.64, 128.37, 128.25, 128.21, 127.81, 127.45, 127.24, 126.91, 126.61, 126.41, 125.32, 125.07, 124.63, 123.33, 120.42, 118.06, 117.72, 112.80, 102.80 (O-CH₂-O), 79.87 (N-CH₂O), 56.33 (Ar-CH₂N), 47.53 (N-CH₂Ph), 21.12 (CH₃).

IR (KBr) ν 3058, 2968, 2894, 1611, 1509, 1463, 1449, 1326, 1268, 1233, 1200, 1155, 1129, 1104, 1039, 997, 927, 838, 754, 700.

MS (ESI⁺): m/z , (%) 460 [M+1]

HRMS (ESI⁺) calcd for C₃₁H₂₆NO₃ [M + 1]⁺ 460.1913, found 460.1938.

(*S_a*)-10-((*S*)-1-phenylethyl)-10,11-dihydro-9H-naphtho[1'',2'':6',7']-[1,3]dioxepino [4',5':7,8]naphtho[1,2-e][1,3]oxazine [(*S_a,S*)-78]



Compound (*S_a,S*)-78 was prepared by same procedure as that of 78.

Yield = 68.2 %.

M.p. 182-184 °C.

$[\alpha]_D^{28} = +742$ ($c = 0.1$, CHCl₃).

¹H NMR (CDCl₃, 400 MHz): δ 7.87 (d, *J* = 8.8 Hz, 1H), 7.83 (d, *J* = 8.4 Hz, 1H), 7.78 (d, *J* = 8.8 Hz, 2H), 7.36-7.34 (m, 1H), 7.29-7.14 (m, 7H) 7.05 (d, *J* = 8.8 Hz, 1H), 6.82 (dd, *J* = 8 & 1.6 Hz, 2H), 5.62 (d, *J* = 3.2 Hz, 1H) 5.56 (d, *J* = 3.2 Hz, 1H), 4.93 (dd, *J* = 9.6 & 2.4 Hz, 1H), 4.57 (d, *J* = 10 & 0.8 Hz, 1H), 3.39 (q, *J* = 6.8 Hz, 1H), 2.85 (dd, *J* = 16.8 & 1.6 Hz, 1H), 2.65 (d, *J* = 16.4 Hz, 1H), 1.18 (d, *J* = 6.8 Hz, 3H).

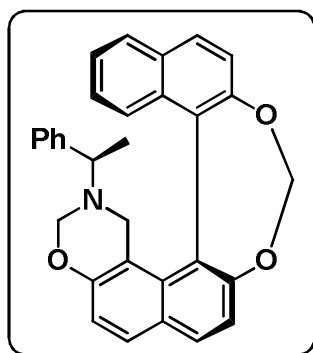
¹³C NMR (CDCl₃, 100.6 MHz): δ 153.67, 152.20, 149.35, 143.46, 133.25, 132.69, 131.99, 130.91, 129.53, 129.14, 128.62, 128.47, 128.21, 127.84, 126.91, 126.42, 124.85, 124.54, 123.46, 120.16, 117.96, 117.66, 113.08, 102.54 (O-CH₂-O), 78.69 (NCH₂O), 57.13 (ArCH₂N), 48.83 (NCH₂Ph), 20.24 (CH₃).

IR (KBr): ν 3054, 3020, 2974, 2911, 2850, 1610, 1509, 1454, 1323, 1275, 1246, 1140, 1007, 989, 891, 757, 700.

MS (ESI⁺): *m/z*, (%) 460 [M+1].

HRMS (ESI⁺) calcd for C₃₁H₂₆NO₃ [M + 1]⁺ 460.1913, found 460.1907.

(*S_a*)-10-((*R*)-1-phenylethyl)-10,11-dihydro-9H-naphtho[1'',2'':6',7']-[1,3]dioxepino[4',5':7,8]naphtho[1,2-*e*][1,3]oxazine [(*S_a*,*R*)-78]



Compound (*S_a*,*R*)-78 was prepared by same procedure as that of (±)-78.

Yield = 53.0 %.

M.p. 80-82 °C.

[α]_D²⁸ = + 638 (*c* = 0.4, CHCl₃).

¹H NMR (CDCl₃, 400 MHz): δ 7.98 (d, *J* = 8.8 Hz, 1H), 7.92 (m, 2H), 7.82 (d, *J* = 9.2 Hz, 1H), 7.49 (d, *J* = 8.4 Hz, 1H), 7.44-7.39 (m, 1H), 7.32 (d, *J* = 8.4 Hz, 1H), 7.27-7.16 (m, 5H), 7.11-7.06 (m, 3H), 5.72-5.69 (broad singlet, 2H), 4.45 (d, *J* = 9.6 Hz, 1H), 4.35 (dd, *J* = 9.6 & 2.8 Hz, 1H), 3.53 (q, *J* = 6.4 Hz, 1H), 3.42 (d, *J* = 9.6 Hz, 1H), 2.93 (d, *J* = 16.8 Hz, 1H), 0.95 (d, *J* = 6.8 Hz, 1H).

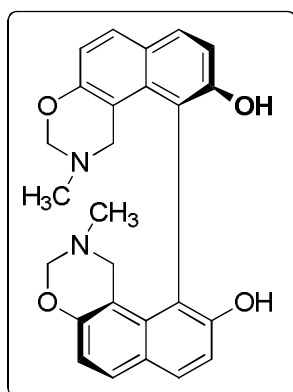
¹³C NMR (CDCl₃, 100.6 MHz): δ 153.53, 152.39, 149.65, 143.42, 133.20, 132.64, 131.30, 131.12, 130.09, 129.37, 129.07, 128.65, 128.37, 128.26, 128.21, 127.81, 127.46, 127.24, 126.91, 126.62, 125.07, 124.63, 123.33, 120.42, 118.06, 117.73, 112.29, 102.81 (O-CH₂-O), 79.87 (NCH₂O), 56.32 (ArCH₂N), 47.53 (NCH₂Ph), 21.13 (CH₃).

IR (KBr) ν 3058, 2968, 2894, 1611, 1509, 1463, 1449, 1326, 1268, 1233, 1200, 1155, 1129, 1104, 1039, 997, 927, 838, 754, 700.

MS (ESI⁺): m/z , (%) 460 [M+1]

HRMS (ESI⁺) calcd for C₃₁H₂₆NO₃ [M + 1]⁺ 460.1913, found 460.1927.

(*R_a*)-(-)-2,2'-Dimethyl-2,3,2',3'-tetrahydro-1H,1'H-[10,10']bi[naphtho[1,2-e][1,3]oxazinyl]-9,9'-diol [(*R_a*)-50]:



A solution of formaldehyde (0.324 g, 0.87 mL, 37 % w/v, 10.8 mmol) and methylamine (0.167 g, 0.42 mL, 40 % w/v, 6.91 mmol) in methanol (10 mL) was stirred at room temperature (30 min) under nitrogen atmosphere. This solution was treated with (*R_a*)-2,2',7,7'-tetrahydroxy-1,1'-binaphthyl (0.715 g, 2.24 mmol) and the solution was stirred at 60 °C (48 h). After the completion of the reaction the mixture was concentrated and the crude product was purified by column chromatography on silica

gel using light petroleum ether:ethyl acetate (100:0 to 60:40) as eluent to obtain a white solid (0.902 g, 94%).

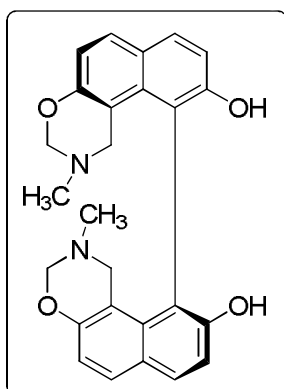
M.p. 190-192 °C.

$[\alpha]_D^{28} = -135$ ($c = 0.10$, CHCl₃).

¹H NMR (CDCl₃, 400 MHz) δ 7.84-7.82 (d, $J = 8.8$ Hz, 2H), 7.69-7.67 (d, $J = 8.8$ Hz, 2H), 7.15-7.13 (d, $J = 8.8$ Hz, 2H), 6.96-6.94 (d, $J = 8.8$ Hz), 5.07 (s, 2H, -OH), 4.74-4.72 (d, $J = 9.6$ Hz, 2H), 4.61-4.58 (d, $J = 9.6$ Hz, 2H), 3.64-3.60 (d, $J = 16.8$ Hz, 2H), 3.21-3.17 (d, $J = 16.8$ Hz, 2H), 2.28 (s, 6H).

MS (EI): m/z , (%) 429 (20), 428 (100), 427 (88), 426(82), 384 (31), 383 (36), 369 (42), 368 (54), 367 (43), 366 (50), 325 (37), 324 (33), 323 (30), 313 (69), 311 (50), 297 (35), 297 (35), 296 (44), 255 (30), 239 (32), 238 (40), 97 (31).

(*S_a*)-2,2'-dimethyl-2,2',3,3'-tetrahydro-1H,1'H-[10,10'-binaphtho[1,2-e][1,3]oxazine]-9,9'-diol [(*S_a*)-50]



Compound (*S_a*)-50 was prepared by same procedure as that of (*R_a*)-50.

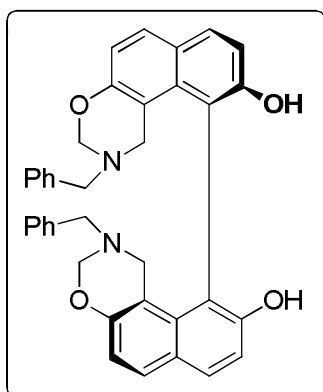
Yield = 0.824 g (86%).

M.p.190-192°C.

$[\alpha]_D^{28} = +137$ ($c = 0.1$ in CHCl_3).

$^1\text{H NMR}$ (CDCl_3 , 400 MHz): δ 7.84-7.82 (d, $J = 8.8$ Hz, 2H), 7.68-7.66 (d, $J = 8.8$ Hz, 2H), 7.15-7.12 (d, $J = 8.8$ Hz, 2H), 6.96-6.94 (d, $J = 8.8$ Hz), 5.07 (s, 2H, -OH), 4.74-4.72 (d, $J = 9.6$ Hz, 2H), 4.61-4.58 (d, $J = 9.6$ Hz, 2H), 3.64-3.60 (d, $J = 16.8$ Hz, 2H), 3.21-3.17 (d, $J = 16.8$ Hz, 2H), 2.28 (s, 6H).

(*R_a*)-(-)-2,2'-dibenzyl-2,2',3,3'-tetrahydro-1H,1'H-[10,10'-binaphtho[1,2-e][1,3]oxazine]-9,9'-diol [(*R_a*)-51]



A solution of formaldehyde solution (0.27 g, 37% w/v, 0.734 mL, 9.04 mmol) and benzylamine (0.49 g, 4.52 mmol) in methanol was stirred for 30 min under nitrogen atmosphere, to this solution (*aR*)-2,7,2',7'-tetrahydroxy-1,1'-binaphthyl (0.60 g, 1.88 mmol) was added in one portion. The solution was stirred for 48 h at 60 °C. After the completion of the reaction the mixture was concentrated and the crude product was purified by column chromatography on silica gel using

light petroleum ether:ethyl acetate (100:0 to 60:40) as eluent to obtain a white solid which was dried in vacuum (0.96 g, 87 %).

M.p.152-154 °C.

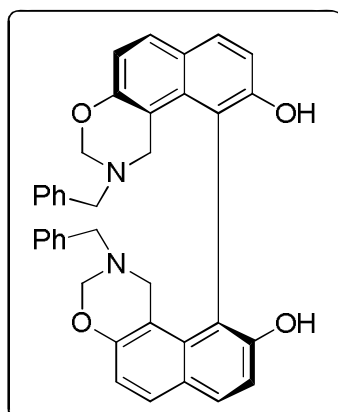
$[\alpha]_D^{28} = -257$ ($c = 0.10$, CHCl_3).

$^1\text{H NMR}$ (CDCl_3 , 400 MHz): δ 7.77-7.75 (d, $J = 8.8$ Hz, 2H), 7.64-7.62 (d, $J = 8.8$ Hz, 2H), 7.21-7.16 (m, 6H), 6.99-6.96 (m, 6H), 6.93-6.90 (d, $J = 8.8$ Hz, 2H) 4.98 (s, 2H), 4.66-4.63 (d, $J = 9.6$ Hz, 2H), 4.52-4.49 (d, $J = 9.2$ Hz, 2H), 3.55-3.54 (d, $J = 2$ Hz, 4H), 3.52-3.47 (d, $J = 16.8$ Hz, 2H), 3.24-3.20 (d, $J = 16.8$ Hz, 2H).

MS (EI) *m/z*, (%): 579 (09), 550 (06), 488 (11), 460 (10), 369 (09), 342 (13), 340 (07), 313 (48), 312 (52), 311 (62), 296 (24), 238 (48), 194 (78), 134 (32), 118 (94), 92 (12), 91 (100), 89 (08).

Anal. Calcd. for C₃₈H₃₂N₂O₄: C 78.60, H 5.55; N 4.82. Found: C 78.22, H 5.19, N 4.77.

(S_a)-2,2'-dibenzyl-2,2',3,3'-tetrahydro-1H,1'H-[10,10'-binaphtho[1,2-e][1,3]oxazine]-9,9'-diol [(S_a)-51]



Compound (S_a)-51 was prepared by same procedure as that of (R_a)-51.

Yield = 0.987 g (90%).

M.p. 152-154°C.

$[\alpha]_D^{28} = +234$ (*c* = 0.1 in CHCl₃).

¹H NMR (CDCl₃, 400 MHz): δ 7.77-7.75 (d, *J* = 8.8 Hz, 2H), 7.64-7.62 (d, *J* = 8.8 Hz, 2H), 7.21-7.16 (m, 6H), 6.99-6.96 (m, 6H), 6.93-6.91 (d, *J* = 8.8 Hz, 2H), 4.97 (s, 2H), 4.66-4.64 (d, *J* = 9.2 Hz, 2H), 4.52-4.49 (d, *J* = 9.6 Hz, 2H), 3.56-3.55 (d, *J* = 2 Hz, 4H), 3.52-3.47 (d, *J* = 17.2 Hz, 2H), 3.24-3.20 (d, *J* = 16.8 Hz, 2H).

¹³C NMR (CDCl₃, 100.6 MHz): δ 153.96 (Cq), 153.86 (Cq), 137.49 (Cq), 132.99 (CH), 132.80 (Cq), 129.55 (CH), 128.38 (2 X CH), 128.30 (2 X CH), 127.06 (CH), 125.55 (Cq), 117.25 (CH), 114.17 (CH), 111.90 (Cq), 111.84 (Cq), 80.78 (OCH₂N), 55.41 (ArCH₂N), 48.63 (NCH₂Ph).

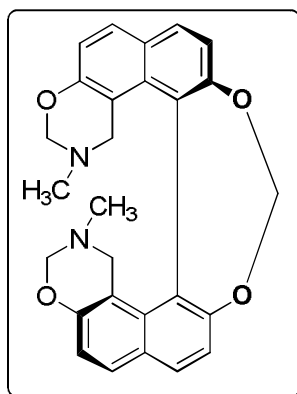
HPLC analysis:

Observed one peak of single enantiomer at R_t – 13.29 min.

Solvent System: Hexane: *Iso*-propanol (70:30), Flow rate: 0.5 mL/min.

Chiral Column: OD-H, UV: 233nm.

Synthesis of helicene like (*M*)-bis-oxazine [(*M*)-74]



A solution of pure (*R_d*)-**50** (0.70 g, 1.63 mmol) and Cs₂CO₃ (2.66 g, 8.16 mmol) in dry DMF (10 mL) was added CH₂I₂ (0.656 g, 2.44 mmol) and the mixture was stirred for 48 h at room temperature under nitrogen atmosphere. After the completion of the reaction (monitored by tlc) the mixture was poured in ice cold water. The aqueous layer was extracted with chloroform (3 X 100 mL) combine the extract and washed with water (2 X 100 mL) and the organic layer was dried over

Na₂SO₄ and evaporated to obtain brown viscous oil. The crude product was purified by column chromatography over silica gel using light petroleum ether:ethyl acetate (100:00 to 70:30) as eluent to get a white solid (0.220 g, 31 %).

M.p.196-198 °C.

$[\alpha]_D^{28} = -747$ ($c = 0.10$, CHCl₃).

¹H NMR (CDCl₃, 400 MHz): δ 7.88-7.85 (d, $J = 8.8$ Hz, 2H), 7.73-7.61 (d, $J = 8.8$ Hz, 2H), 7.31-7.29 (d, $J = 8.8$ Hz, 2H), 6.99-6.96 (d, $J = 8.8$ Hz, 2H), 5.67 (s, 2H), 4.56-4.54 (d, $J = 9.2$ Hz, 2H), 4.53-4.50 (dd, $J = 2.4$ Hz, 9.2 Hz, 2H), 2.70-2.66 (d, $J = 16.4$ Hz, 2H), 2.43-2.39 (d, $J = 16.4$ Hz, 2H), 2.06 (s, 6H).

MS (EI): m/z , (%) 440 (35), 439 (100), 410 (16), 408 (12), 396 (09), 382 (18), 380 (22), 354 (07), 353 (12), 352 (08), 323 (10), 312 (15), 311 (11), 278 (08), 239 (09), 238 (07).

HPLC condition:

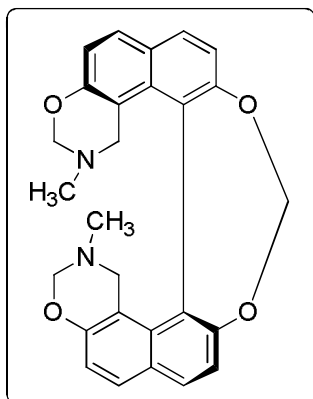
Observed one peak of single enantiomer at $R_t = 10.38$ min.

Solvent System: Hexane: *Iso*-propanol (70:30),

Flow rate: 0.5 mL/min,

Column: Lux Amylose 2, UV: 254 nm.

Synthesis of helicene like (*P*)-bis-oxazine [(*P*)-74]



Compound (*P*)-74 was prepared by same procedure as that of (*M*)-74.

Yield = 0.215 g (30%).

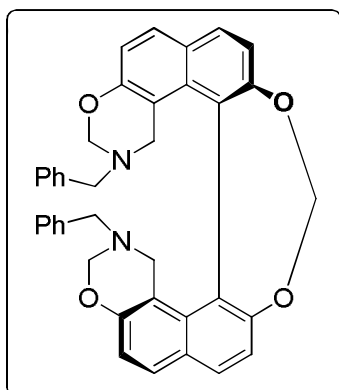
M.p.198-200°C.

$[\alpha]_D^{28} = +787$ ($c = 0.1$ in CHCl_3).

¹H NMR (CDCl_3 , 400 MHz): δ 7.88-7.85 (d, $J = 8.8$ Hz, 2H),

7.73-7.61 (d, $J = 8.8$ Hz, 2H), 7.31-7.29 (d, $J = 8.8$ Hz, 2H), 6.99-6.96 (d, $J = 8.8$ Hz, 2H), 5.67 (s, 2H), 4.56-4.54 (d, $J = 9.2$ Hz, 2H), 4.53-4.50 (dd, $J = 2.4$ Hz, 9.2 Hz, 2H), 2.70-2.66 (d, $J = 16.4$ Hz, 2H), 2.43-2.39 (d, $J = 16.4$ Hz, 2H), 2.06 (s, 6H).

Synthesis of helicene like (*M*)-bis-oxazine [(*M*)-75]



A solution of pure (*R_a*)-51 (0.70 g, 1.25 mmol) and anhydrous Cs_2CO_3 (2.04 g, 6.03 mmol) in dry DMF (10 mL) and CH_2I_2 (0.502 g, 1.87 mmol) was added and the mixture was stirred 48 h at room temperature under nitrogen atmosphere. After the completion of the reaction (tlc) the reaction mixture was poured in ice cold water. The aqueous layer was extracted with chloroform (3 X 100 mL) combine the extract and washed with water (2 X 100 mL) and the

organic layer was dried over Na_2SO_4 and evaporated to obtained crude solid. The crude product was purified by column chromatography over silica gel using a light petroleum ether/ethyl acetate as eluent (100:00 to 80:20) furnishing a white solid (0.385 g, 54%).

M.p.218-220°C.

$[\alpha]_D^{28} = -930$ ($c = 0.10$, CHCl_3).

¹H NMR (CDCl_3 , 400 MHz): δ 7.79-7.77 (d, $J = 8.8$ Hz, 2H), 7.72-7.70 (d, $J = 8.8$ Hz, 2H), 7.25-7.22 (m, 6H), 7.16-7.14 (d, $J = 8.8$ Hz, 2H), 7.01-6.97 (m, 6H), 5.61 (s, 2H), 4.61-4.58 (d, $J = 9.6$ Hz, 2H), 4.54-4.52 (dd, $J = 2$ Hz, 9.2 Hz, 2H), 3.42-3.39 (d, $J = 12.8$ Hz, 2H), 3.27-3.24 (d, $J = 12.8$ Hz, 2H), 2.75-2.71 (d, $J = 16.8$ Hz, 2H), 2.57-2.53 (d, $J = 16.4$ Hz, 2H).

¹³C NMR (CDCl₃, 100.6 MHz): δ 152.9 (Cq), 150.9 (Cq), 137.5 (Cq), 133.8 (Cq), 131.0 (CH), 129.6 (CH), 129.1 (2 X CH), 128.3 (2 X CH), 127.8 (Cq), 127.2 (CH), 126.3 (Cq), 118.0 (CH), 117.2 (CH), 112.1 (Cq), 102.1 (O-CH₂-O), 80.4 (NCH₂O), 54.5 (ArCH₂N), 49.5 (NCH₂Ph).

MS (EI) *m/z*, (%): 591 (16), 501 (11), 458 (09), 354 (10), 342 (18), 341 (21), 340 (15), 324 (13), 310 (16), 298 (15), 256 (27), 255 (28), 236 (31), 182 (36), 133 (16), 118 (22), 91 (100).

Anal. Calcd. for C₃₉H₃₂N₂O₄: C 79.03, H 5.44, N 4.73. Found: C 78.64, H 5.30, N 4.65.

HPLC condition:

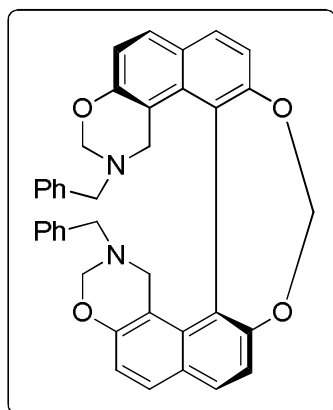
Observed one peak of single enantiomer at R_t = 15.25 min.

Solvent System: Hexane: *Iso*-propanol (85:15),

Flow rate: 0.5 mL/min.

Column: Lux Amylose 2, UV: 254nm.

Synthesis of helicene like (*P*)-bis-oxazine [(*P*)-75]



Compound (*P*)-75 was prepared by same procedure as that of (*M*)-75.

Yield = 0.398 g (65%).

M.p.218-220°C.

$[\alpha]_D^{28} = + 889$ ($c = 0.1$ in CHCl₃).

¹H NMR (CDCl₃, 400 MHz): δ 7.79-7.77 (d, *J* = 8.4 Hz, 2H), 7.73-7.70 (d, *J* = 8.8 Hz, 2H), 7.26-7.22 (m, 6H), 7.17-7.14 (d, *J* = 8.4 Hz, 2H), 7.02-6.97 (m, 6H), 5.62 (s, 2H), 4.61-4.59 (d, *J* = 9.2 Hz, 2H), 4.55-4.52 (dd, *J* = 2.4 Hz, 9.6 Hz, 2H), 3.42-3.39 (d, *J* = 12.8 Hz, 2H), 3.27-3.24 (d, *J* = 12.8 Hz, 2H), 2.75-2.71 (d, *J* = 16.8 Hz, 2H), 2.57-2.53 (d, *J* = 16.4 Hz, 2H).

¹³C NMR (CDCl₃, 100.6 MHz): δ 152.90 (Cq), 150.90 (Cq), 137.50 (Cq), 133.79 (Cq), 130.94 (CH), 129.61 (CH), 129.08 (2 X CH), 128.28 (2 X CH), 127.84 (Cq), 127.16 (CH), 126.31 (Cq), 118.03 (CH), 117.18 (CH), 112.09 (Cq), 102.09 (O-CH₂-O), 80.40 (NCH₂O), 54.49 (ArCH₂N), 49.45 (NCH₂Ph).

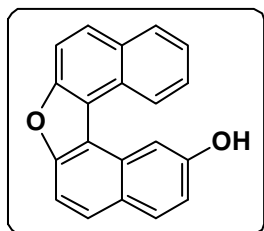
HPLC analysis:

Observed one peak of single enantiomer at R_t – 13.59 min.

Solvent System: Hexane: *Iso*-propanol (85:15),

Flow rate: 0.5 mL/min.

Chiral Column: Lux Amylose 2, UV: 254nm.

dinaphtho[2,1-b:1',2'-d]furan-2-ol or 2-hydroxy-7-oxa[5]helicene (80)

[1,1'-binaphthalene]-2,2',7-triol compound (**44**) (1 g, 3.31 mmol) was refluxed in toluene (20 mL) in the presence of *p*-TsOH (0.63 g 3.31 mmol) for 24 h. After quenching with saturated potassium carbonate solution, the crude product was extracted with ethyl acetate. The combine the extract and washed with water (2 X 100 mL) and the organic layer was dried over Na_2SO_4 and evaporated to obtained crude solid. The crude product was purified by column chromatography over silica gel using light petroleum ether/ethyl acetate as eluent (100:00 to 90:10) furnishing a white solid (0.58 g, 62%).

M.p.180-182 °C.

$^1\text{H NMR}$ (CDCl_3 , 400 MHz): δ 9.12 (d, J = 8.8 Hz, 1H, ArH), 8.50 (d, J = 2.4 Hz, ArH), 8.09 (d, J = 8.8 Hz, 1H, ArH), 7.99 (d, J = 8.4 Hz, 1H, ArH), 7.97 (d, J = 8.4 Hz, 1H, ArH), 7.90 (d, J = 8.8 Hz, 1H, ArH), 7.85 (d, J = 8.8 Hz, 1H, ArH), 7.77 (td, J = 6.8, 1.2 Hz, 1H, ArH), 7.71 (d, J = 8.8 Hz, 1H, ArH), 7.61 (td, J = 6.8, 1.2 Hz, 1H, ArH), 7.20 (dd, J = 8.8, 2.4 Hz, 1H, ArH), 5.37 (s, 1H, OH).

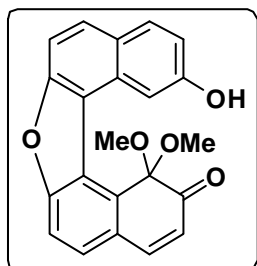
$^{13}\text{C NMR}$ (CDCl_3 , 100.6 MHz): δ 155.05 (Cq), 154.13 (Cq), 154.05 (Cq), 131.43 (CH), 131.21 (Cq), 130.04 (Cq), 129.55 (CH), 128.75 (Cq), 128.49 (Cq), 128.28 (CH), 128.10 (CH), 126.36 (Cq), 126.10 (CH), 125.58 (CH), 124.34 (CH), 118.46 (Cq), 115.54 (CH), 112.37 (CH), 110.37 (CH), 109.08 (CH).

IR (KBr): ν 3535, 3230 (OH), 3050, 1621, 1447, 1375, 1236, 1202, 1030, 996, 829, 803.

Mass (EI) m/z , (%): (M+1) 285 (21), (M) 284 (99), (M-H) 283 (100) and (ESI^{ve}) [M] 284.3.

HRMS (ESI⁺) calcd for $\text{C}_{20}\text{H}_{21}\text{O}_2$ (M)⁺ 284.0837, found 284.0839.

Synthesis of Compound (81)



Copper (II) chloride dihydrate (0.60 g, 3.52 mmol) and TEMED (0.43 g, 3.69 mmol) were taken in methanol (2 ml) under a nitrogen atmosphere. The solution was allowed to stand for 30 min at room temperature. After the solution had been purged with nitrogen for 5 min, a solution of 2-hydroxy-7-oxa[5]helicene **80** (0.1 g, 0.35 mmol) in degassed methanol (5 ml) was added, and the mixture was stirred at room temperature for 24 h under nitrogen. The reaction mixture was poured into the mixed solvent of 1 M hydrochloric acid solution and ethyl acetate. The organic layer was separated, washed successively with water and brine, and dried over sodium sulfate, and the solvent was evaporated to give a residue. The residue was purified by column chromatography on silica gel using light petroleum ether:ethyl acetate (100:0 to 95:5) as eluent to obtain an orange solid **81** (33 mg, 27%), M.p. 190-192 °C. And using ethyl acetate to collect impure **79** compound which was without purification converted to **78** compound.

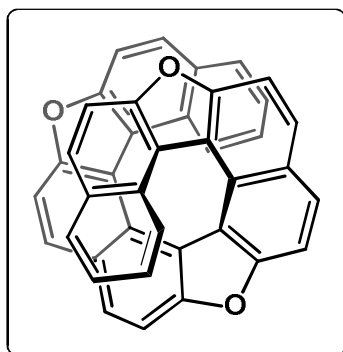
¹H NMR (CDCl₃, 400 MHz) δ 9.62 (d, *J* = 8.8 Hz, 1H, ArH), 8.04 (d, *J* = 8.8 Hz, 1H, ArH), 7.98 (dd, *J* = 8, 1.2 Hz, 1H, ArH), 7.77 (d, *J* = 8 Hz, 1H, ArH), 7.75 (d, *J* = 8 Hz, 1H, ArH), 7.70-7.67 (m, 1H, ArH), 7.58 (d, *J* = 10 Hz, 1H, ArH), 7.57 – 7.55 (m, 1H, ArH), 7.48 (d, *J* = 8.4 Hz, 1H, ArH), 6.26 (d, *J* = 10 Hz, 1H), 3.22 (s, 6H, OCH₃)

¹³C NMR (CDCl₃, 100.6 MHz) δ 194.71 (C=O), 158.01 (Cq), 156.17 (Cq), 147.75 (CH), 133.35 (Cq), 131.62 (CH), 131.26 (Cq), 129.95 (Cq), 129.49 (CH), 129.08 (CH), 128.38 (CH), 127.74 (Cq), 125.76 (CH), 125.04 (Cq), 124.49 (CH), 122.71 (CH), 117.43 (Cq), 113.56 (CH=CH), 112.07 (CH=CH), 97.64 [C(OCH₃)₂], 51.87 (2 × OCH₃).

IR (KBr) ν 3043, 1759, 1681, 1600, 1541, 1394, 1222, 1084, 998, 887, 800, 743, 624.

Mass (EI): *m/z*, (%) 344 (100).

HRMS [ESI⁺] calcd for C₂₂H₁₆O₄Na [M+Na]⁺ 367.0946, found 367.0951.

7, 12, 17-trioxa[11]helicene (78)

Compound **79** was refluxed in toluene (20 mL) in the presence of *p*-TsOH (80 mg w/w) for 24 h. After quenching with saturated potassium carbonate solution, the crude product was extracted with ethyl acetate. The combine the extract and washed with water (2 X 100 mL) and the organic layer was dried over Na₂SO₄ and evaporated to obtained crude solid. The crude product was purified by

column chromatography over silica gel using light petroleum ether/ethyl acetate as eluent (100:00 to 98:2) furnishing a yellow solid (36 mg, 37%).

M.p. 345 °C.

¹H NMR (CDCl₃, 400 MHz) δ 8.06 (d, *J* = 8.8 Hz, 1H, ArH), 8.01 (d, *J* = 8.4 Hz, 1H, ArH), 7.67 (d, *J* = 8.8 Hz, 1H, ArH), 7.61 (d, *J* = 8.4 Hz, 1H, ArH), 7.58 (d, *J* = 8.8 Hz, 1H, ArH), 7.36 (d, *J* = 8.8 Hz, 1H, ArH), 7.08 (d, *J* = 8.8 Hz, 1H, ArH), 7.07 (d, *J* = 8.4 Hz, 1H, ArH), 6.95 (td, *J* = 6.8, 1.2 Hz, 1H, ArH), 6.26 (td, *J* = 6.8, 1.2 Hz, 1H, ArH).

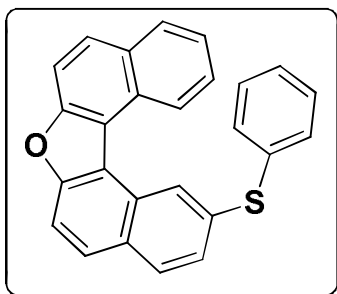
¹³C NMR (CDCl₃, 100.6 MHz) δ 154.97 (2 × Cq), 154.58 (2 × Cq), 152.27 (2 × Cq), 130.45 (2 × Cq), 129.26 (2 × CH), 128.73 (2 × Cq), 128.66 (2 × CH), 128.51 (2 × CH), 127.54 (2 × Cq), 127.05 (2 × CH), 125.06 (2 × CH), 124.65 (2 × CH), 123.68 (2 × Cq), 123.20 (2 × CH), 121.07 (2 × Cq), 120.58 (2 × Cq), 118.66 (2 × Cq), 110.78 (2 × CH), 110.64 (2 × CH), 110.39 (2 × CH).

IR (KBr) ν 1671, 1568, 1551, 1519, 1441, 1379, 1220, 1074, 1004, 840, 809.

MS (EI) *m/z*, (%) 548 (100).

HRMS [ESI⁺] calcd for C₄₀H₂₀O₃ [M]⁺ 548.1412, found 548.1422.

2-(phenylthio)dinaphtho[2,1-b:1',2'-d]furan (**83**)



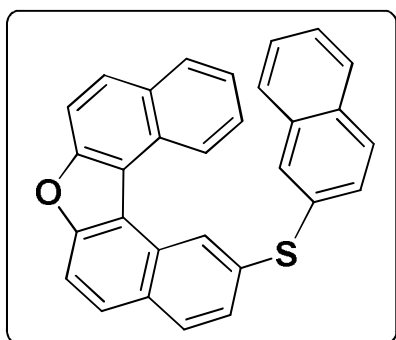
A solution of 2-hydroxy-7-oxa[5]helicene **80** (0.15 g, 0.05 mmol) and benzenethiol (7.3 mg, 0.08 mmol) in the presence of p-TsOH (0.10 g, 0.05 mmol) was refluxed in toluene for 24 h. The reaction was cooled down and then quenched with saturated NaHCO₃ solution. The crude product was extracted with ethyl acetate. The combine the extract and washed with water (2 X 100 mL) and the organic layer was dried over Na₂SO₄ and evaporated to obtained crude solid. The crude product was purified by column chromatography over silica gel using light petroleum ether/ethyl acetate as eluent (100:00 to 95:5) furnishing a white solid (0.165 g, 83%).

M.p. 146-148 °C.

¹H NMR (CDCl₃, 400 MHz): δ 9.14(d, *J* = 0.8 Hz, 1H), 8.76 (d, *J* = 8.4 Hz, 1H), 8.04 (d, *J* = 7.6 Hz, 1H), 7.99 (d, *J* = 8.4 Hz, 1H), 7.95 (d, *J* = 8.4 Hz, 1H), 7.92 (d, *J* = 8 Hz, 1H), 7.82 (d, *J* = 8.8 Hz, 2H), 7.59-7.51 (m, 4H), 7.46-7.37 (m, 4H).

¹³C NMR (CDCl₃, 100.6 MHz): 154.70, 154.37, 135.61, 134.86, 131.87, 131.13, 130.16, 129.90, 129.52, 129.43, 129.15, 128.51, 128.41, 128.01, 127.61, 126.97, 126.55, 126.33, 125.21, 124.30, 119.12, 118.98, 112.77, 112.58.

2-(naphthalen-2-ylthio)dinaphtho[2,1-b:1',2'-d]furan (**85**)



Compound **85** was prepared by same procedure as that of **83**.

Yield = 70%.

M.p. 166-168 °C.

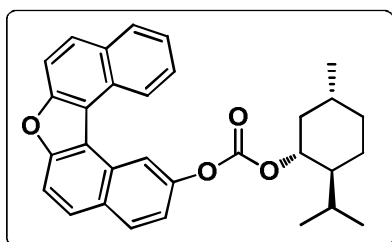
¹H NMR (CDCl₃, 400 MHz) δ 9.11(d, *J* = 1.2 Hz, 1H), 8.58 (d, *J* = 8.4 Hz, 1H), 8.14 (d, *J* = 1.2 Hz, 1H), 8.02 (d, *J* = 8.4 Hz, 1H), 7.94 (d, *J* = 8.8 Hz, 1H), 7.92-7.79 (m, 7H), 7.62-7.55 (m, 4H), 7.29-7.28 (m, 1H), 6.73-6.69 (m, 1H).

¹³C NMR (CDCl₃, 100.6 MHz): δ 154.69, 154.32, 135.24, 134.03, 132.75, 132.43, 131.25, 131.01, 130.18, 129.62, 129.27, 129.23, 129.19, 128.47, 128.32, 128.02, 127.88, 127.67, 126.80, 126.59, 126.45, 126.18, 126.00, 124.96, 124.22, 119.07, 118.95, 112.71, 112.49.

MS (EI): *m/z*, (%) 427 (23), 426 (91), 425 (87), 424(100), 423 (23).

HRMS [ESI⁺] calcd for C₃₀H₁₈OS (M)⁺ 426.1078 found 426.1051.

Dinaphtho[2,1-b:1',2'-d]furan-2-yl((1R,2S,5R)-2-isopropyl-5-methylcyclohexyl) carbonate (87)



To the solution of 2-hydroxy-7-oxa[5]helicene **80** (0.20 g, 0.70 mmol) and triethylamine (0.08 g, 0.77 mmol) in dichloromethane was added (1R,2S,5R)-(-)-menthyl chloroformate (0.17 g, 0.77 mmol) drop wise at 0 °C under N₂ atmosphere. After the completion of the

reaction (tlc) the reaction mixture was poured in ice cold water. The aqueous layer was extracted with dichloromethane (2 X 50 mL) combine the extract and washed with water (2 X 50 mL) and the organic layer was dried over Na₂SO₄ and evaporated to obtained crude solid. The crude product was purified by column chromatography over silica gel using petroleum ether/ethyl acetate as eluent (100:00 to 95:5) furnishing a white solid (0.325 g, 99%).

M.p. 106-108 °C.

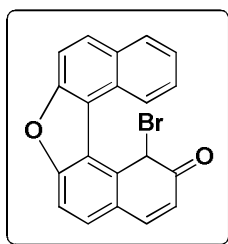
$[\alpha]_D^{28} = -40$ (*c* = 0.3, chloroform).

¹H NMR (CDCl₃, 400 MHz): δ 9.15 (d, *J* = 8.8 Hz, 1H), 9.04 (d, *J* = 2 Hz, 1H), 8.10 (d, *J* = 8.8 Hz, 2H), 7.97 (d, *J* = 8.8 Hz, 2H), 7.84 (d, *J* = 8.8 Hz, 2H), 7.79-7.75 (m, 1H), 7.63-7.59 (m, 1H), 7.44 (dd, *J* = 8.8 & 2.4 Hz, 1H), 4.77 (m, 1H), 2.32-2.27 (m, 1H), 2.17-2.13 (m, 1H), 1.80-1.74 (m, 2H), 1.62-1.54 (m, 3H), 1.29-1.11 (m, 2H), 1.01 (d, *J* = 6.8 Hz, 6H), 0.92 (d, *J* = 7.2 Hz, 3H).

¹³C NMR (CDCl₃, 100.6 MHz): δ 154.71, 154.35, 153.53, 149.13, 131.21, 130.80, 129.49, 129.00, 128.53, 128.49, 127.95, 126.50, 125.63, 124.50, 119.55, 119.13, 118.63, 116.82, 112.65, 112.57, 79.76, 47.08, 40.73, 34.09, 31.51, 26.33, 23.42, 22.06, 20.79, 16.46.

IR (KBr): ν 3052, 2953, 2867, 1746, 1623, 1529, 1375, 1260, 1242, 1192, 1027, 949, 830, 807, 743cm⁻¹.

1-bromodinaphtho[2,1-b:1',2'-d]furan-2(1H)-one (**89**)



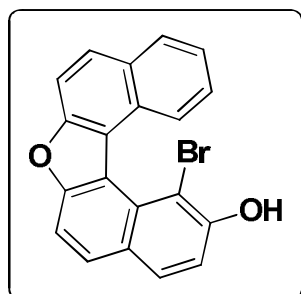
A solution of KBrO_3 (0.02 g, 0.12 mmol) and KBr (0.03 g, 0.23 mmol) in $\text{MeOH-H}_2\text{O}$ (2:1) was added compound **80** (0.10 g, .35 mmol) then slowly added HCl (0.026 g, 30%, 0.70 mmol) at room temperature. After completion of the reaction, it was poured on ice-cold water and extracted with ethylacetate (2 X 50 mL), the organic layer was washed with water, dried over sodium sulphate and concentrated at reduced pressure to obtain the crude product. The purification of the compound by crystallization in ethyl acetate gave orange product **89** (0.0.75 g, 59%).

M.p. 142-144 °C.

$^1\text{H NMR}$ (CDCl_3 , 400 MHz): δ 9.10 (d, $J = 8.8$ Hz, 1H), 8.07-8.03 (two doublet merged, $J = 8.4$ Hz, 2H), 7.87-7.82 (m, 1H), 7.76 (d, $J = 8.8$ Hz, 1H), 7.72 (d, $J = 8.4$ Hz, 1H), 7.65-7.61 (m, 2H), 7.51 (d, $J = 8.4$ Hz, 1H), 6.44 (s, 1H), 6.39 (d, $J = 9.6$ Hz)

IR (KBr): ν 3066, 3019, 2891, 1560, 1481, 1463, 1430, 1213, 1158, 930, 767, 747, 641.

1-bromodinaphtho[2,1-b:1',2'-d]furan-2-ol (**90**)

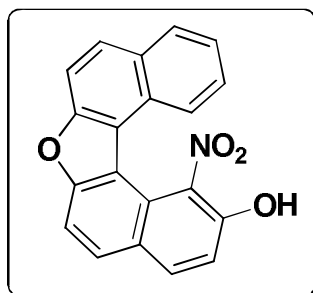


A solution of 2-hydroxy-7-oxa[5]helicene **80** (0.10 g, 0.35 mmol), N -bromosuccinimide (0.06 g, 0.35 mmol) acetonitrile (5 mL) was stirred at room temperature for 12 h. After the completion of the reaction, the mixture was poured in water and extracted with chloroform (2 X 25 mL), the organic layer was washed with the water, dried over sodium sulphate and concentrated at reduced pressure to obtain the crude solid. The purification of the compound by column chromatography over silica gel using (petroleum ether:ethylacetate, 100:00 to 95:5) gradient for the elution to obtain the compound (0.08 g, 68%).

$^1\text{H NMR}$ (CDCl_3 , 400 MHz): δ 8.43-8.40 (m, 1H), 8.00-7.99 (m, 1H), 7.98-7.94 (two doublets merged, $J = 8.8$ Hz, 2H), 7.84-7.81 (two doublets merged, $J = 8.8$ Hz, 2H), 7.69 (d, $J = 8.8$ Hz, 1H), 7.55-7.49 (m, 2H), 7.38 (d, $J = 8.8$ Hz, 1H), 6.22 (s, 1H).

MS (ESI) ($\text{M} + 1$) 384.

1-nitrodinaphtho[2,1-b:1',2'-d]furan-2-ol (**92**)



A solution of 2-hydroxy-7-oxa[5]helicene **80** (0.20 g, 0.70 mmol) and nitric acid (0.066 g, 0.047 mL, 1.05 mmol) in chloroform (5 mL) was kept in ultrasound sonicator at room temperature for 2 h. After completion of the reaction, it was poured on ice-cold water and extracted with ethylacetate (2 X 50 mL), the organic layer was washed with water, dried over sodium sulphate and concentrated at reduced pressure to obtain the crude yellow solid. The purification of the compound by column chromatography over silica gel using (petroleum ether:ethylacetate, 100:00 to 80:20) gradient for the elution obtained the compound (0.194 g, 84%).

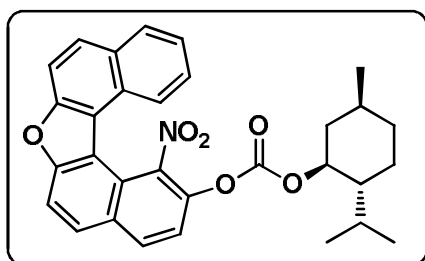
¹H NMR (CDCl₃, 400 MHz): δ 8.33 (d, *J* = 9.2 Hz, 1H), 8.15-8.06 (three doublets merged, *J* = 8.8 Hz, 3H), 7.97-7.94 (two doublets merged, *J* = 8.8 & 9.2 Hz, 2H), 7.55-7.46 (m, 2H), 7.42 (d, *J* = 8.8 Hz, 1H).

¹³C NMR (CDCl₃, 100.6 MHz): δ 161.18, 160.08, 157.98, 142.40, 136.84, 135.21, 134.42, 134.08, 133.88, 130.76, 130.68, 129.78, 129.61, 126.99, 124.17, 122.94, 121.37, 117.44, 116.62.

MS (ESI) [M + Na] 352.0577 *m/z*.

HRMS [ESI⁺] calcd for C₂₀H₁₁NO₄ [M + Na] 352.0586 found 352.0576.

(1R,2S,5R)-2-isopropyl-5-methylcyclohexyl(1-nitrodinaphtho[2,1-b:1',2'-d]furan-2-yl)carbonate (**93**)



Compound **93** was prepared by same procedure as that of **87**.

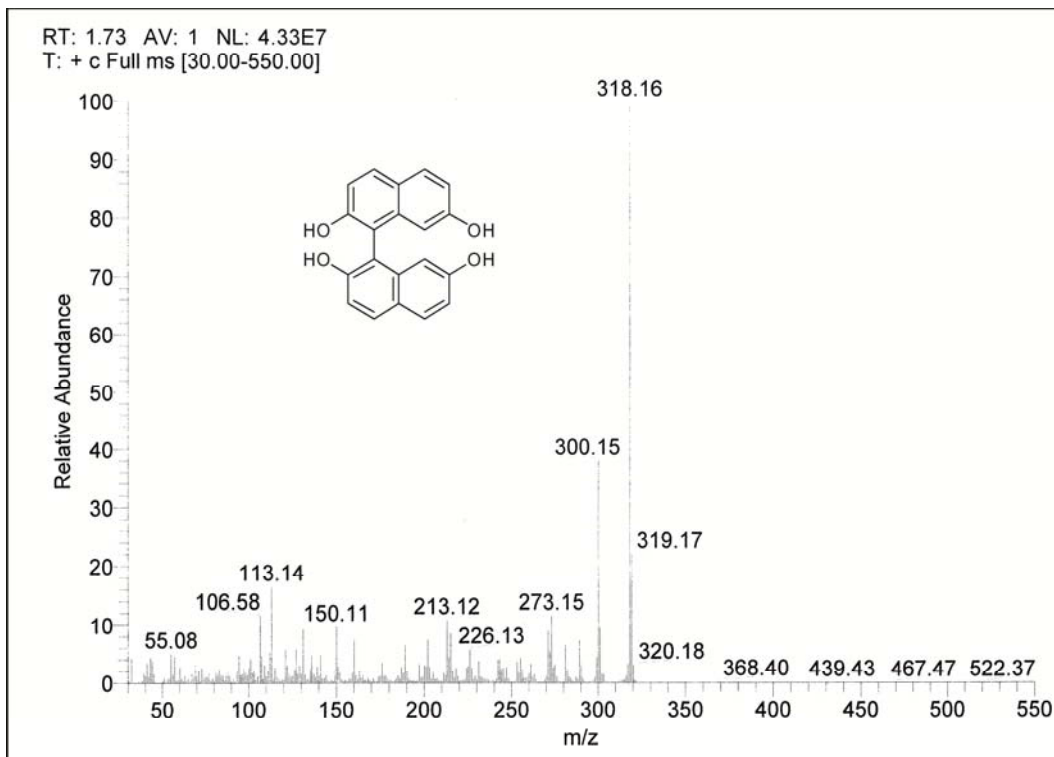
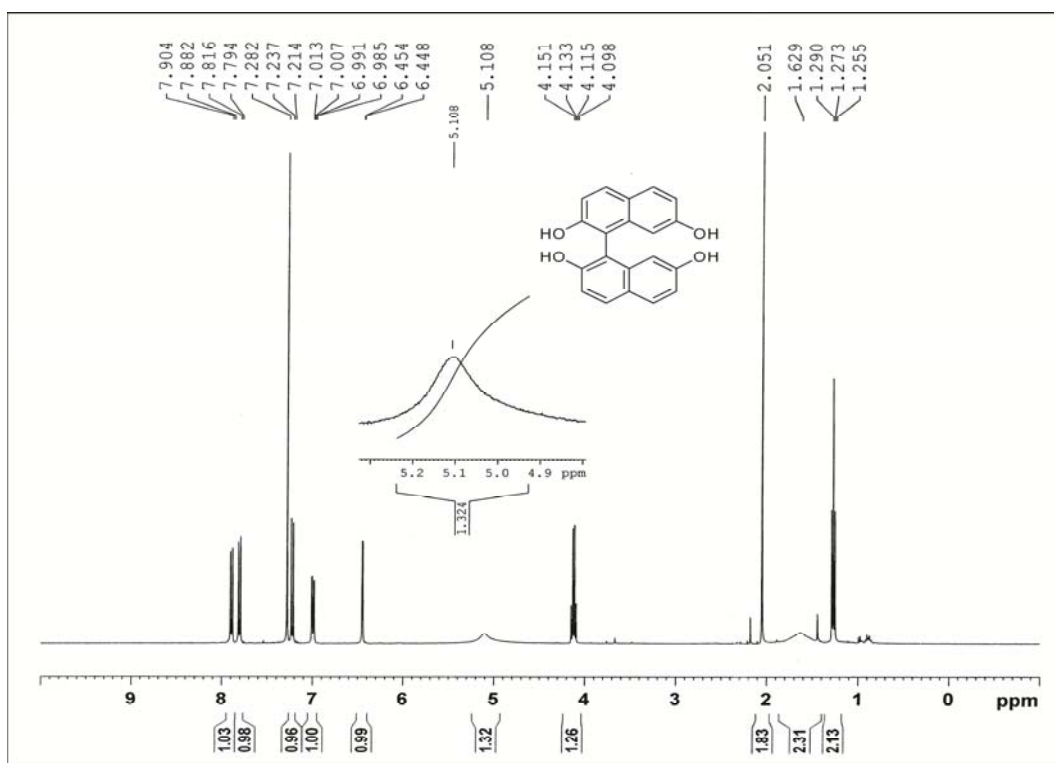
Yield = 96 %

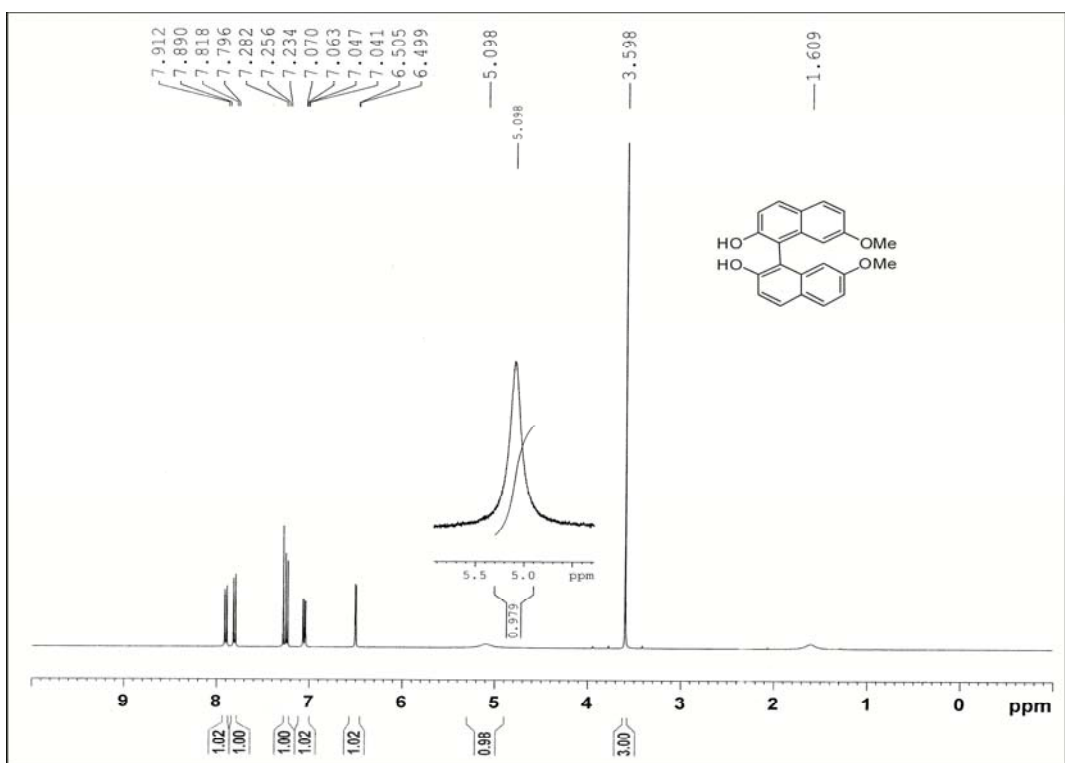
¹H NMR (CDCl₃, 400 MHz): δ 8.30 (d, *J* = 8.8 Hz, 1H), 8.25-8.23 (m, 1H), 8.02-7.96 (m, 4H), 7.81 (d, *J* = 9.2 Hz, 1H), 7.54-7.52 (m, 2H), 7.50 (d, *J* = 8.8 Hz, 1H), 4.86 (broad multiplet signal, 1H), 2.92 (broad multiplet signal, 2H), 1.82-1.81 (m, 2H), 1.79-1.76 (m, 3H), 1.64-1.60 (m, 1H), 1.58-1.28 (m, 1H), 1.20-0.97 (m, 9H).

¹³C NMR (CDCl₃, 100.6 MHz): δ 156.31, 153.87, 152.90, 145.28, 138.96, 135.84, 130.45, 130.36, 129.52, 129.38, 128.73, 127.74, 125.81, 124.92, 121.93, 120.31, 119.27, 117.48, 114.56, 112.11, 101.59, 81.04, 46.98, 34.05, 31.55, 26.05, 23.26, 22.09, 20.79, 16.26.

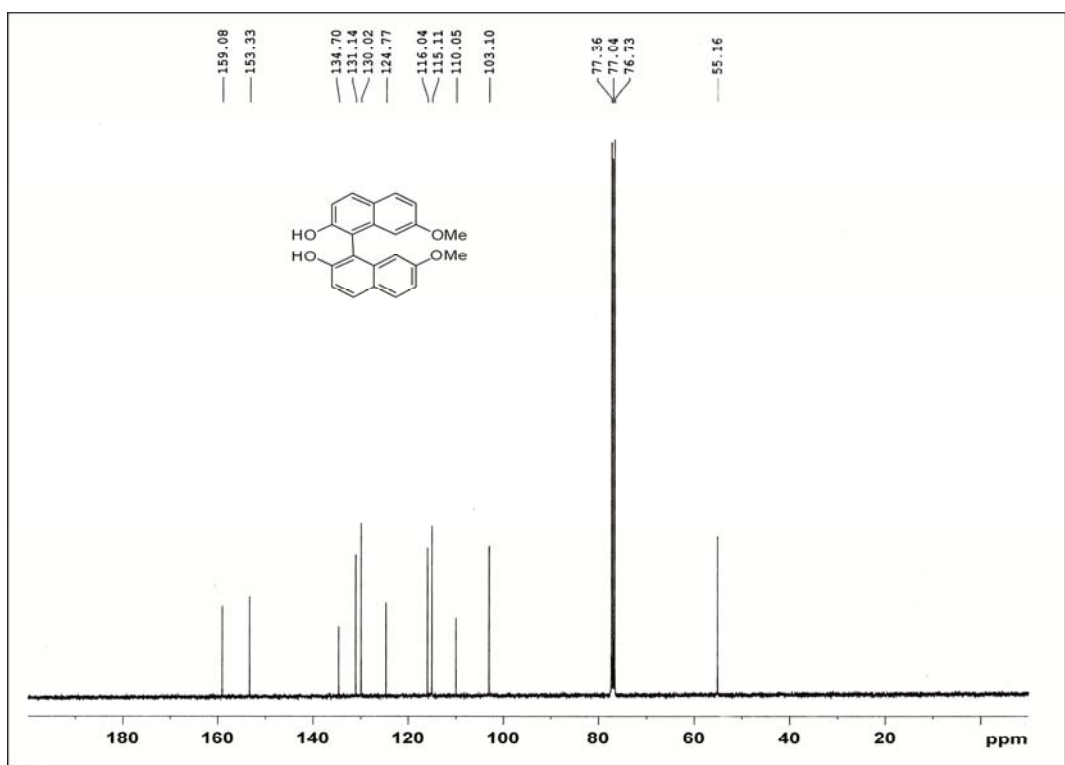
HRMS [ESI⁺] calcd for C₃₁H₂₉NO₆ [M + Na] 534.1893 found 534.1888

3.5 Spectral data

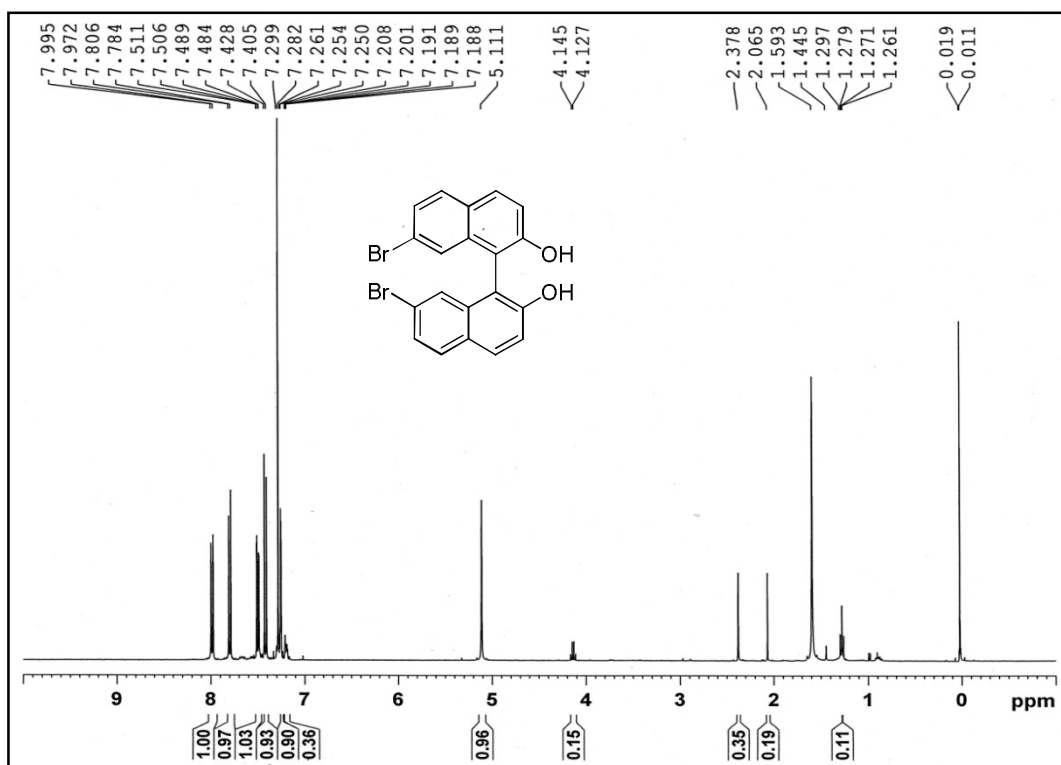




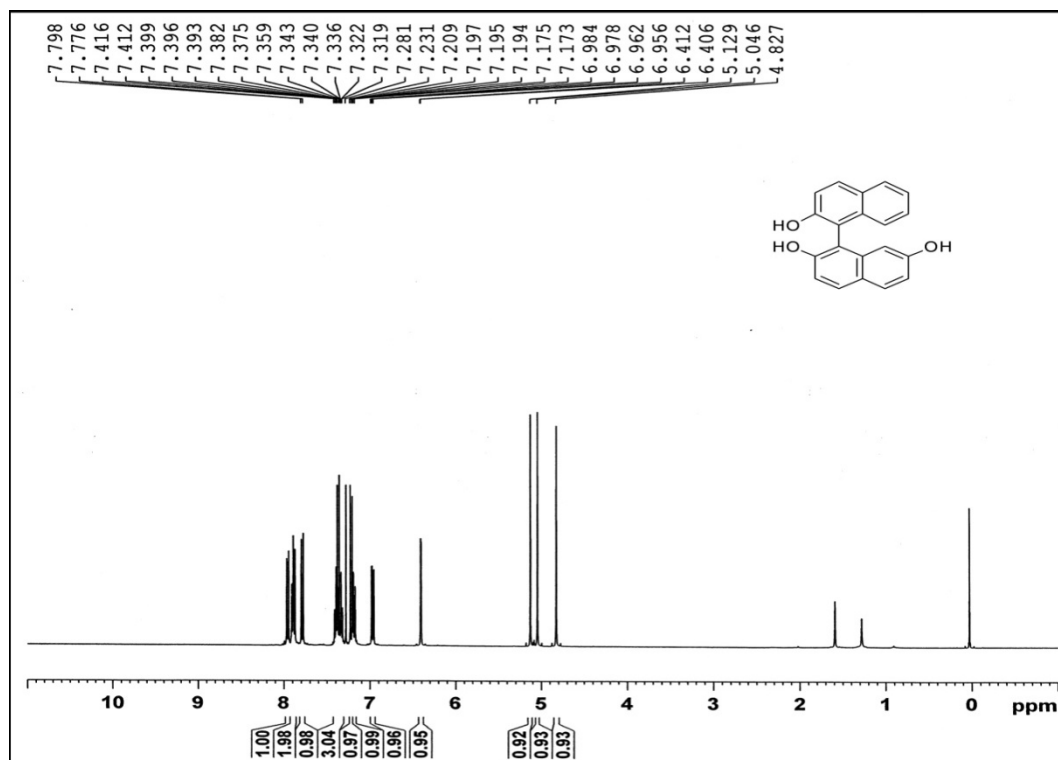
¹H-NMR spectrum of 7,7'-dimethoxy-2,2'-binaphthol (42)



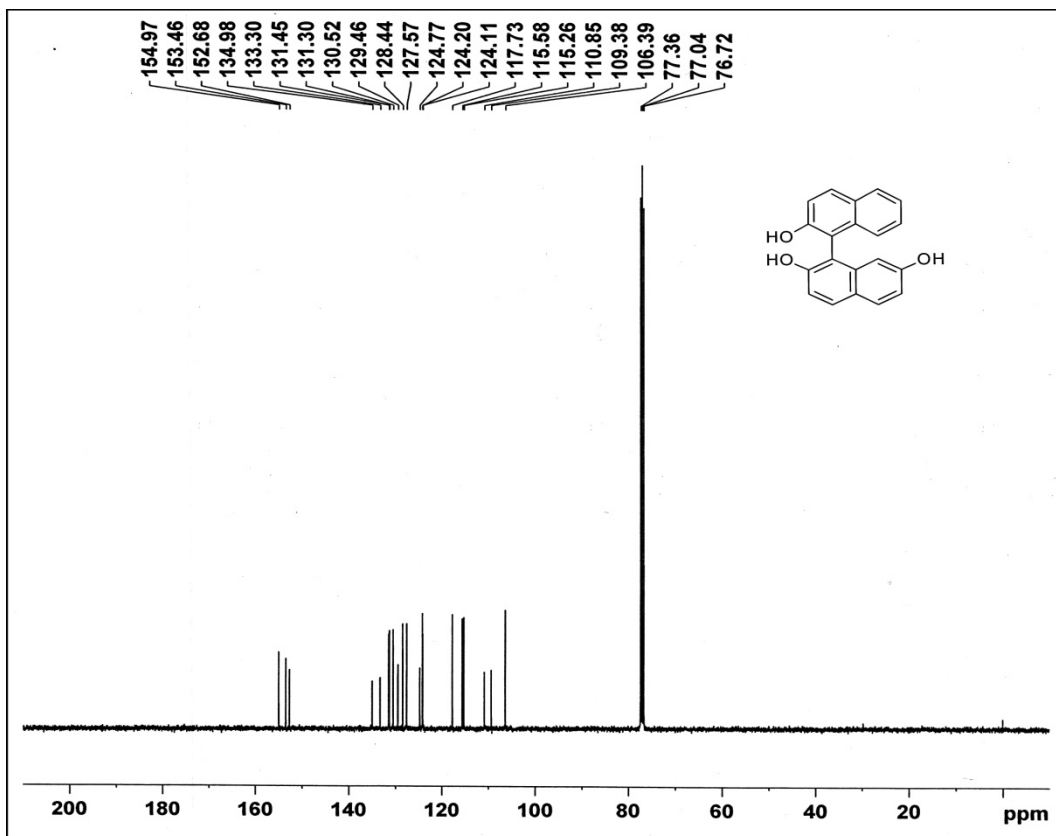
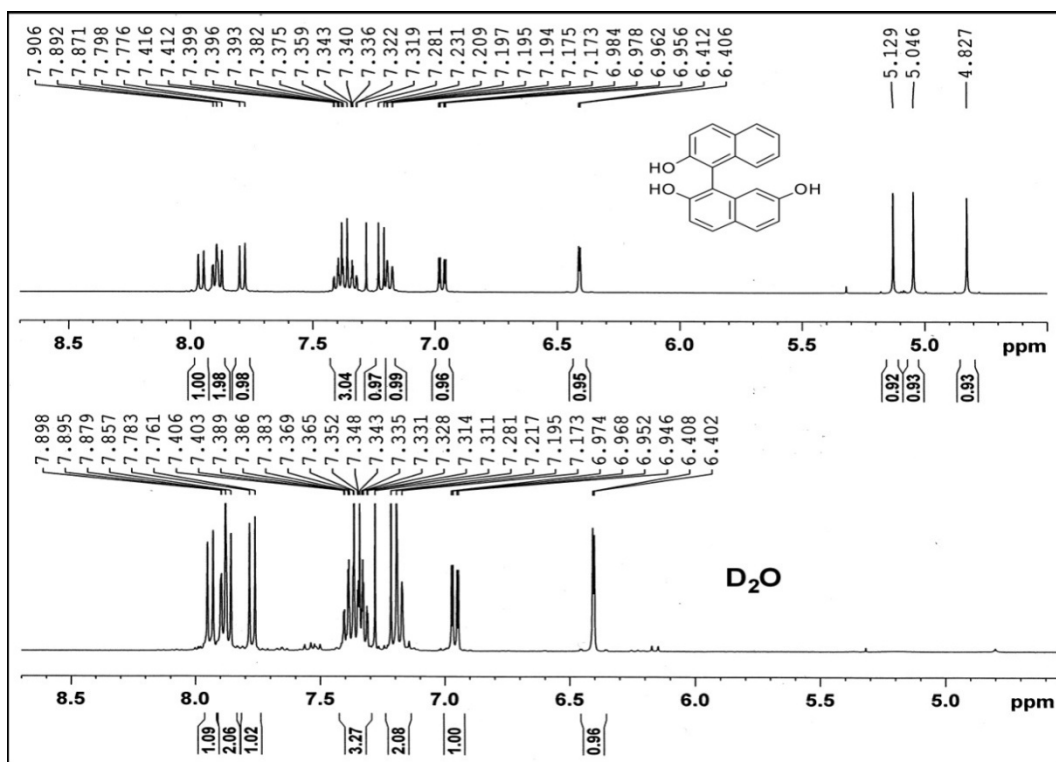
¹³C-NMR spectrum of 7,7'-dimethoxy-2,2'-binaphthol (42)



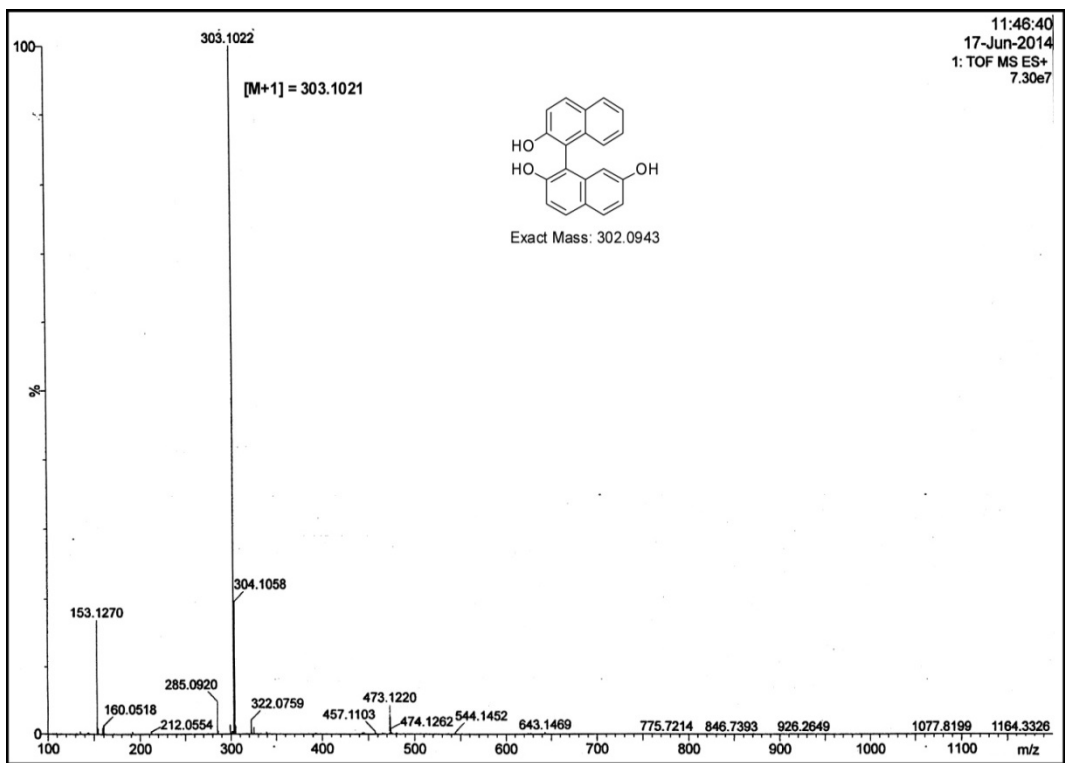
¹H-NMR spectrum of 7,7'-dibromo-[1,1'-binaphthalene]-2,2'-diol (43)



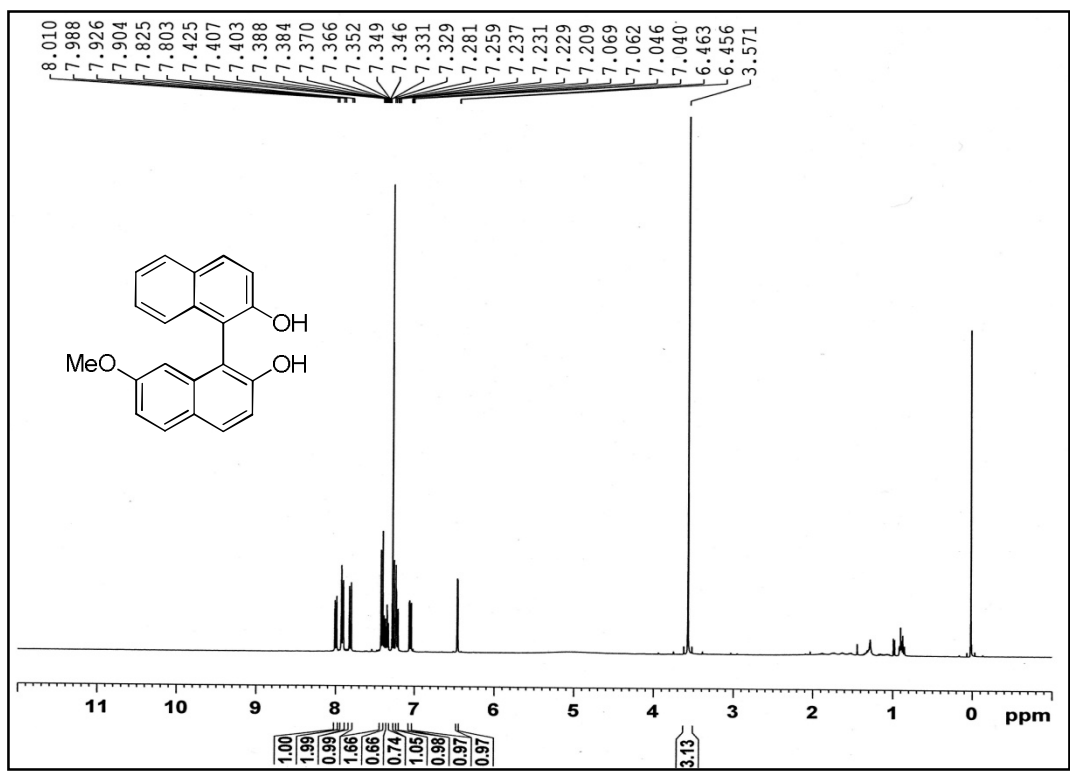
¹H-NMR Spectrum of 1,1'-binaphthalenyl-2,2',7-triol (44)



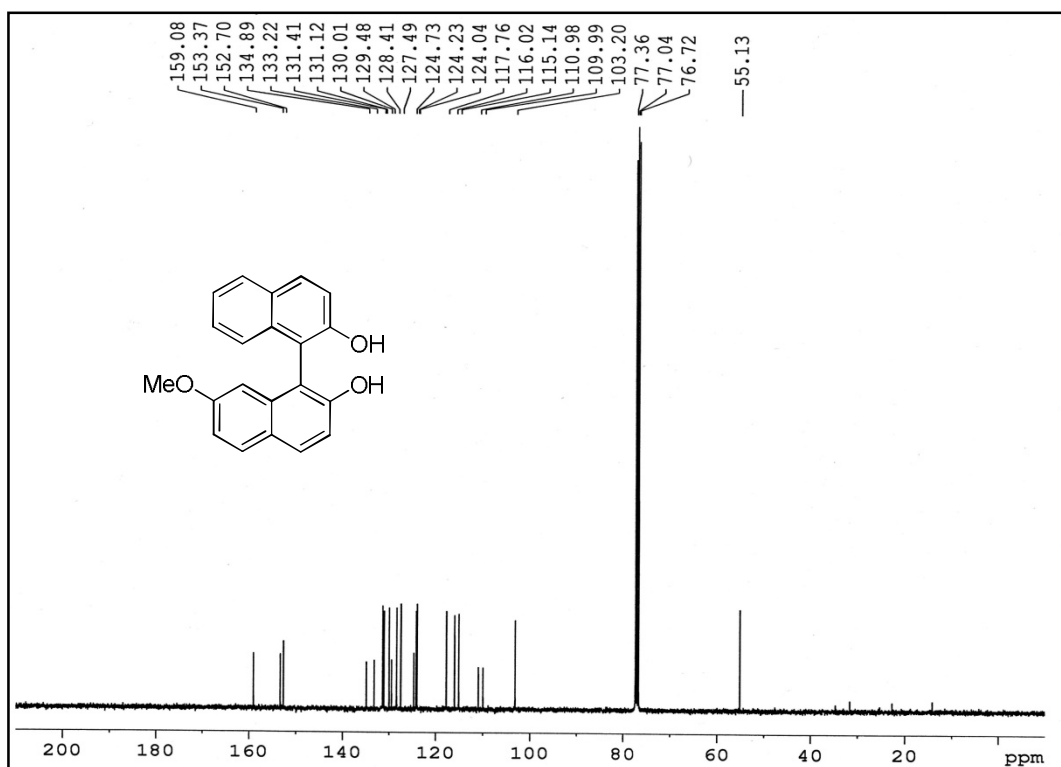
¹³C-NMR spectrum of 1,1'-binaphthalenyl-2,2',7-triol (44) in CDCl₃ on 100.6 MHz



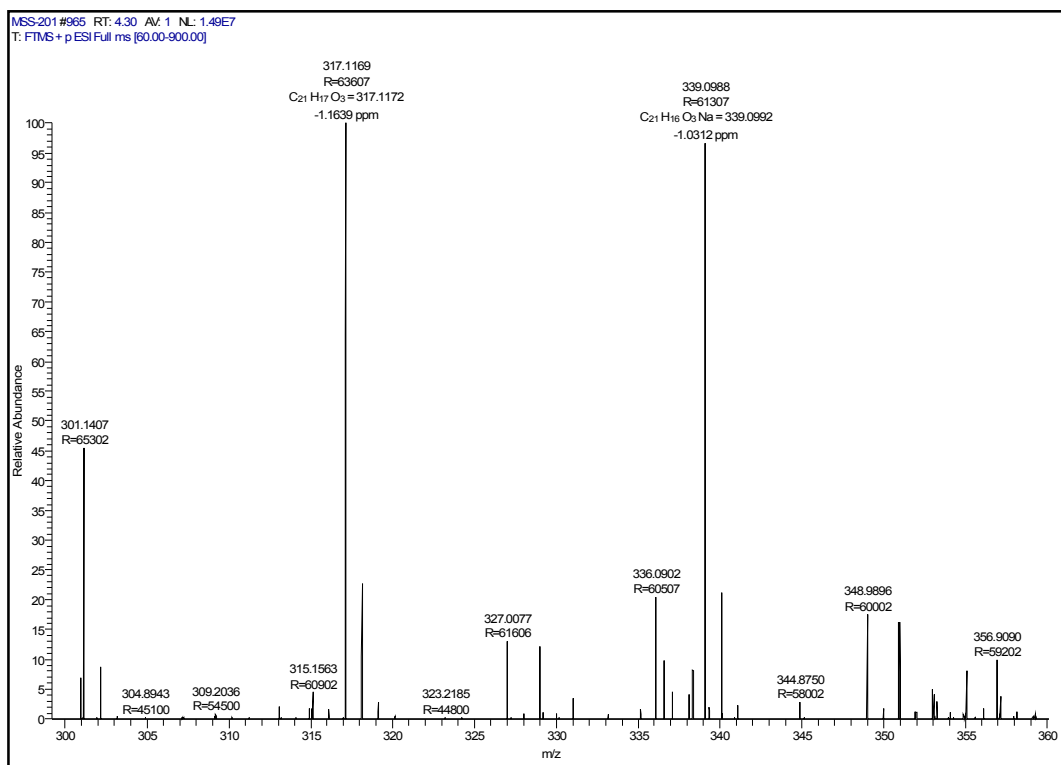
HRMS spectrum of 1,1'-binaphthalenyl-2,2',7-triol (44)



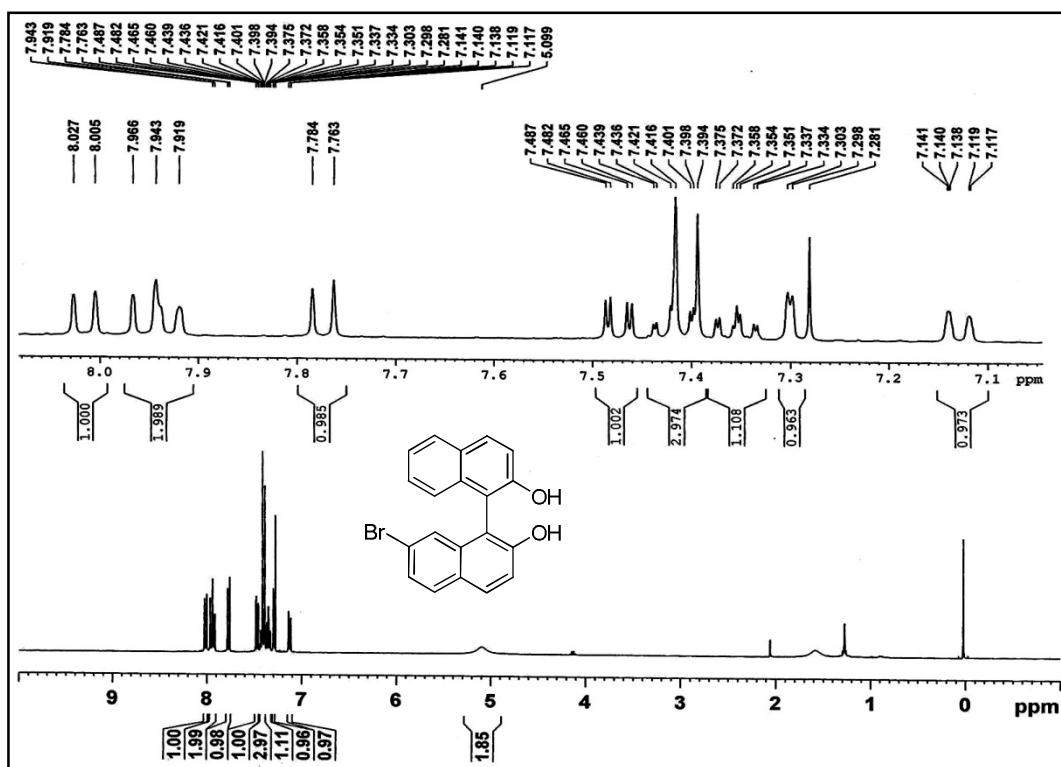
¹H-NMR spectrum of 7-methoxy-[1,1'-binaphthalene]-2,2'-diol (45)



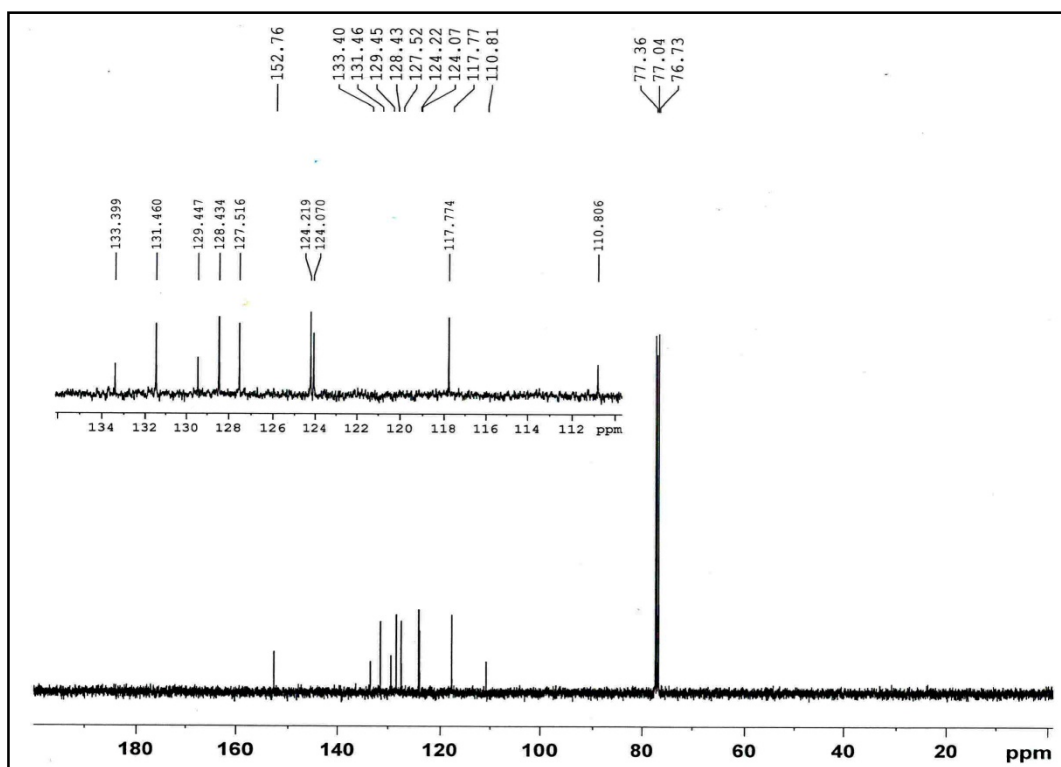
¹³C-NMR spectrum of 7-methoxy-[1,1'-binaphthalene]-2,2'-diol (45)



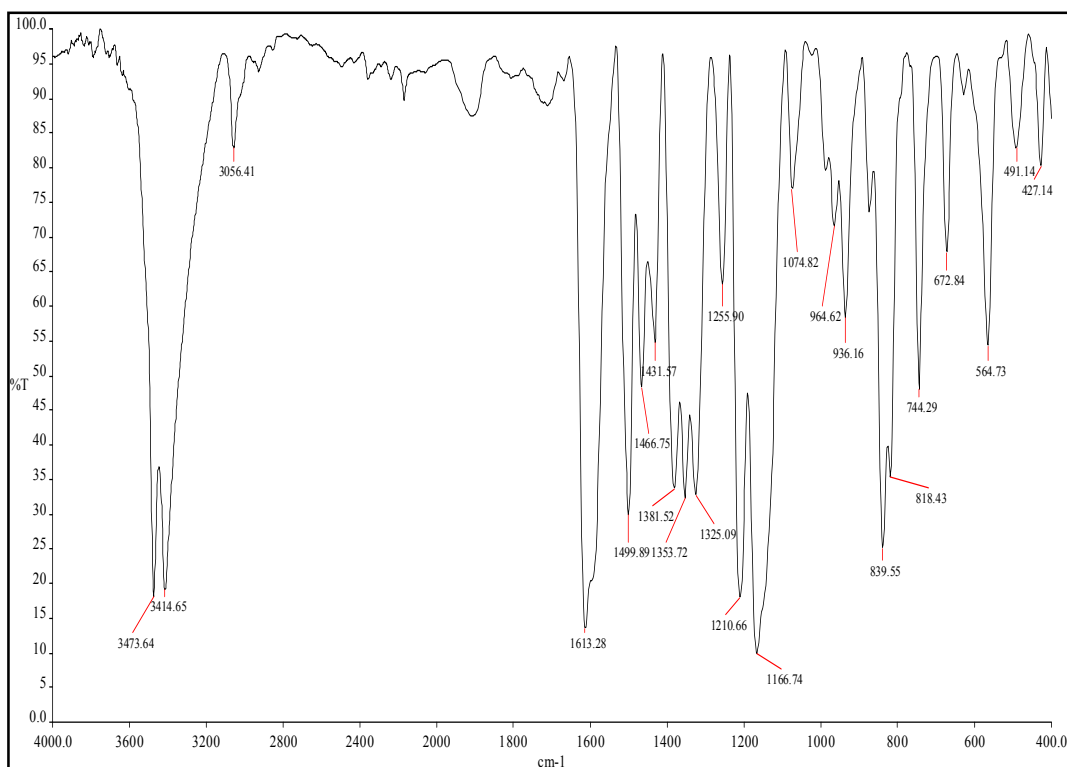
HRMS spectrum of 7-methoxy-[1,1'-binaphthalene]-2,2'-diol (45)



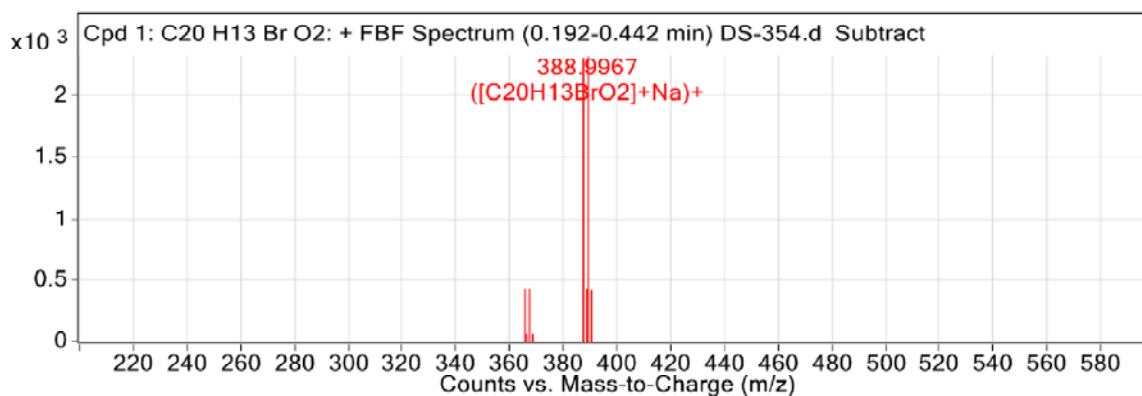
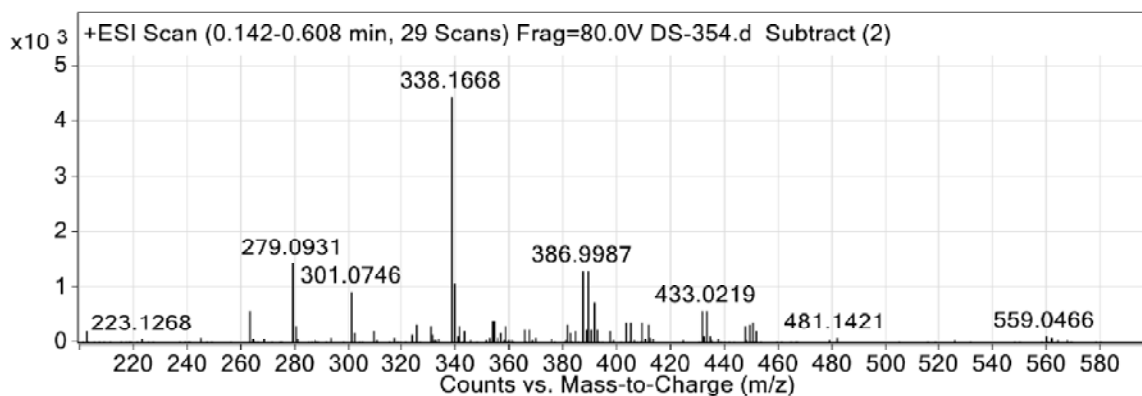
¹H-NMR spectrum of 7-bromo-[1,1'-binaphthalene]-2,2'-diol (46)



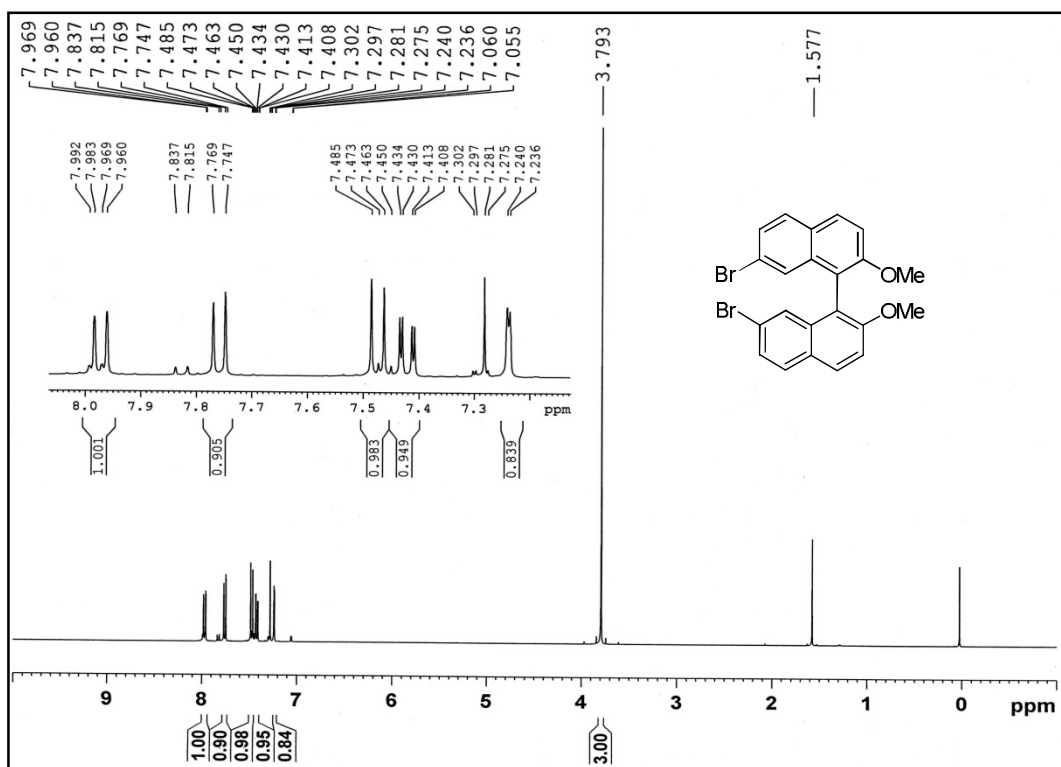
¹³C-NMR spectrum of 7-bromo-[1,1'-binaphthalene]-2,2'-diol (46)



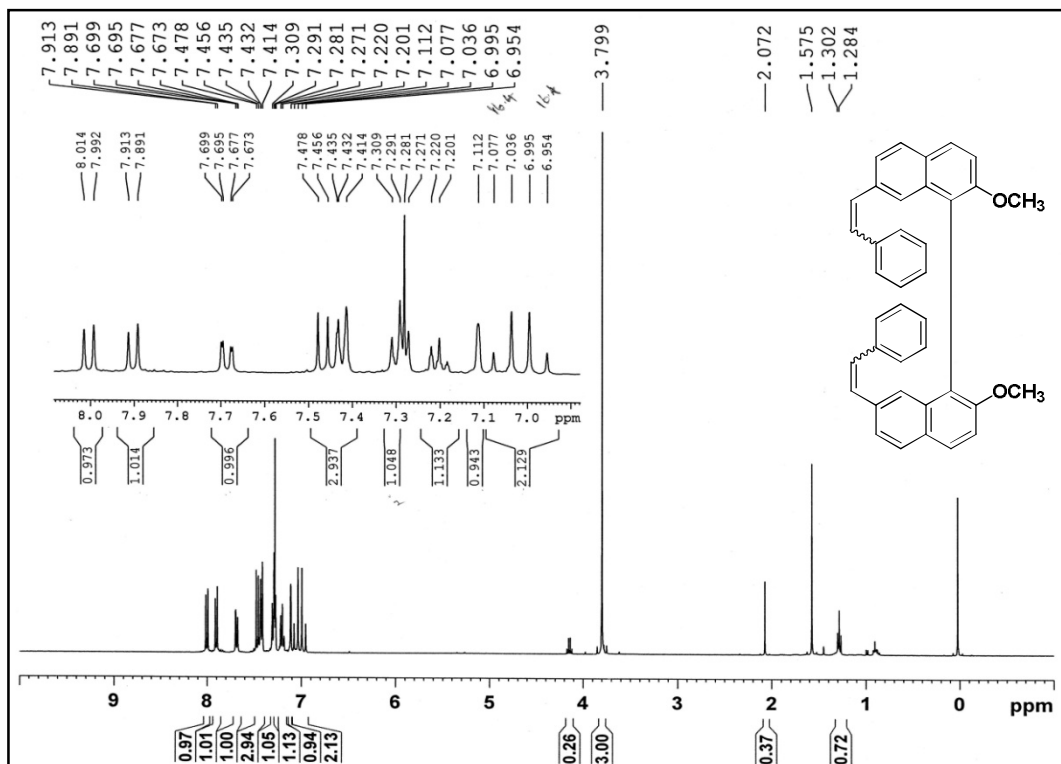
IR spectrum of 46



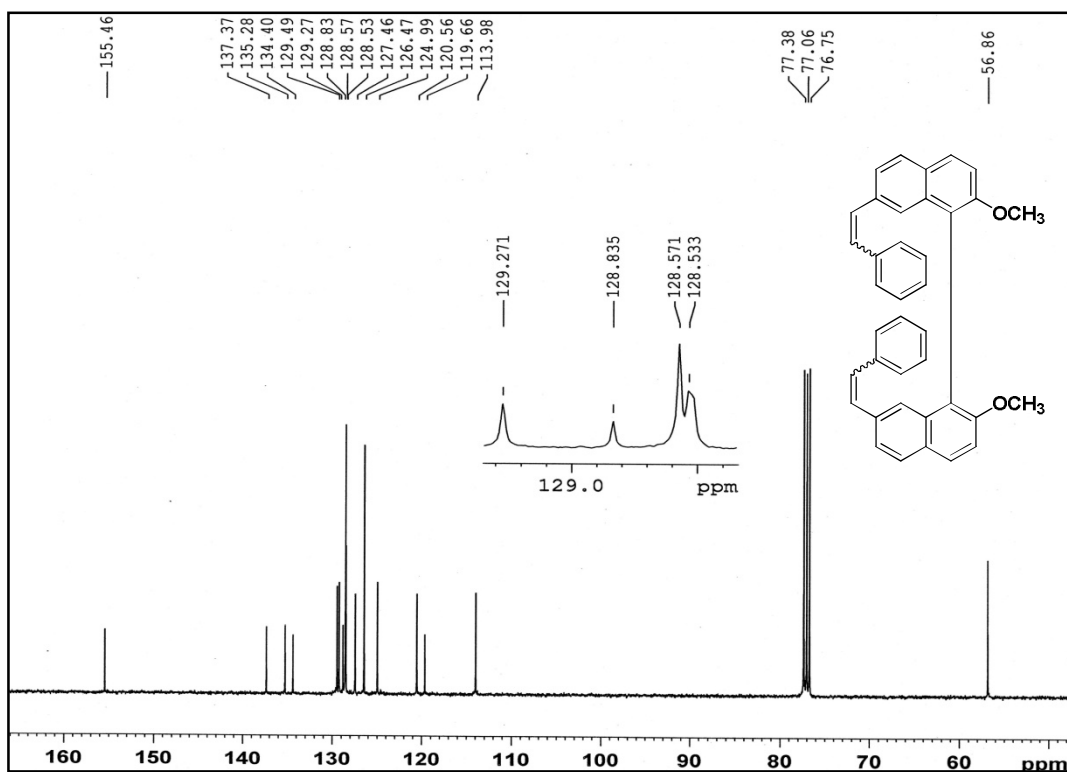
HRMS spectrum of 7-bromo-[1,1'-binaphthalene]-2,2'-diol (46)



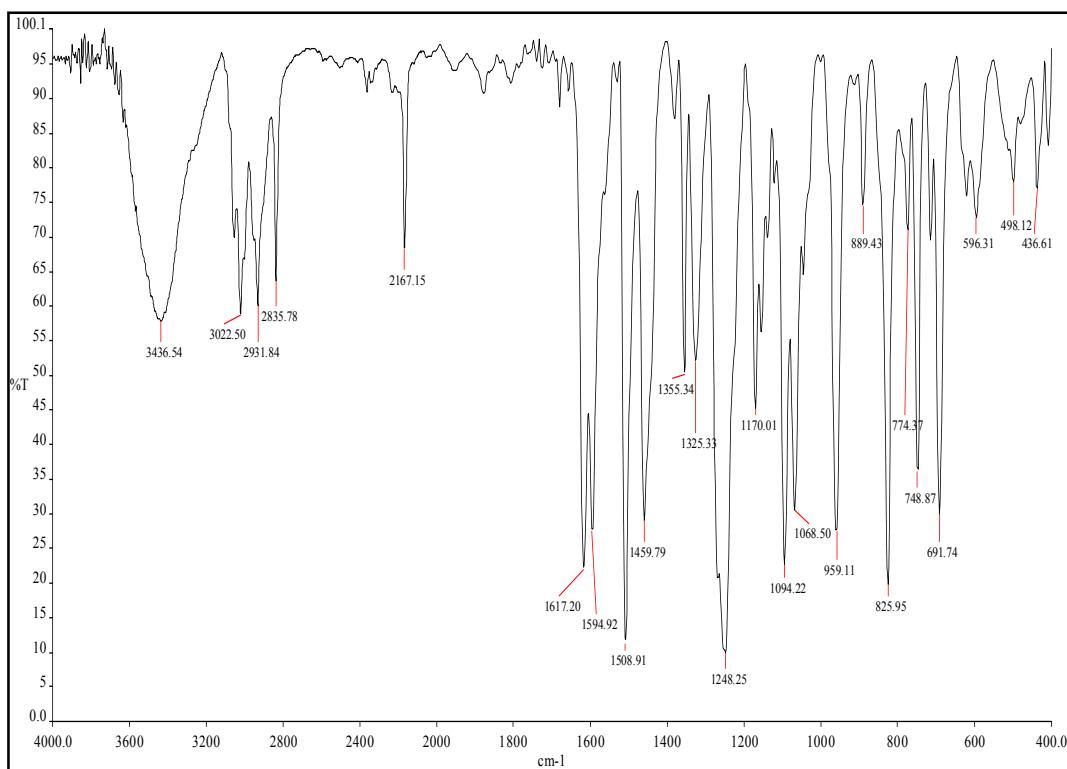
¹H-NMR spectrum of 7,7'-dibromo-2,2'-dimethoxy-1,1'-binaphthalene (63)



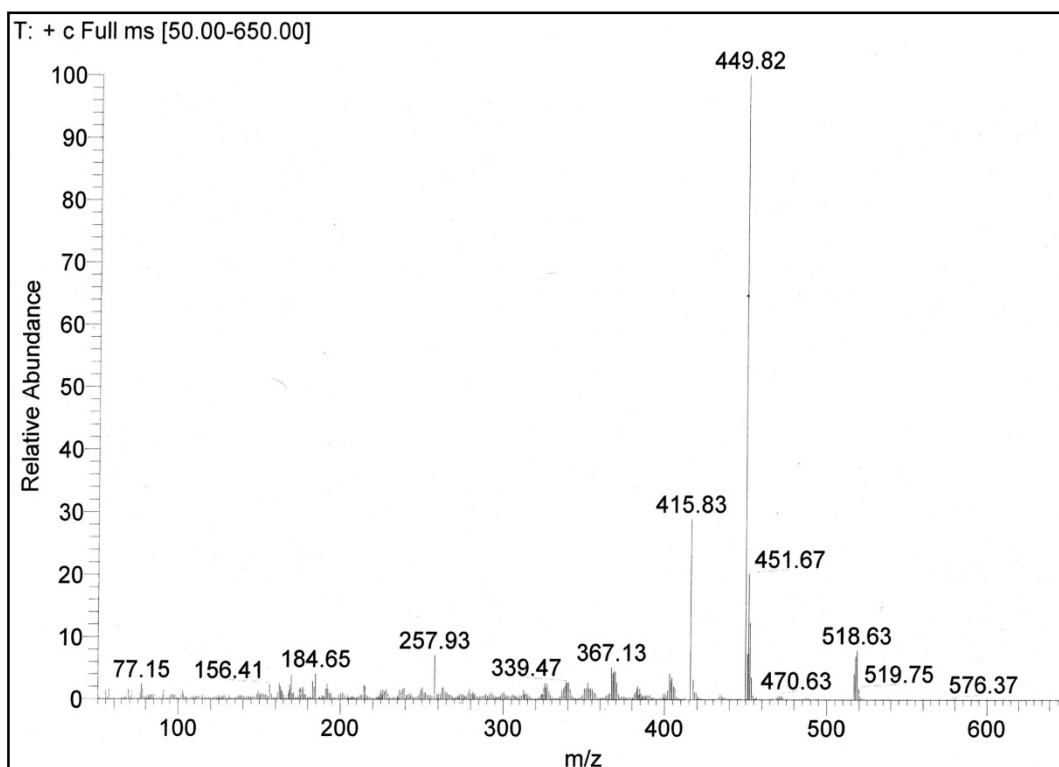
¹H-NMR spectrum of 2,2'-dimethoxy-7,7'-di((E)-styryl)-1,1'-binaphthalene (64)



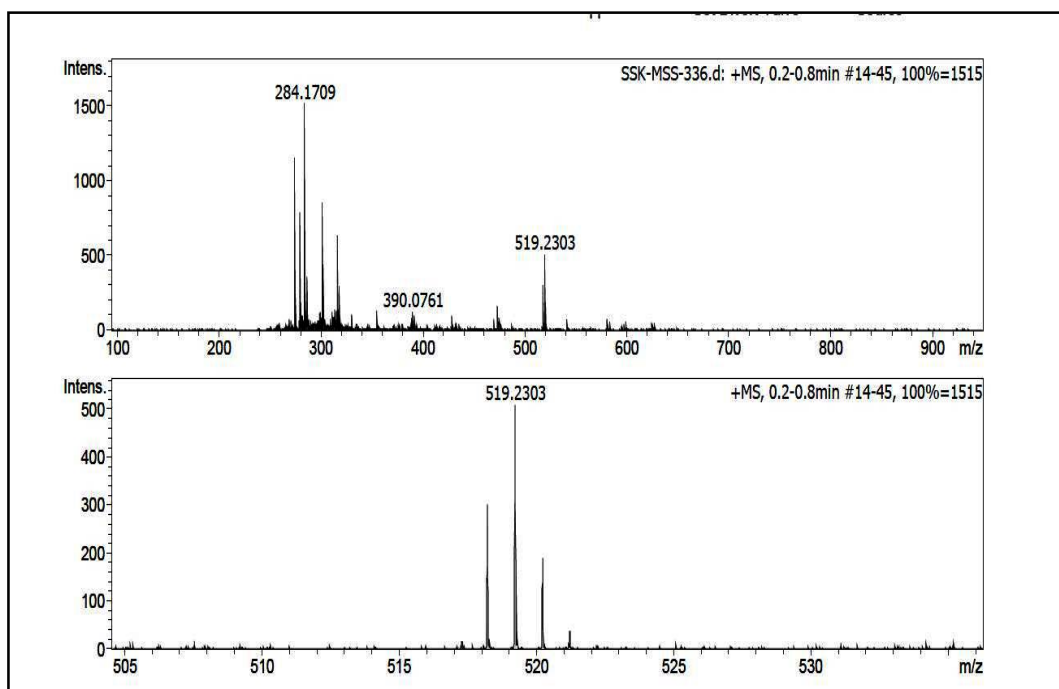
¹³C-NMR spectrum of 64



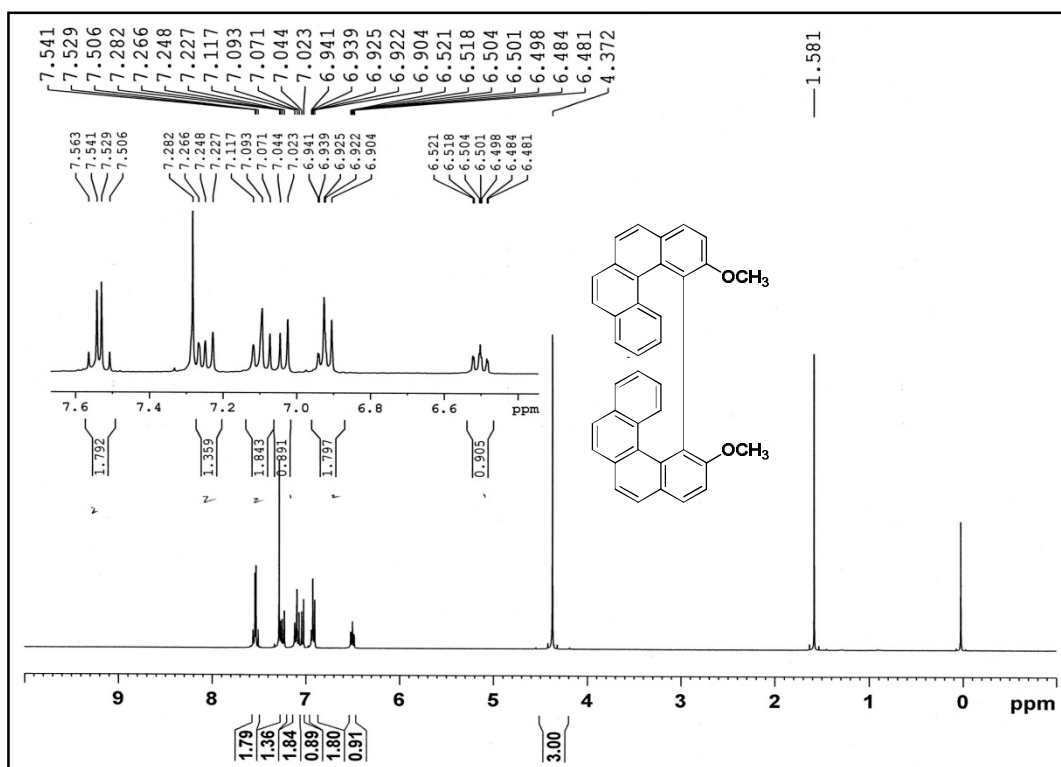
IR spectrum of 64



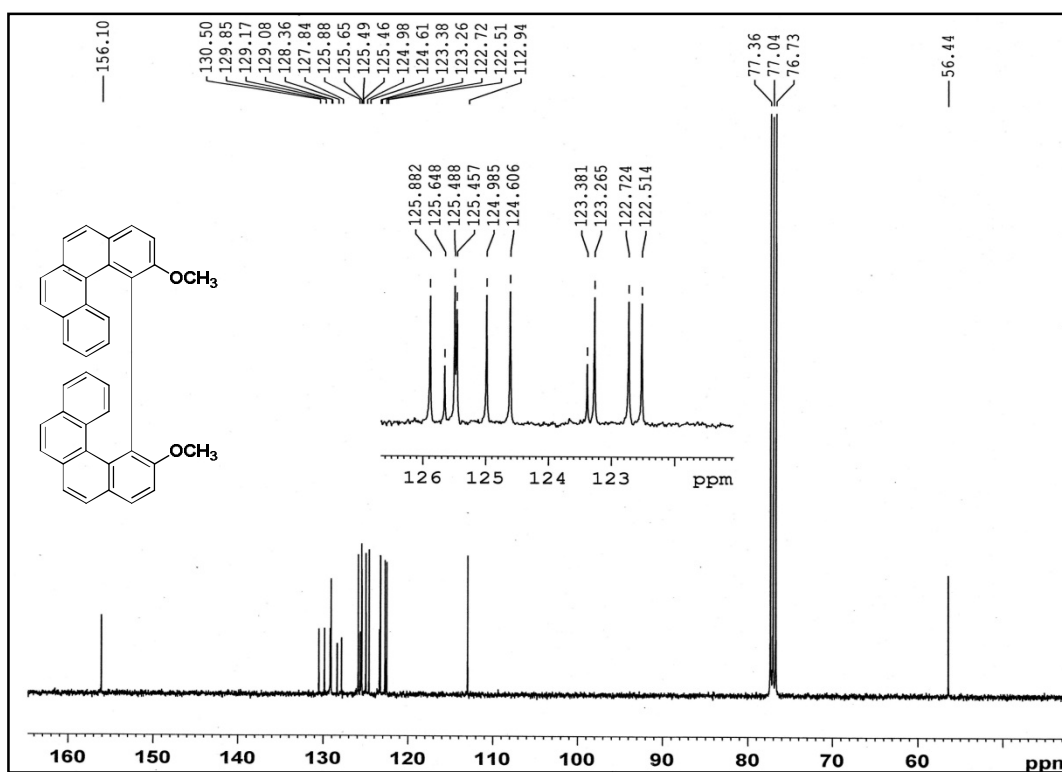
EI mass spectrum of 64



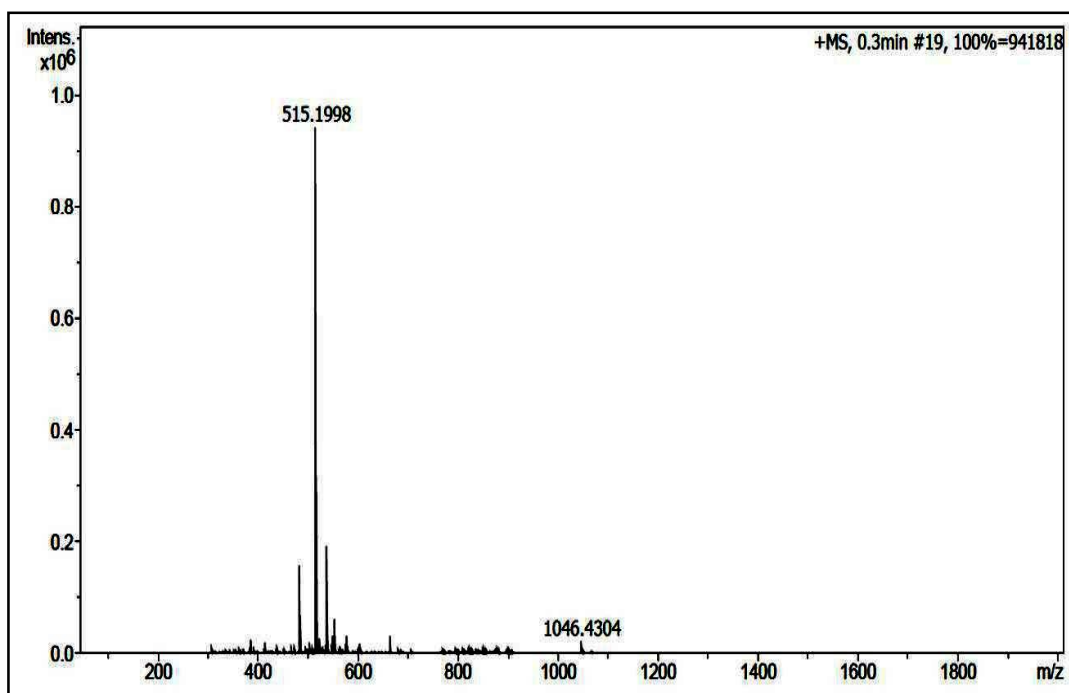
HRMS spectrum of 64



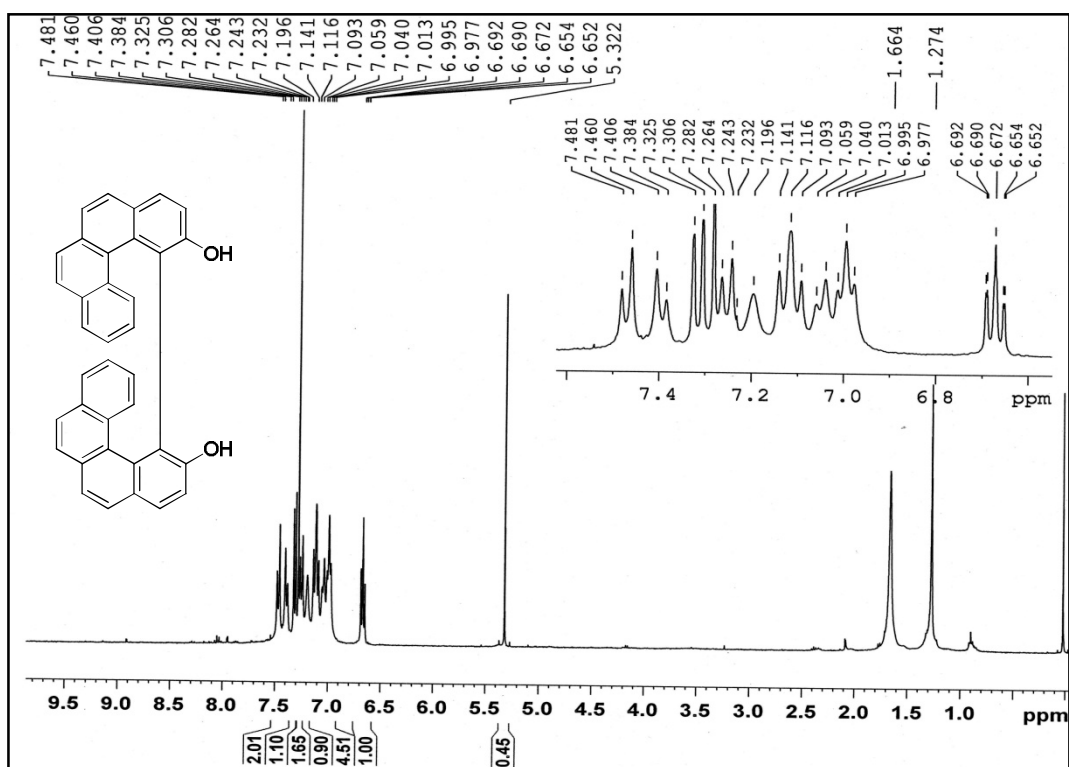
¹H-NMR spectrum of 2,2'-dimethoxy-1,1'-bibenzo[c]phenanthrene (65)



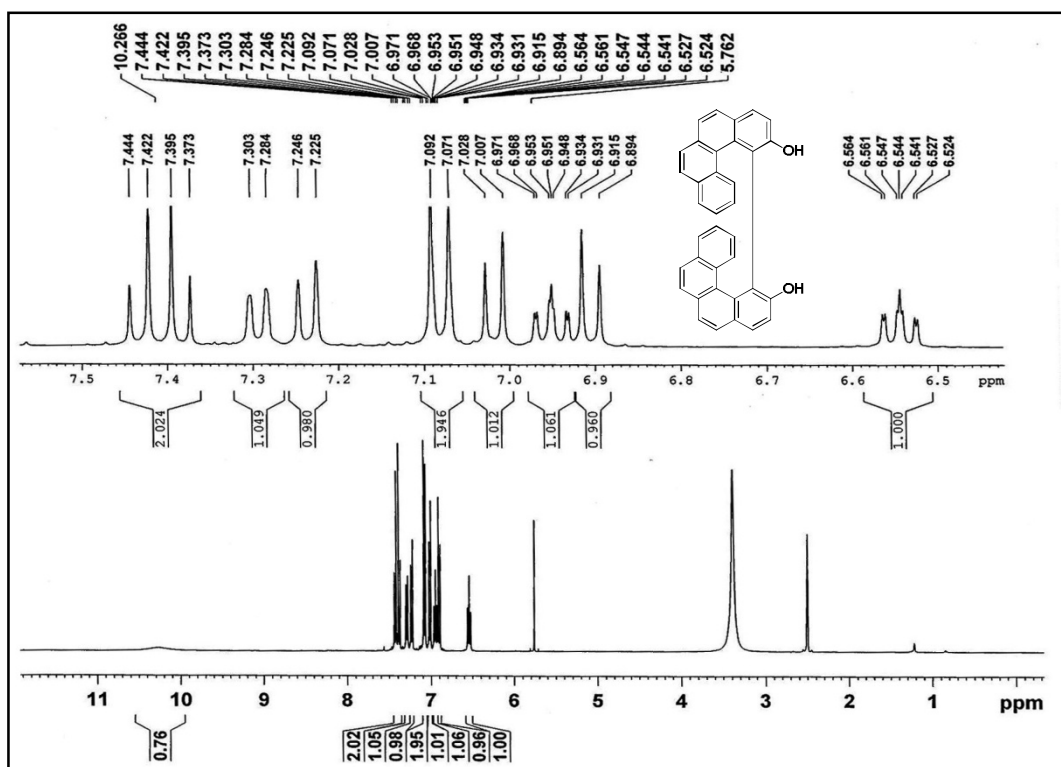
¹³C-NMR spectrum of 65



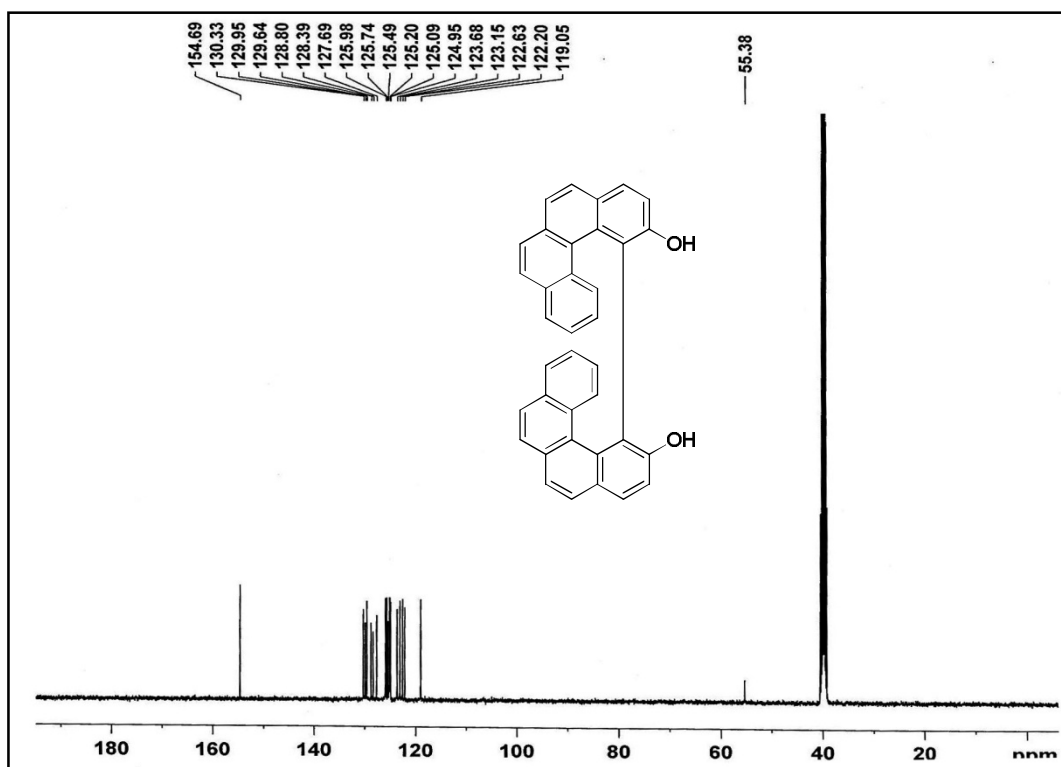
HRMS spectrum of 65



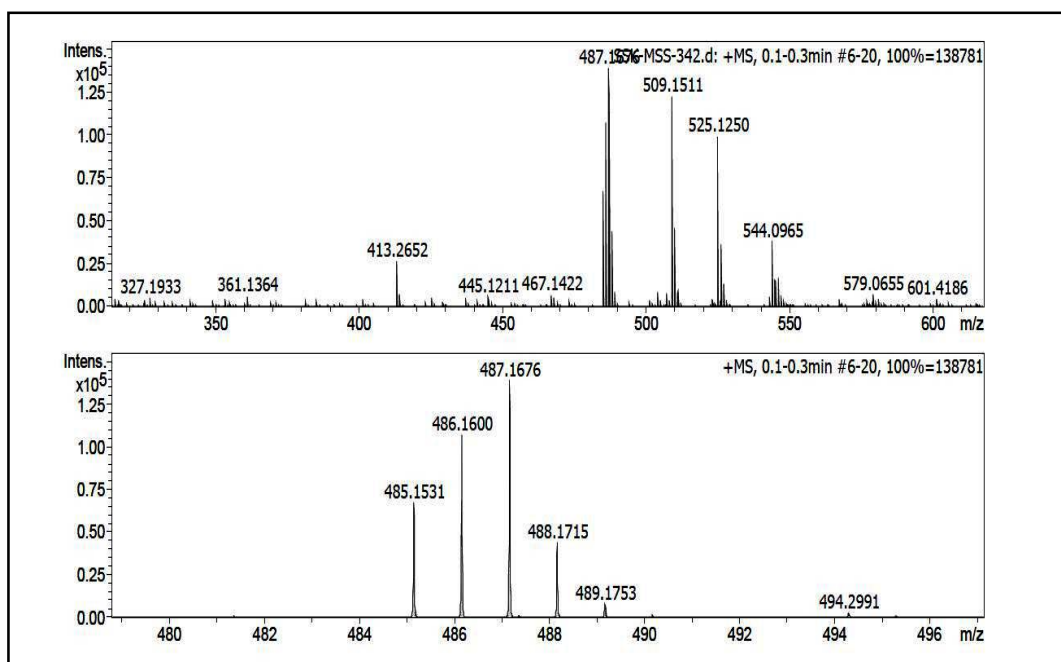
¹H-NMR spectrum of [1,1'-bibenzo[c]phenanthrene]-2,2'-diol (52) in CDCl₃



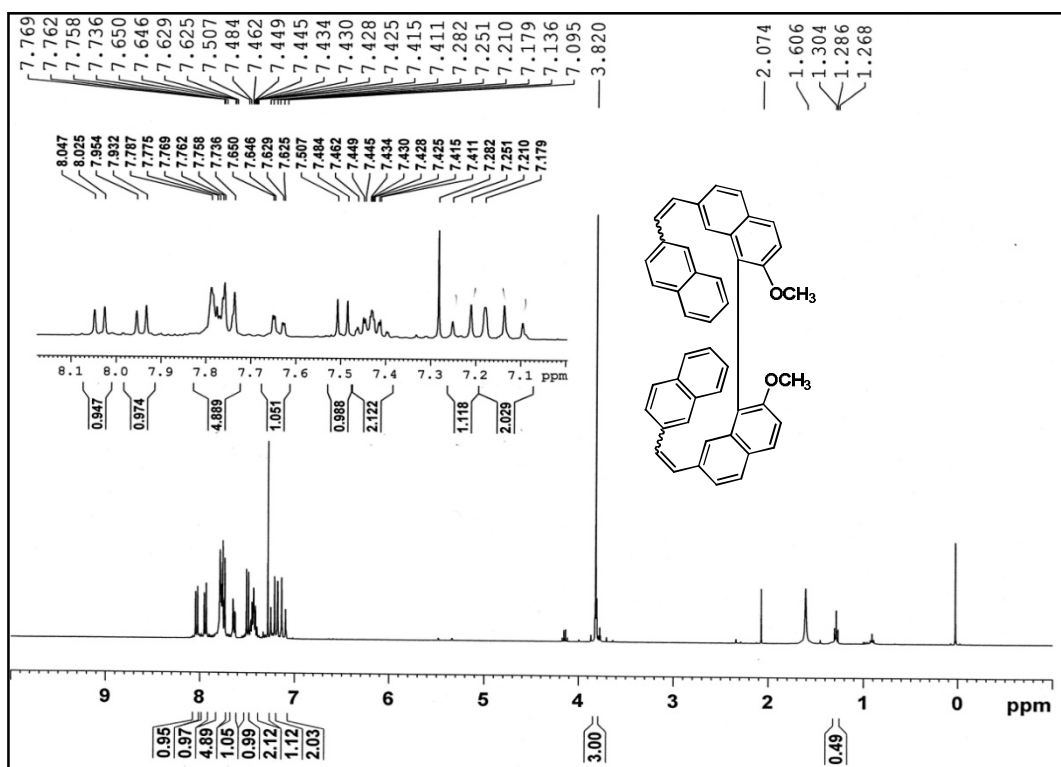
¹H-NMR spectrum of [1,1'-bibenzo[c]phenanthrene]-2,2'-diol (52) in DMSO-d₆



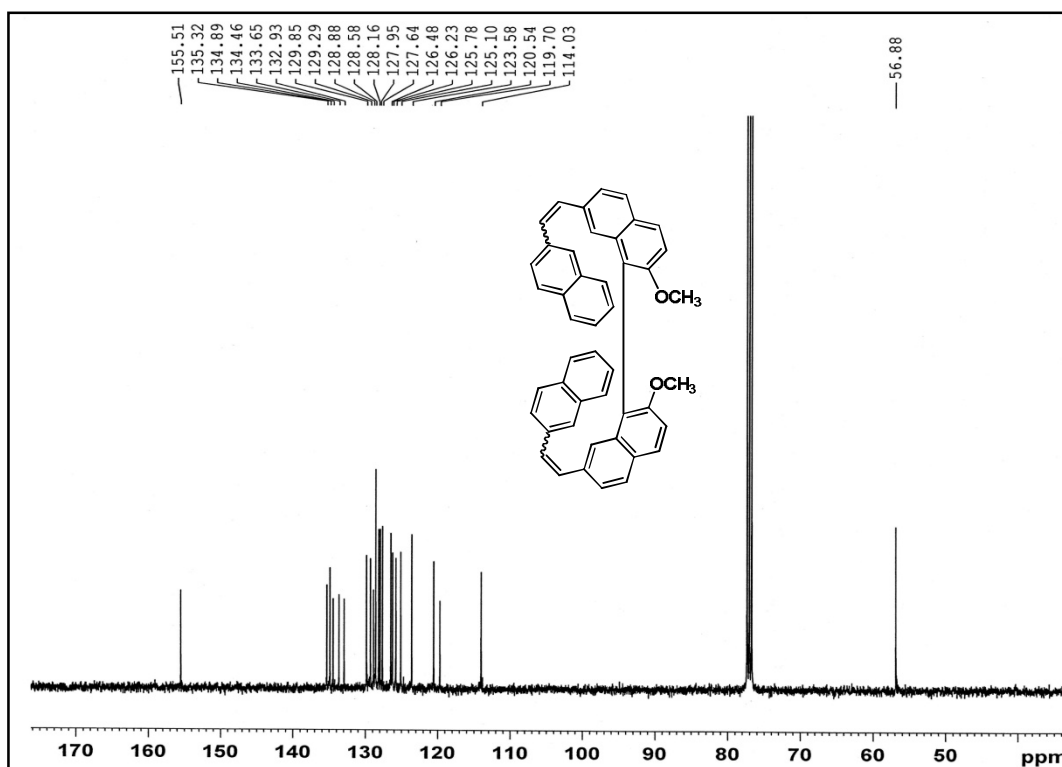
¹³C-NMR spectrum of [1,1'-bibenzo[c]phenanthrene]-2,2'-diol (52) in DMSO-d₆



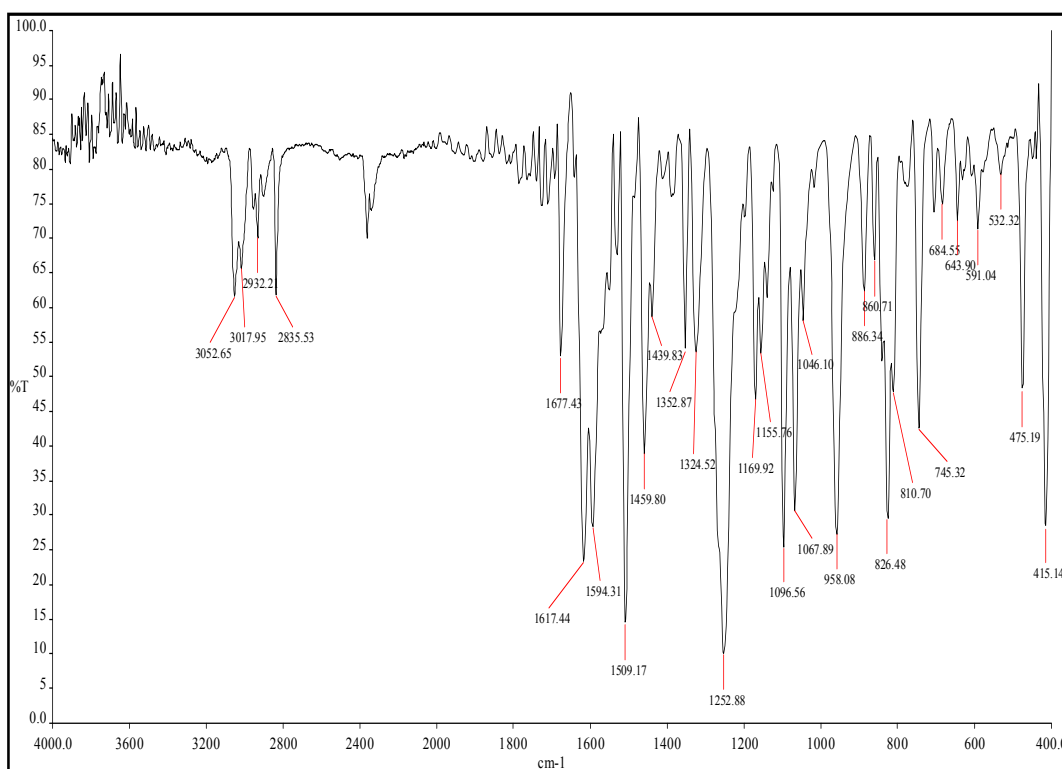
HRMS spectrum of 52



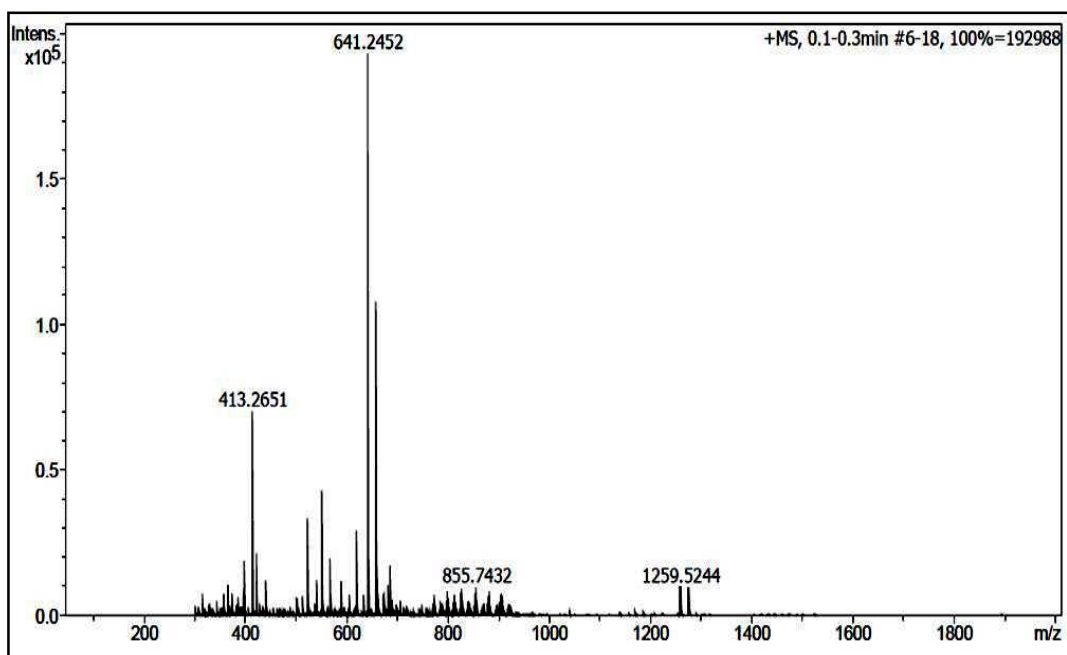
¹H-NMR spectrum of 2,2'-dimethoxy-7,7'-bis(2-(naphthalen-2-yl)vinyl)-1,1'-binaphthalene (66)



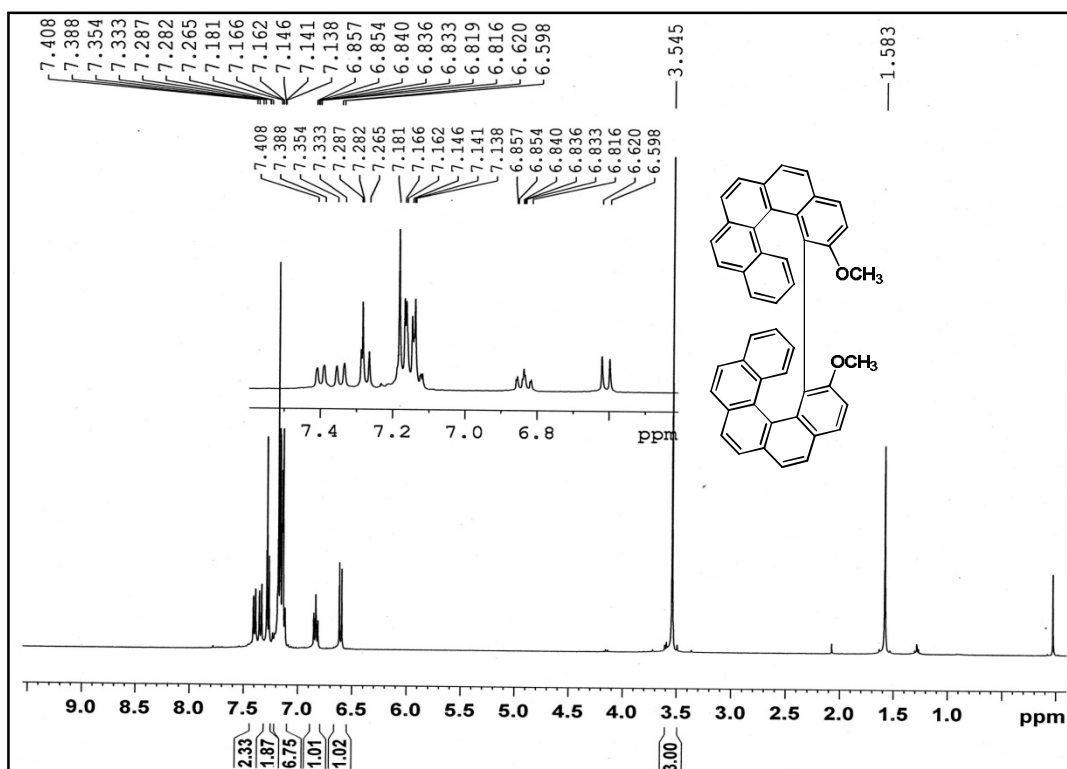
¹³C-NMR spectrum of 66



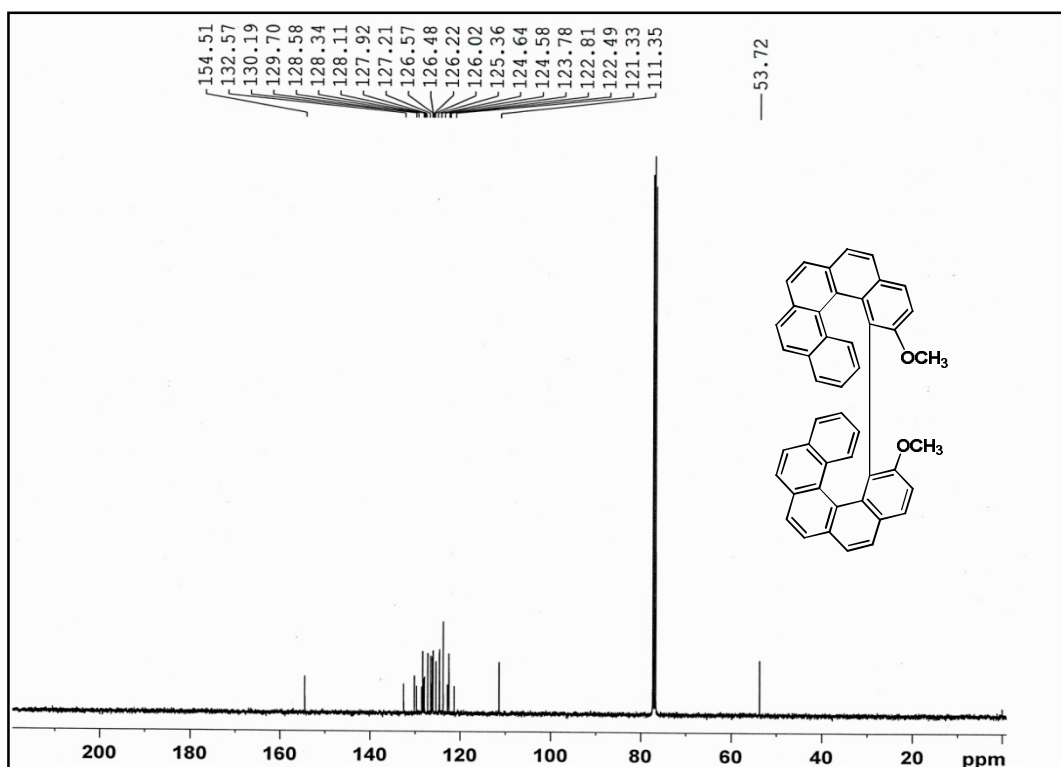
IR spectrum of 66



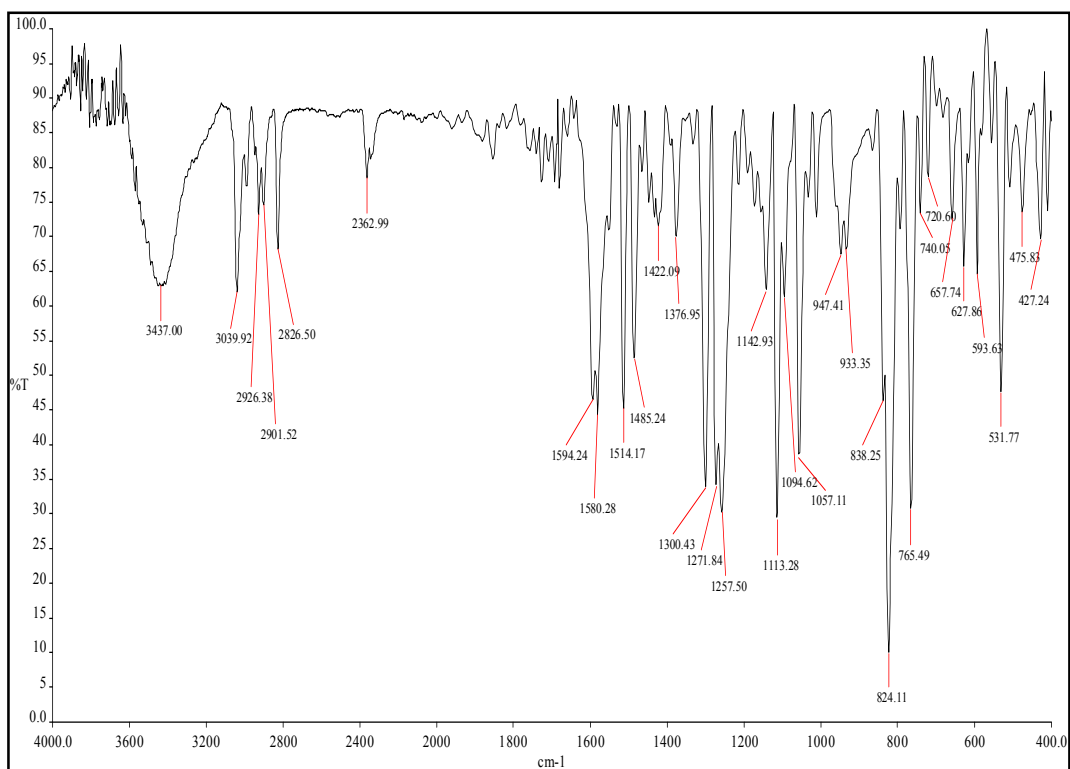
HRMS spectrum of 66



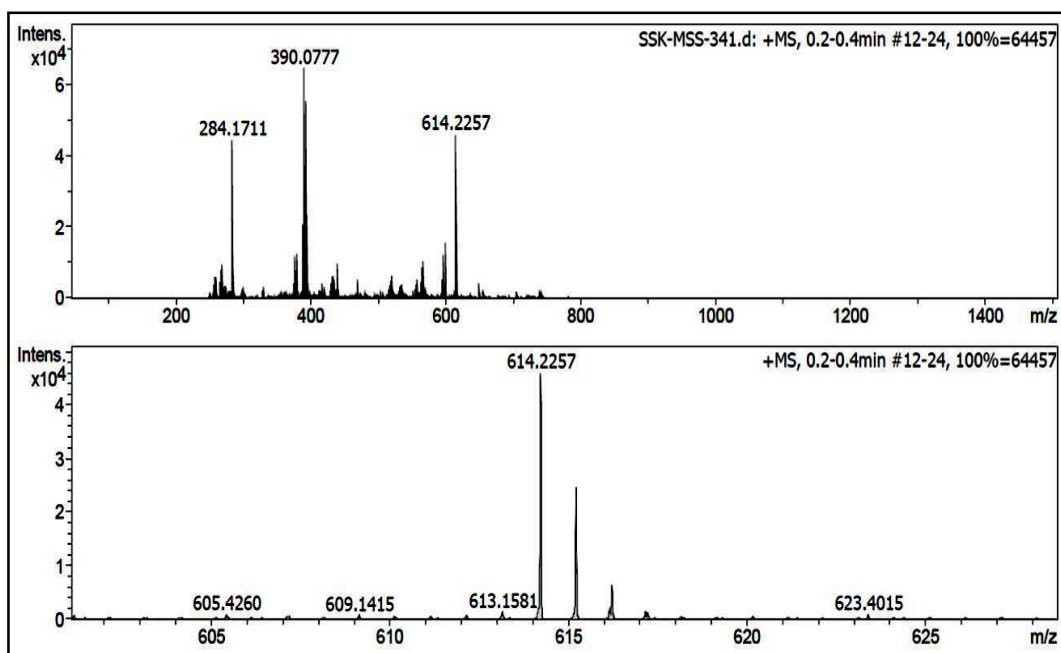
¹H-NMR spectrum of 9,9'-dimethoxy-10,10'-bidibenzo[*c,g*]phenanthrene (67)



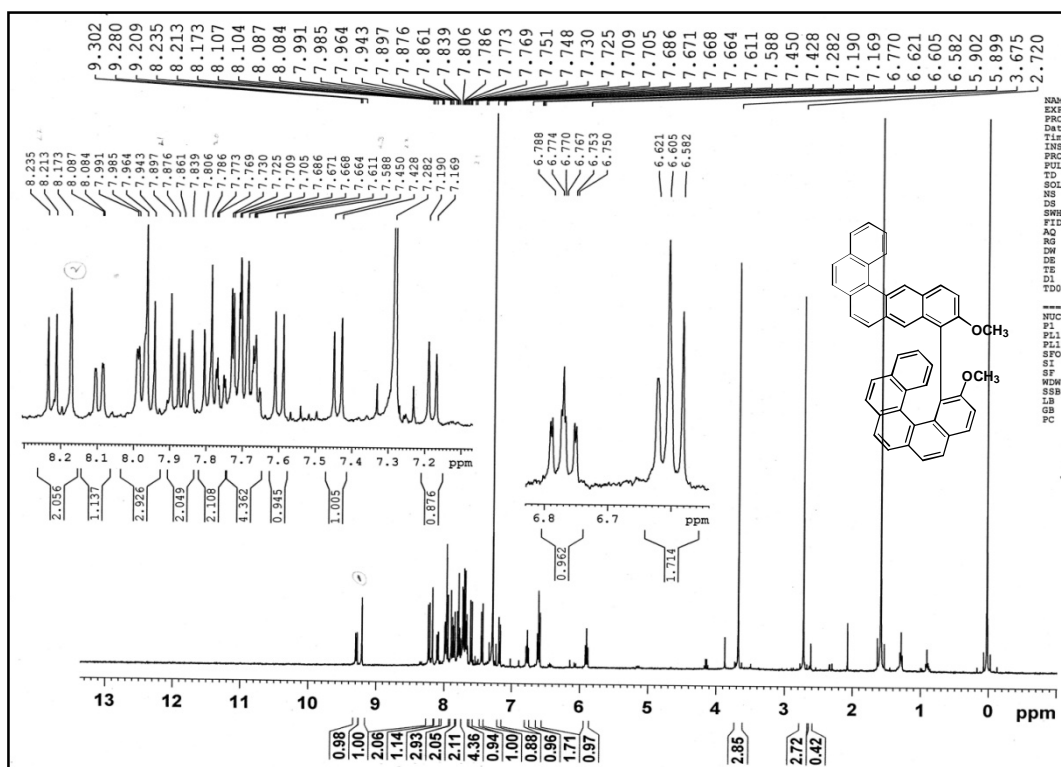
¹³C-NMR spectrum of 67



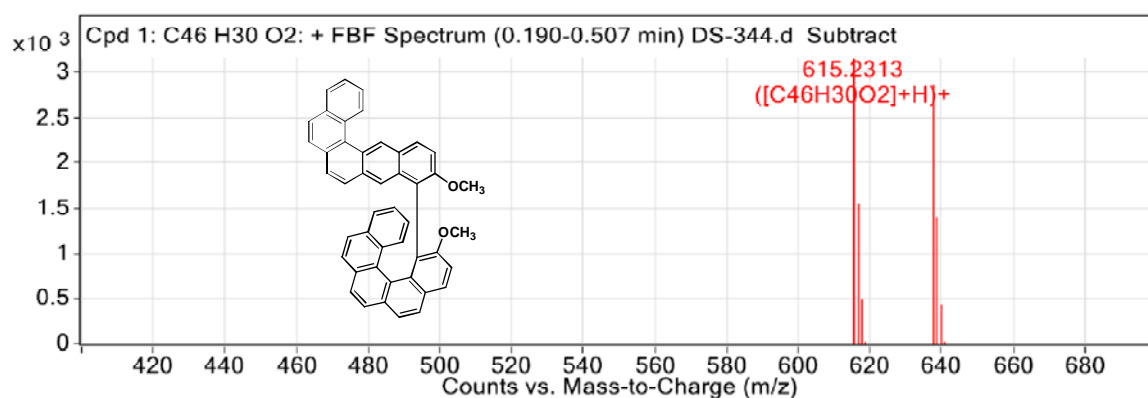
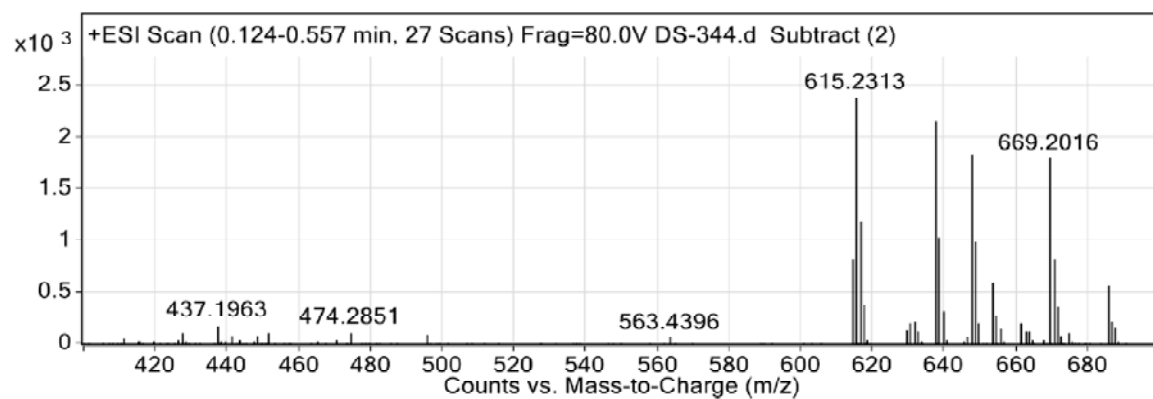
IR Spectrum of 67



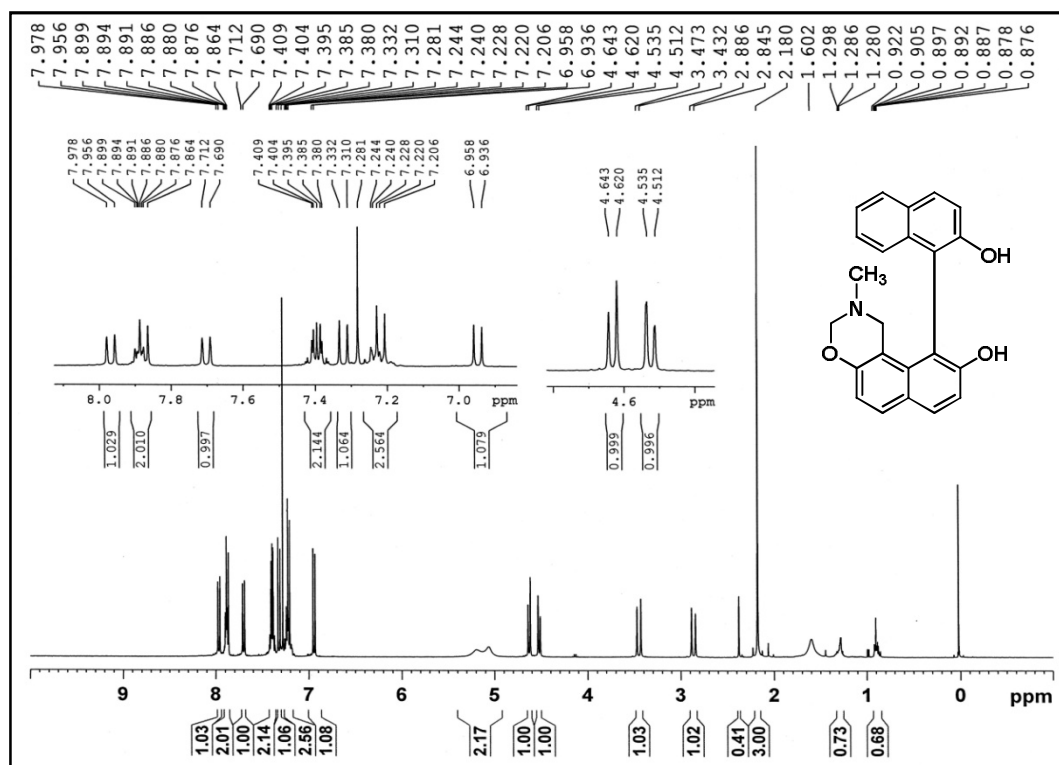
HRMS spectrum of 67



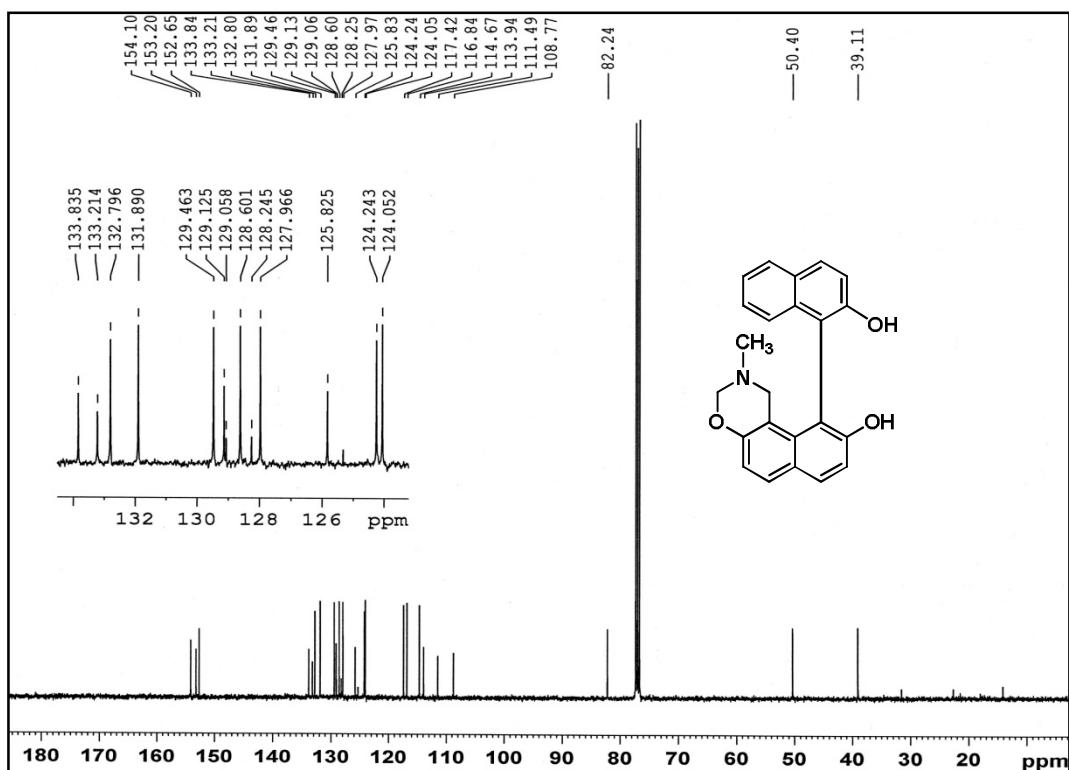
¹H NMR spectrum of 69



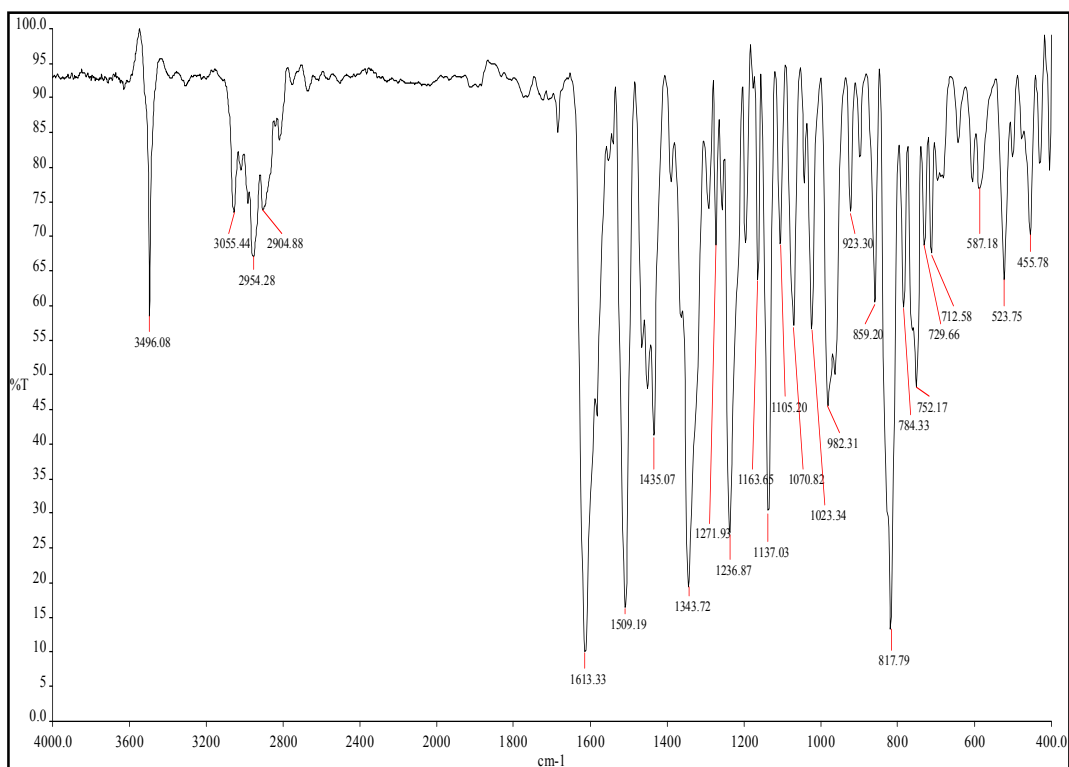
HRMS spectrum of 69



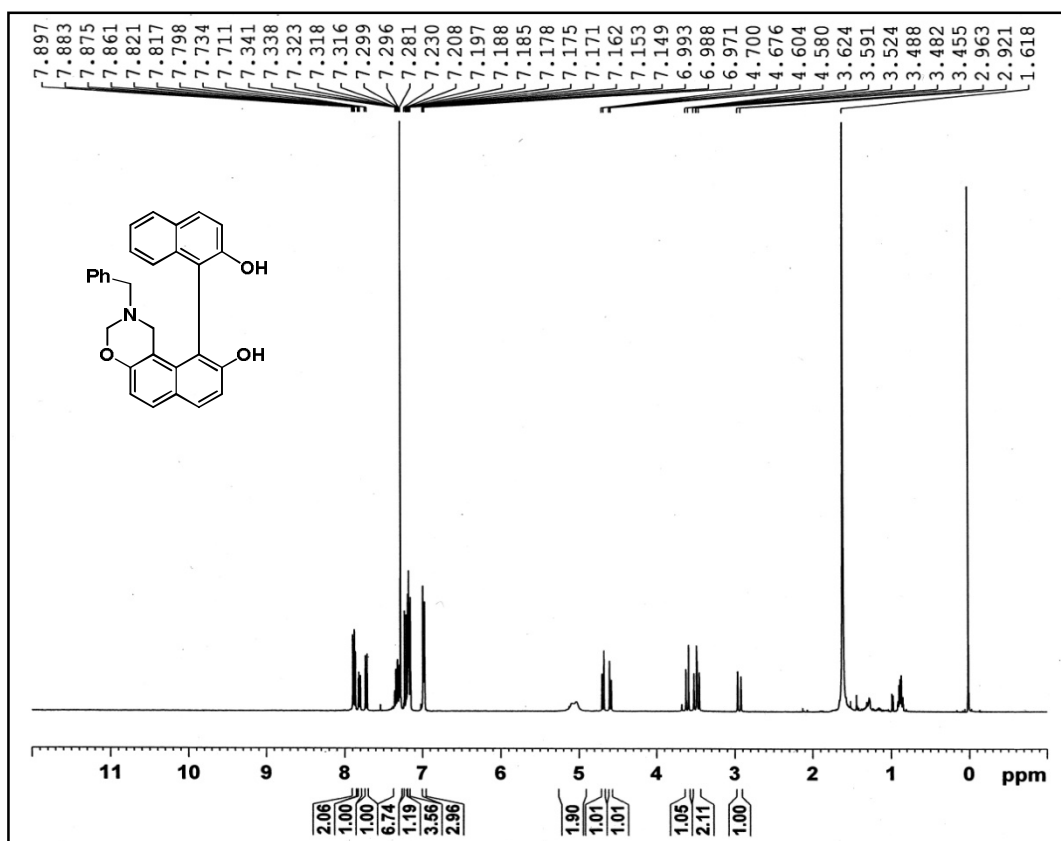
¹H-NMR spectrum of 10-(2-hydroxynaphthalen-1-yl)-2-methyl-2,3-dihydro-1H-naphtho[1,2-e][1,3]oxazin-9-ol (47)



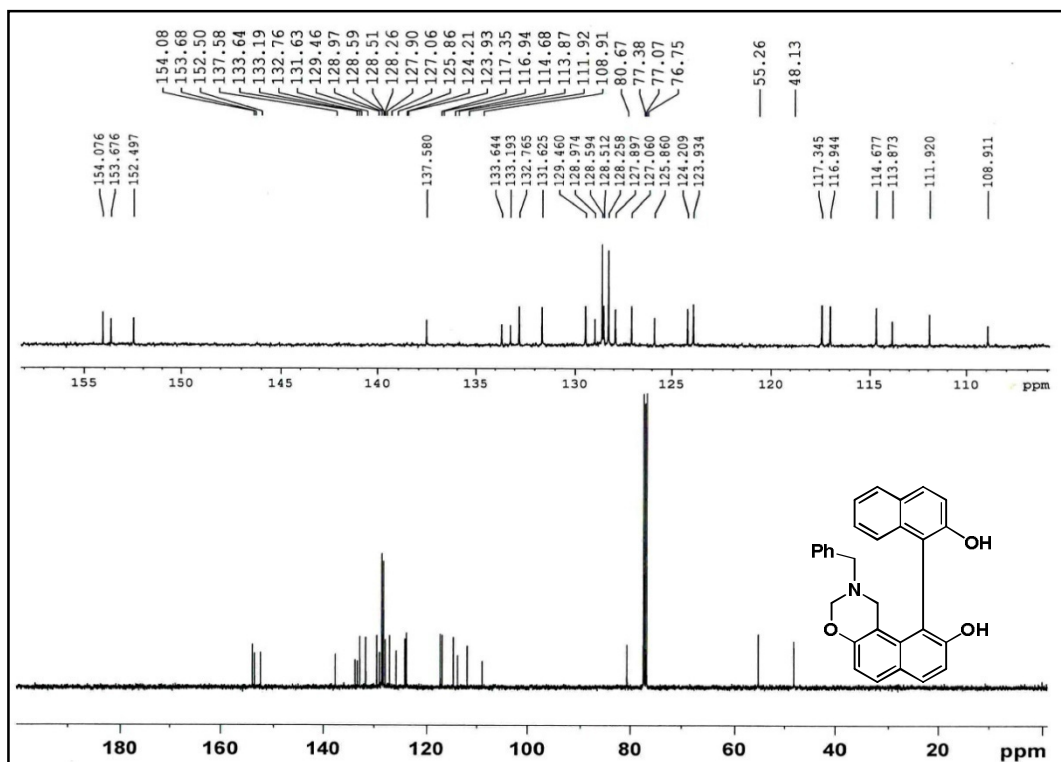
¹³C-NMR spectrum of 47



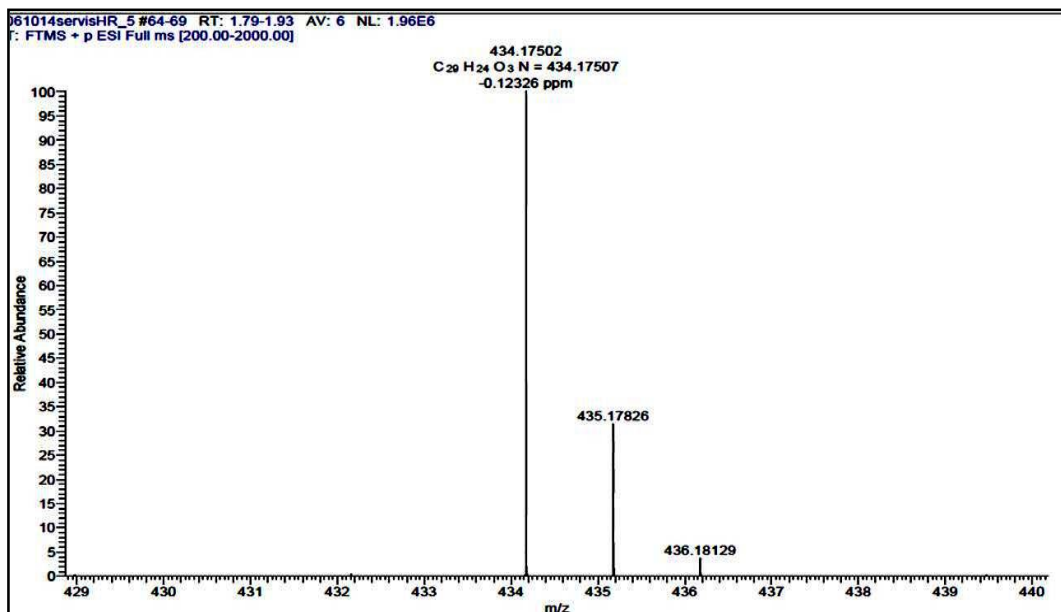
IR spectrum of 47



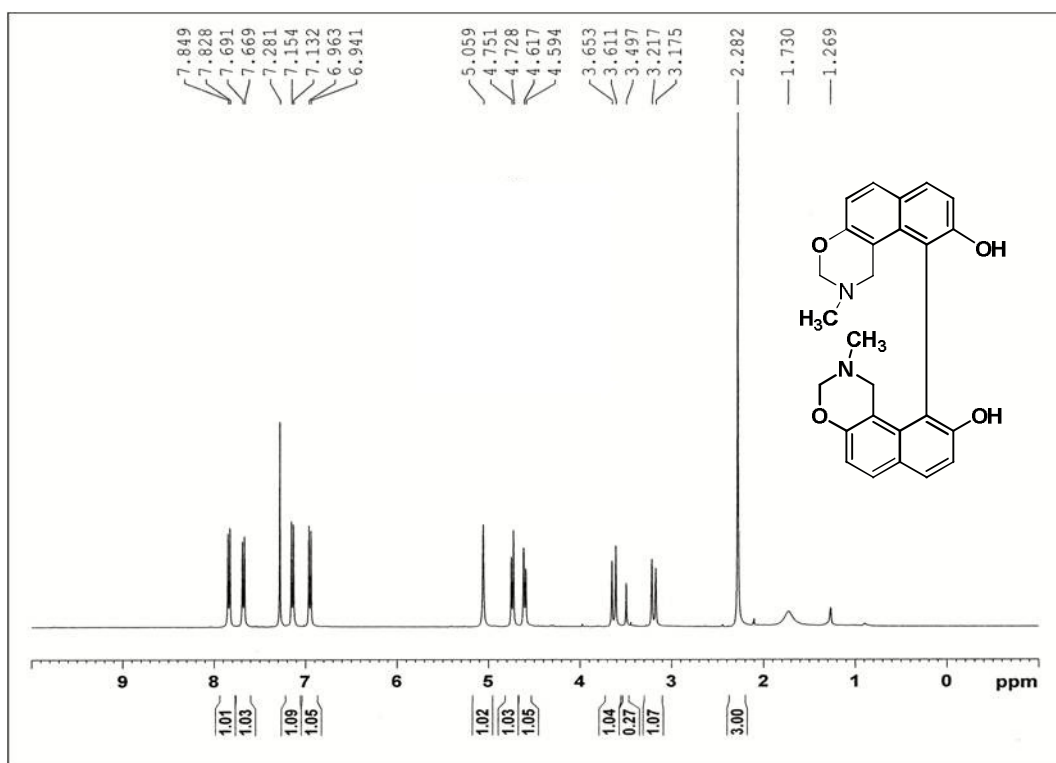
¹H-NMR Spectrum of compound (±) 2-benzyl-10-(2-hydroxynaphthalen-1-yl)-2,3-dihydro-1H-naphtho[1,2-e][1,3]oxazin-9-ol (48)



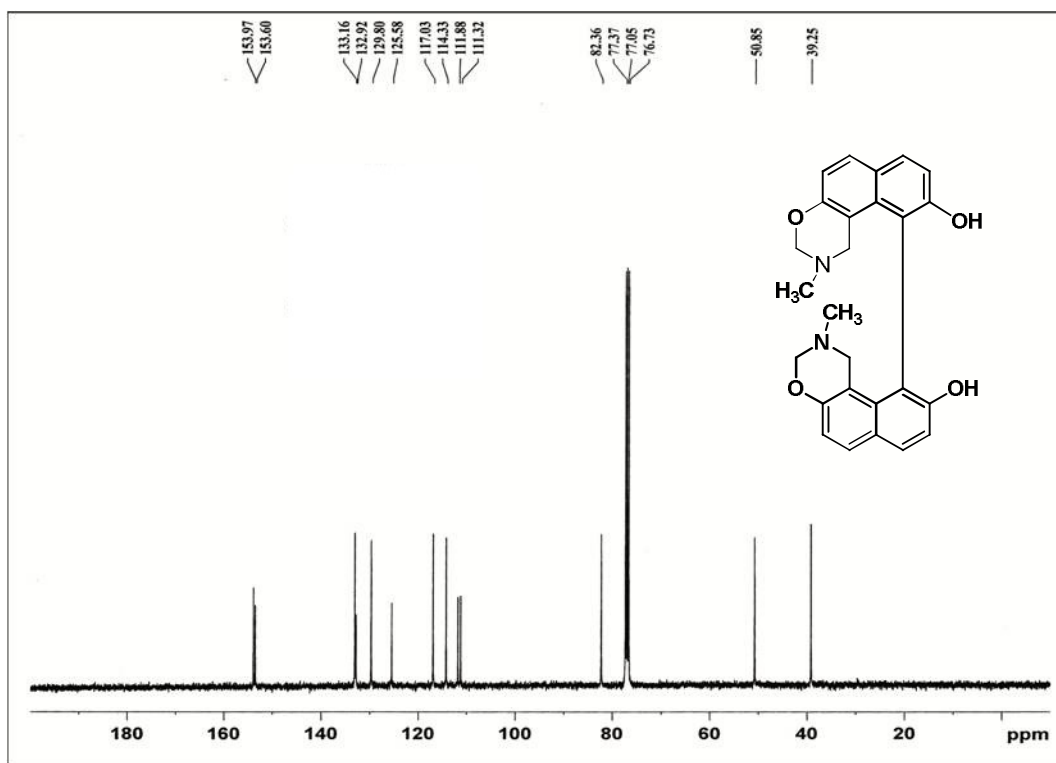
¹³C-NMR spectrum of (±)-48



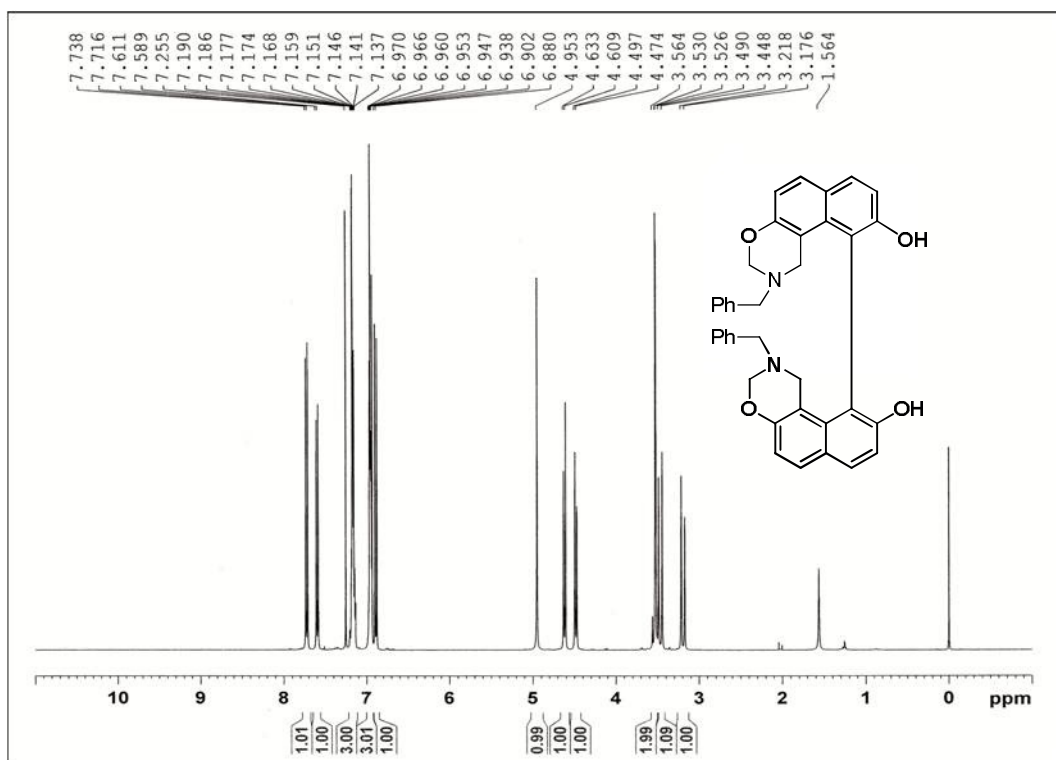
HRMS spectrum of 48



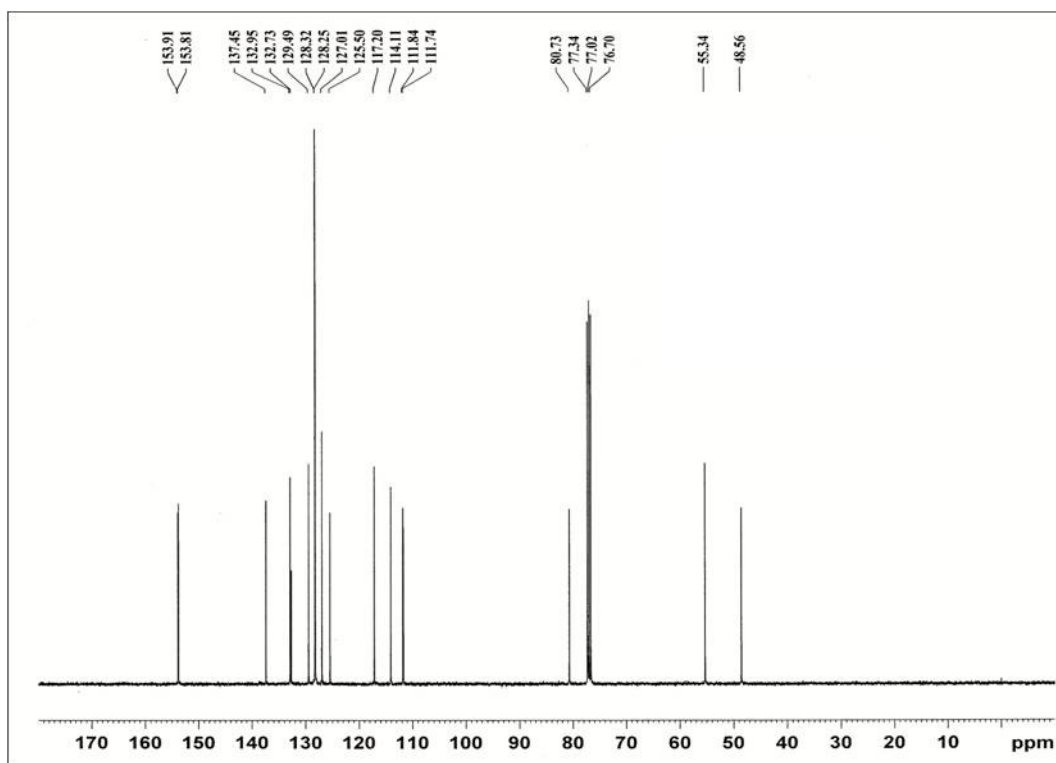
1H -NMR spectrum of 2,2'-Dimethyl-2,3,2',3'-tetrahydro-1*H*,1'*H*-[10,10']bi[naphtho[1,2-*e*][1,3]oxaziny]-9,9'-diol (50)



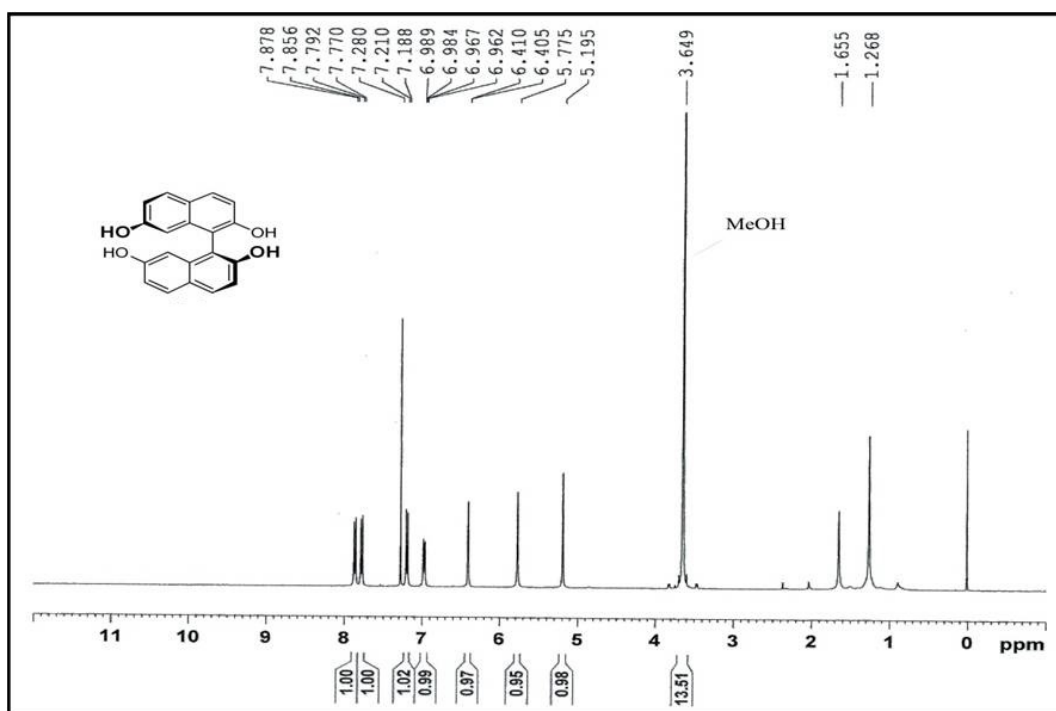
$^{13}\text{C-NMR}$ spectrum of 50



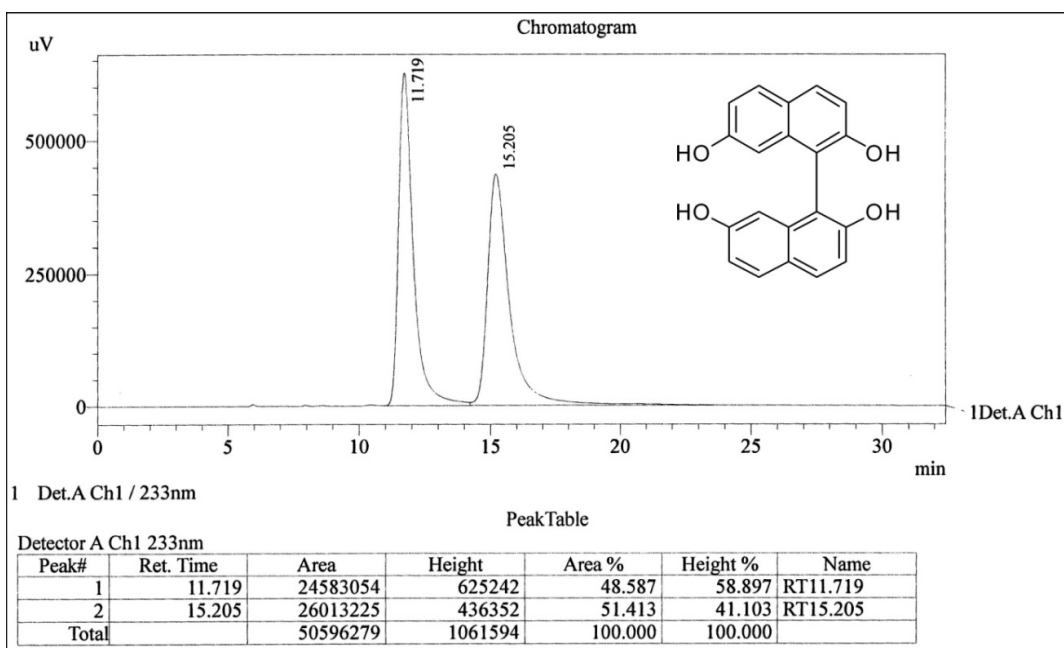
$^1\text{H-NMR}$ spectrum of 2,2'-dibenzyl-2,2',3,3'-tetrahydro-1H,1'H-[10,10'-binaphtho[1,2-e][1,3]oxazine]-9,9'-diol (51)



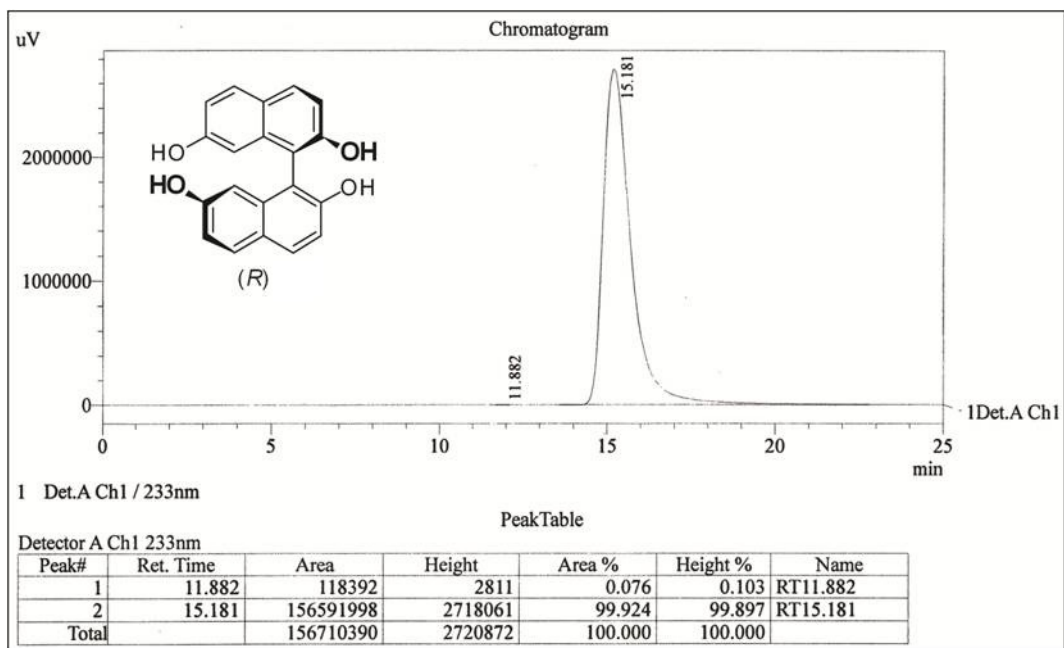
^{13}C -NMR spectrum of 51



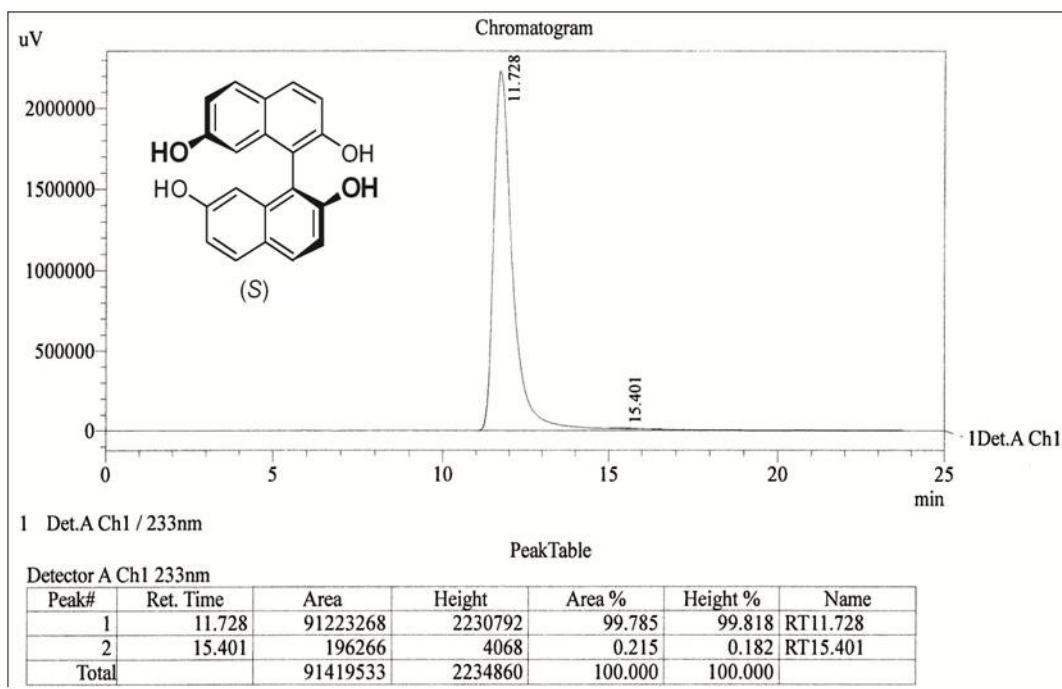
^1H -NMR Spectrum of (*S*)-2,2',7,7'-tetrahydroxy-1,1'-binaphthyl [*S_a*]-41 in CDCl_3 (400 MHz)



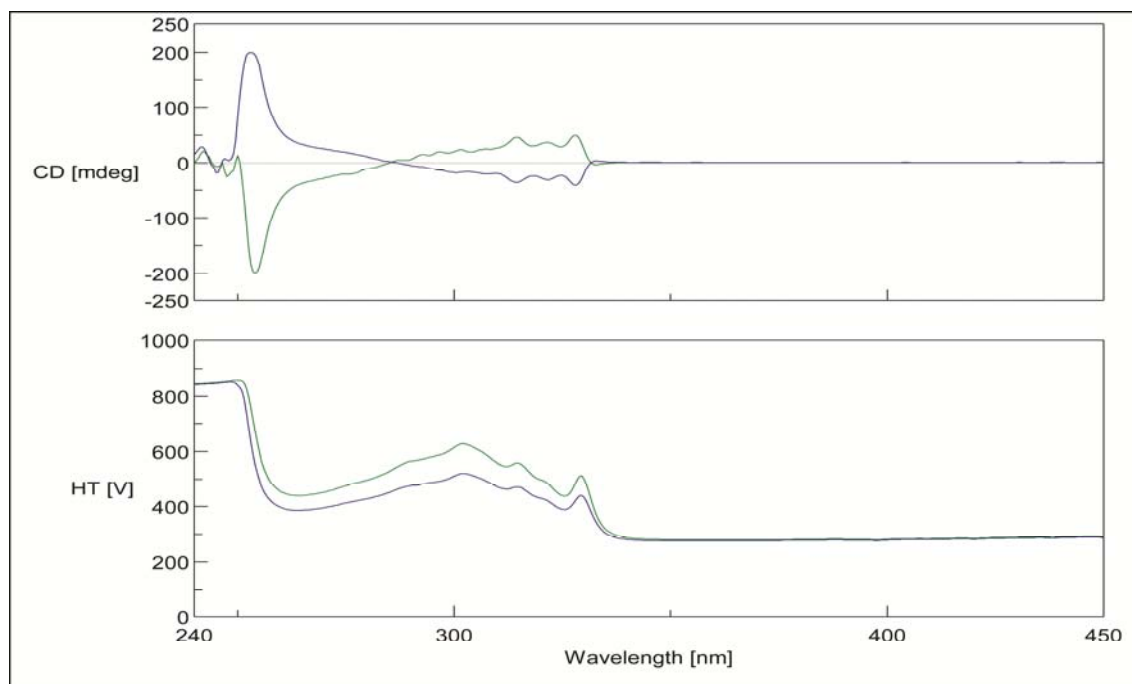
HPLC conditions: Observed two peaks of separated enantiomers at 1) R_t – 11.71 min and 2) R_t – 15.20 min. Solvent System: Hexane: *Iso*-propanol (70:30), Flow rate: 0.5 mL/min. Chiral Column: OD-H. UV : 233nm.



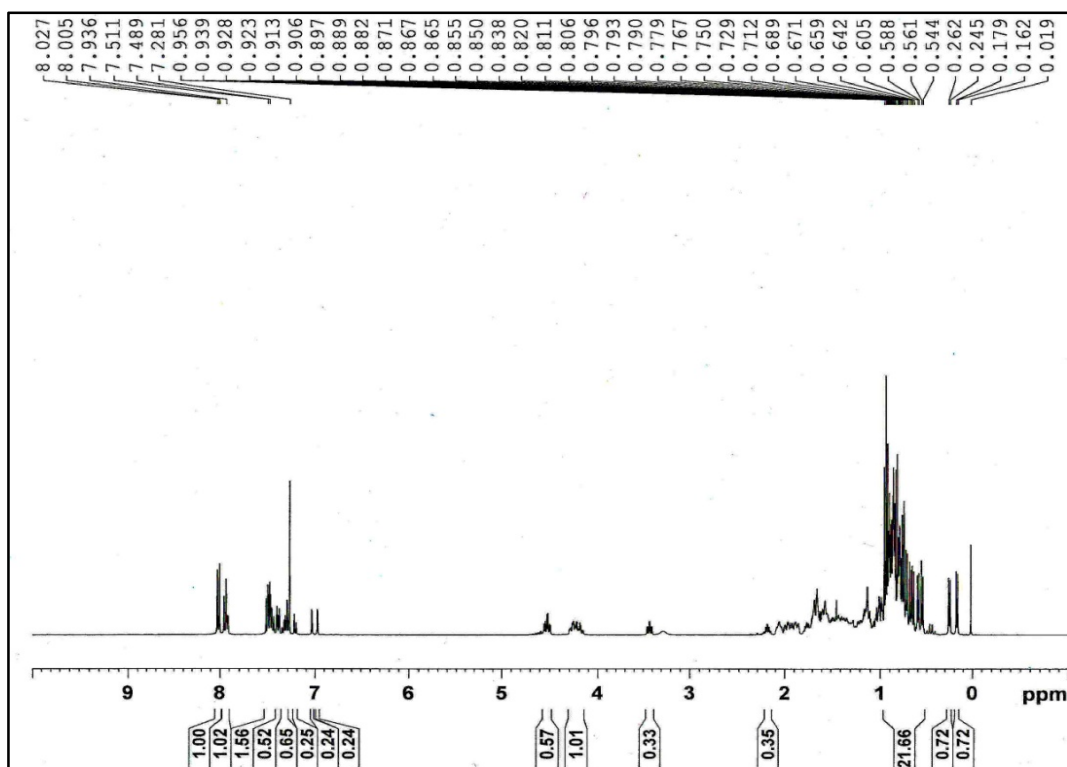
HPLC condition: Observed one peak of single enantiomer at R_t – 15.18 min. Solvent System: Hexane: *Iso*-propanol (70:30), Flow rate: 0.5 mL/min. Chiral Column: Diacel Chiral OD-H. UV : 233nm.



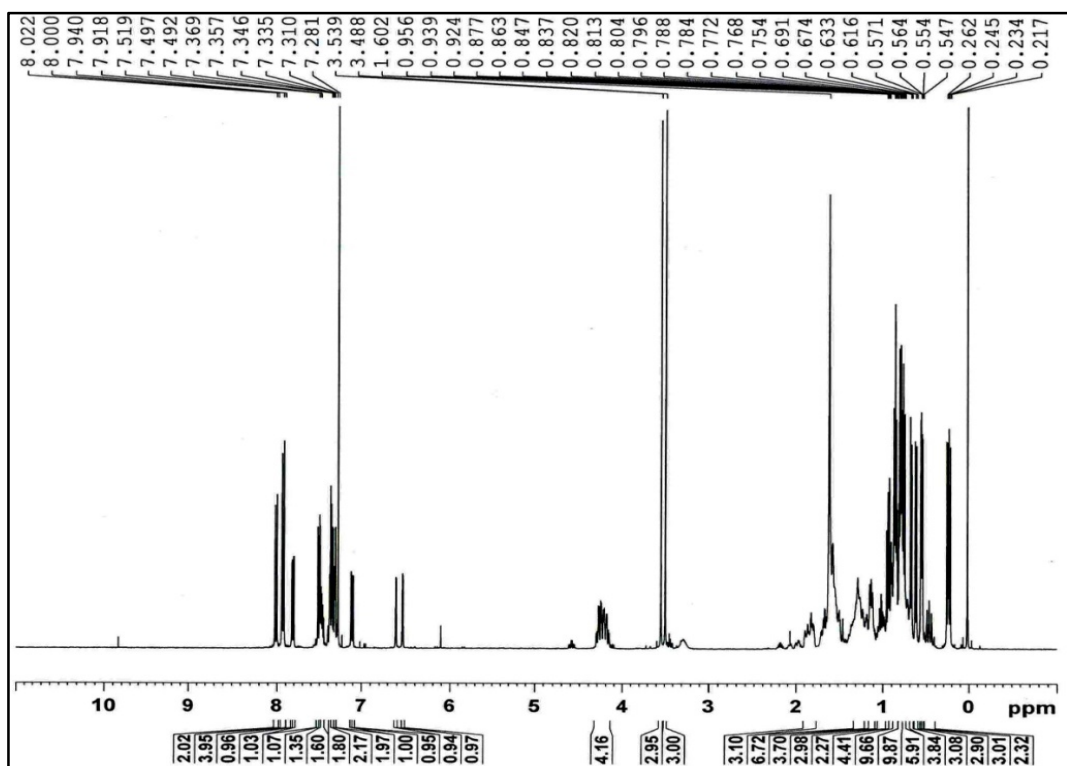
HPLC condition: Observed one peak of single enantiomer at R_t – 11.72 min. Solvent System: Hexane: *Iso*-propanol (70:30), Flow rate: 0.5 mL/min. Chiral Column: Diacel Chiral OD-H. UV: 233nm.



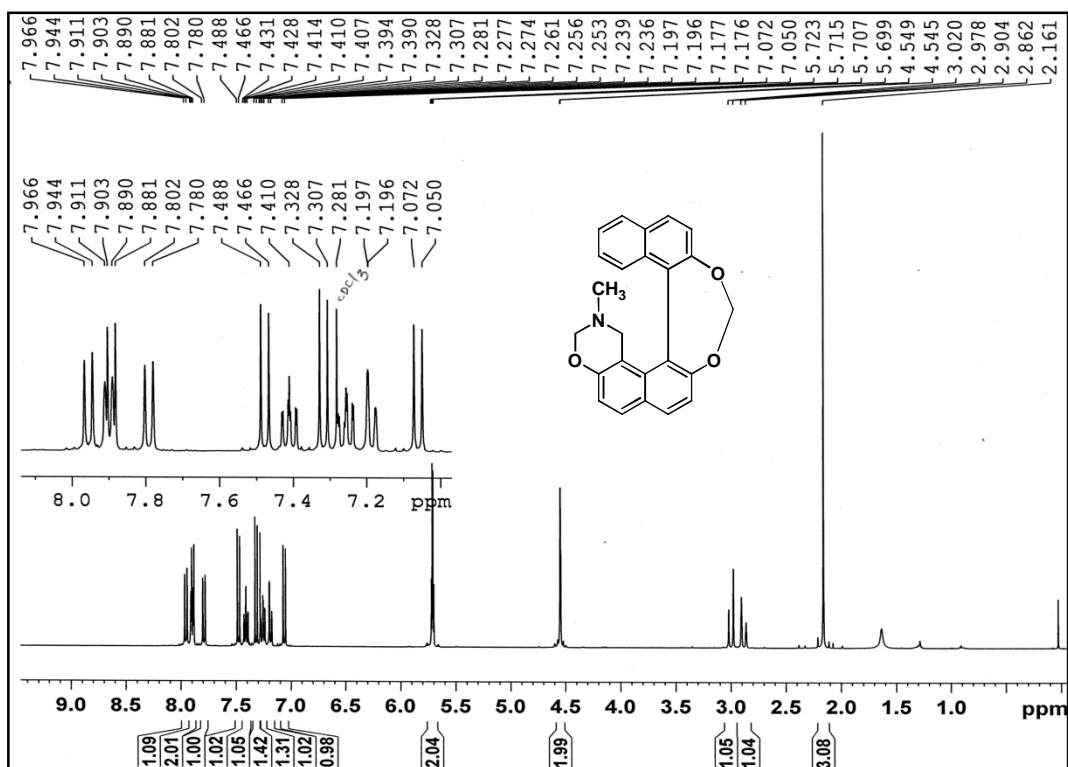
UV and Circular dichroism spectra of resolved 2,2',7,7'-tetrahydroxy-1,1'-binaphthyl : (Blue line) *aR*-**41** and (Green line) *aS*-**41** (c 8.44×10^{-4} M in acetonitrile, 25 °C).



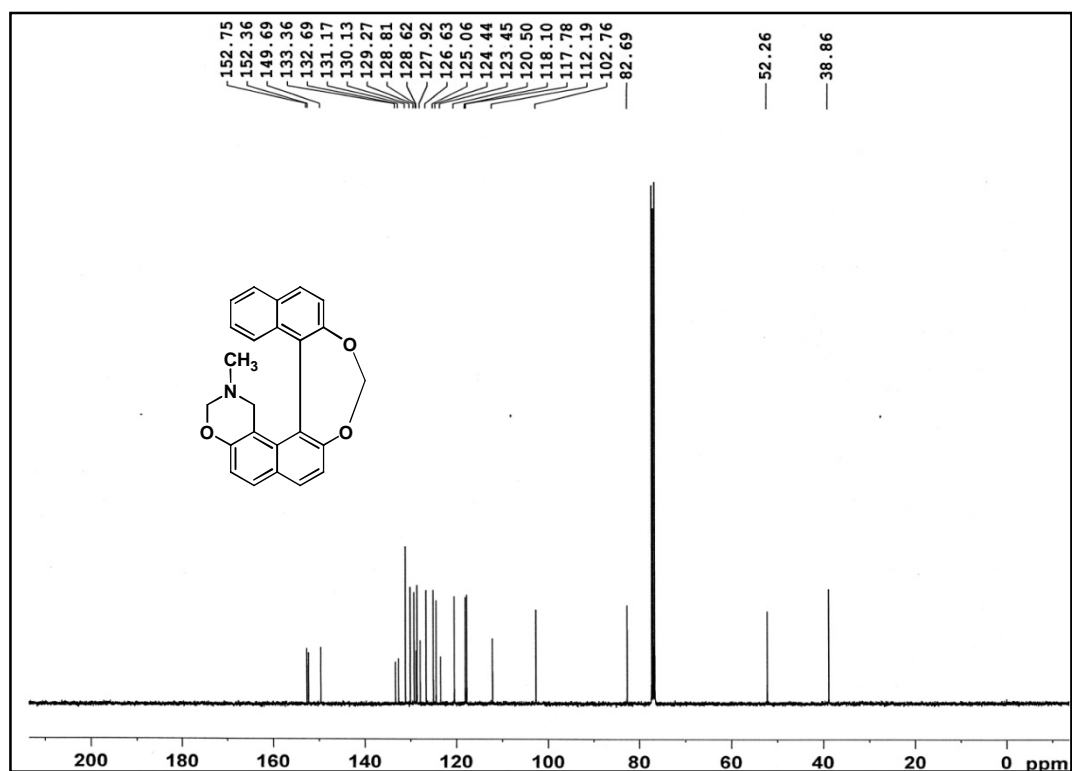
¹H-NMR spectrum of [1,1'-binaphthalene]-2,2',7-triyl tris((1R,2S,5R)-2-isopropyl-5-methylcyclohexyl) tricarbonate (69)



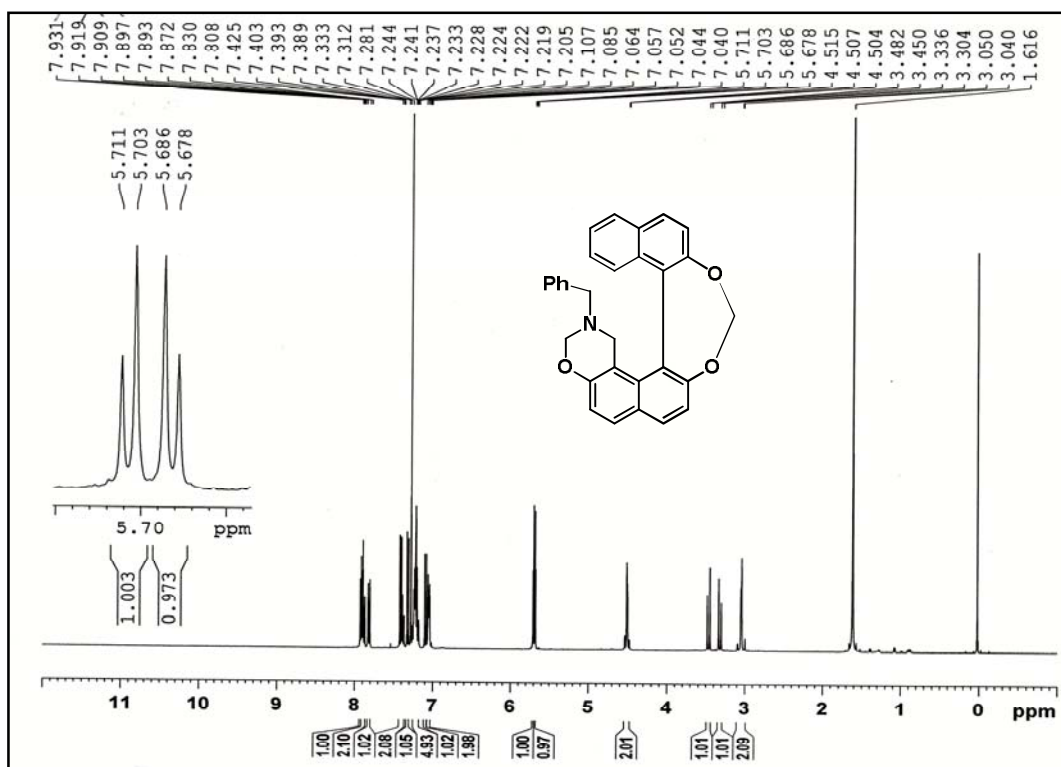
¹H-NMR spectrum of bis((1R,2S,5R)-2-isopropyl-5-methylcyclohexyl)(7-methoxy-[1,1'-binaphthalene]-2,2'-diyl) dicarbonate (70)



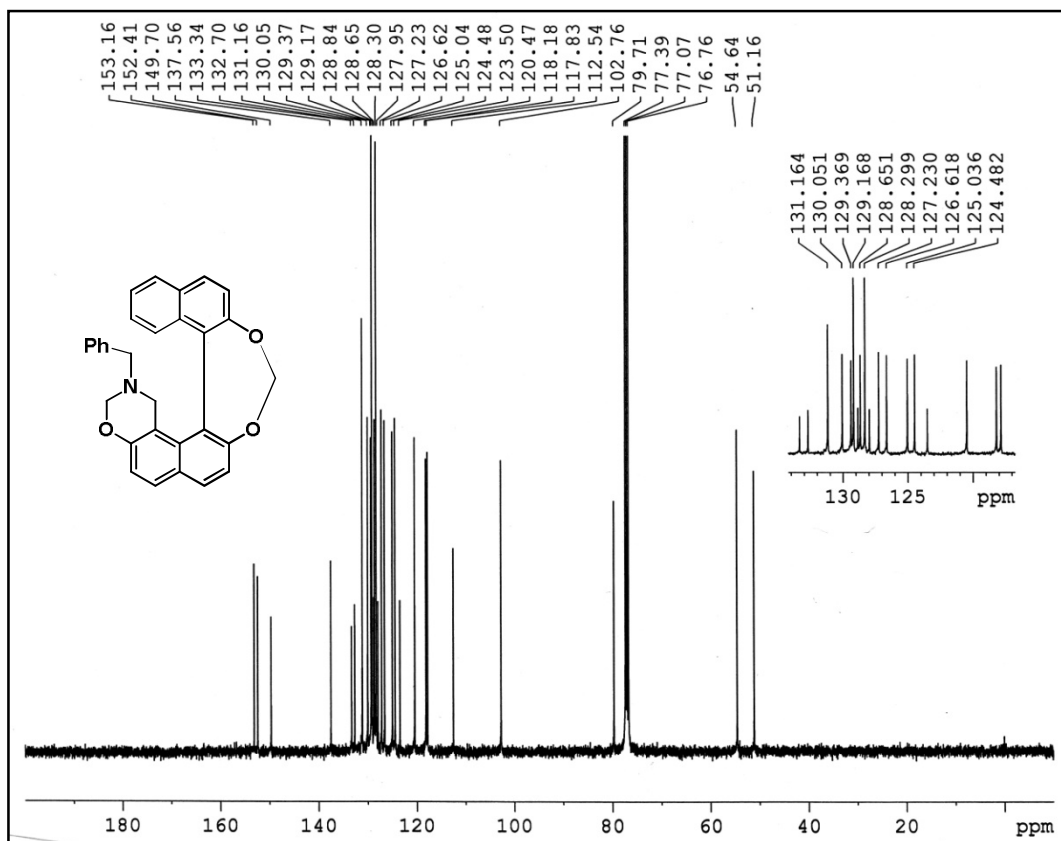
¹H-NMR spectrum of 10-methyl-10,11-dihydro-9H-naphtho[1'',2'':6',7'][[1,3]dioxepino[4',5':7,8]naphtha[1,2-e][1,3]oxazine (72)

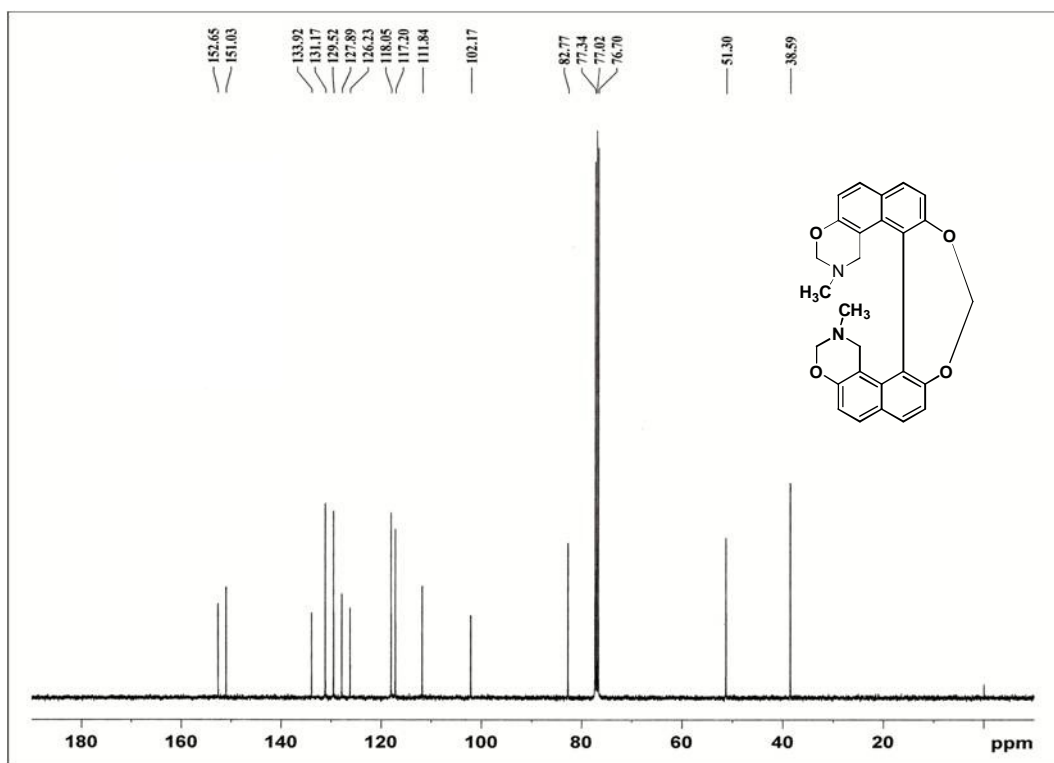


¹³C-NMR spectrum of 72

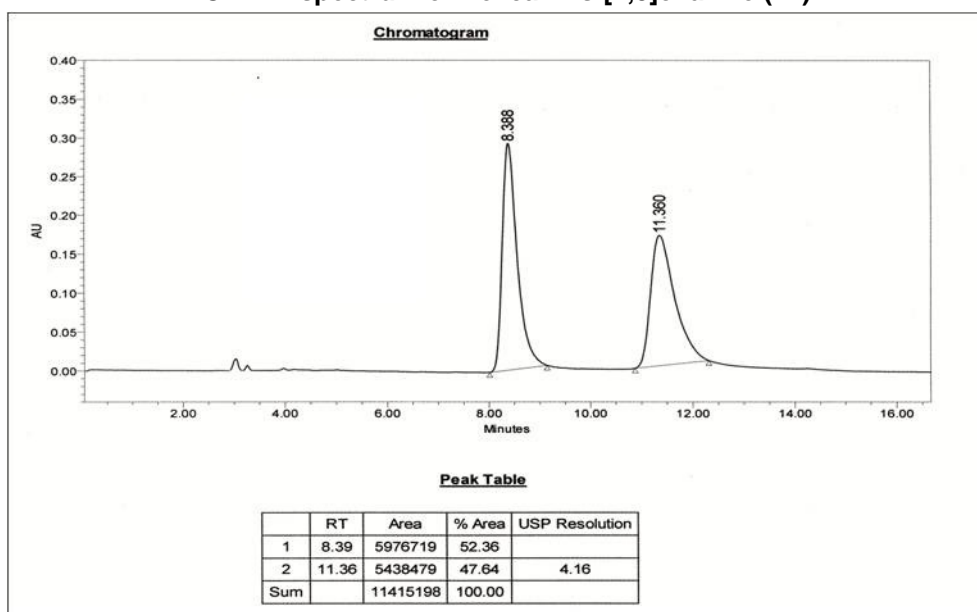


¹H-NMR Spectrum of compound 10-benzyl-10,11-dihydro-9H-naphtho[1',2'':6',7']-[1,3]dioxepino[4',5':7,8]naphtha [1,2-e][1,3]oxazine (73)





¹³C-NMR spectrum of Helical Bis-[1,3]oxazine (74)



HPLC analysis:

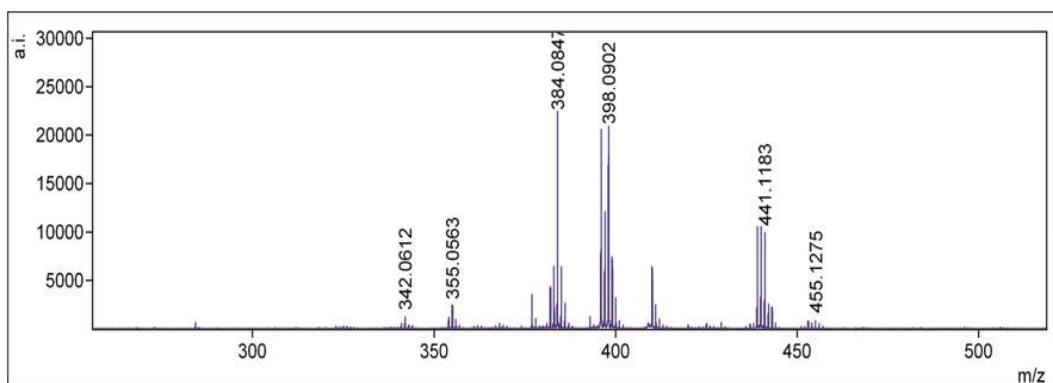
Observed two peaks of separated enantiomers at

- 1) R_t – 8.38 min and
- 2) R_t – 11.36 min.

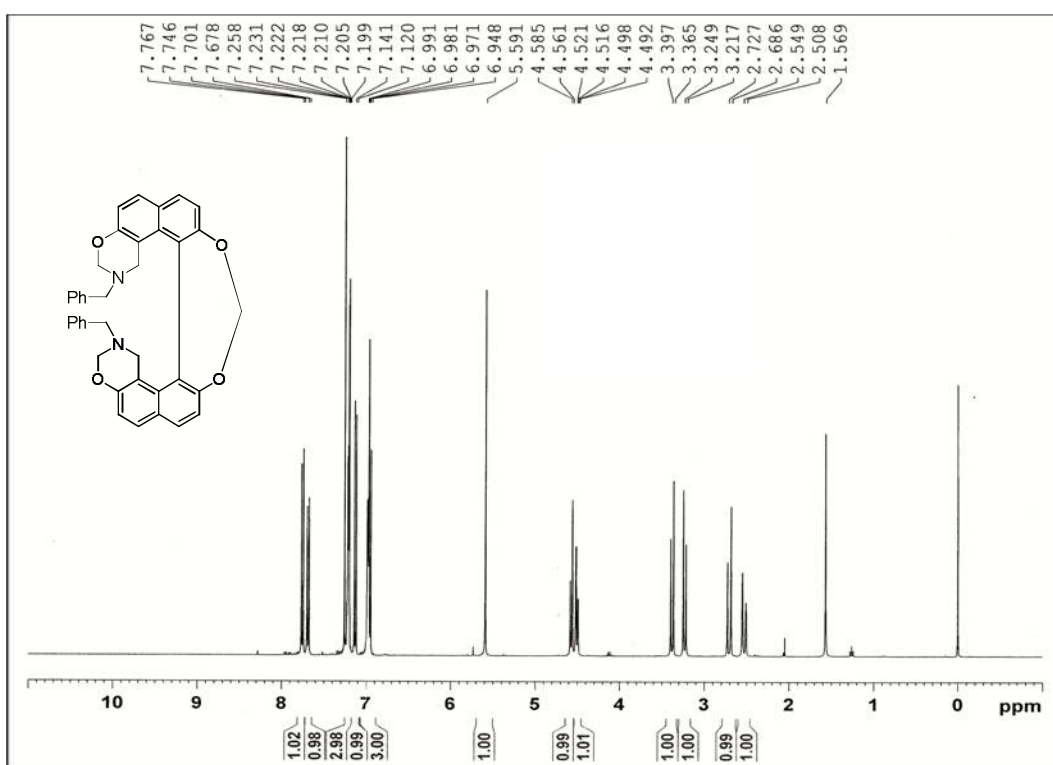
Solvent System: *n*-Hexane: *Iso*-propanol (85:15),

Flow rate: 1mL/min.

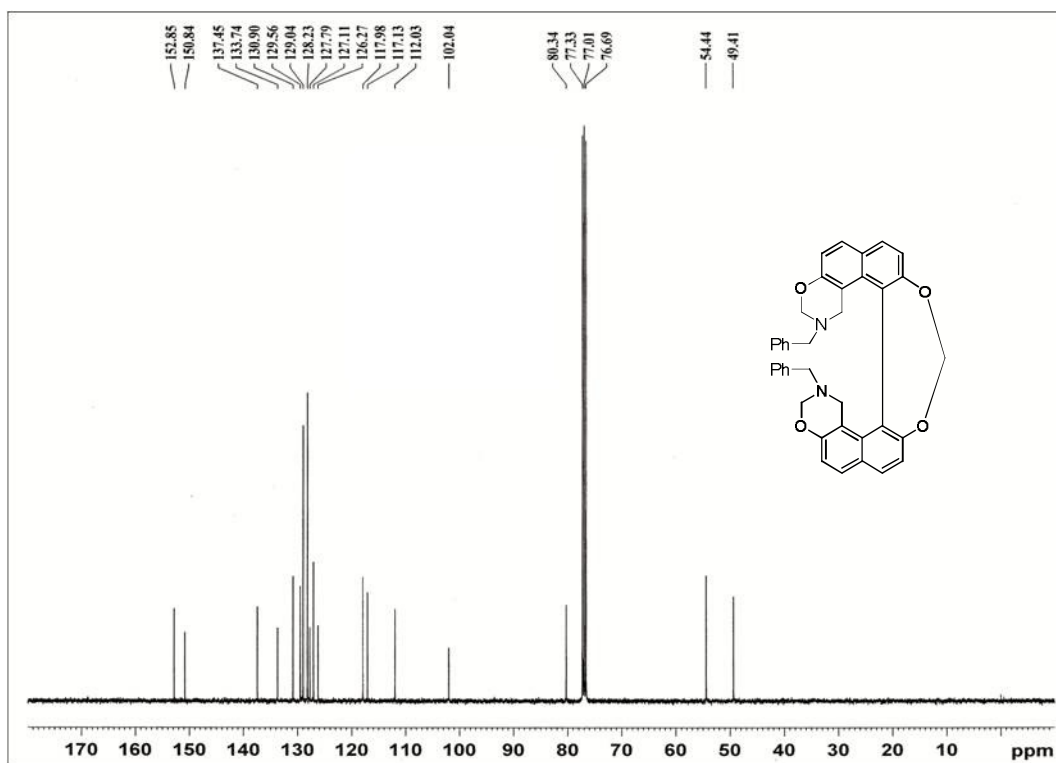
Chiral Column: Lux Amylose 2



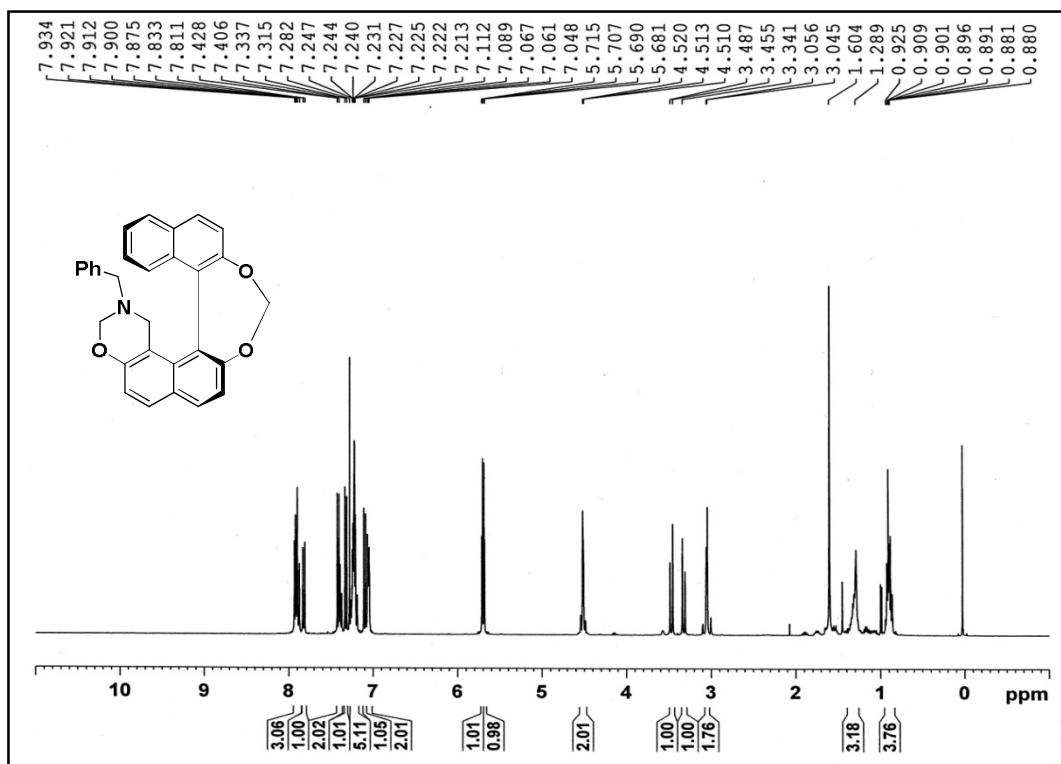
MALDI-TOF-MS spectrum of Helical Bis-[1,3]oxazine (74)



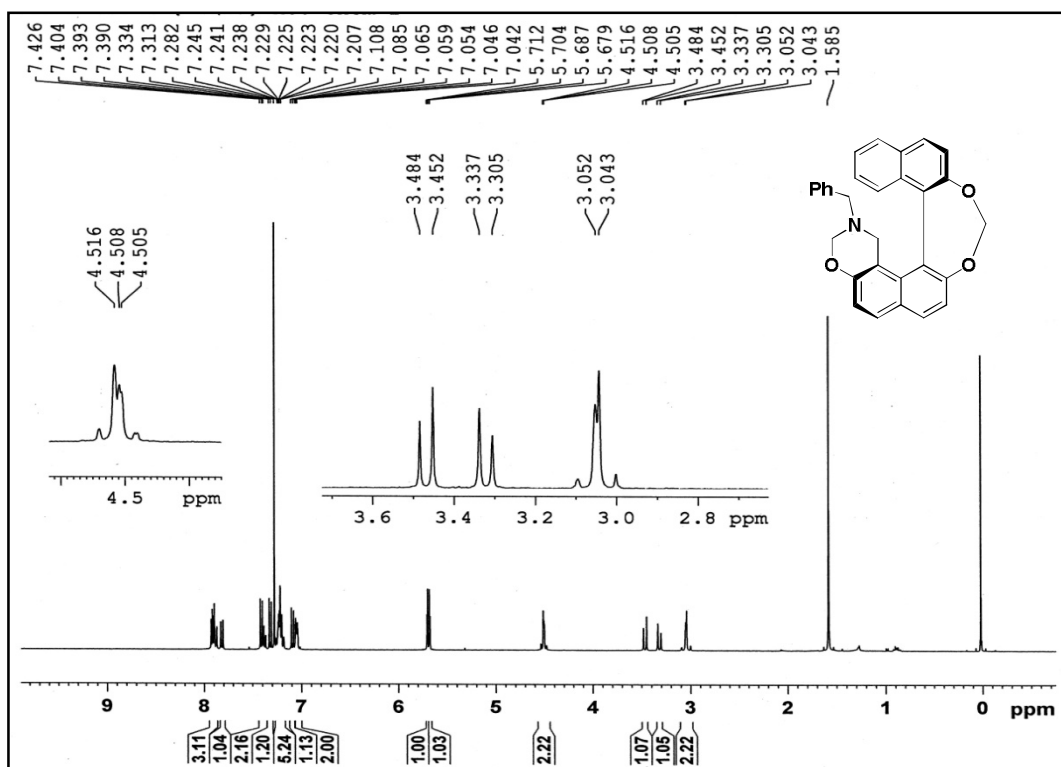
¹H-NMR spectrum of Helical Bis-[1,3]oxazine (75) in CDCl₃ on 400 MHz



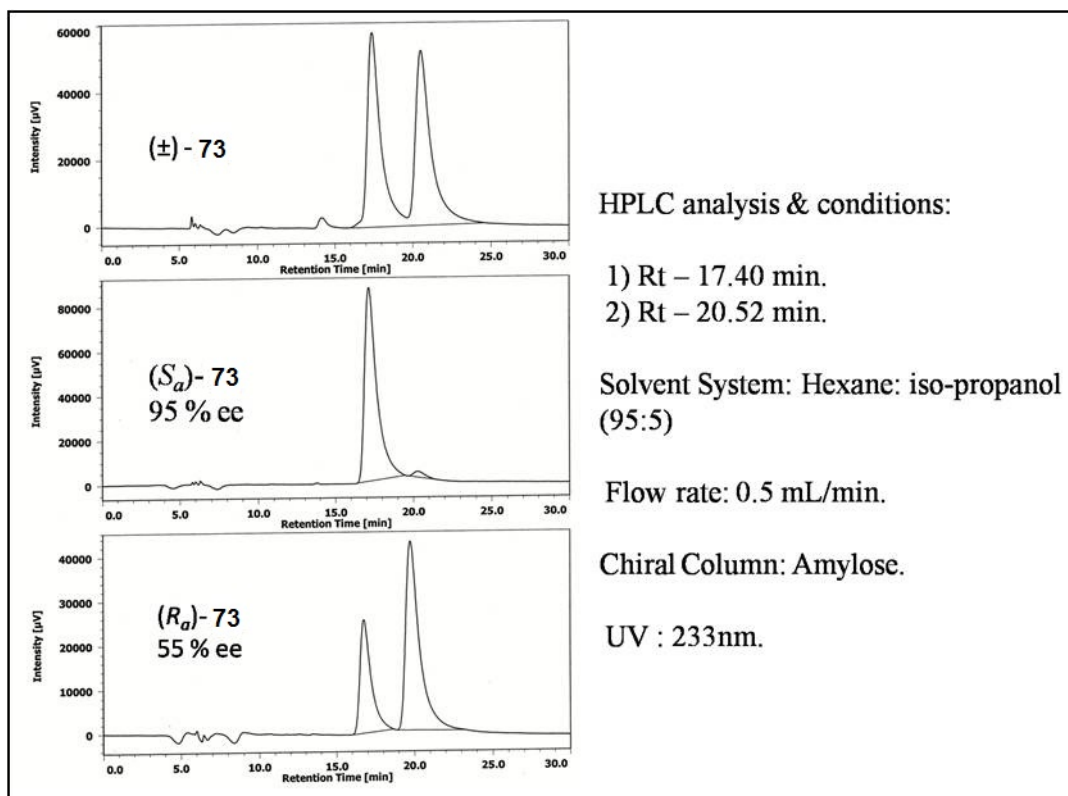
¹³C-NMR spectrum of Helical Bis-[1,3]oxazine (75) in CDCl₃ on 100.6 MHz



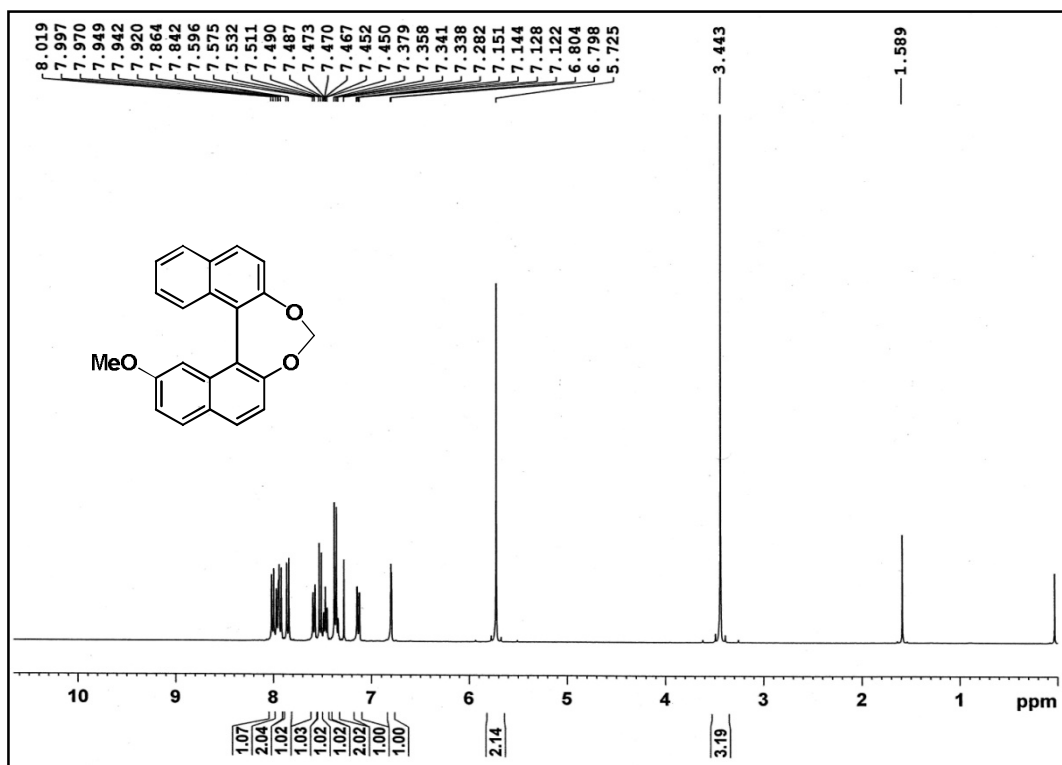
¹H-NMR Spectrum of (*S_a*)-10-benzyl-10,11-dihydro-9H-naphtho[1'',2'':6',7']-[1,3]dioxepino[4',5':7,8]naphtha[1,2-e][1,3]oxazine [(*S_a*)-73]



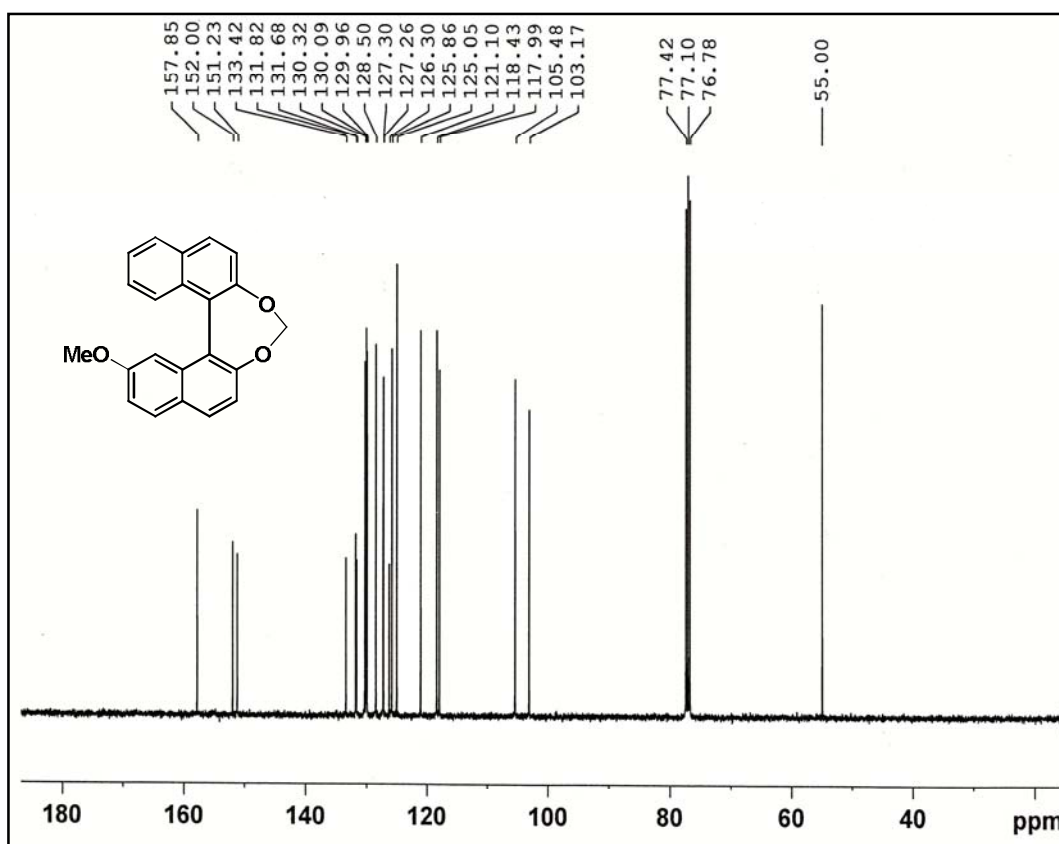
HPLC Analysis of compound 73:



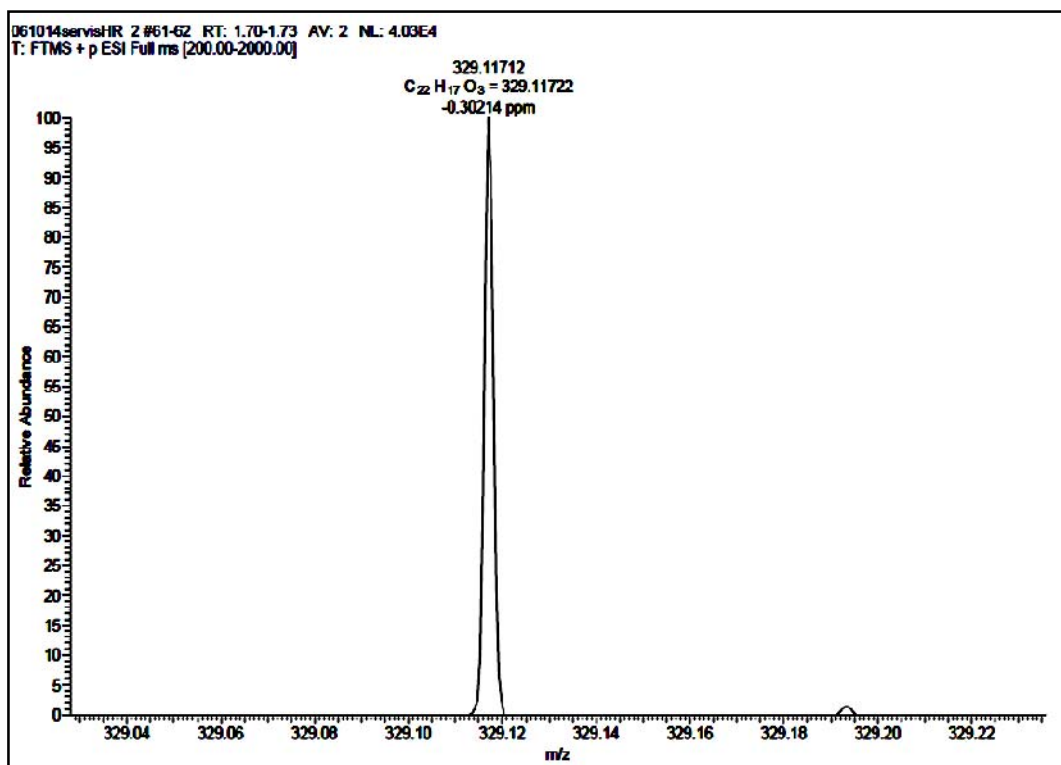
HPLC analysis of enantiomers pair of (S_a) -73 and (R_a) -73



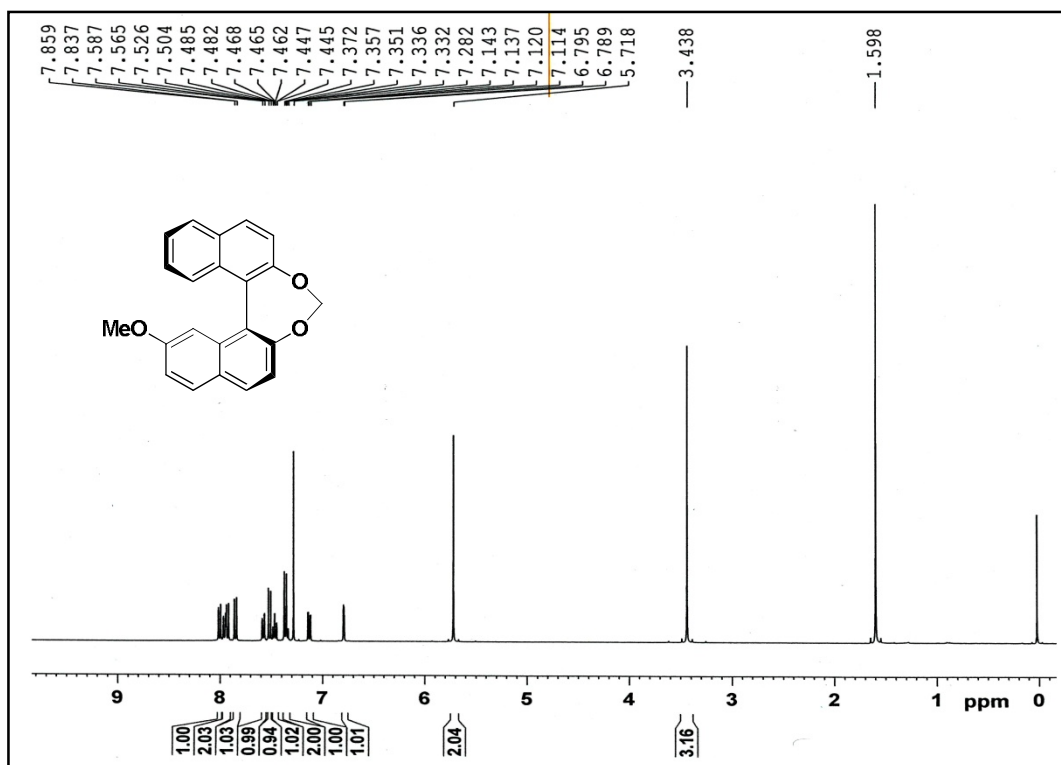
¹H-NMR Spectrum of (±) 10-methoxydinaphtho[2,1-d:1',2'-f][1,3]dioxepine (76)



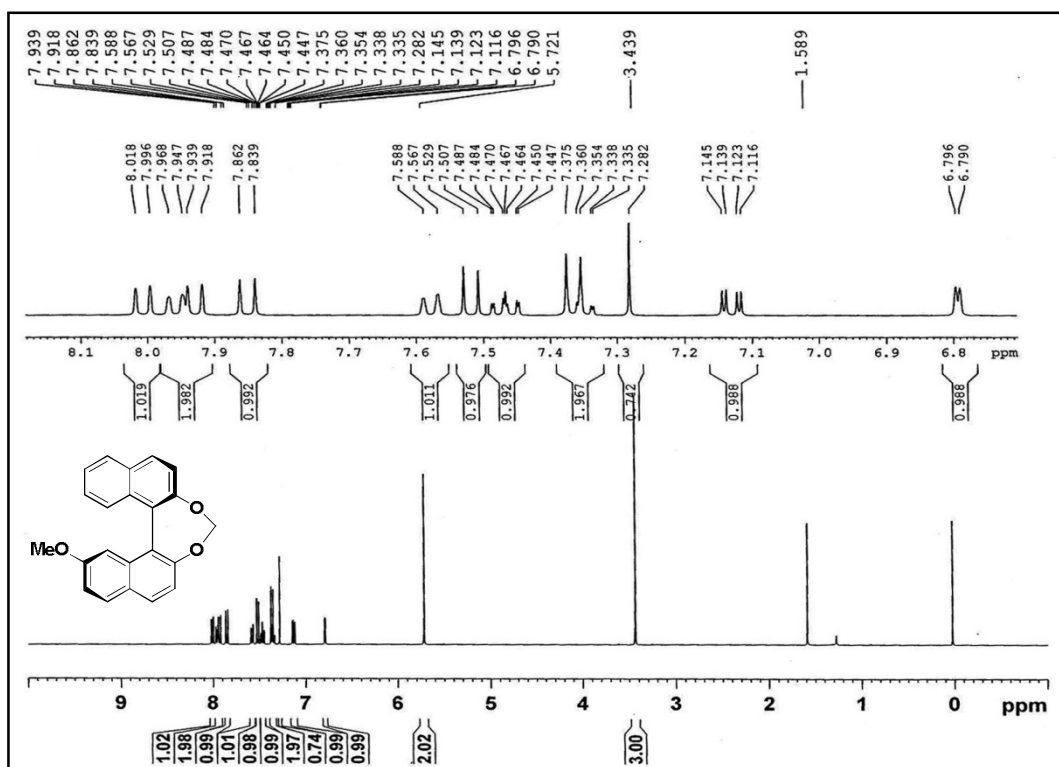
¹³C-NMR spectrum of (±) 10-methoxydinaphtho[2,1-d:1',2'-f][1,3]dioxepine (76)



HRMS spectrum of (±) 10-methoxydinaphtho[2,1-d:1',2'-f][1,3]dioxepine (76)

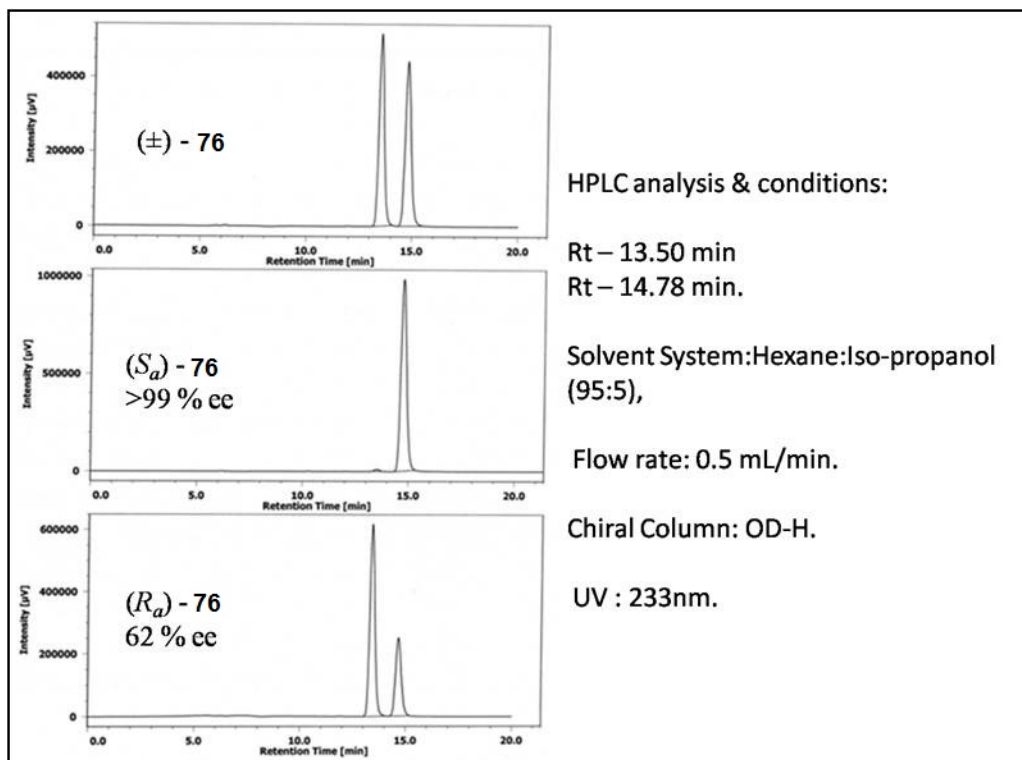


¹H-NMR spectrum of (*S_a*) 10-methoxydinaphtho[2,1-d:1',2'-f][1,3]dioxepine [(*S_a*)-76]

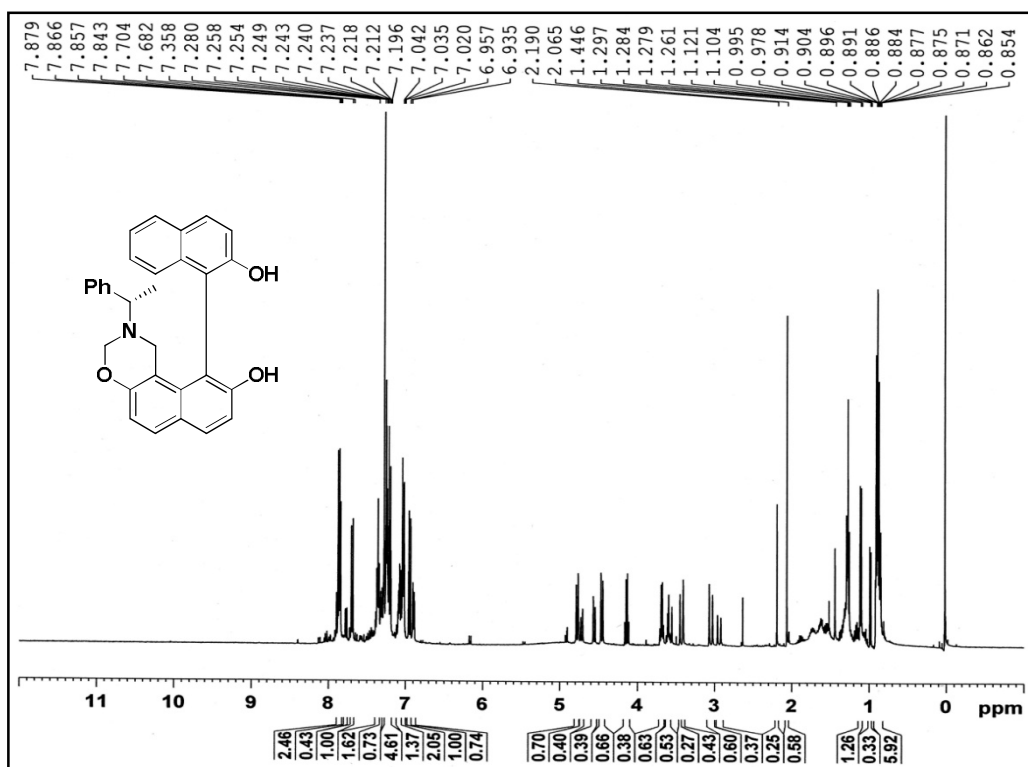


$^1\text{H-NMR}$ spectrum of (R_a) 10-methoxydinaphtho[2,1-d:1',2'-f][1,3]dioxepine [(R_a)-76]

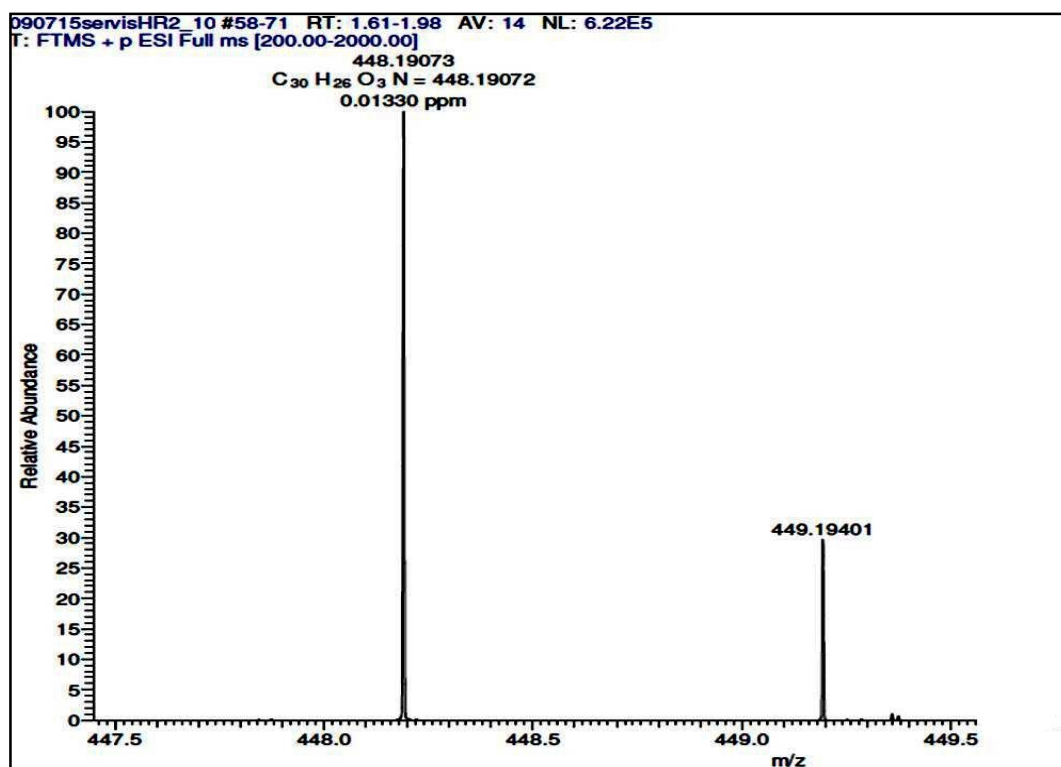
HPLC analysis of compound 76:



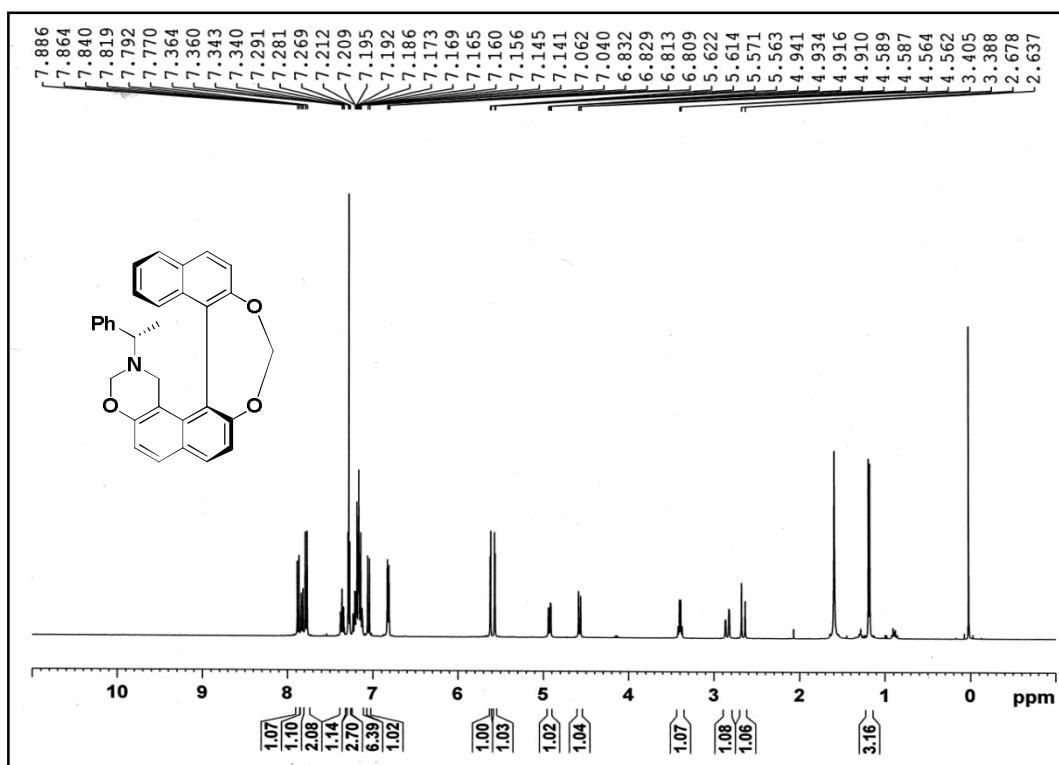
HPLC analysis of enantiomers pair of (S_a)-76 and (R_a)-76



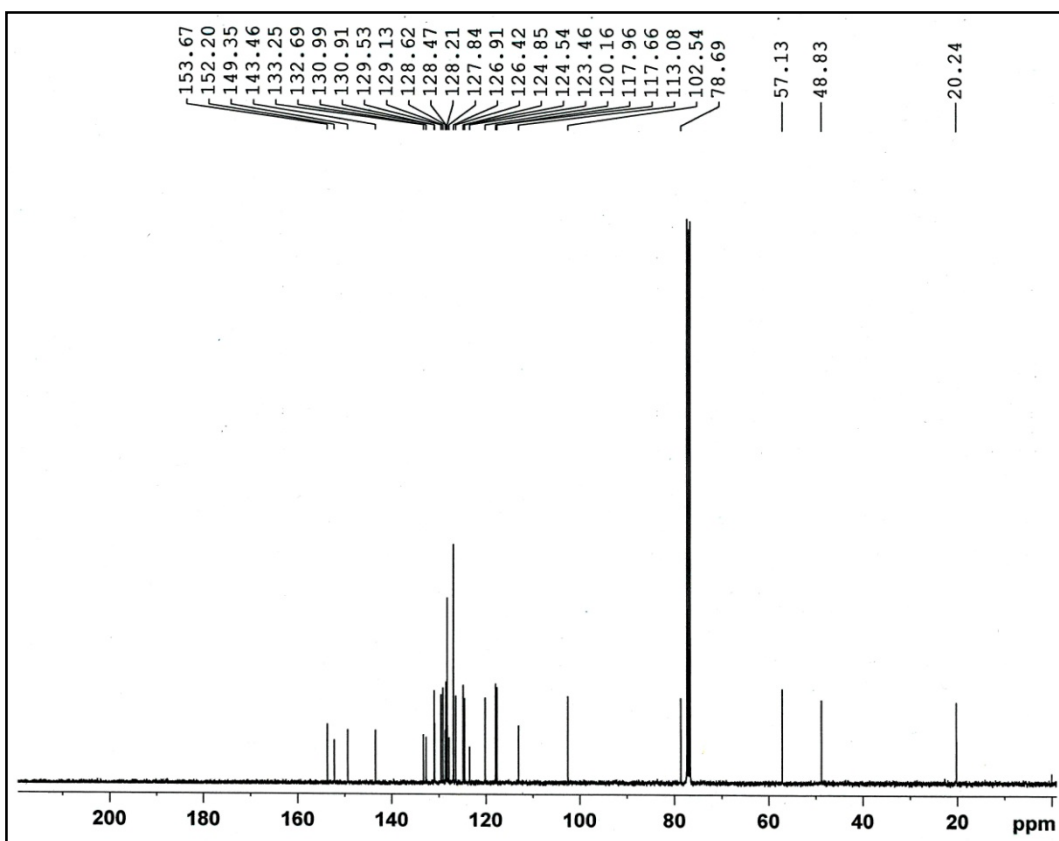
¹H-NMR Spectrum of (±) 10-(2-hydroxynaphthalen-1-yl)-2-((S)-1-phenylethyl)-2,3-dihydro-1H-naphtho [1,2-e][1,3]oxazin-9-ol (77)



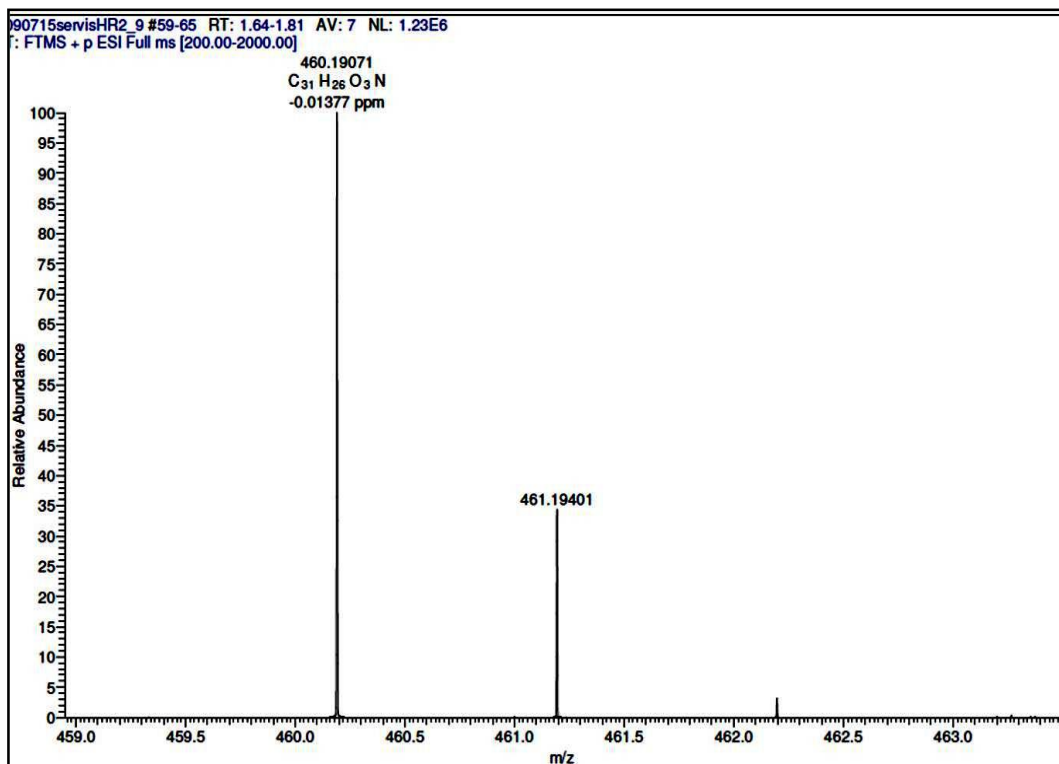
¹H-NMR Spectrum of compound (±)-77



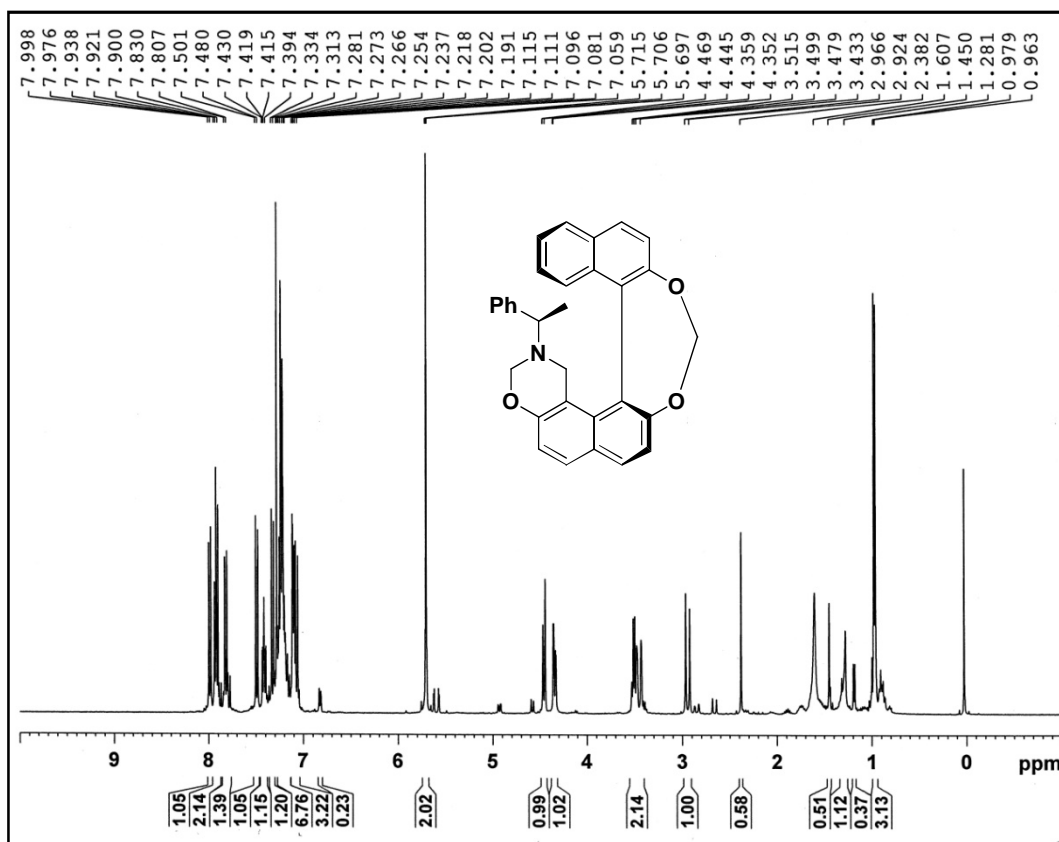
¹H-NMR Spectrum of (S_a)-10-((S)-1-phenylethyl)-10,11-dihydro-9H-naphtho[1'':2'':6',7']-[1,3]dioxepino[4',5':7,8]naphtho[1,2-e][1,3]oxazine [(S_a,S)-77]



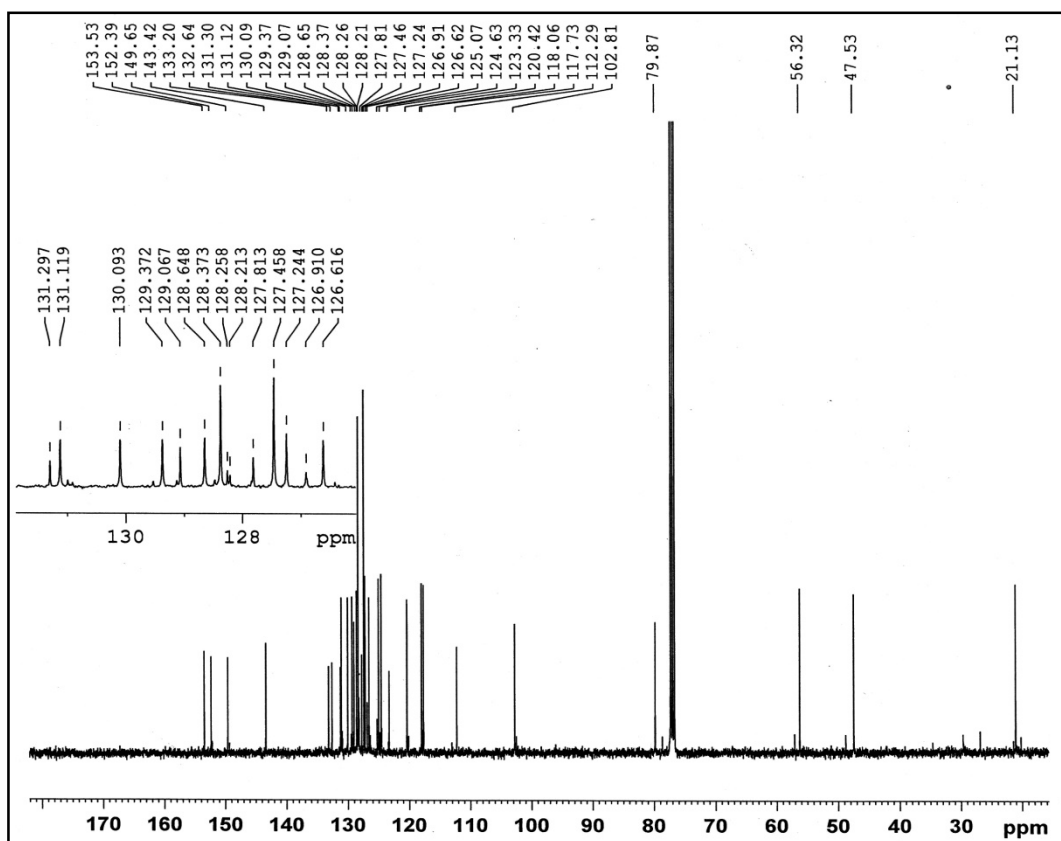
¹³C-NMR spectrum of compound [(S_a,S)-78]



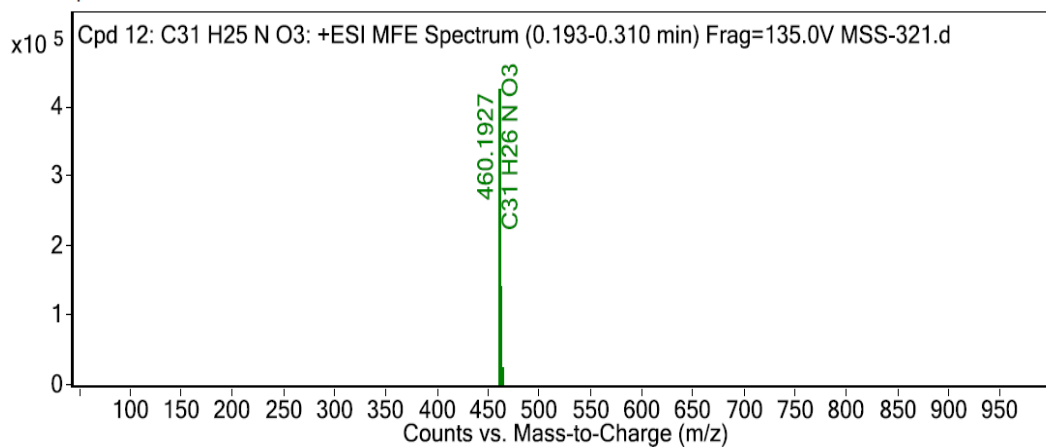
HRMS spectrum of compound [(*S_a*,*S*)-78]



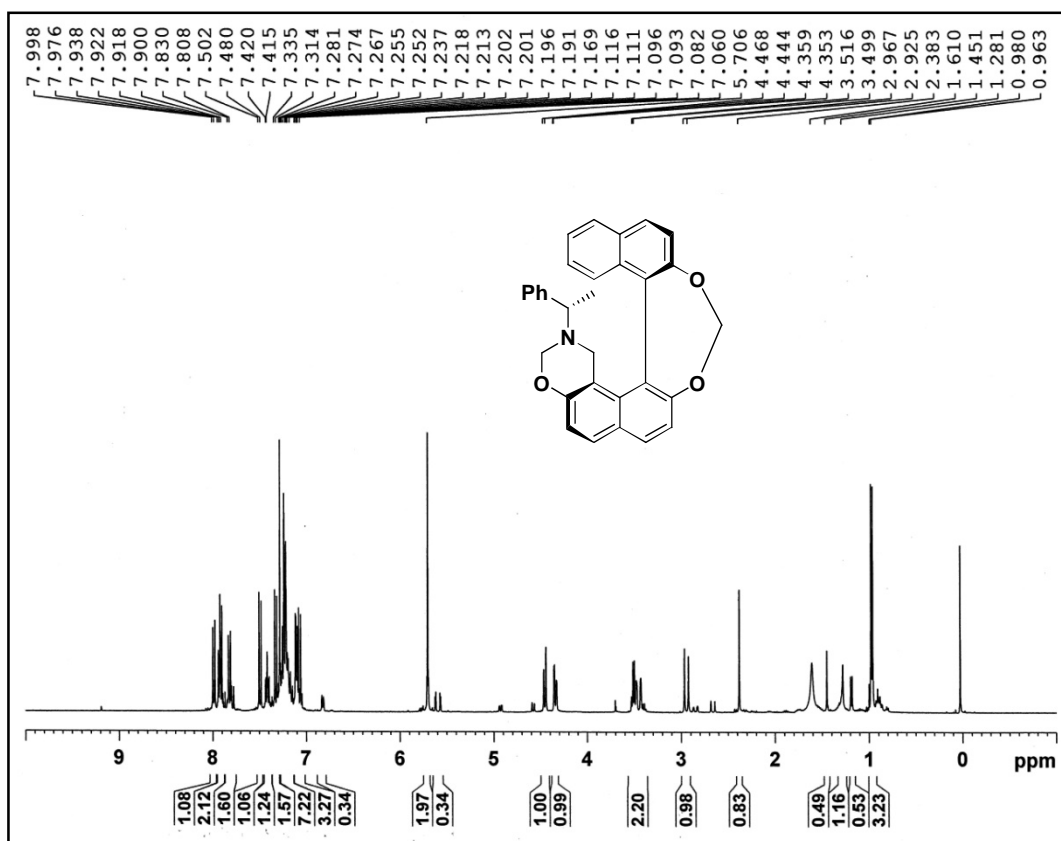
¹H-NMR Spectrum of compound [(*S_a*,*R*)-78]



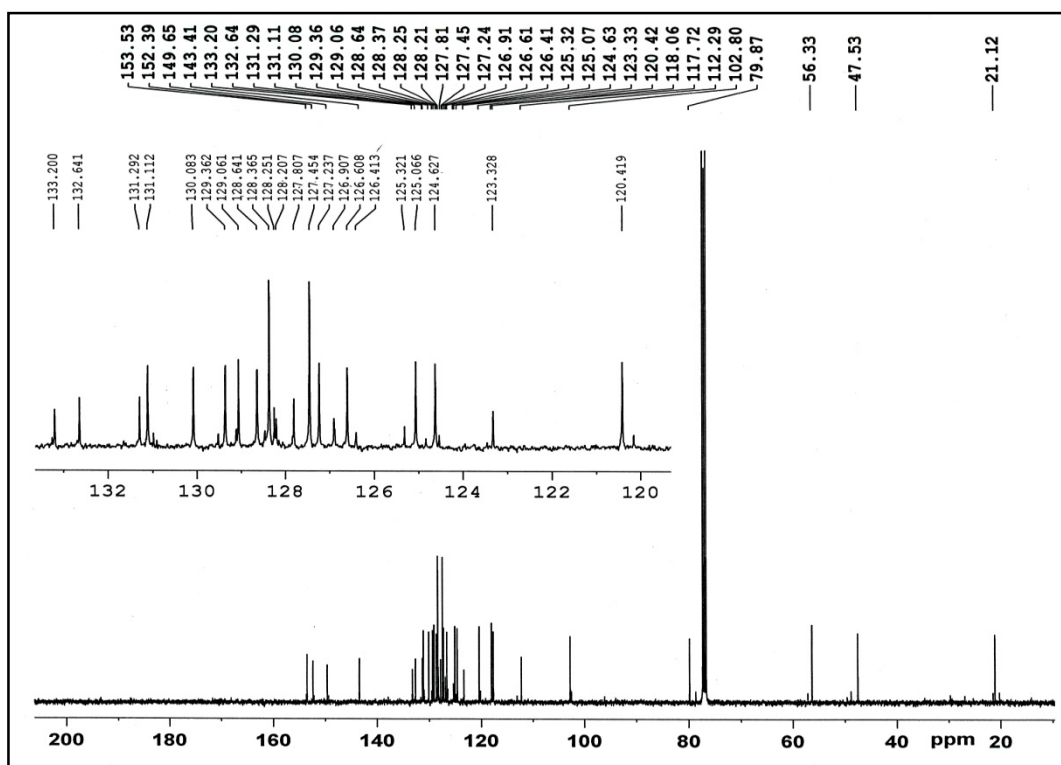
¹³C-NMR spectrum of compound [(*S_a*,*R*)-78]



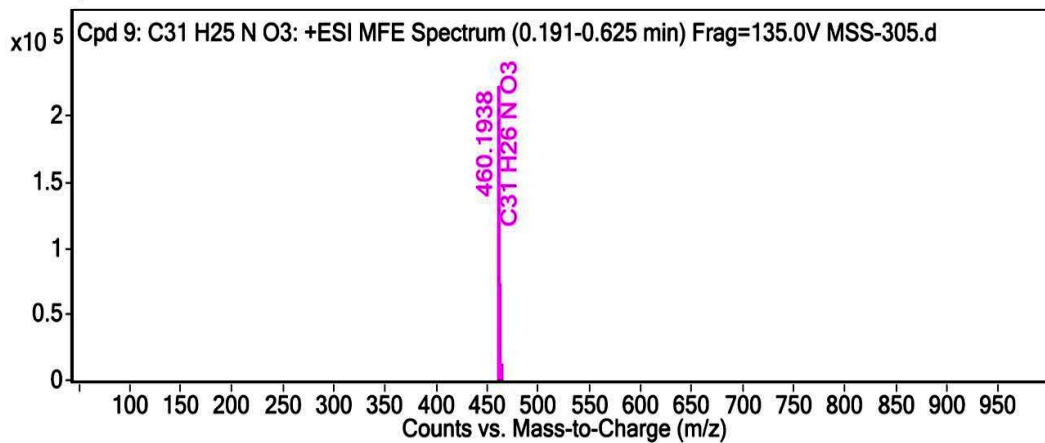
HRMS spectrum of compound [(*S_a*,*R*)-78]



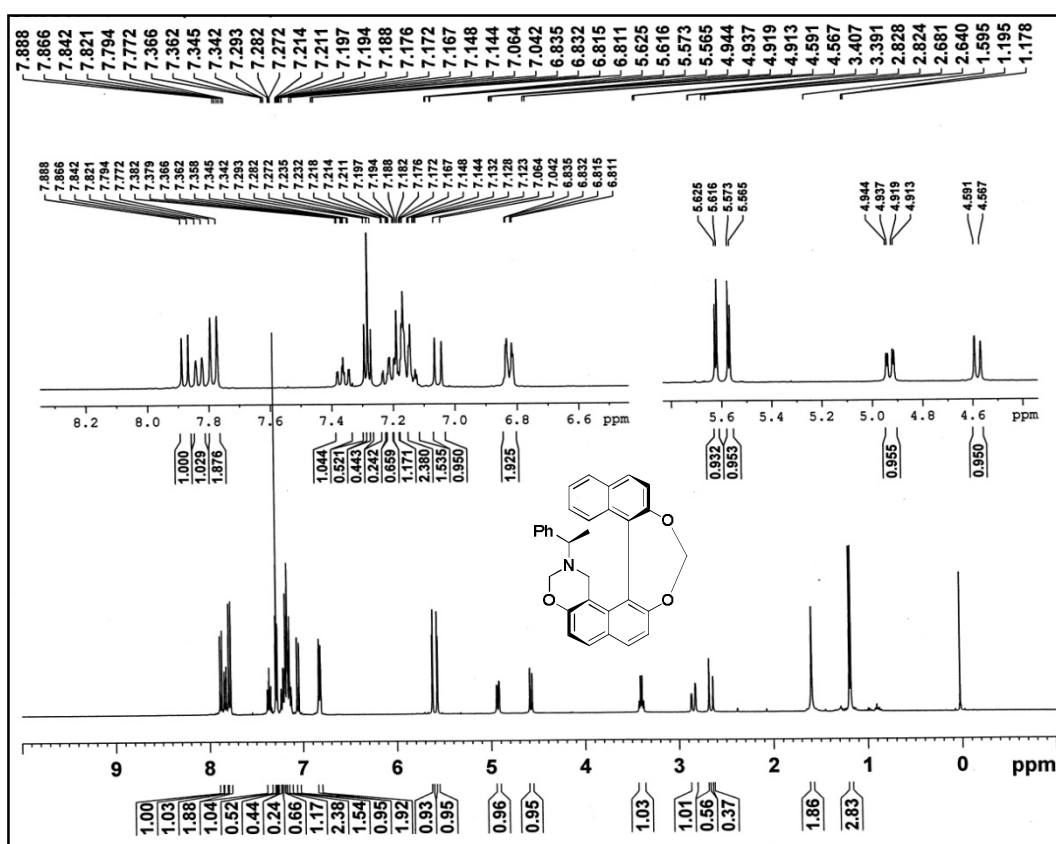
¹H-NMR Spectrum of compound [(*R_a*,*S*)-78]



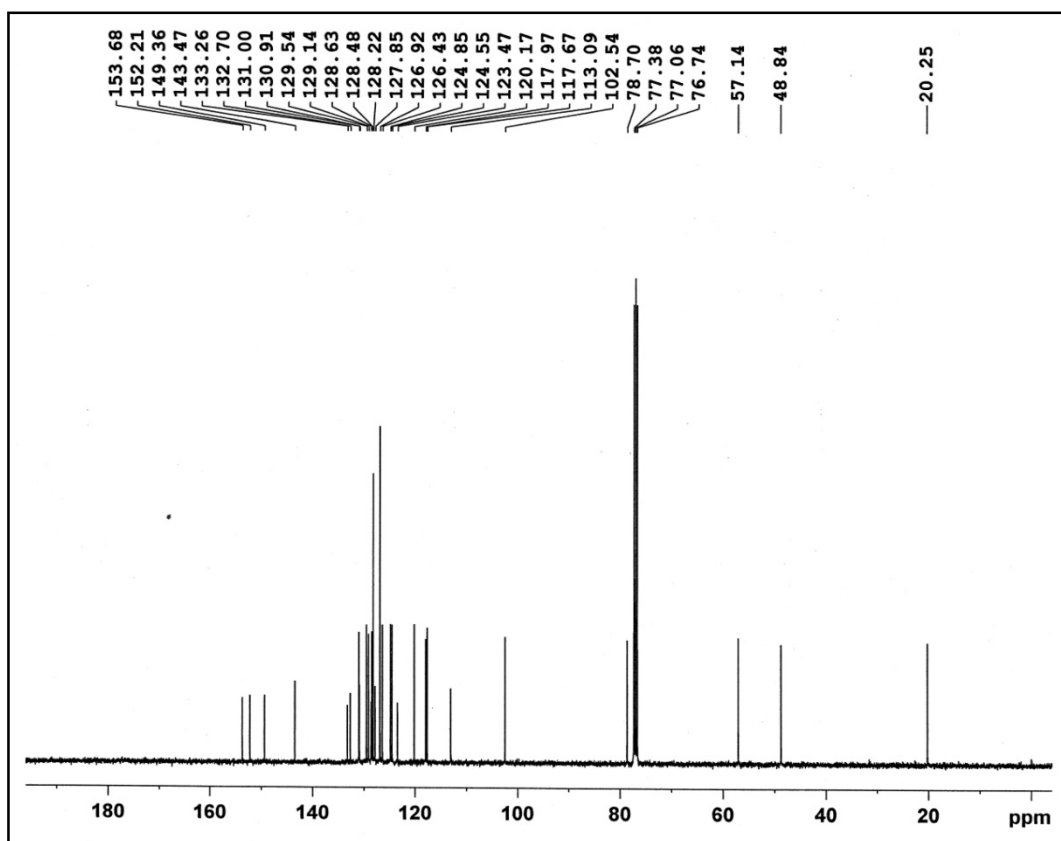
¹³C-NMR spectrum of compound [(*R_a*,*S*)-78]



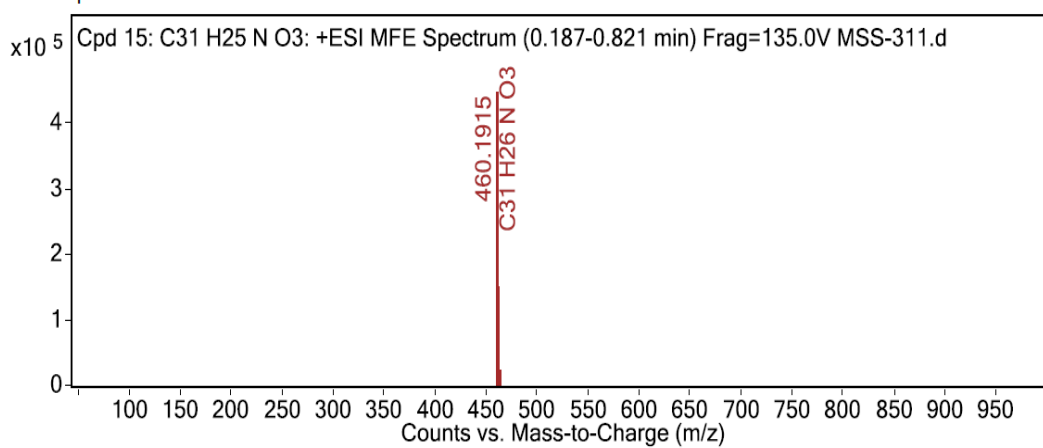
HRMS spectrum of compound [(*R_a*, *S*)-78]



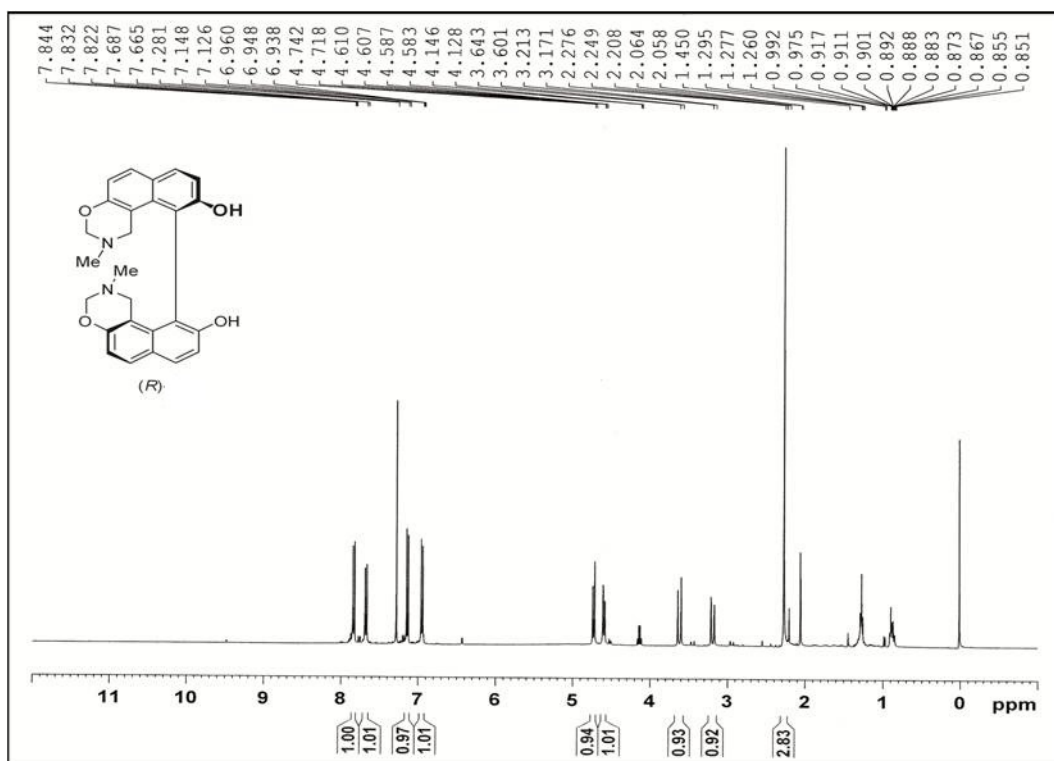
¹H-NMR Spectrum of compound [(*R_a*, *R*)-78]



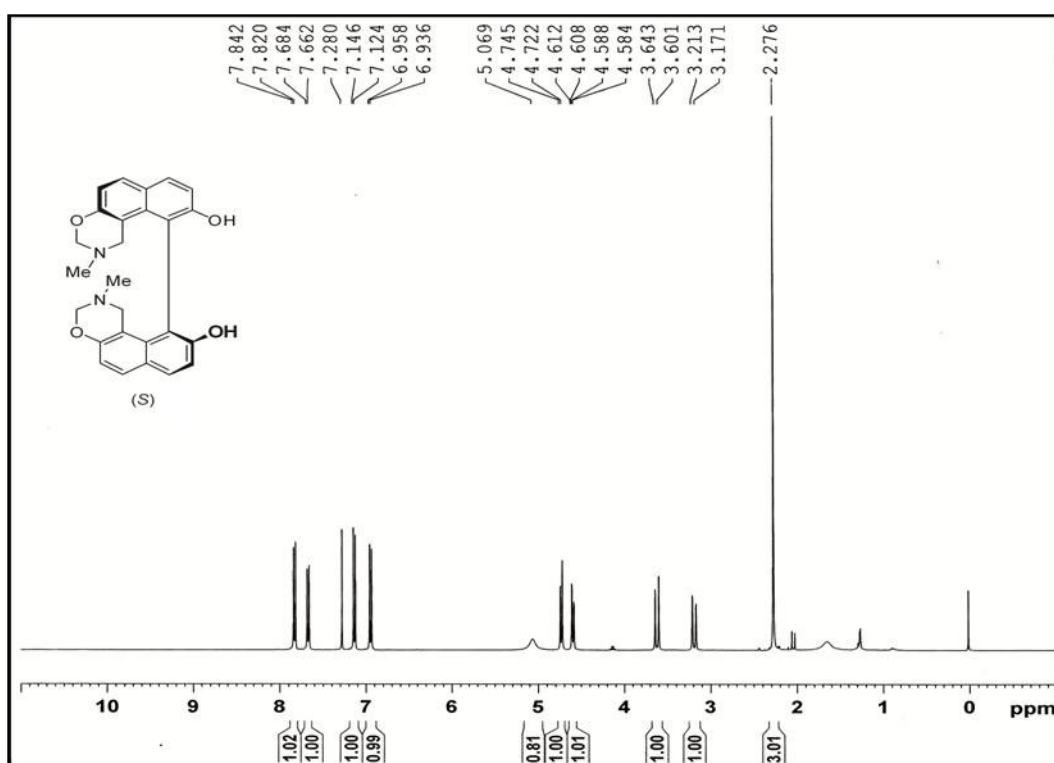
¹³C-NMR spectrum of compound [(*R_a*,*R*)-78]



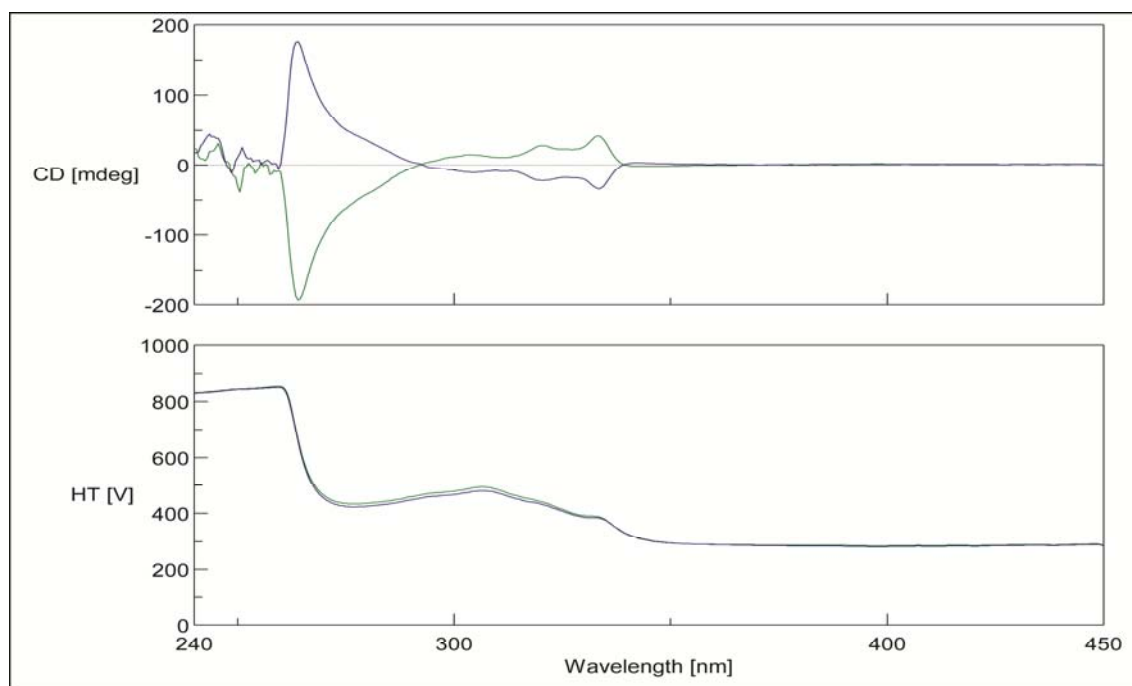
HRMS spectrum of compound [(*R_a*,*R*)-78]



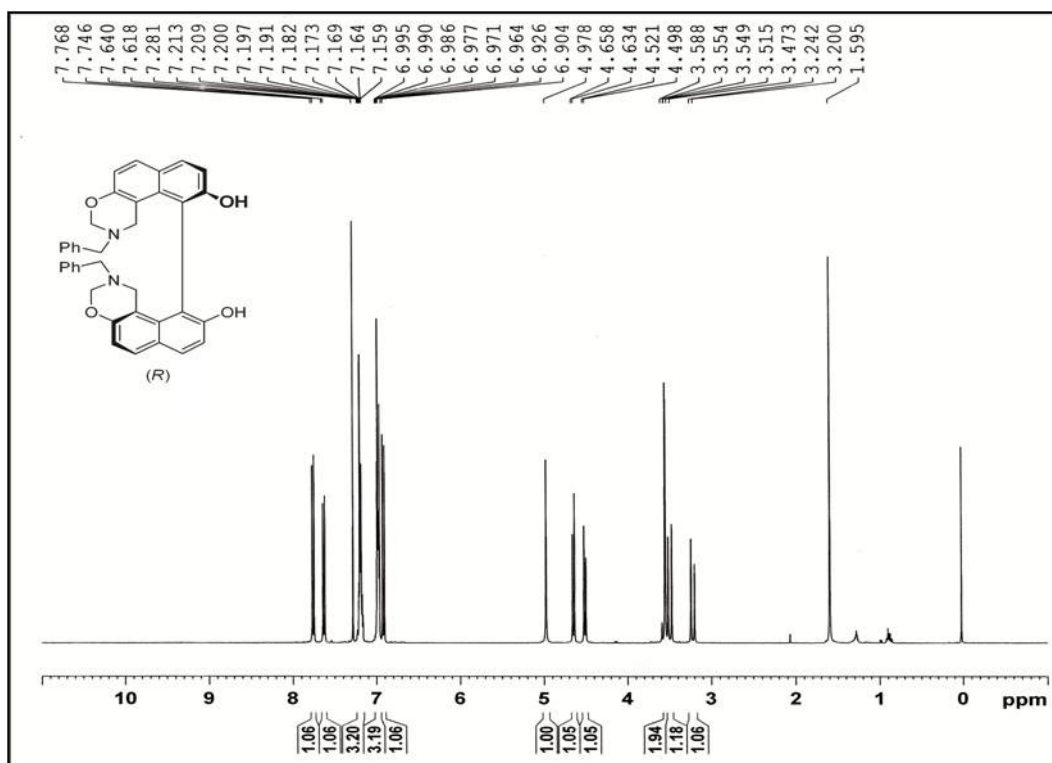
¹H-NMR Spectrum of (*R*)-(-)-2,2'-Dimethyl-2,3,2',3'-tetrahydro-1H,1'H-[10,10']bi[naphtho[1,2-e][1,3]oxaziny]-9,9'-diol [(*R*)-50]



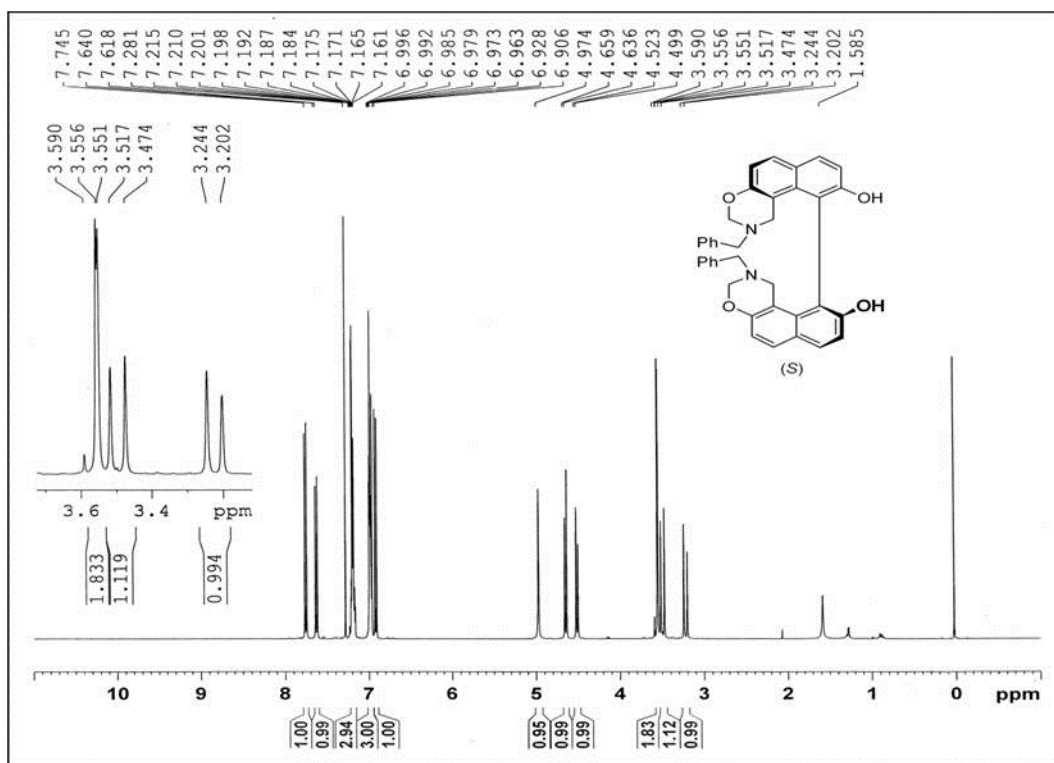
¹H-NMR Spectrum of (*S*)-(+)-2,2'-Dimethyl-2,3,2',3'-tetrahydro-1H,1'H-[10,10']bi[naphtho[1,2-e][1,3]oxaziny]-9,9'-diol [(*S*)-50]



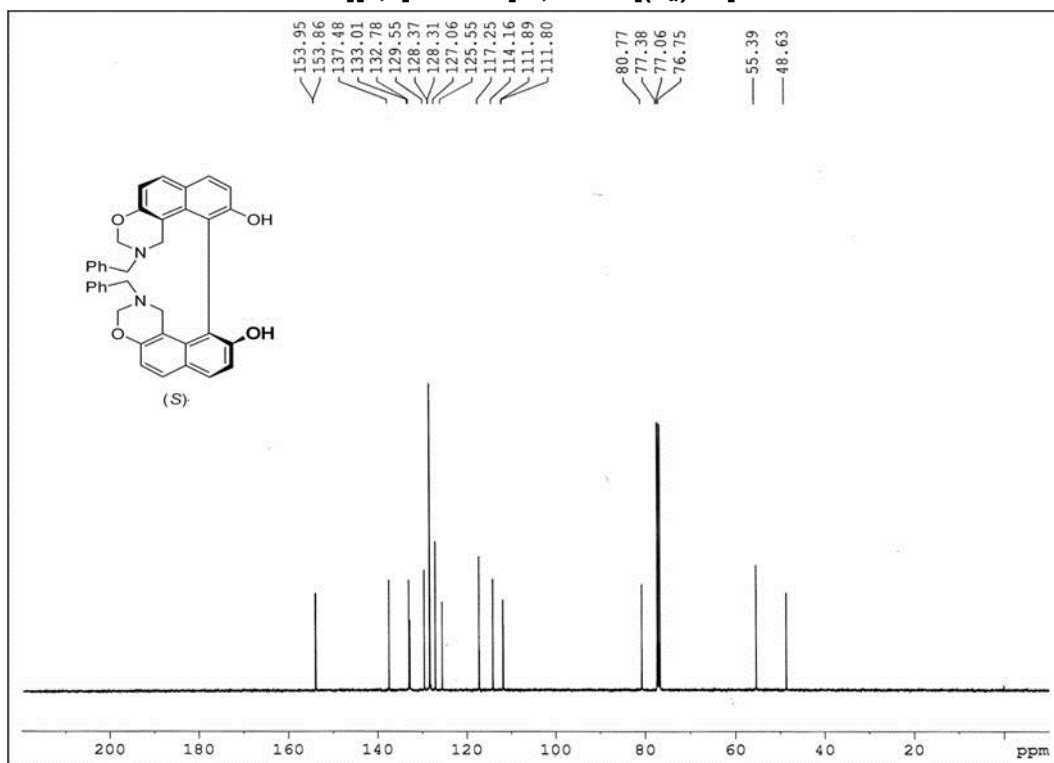
UV and Circular dichroism spectra of resolved 2,2'-Dimethyl-2,3,2',3'-tetrahydro-1H,1'H [10,10']bi[naphtho[1,2-e][1,3]oxaziny]-9,9'-diol: (Blue line) (*R_a*)-**50** and (Green line) (*S_a*)-**50** (*c* 8.44 × 10⁻⁴ M in acetonitrile, 25 °C).



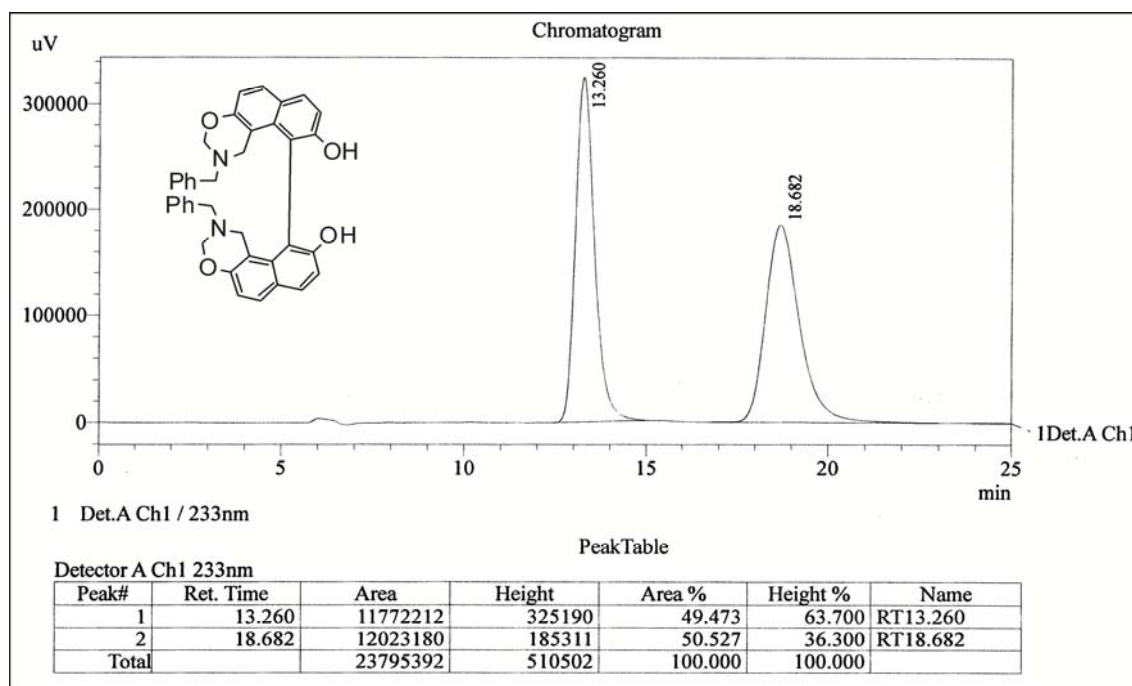
¹H-NMR spectrum of (*R_a*)-(-)-2,2'-dibenzyl-2,2',3,3'-tetrahydro-1H,1'H-[10,10'-binaphtho[1,2-e][1,3]oxazine]-9,9'-diol [(*R_a*)-**51**]



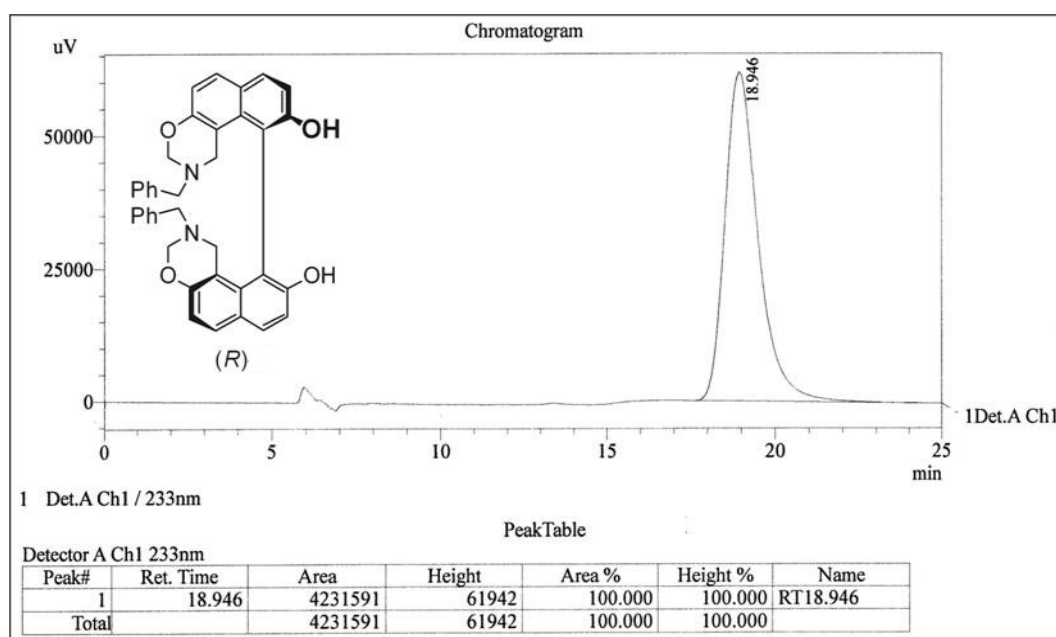
¹H-NMR spectrum of (*S_a*)-(+)-2,2'-dibenzyl-2,2',3,3'-tetrahydro-1H,1'H-[10,10'-binaphtho[1,2-e][1,3]oxazine]-9,9'-diol [(*S_a*)-51]



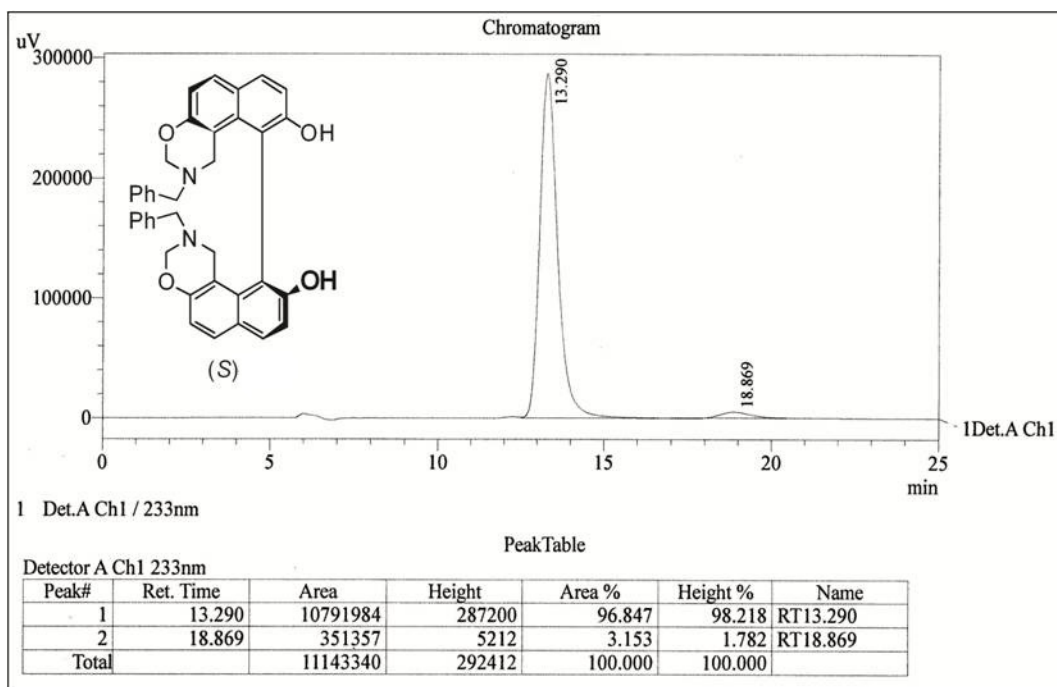
¹³C-NMR spectrum of (*S_a*)-(+)-2,2'-dibenzyl-2,2',3,3'-tetrahydro-1H,1'H-[10,10'-binaphtho[1,2-e][1,3]oxazine]-9,9'-diol [(*S_a*)-51]



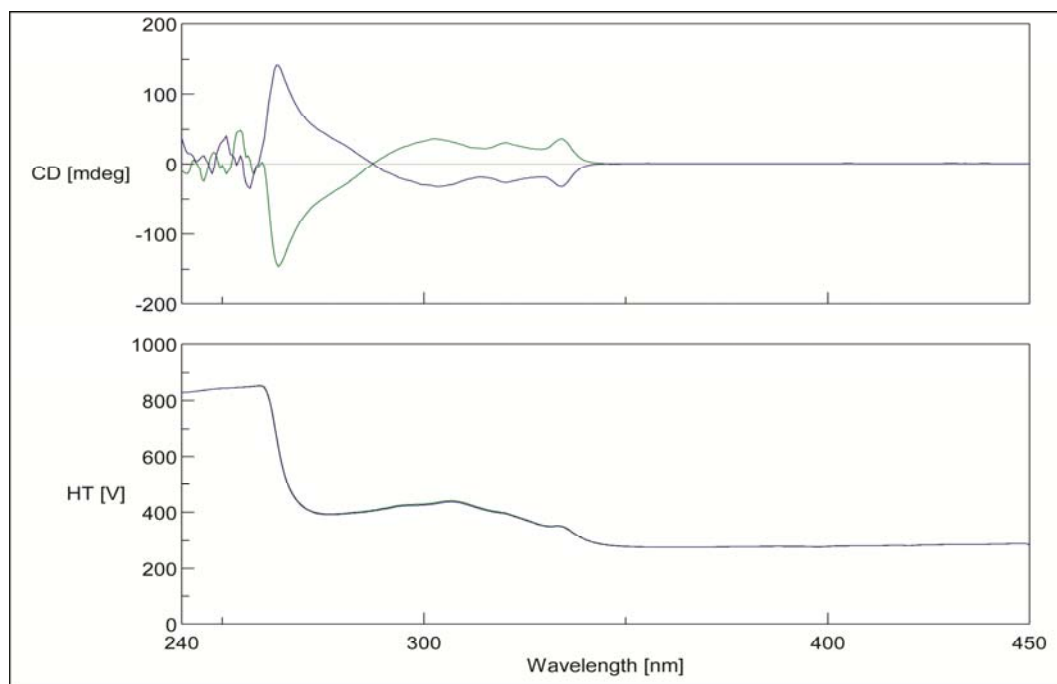
HPLC condition for **51**: Observed two peaks of separated enantiomers at 1) R_t – 13.26 min and 2) R_t – 18.68 min. Solvent System: Hexane: *iso*-propanol (70:30), Flow rate: 0.5 mL/min. Chiral Column: Daicel Chiral OD-H. UV: 233nm.



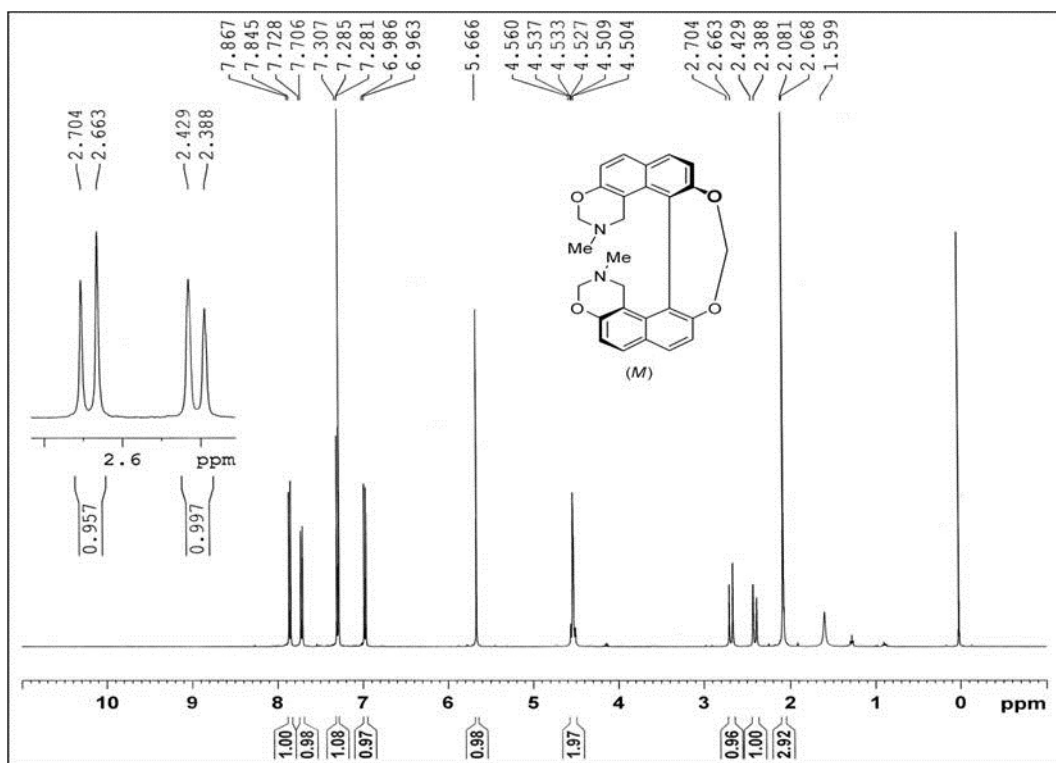
HPLC condition for (R_a)-**51**: Observed one peak of single enantiomer at R_t – 15.23 min. Solvent System: Hexane: *iso*-propanol (70:30), Flow rate: 0.5 mL/min. Chiral Column: Lux Amylose 2, UV: 254nm.



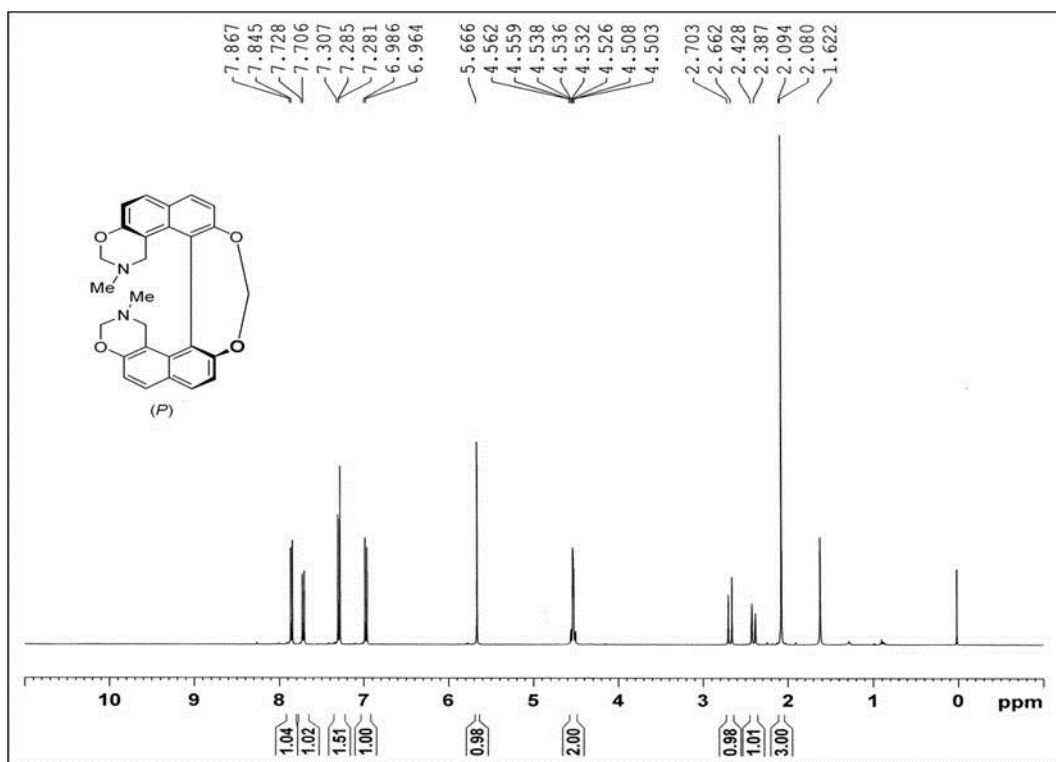
HPLC condition (*S_a*)-**51**: Observed one peak of single enantiomer at R_t – 13.29 min. Solvent System: Hexane: *Is*o-propanol (70:30), Flow rate: 0.5 mL/min. Chiral Column: Diacel Chiral OD-H. UV: 233nm.



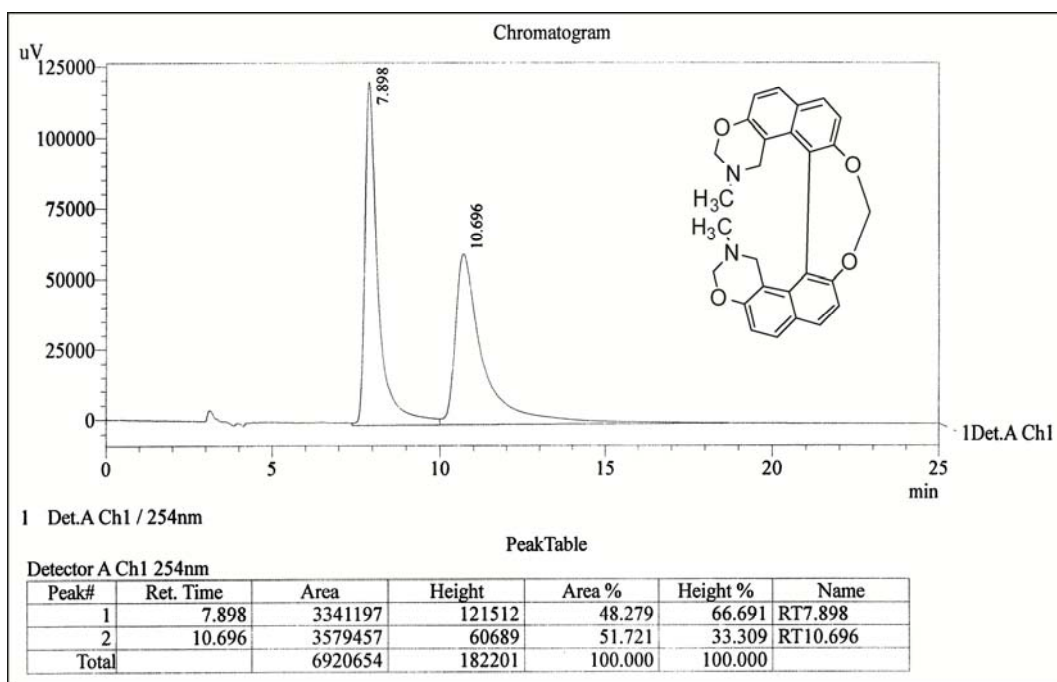
UV and Circular dichroism spectra of resolved 2,2'-dibenzyl-2,2',3,3'-tetrahydro-1H,1'H-[10,10'-binaphtho[1,2-e][1,3]oxazine]-9,9'-diol: (Blue line) (*R_a*)-**51** and (Green line) (*S_a*)-**51** (c 8.44 \times 10⁻⁴ M in acetonitrile, 25 °C).



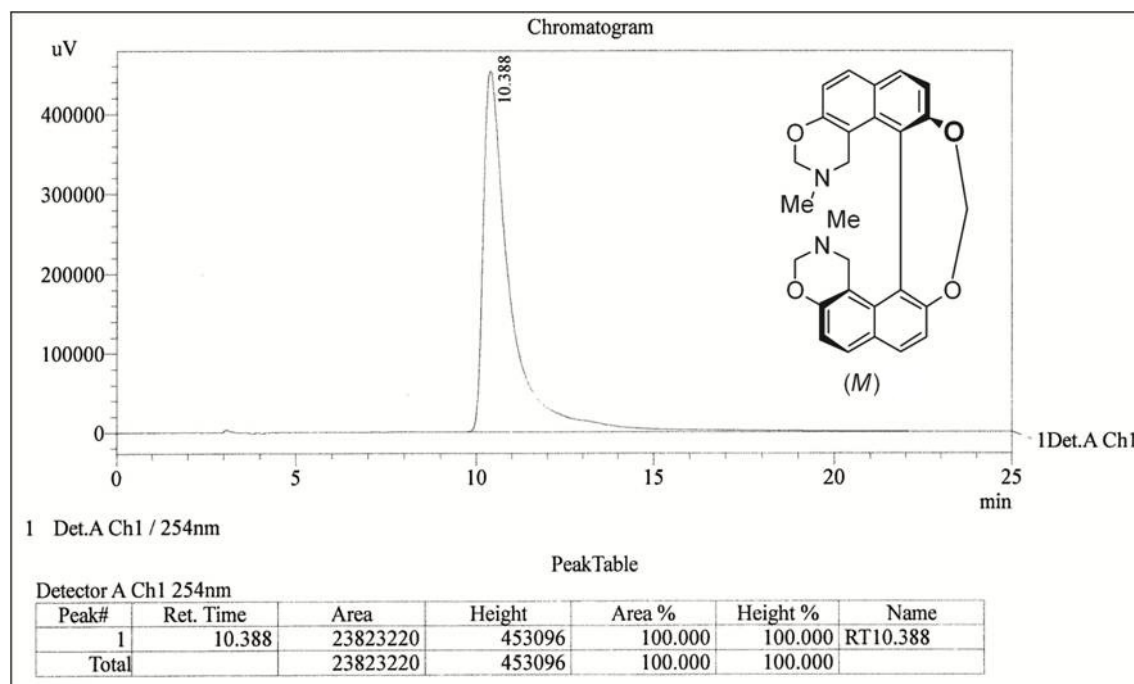
¹H-NMR spectrum of helicene like (*M*)-bis-oxazine [(*M*)-74]



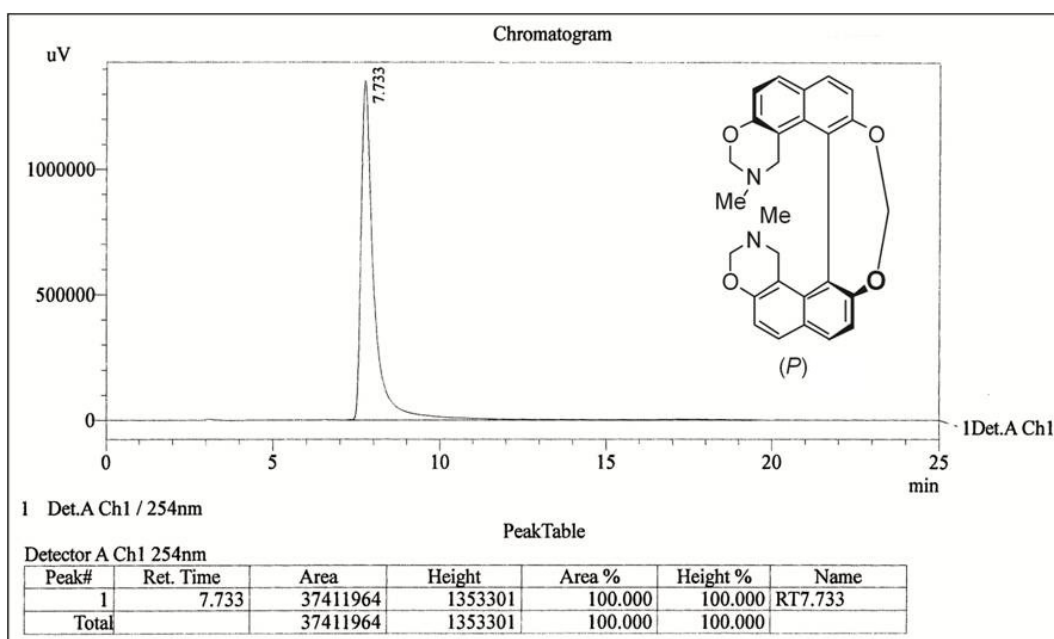
¹H-NMR spectrum of helicene like (*P*)-bis-oxazine [(*P*)-74] in CDCl₃ on 400 MHz



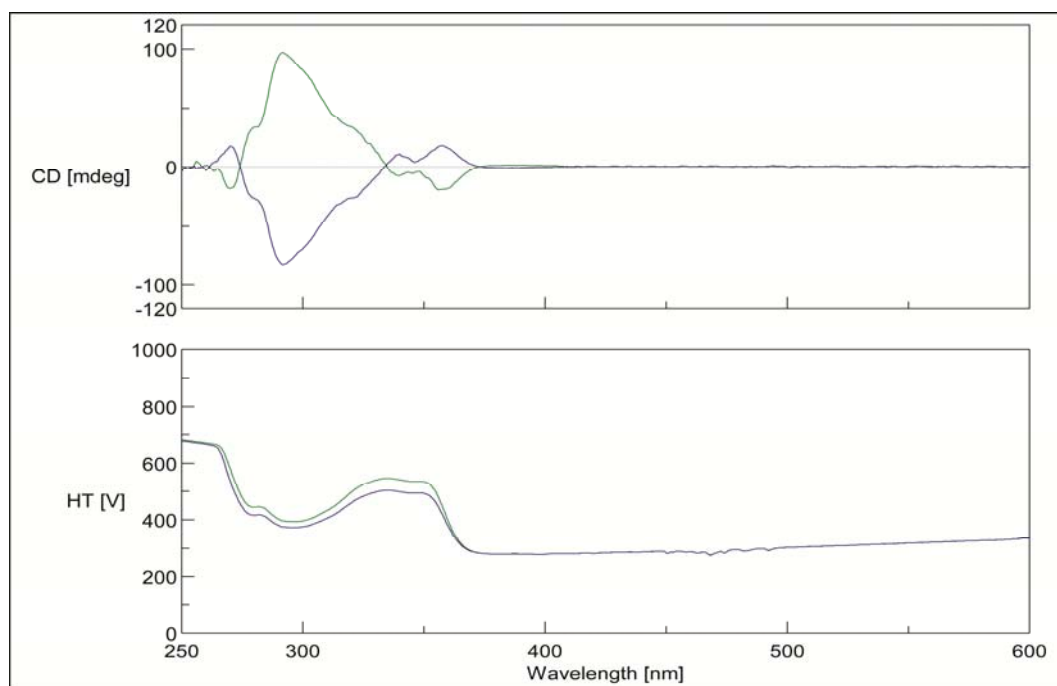
HPLC condition for (\pm)-**74**: Observed two peaks of separated enantiomers at 1). R_t – 7.89 min and 2). R_t – 10.69 min. Solvent System: Hexane: *Is*o-propanol (70:30), Flow rate: 0.5 mL/min. Chiral Column: Lux Amylose 2, UV: 254nm.



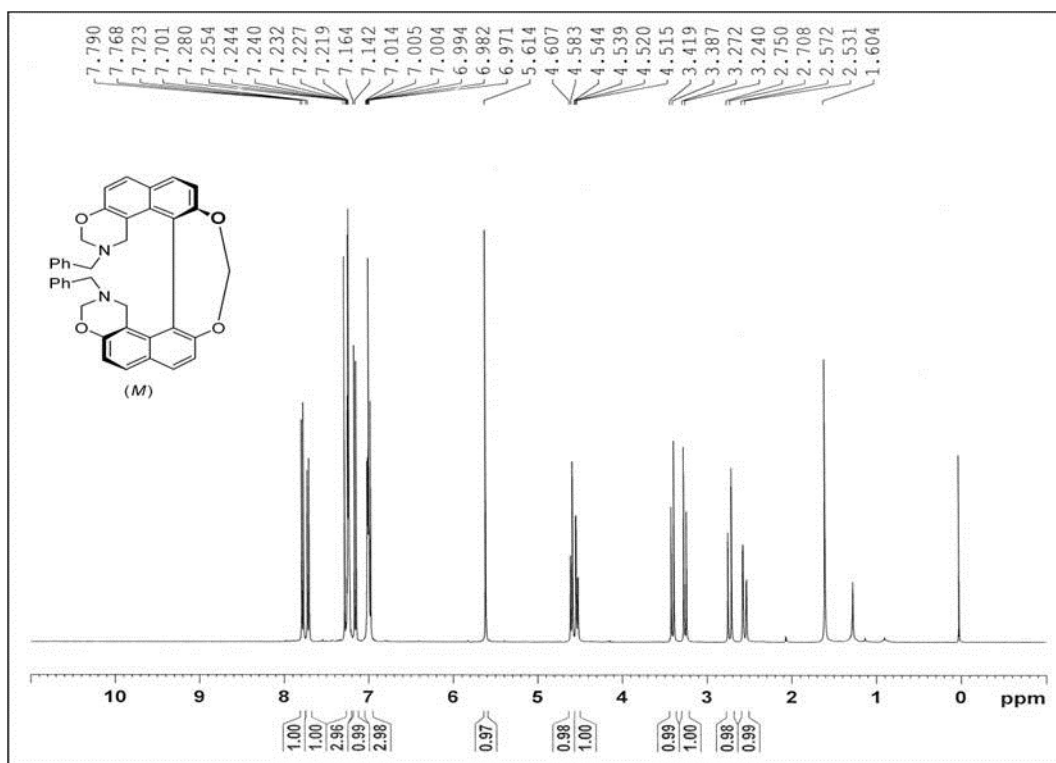
HPLC condition (*M*)-**74**: Observed one peak of single enantiomer at R_t = 10.38 min. Solvent System: Hexane: *Is*o-propanol (70:30), Flow rate: 0.5 mL/min, column: Lux Amylose 2, UV: 254 nm.



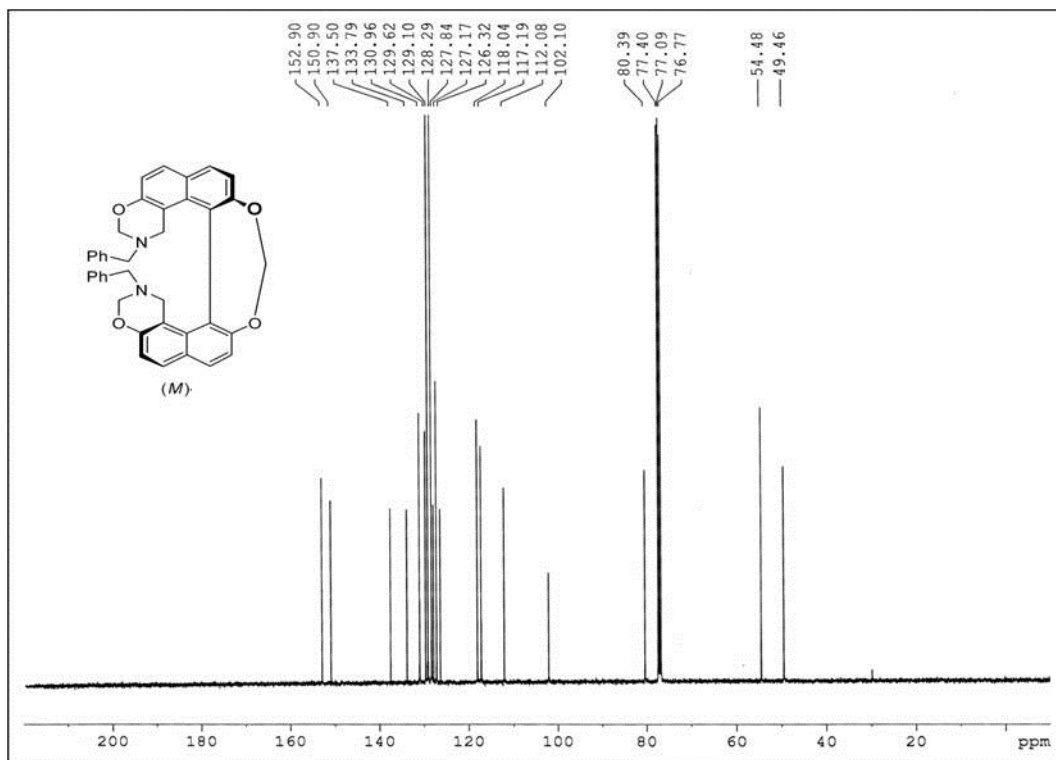
HPLC condition for (*P*)-**74**: Observed one peak of single enantiomer at $R_t = 7.73$ min.
 Solvent System: Hexane: *Iso*-propanol (70:30), Flow rate: 0.5 mL/min, column: Lux Amylose 2, UV: 254 nm.



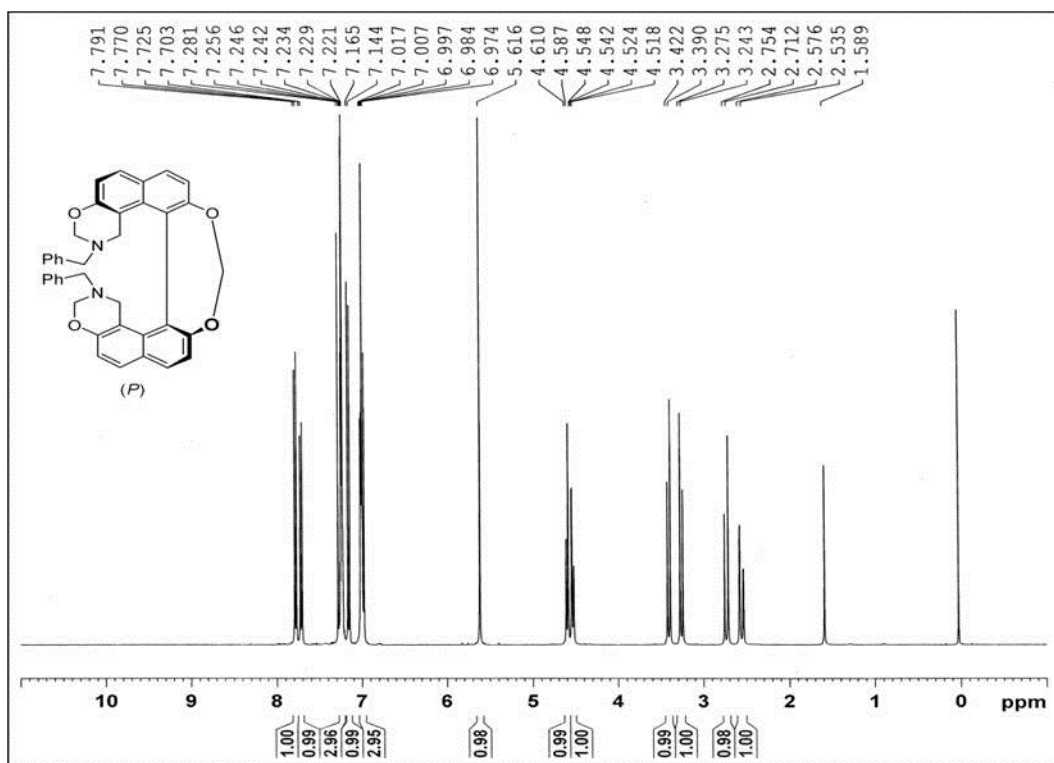
UV and Circular dichroism spectra of resolved helicene like bis-oxazine: (Blue line) (*P*)-**74** and (Green line) (*M*)-**74** ($c\ 1.13 \times 10^{-3}$ M in acetonitrile, 25 °C).



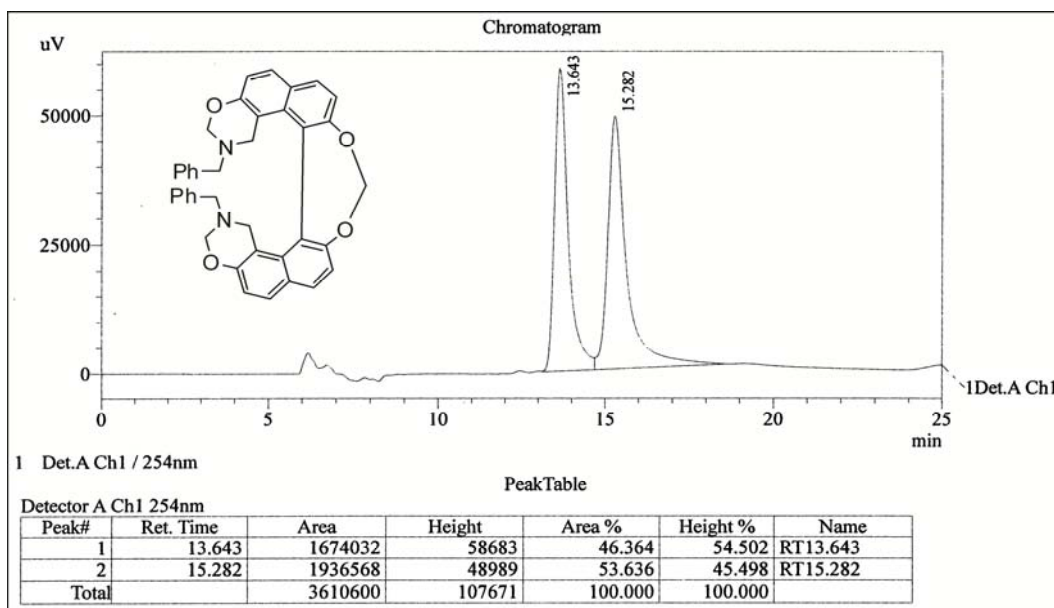
¹H-NMR spectrum of helicene like (M)-bis-oxazine [(M)-75]



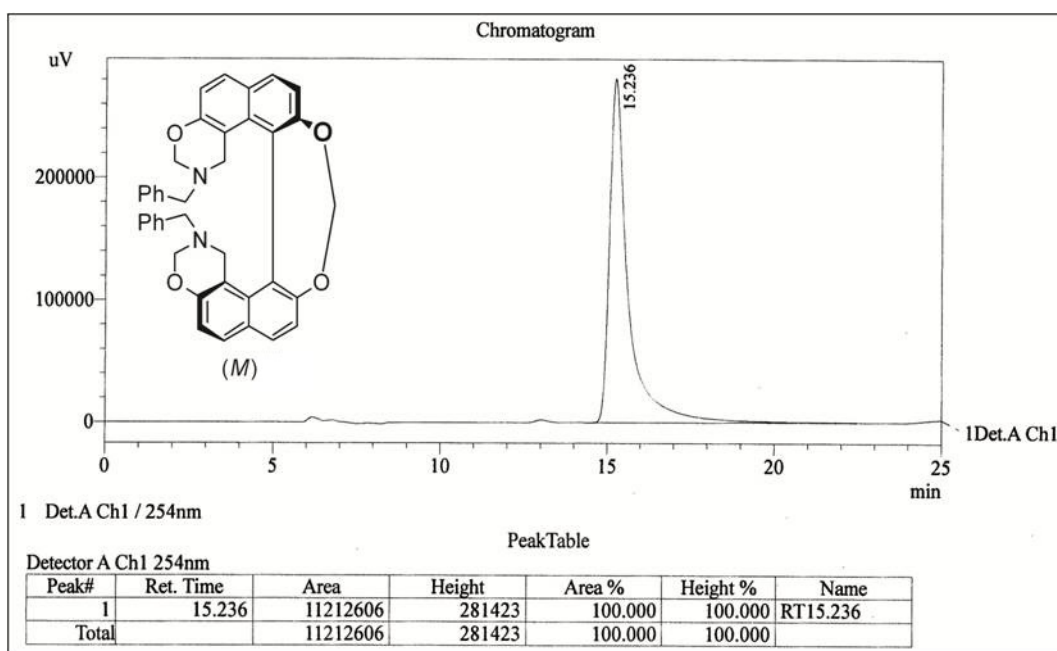
¹³C-NMR spectrum of helicene like (M)-bis-oxazine [(M)-75]



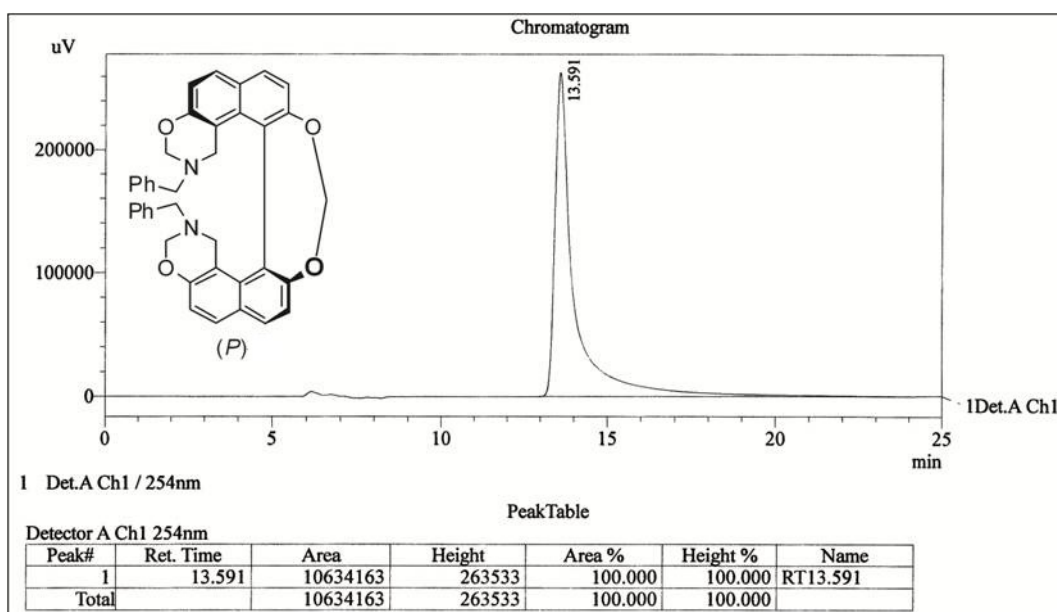
¹H-NMR spectrum of helicene like (*P*)-bis-oxazine [(*P*)-75]



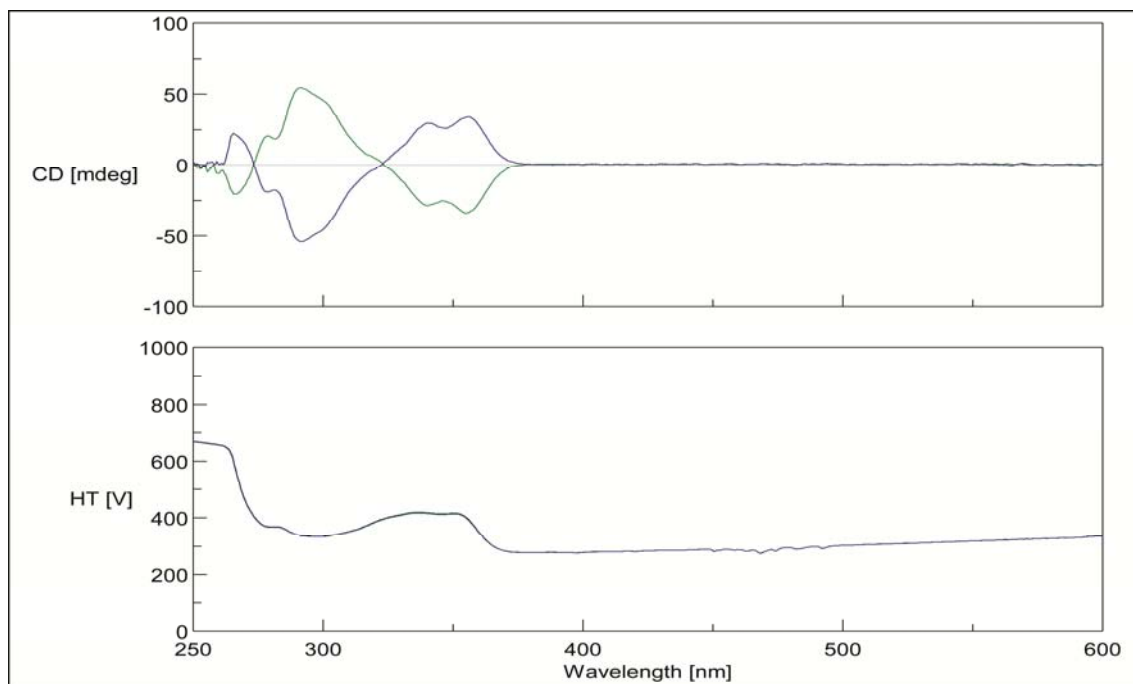
HPLC condition for (\pm)-75: Observed two peaks of separated enantiomers at 1) R_t – 13.64 min and 2) R_t – 15.28 min. Solvent System: Hexane: *Is*o-propanol (70:30), Flow rate: 0.5 mL/min. Chiral Column: Lux Amylose 2, UV: 254nm.



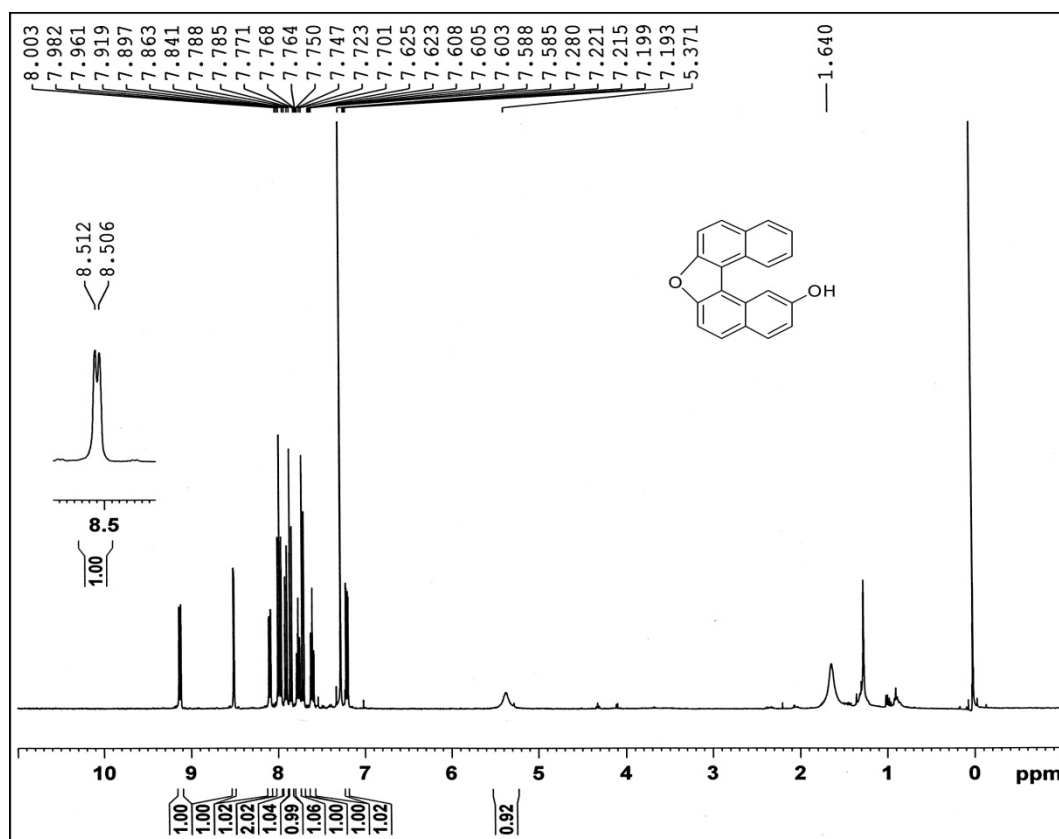
HPLC condition for (*M*)-**75**: Observed one peak of single enantiomer at R_t – 15.23 min. Solvent System: Hexane: *Iso*-propanol (70:30), Flow rate: 0.5 mL/min. Chiral Column: Lux Amylose 2, UV: 254nm.



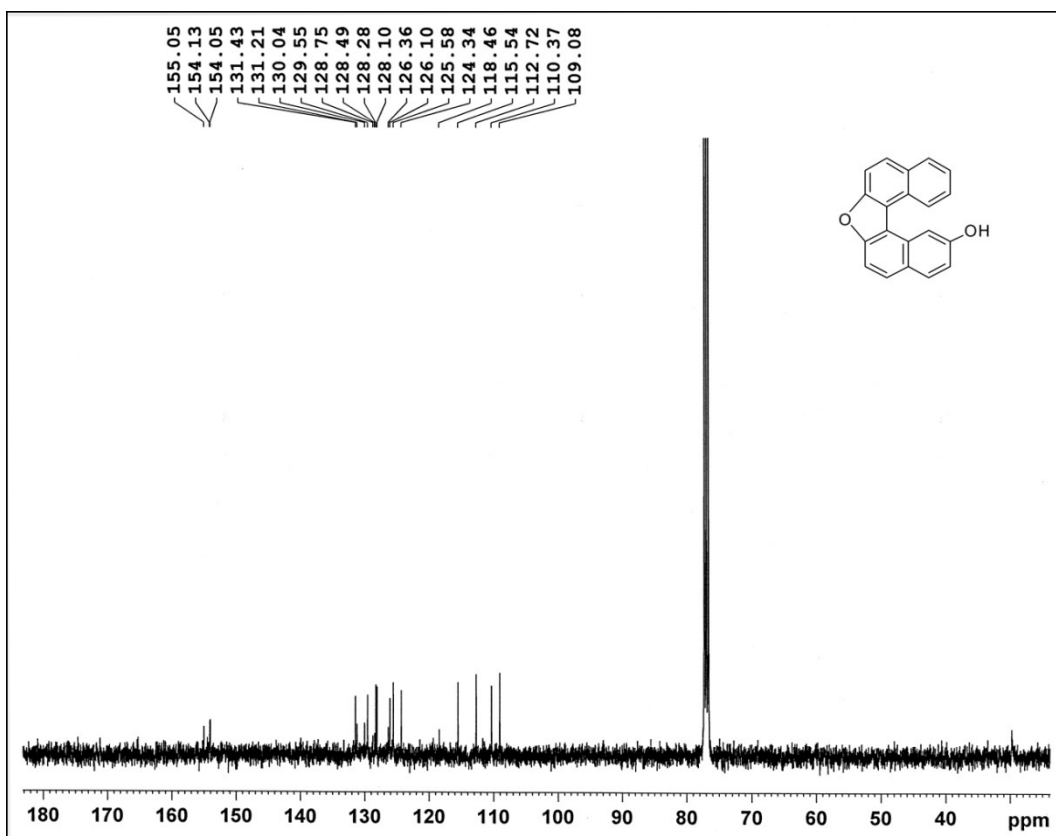
HPLC condition for (*P*)-**75**: Observed one peak of single enantiomer at R_t – 13.59 min. Solvent System: Hexane: *Iso*-propanol (70:30), Flow rate: 0.5 mL/min. Chiral Column: Lux Amylose 2, UV: 254nm.



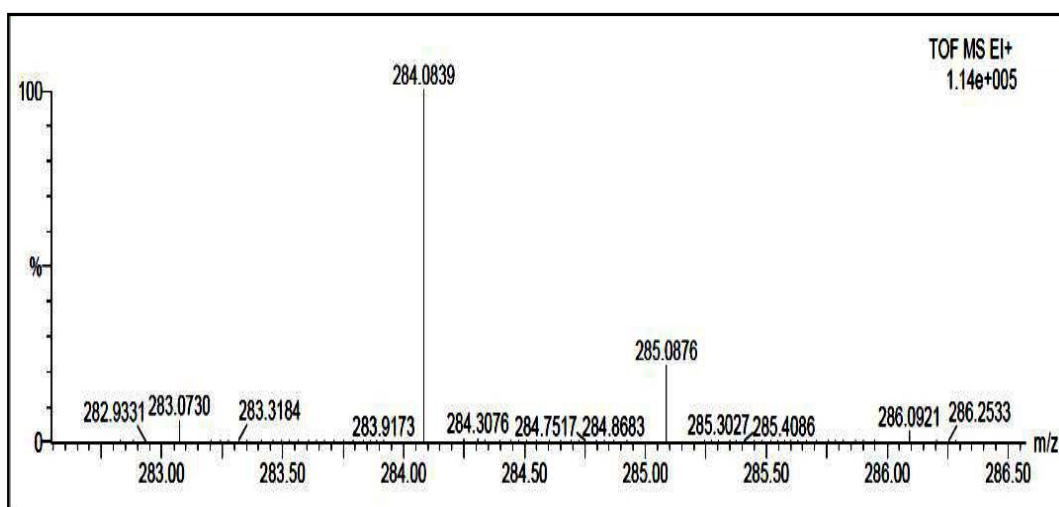
UV and Circular dichroism spectra of resolved helicene like bis-oxazine: (Blue line) **(P)-75** and (Green line) **(M)-75** (c 8.44×10^{-4} M in acetonitrile, 25 °C).



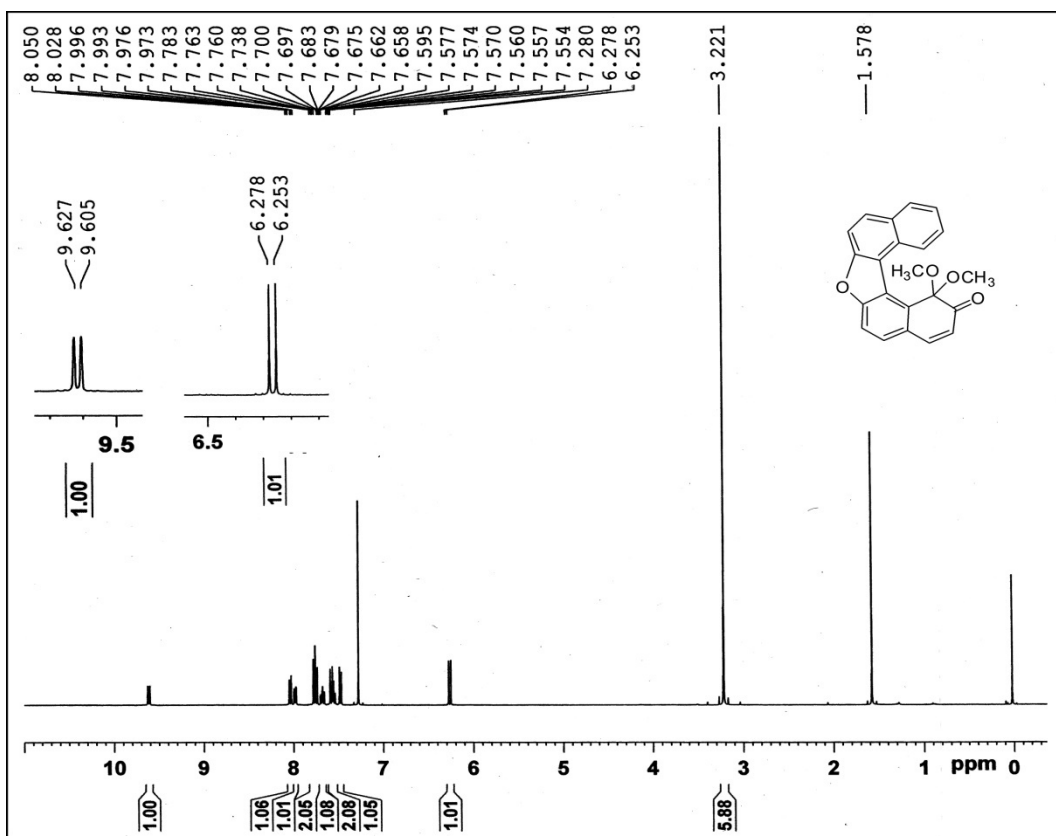
¹H-NMR Spectrum of 2-hydroxy-7-oxa[5]helicene (80) in CDCl₃ (400 MHz)



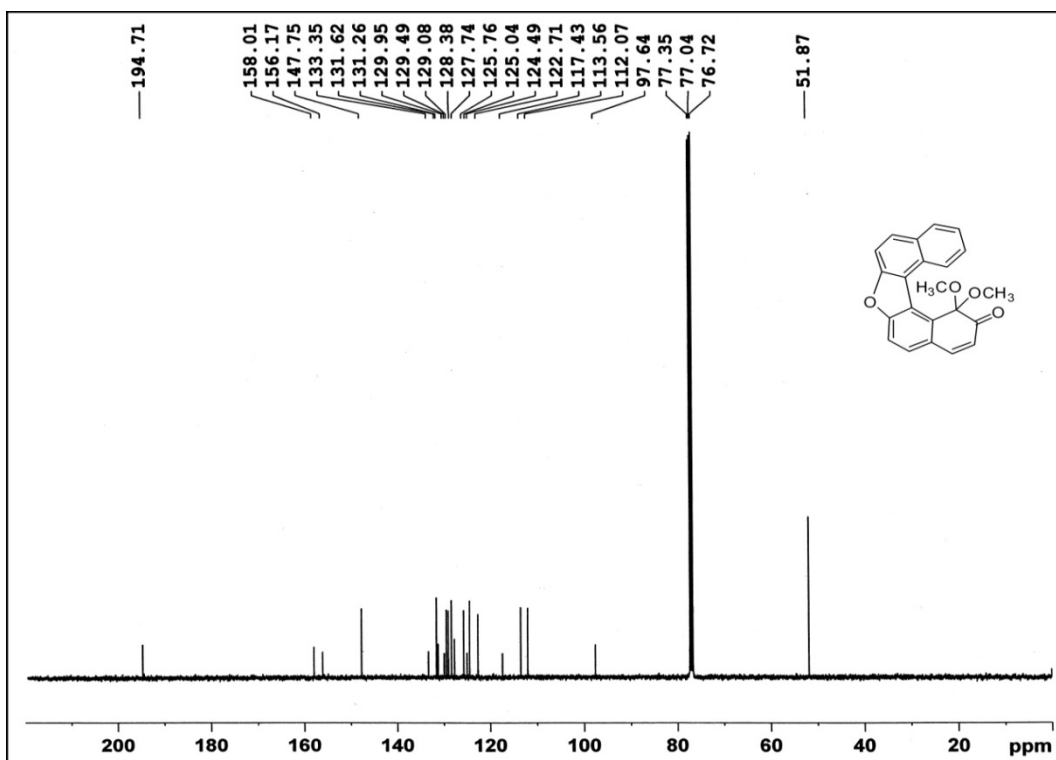
¹³C-NMR spectrum of 2-hydroxy-7-oxa[5]helicene (80) in CDCl₃ on 100.6 MHz



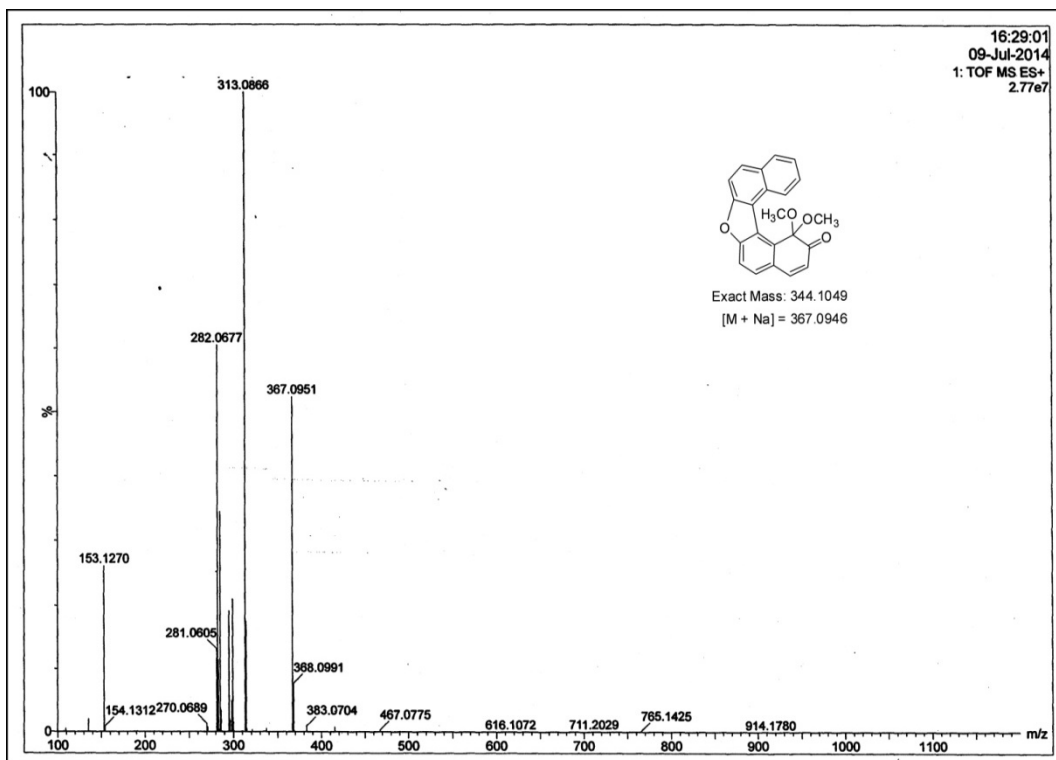
HRMS spectrum of 2-hydroxy-7-oxa[5]helicene (80)



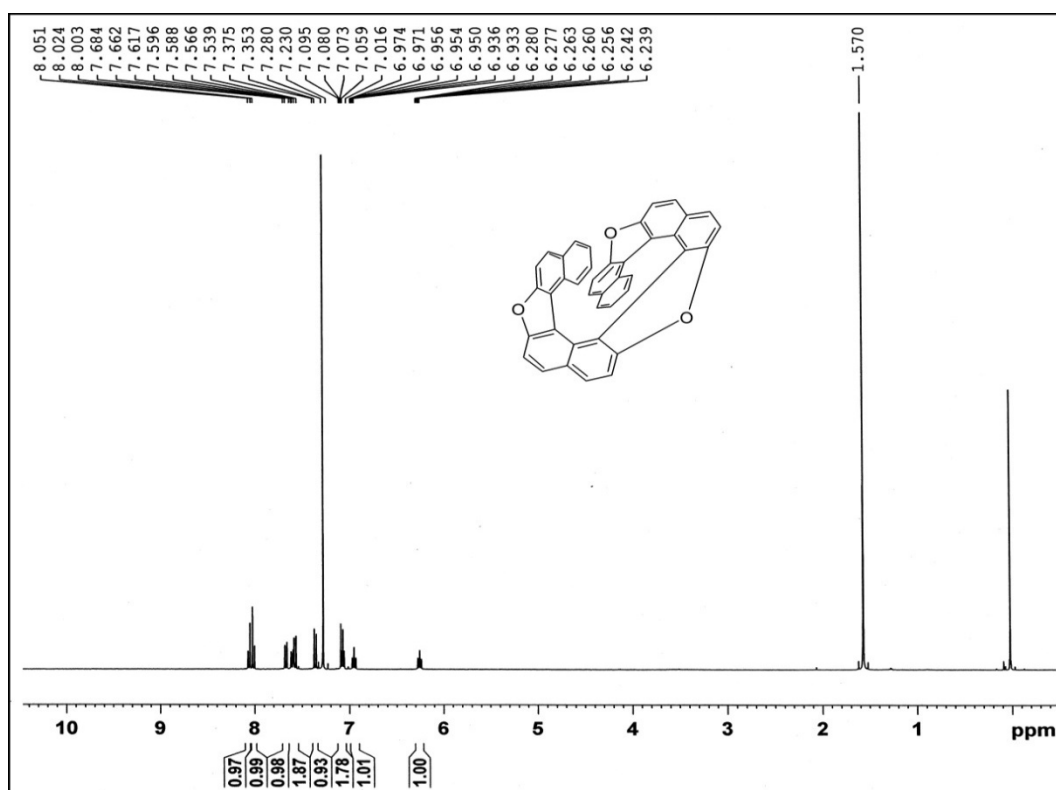
¹H-NMR Spectrum of (81) in CDCl₃ (400 MHz)



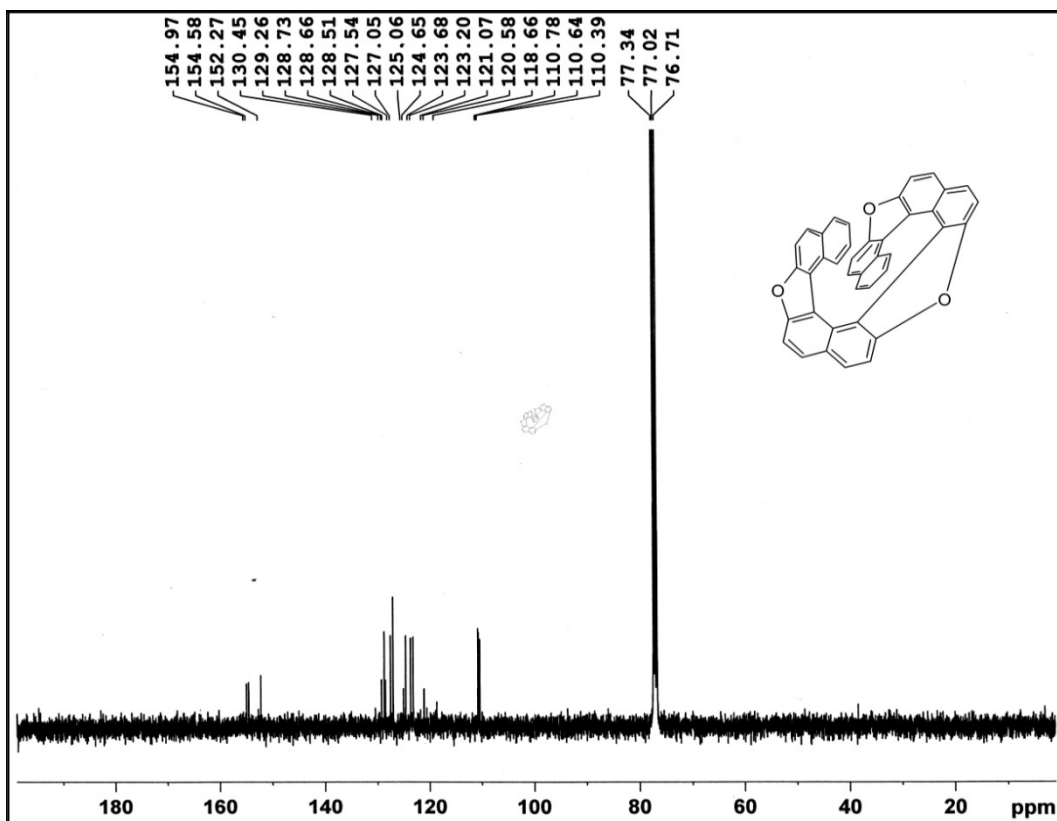
¹³C-NMR spectrum of (81) in CDCl₃ on 100.6 MHz



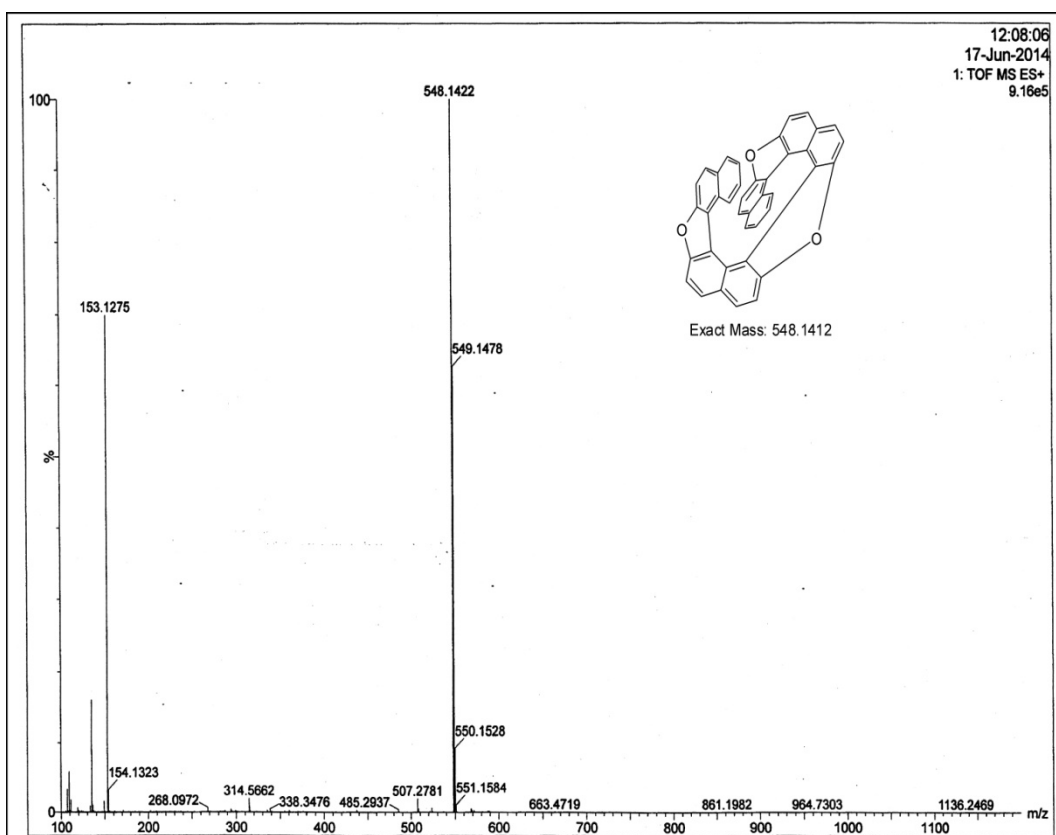
HRMS spectrum of (81)



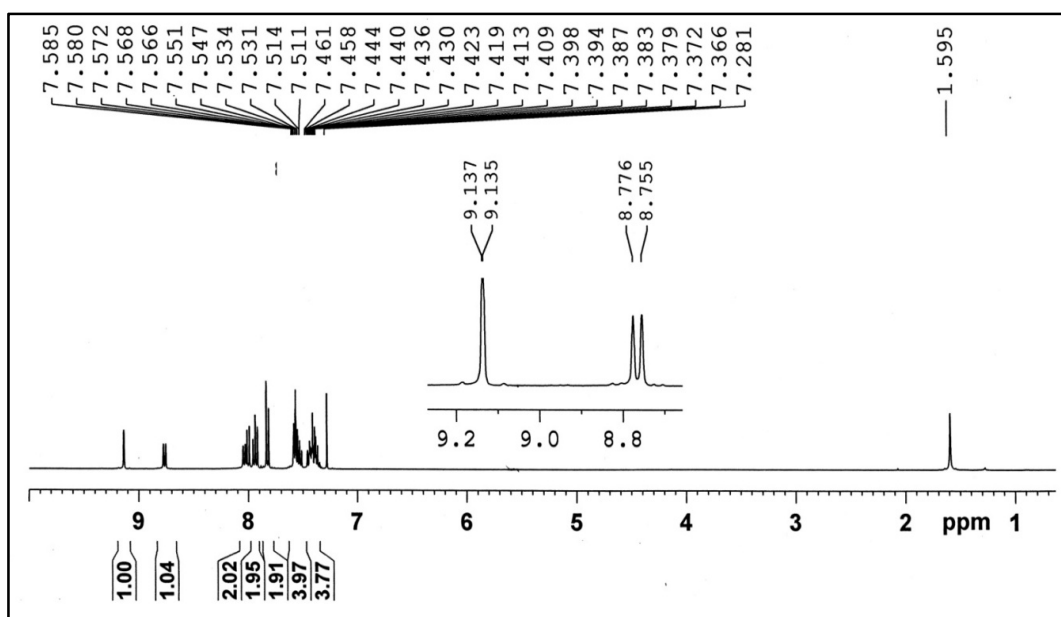
¹H-NMR Spectrum of 7,12,17-trioxa[11]helicene (78) in CDCl₃ (400 MHz)



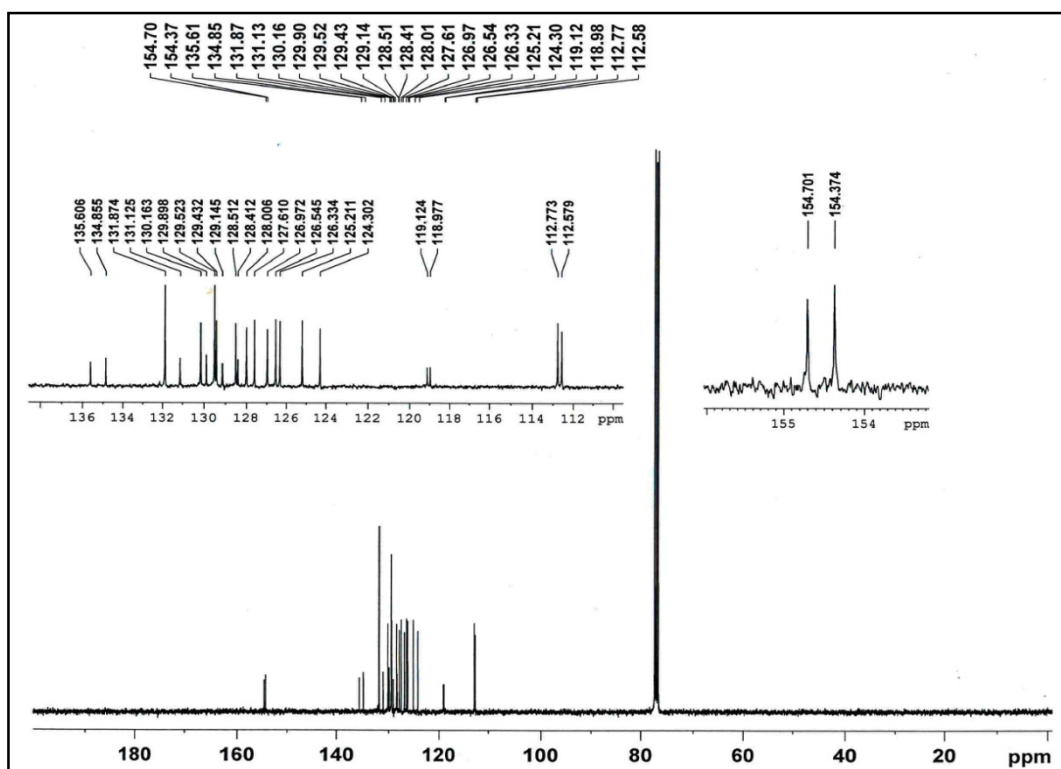
¹³C-NMR spectrum of 7,12,17-trioxa[11]helicene] (78) in CDCl₃ on 100.6 MHz



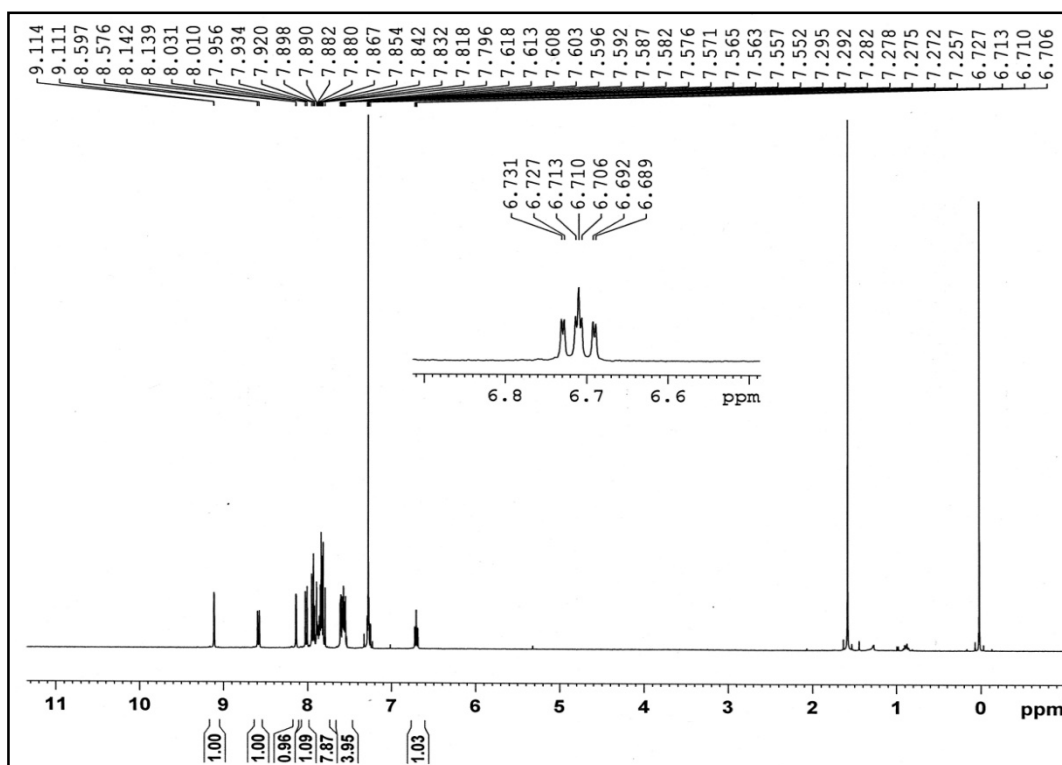
HRMS spectrum of 7,12,17-trioxa[11]helicene] (78)



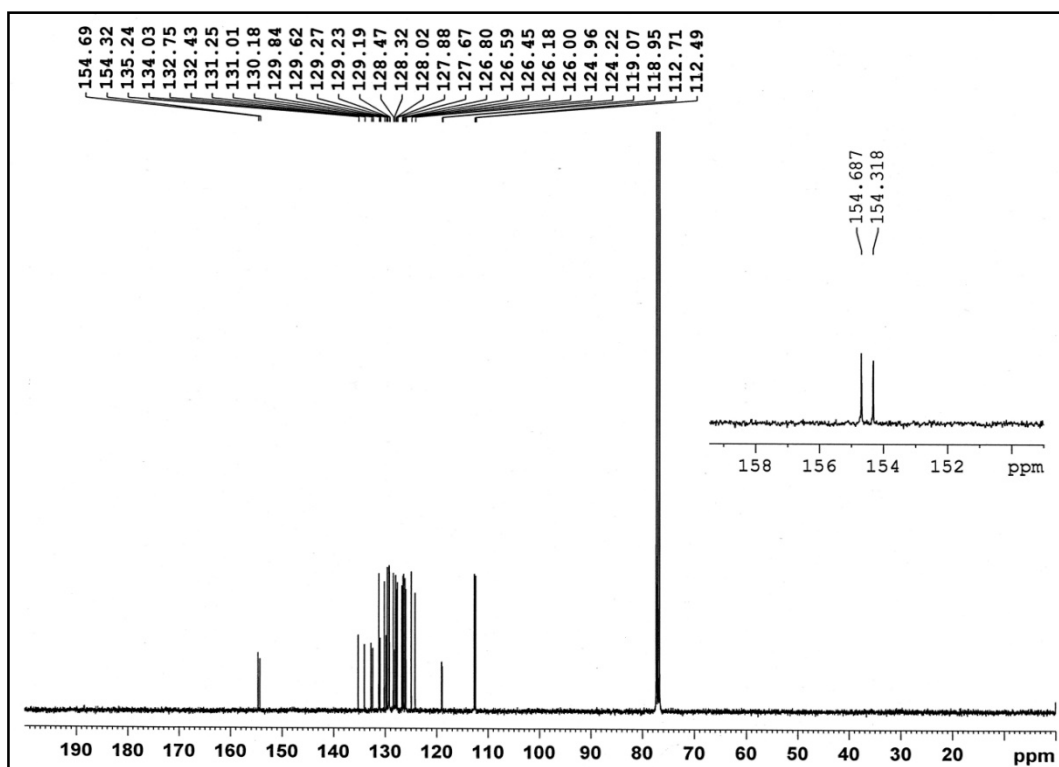
¹H-NMR spectrum of 2-(phenylthio)dinaphtho[2,1-b:1',2'-d]furan (83)



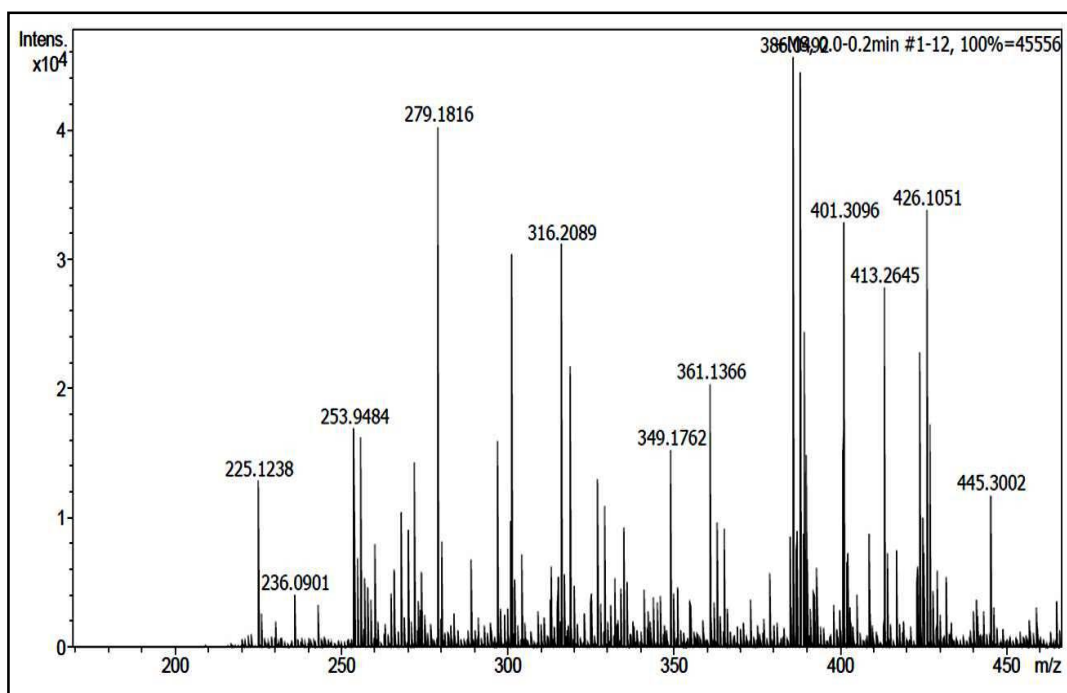
¹³C-NMR spectrum of 83



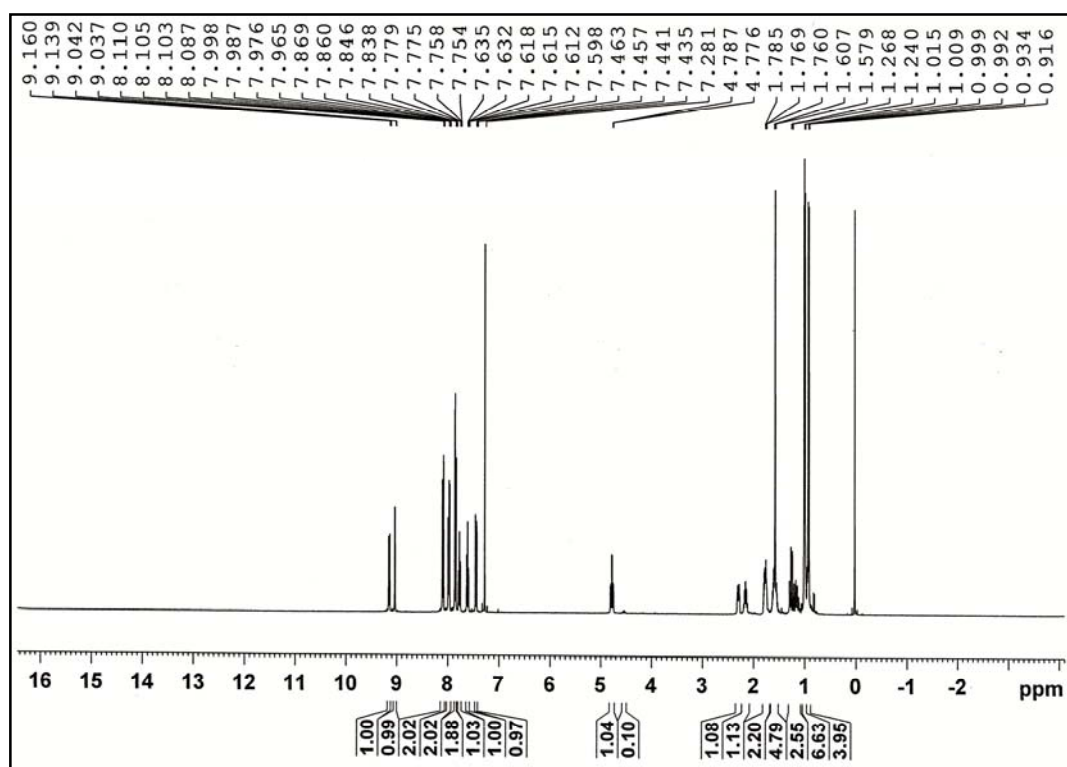
¹H-NMR spectrum of 2-(naphthalen-2-ylthio)dinaphtho[2,1-b:1',2'-d]furan (85)



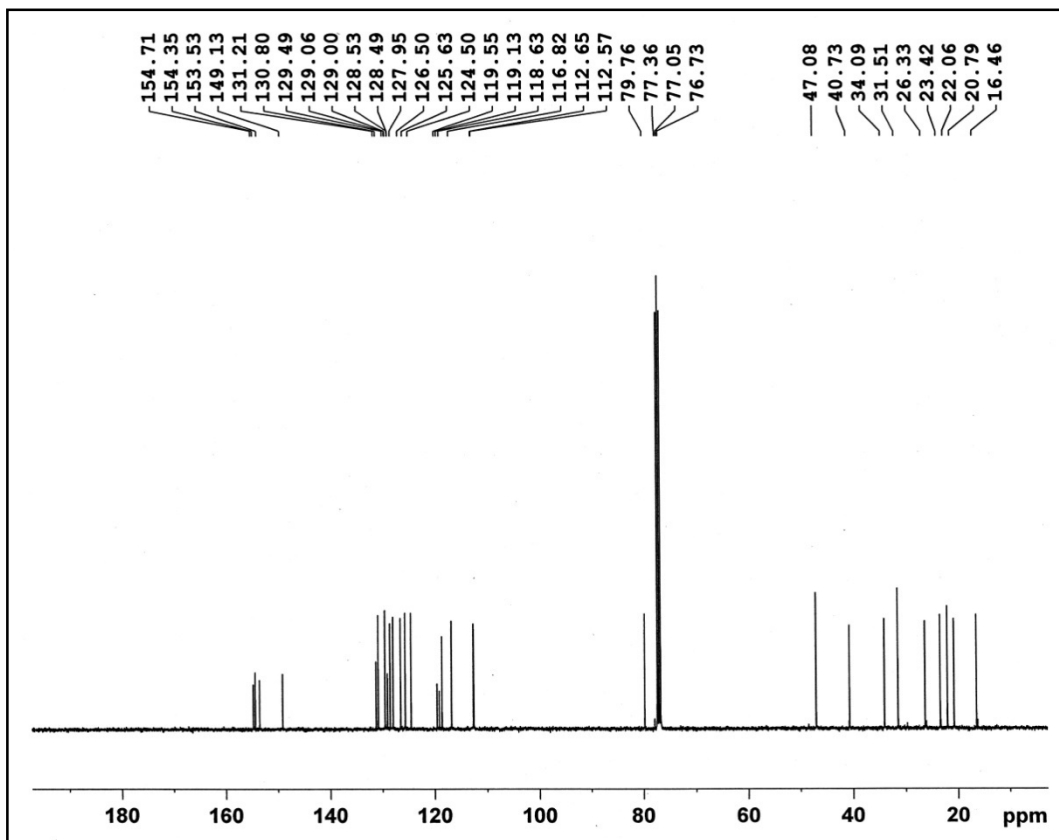
¹³C-NMR spectrum of 2-(naphthalen-2-ylthio)dinaphtho[2,1-b:1',2'-d]furan (85)



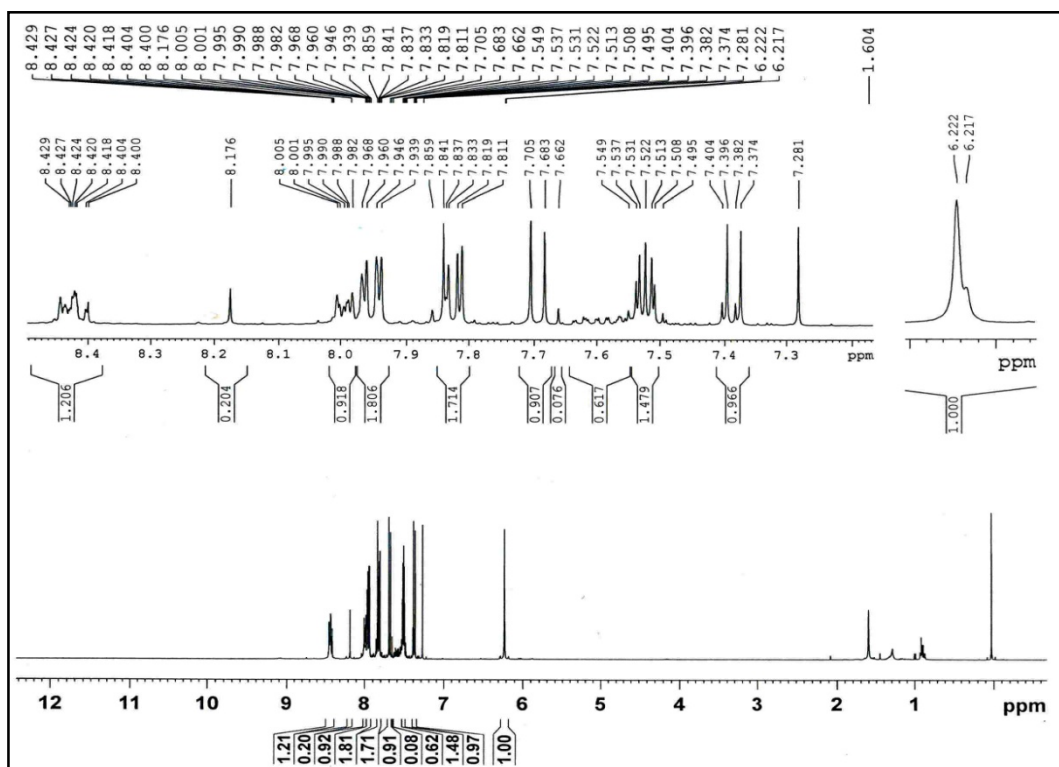
HRMS of 2-(naphthalen-2-ylthio)dinaphtho[2,1-b:1',2'-d]furan (85)



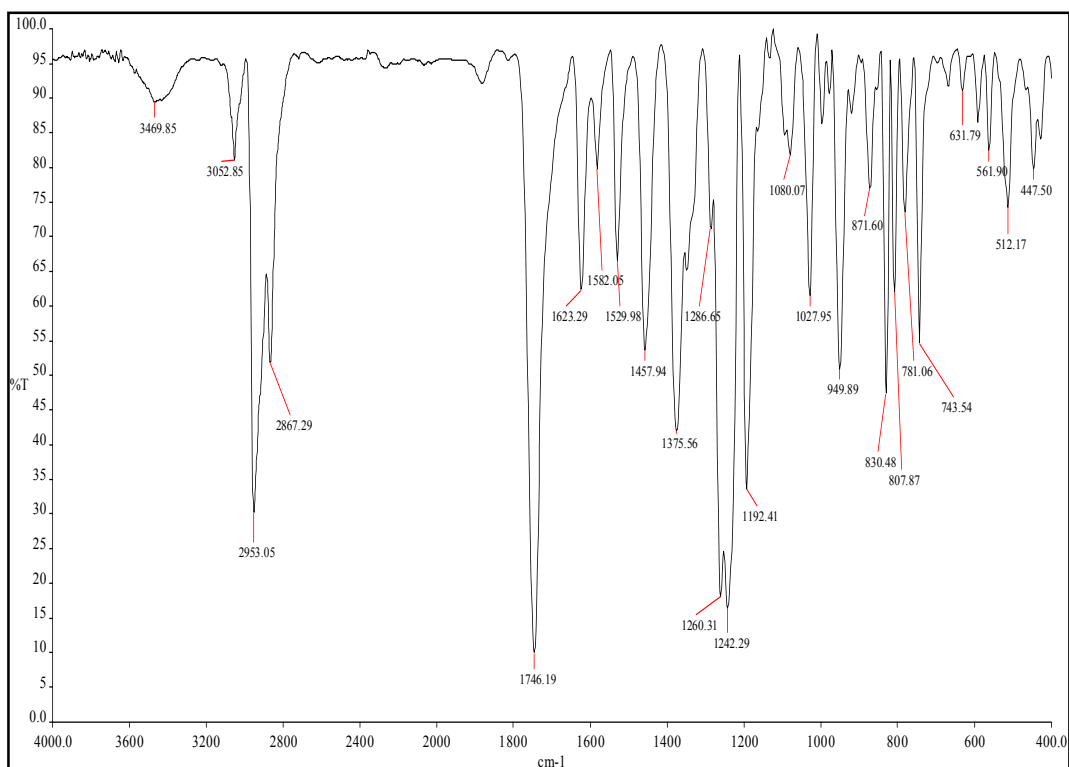
¹H-NMR spectrum of Dinaphtho[2,1-b:1',2'-d]furan-2-yl((1R,2S,5R)-2-isopropyl-5-methylcyclohexyl) carbonate (87)



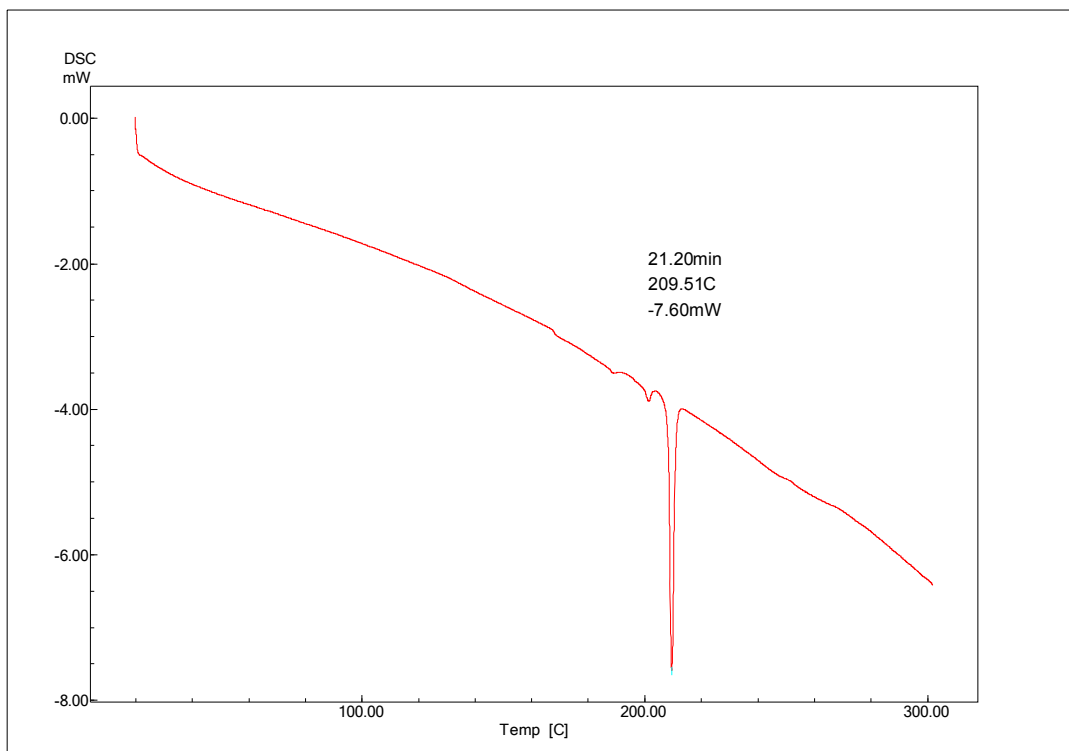
¹³C-NMR spectrum of 87 in CDCl₃ on 100 MHz



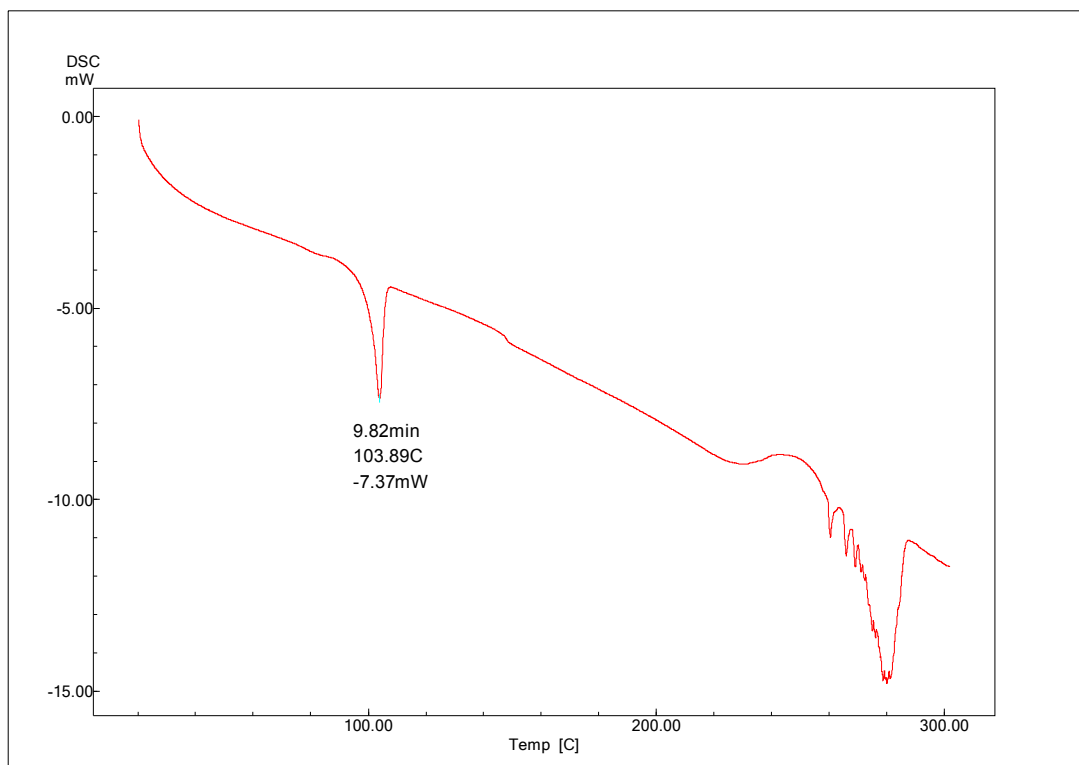
¹H-NMR spectrum of 89



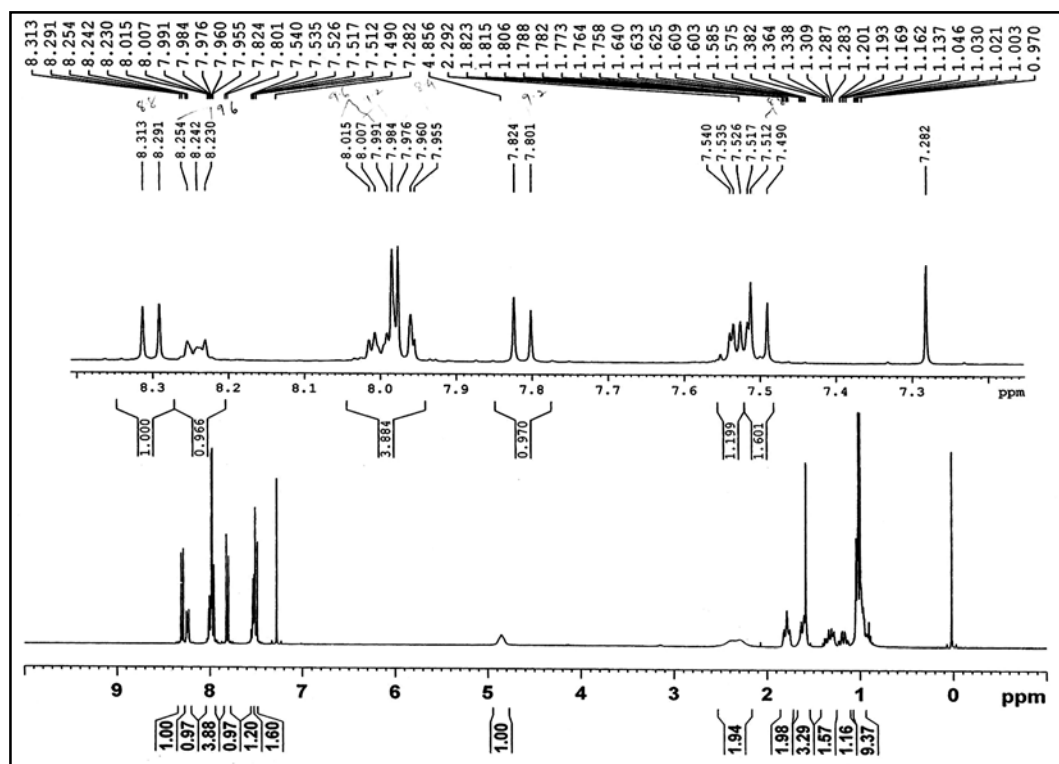
IR spectrum of 97



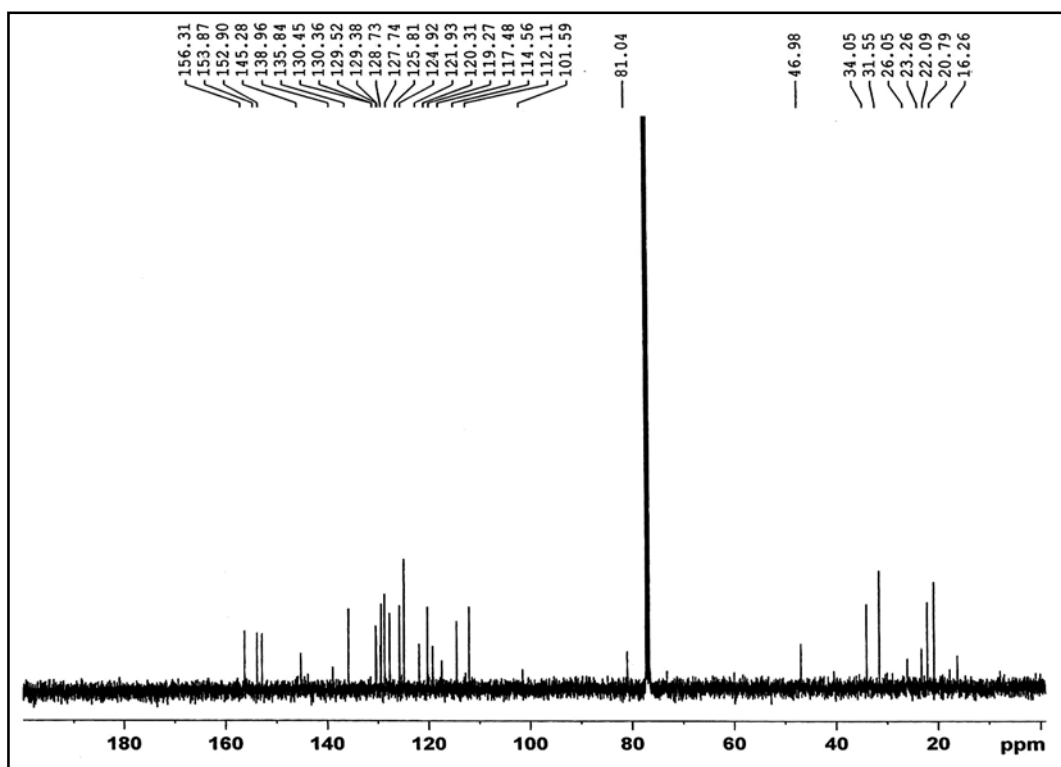
DSC thermogram of 85



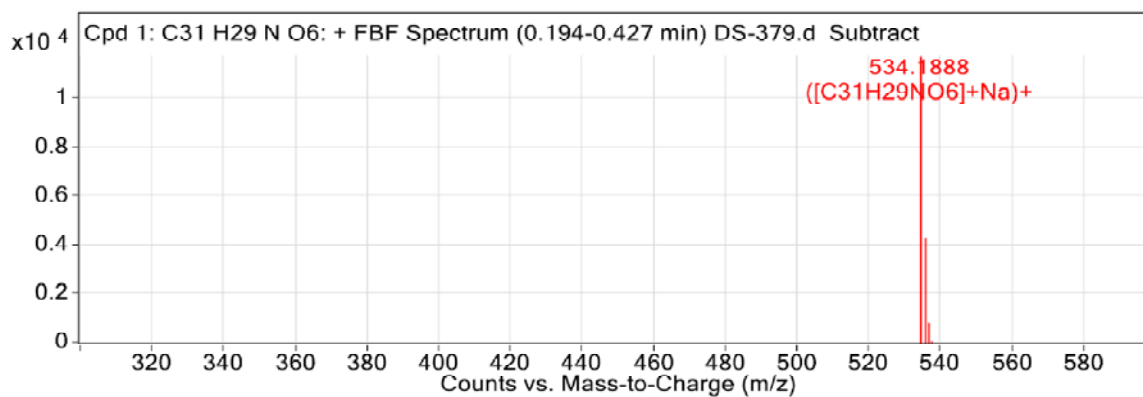
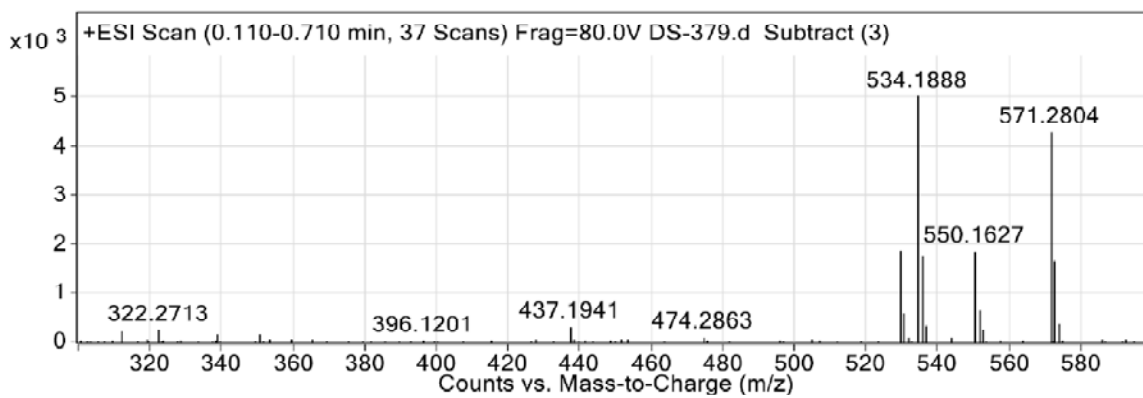
DSC thermogram of **92**



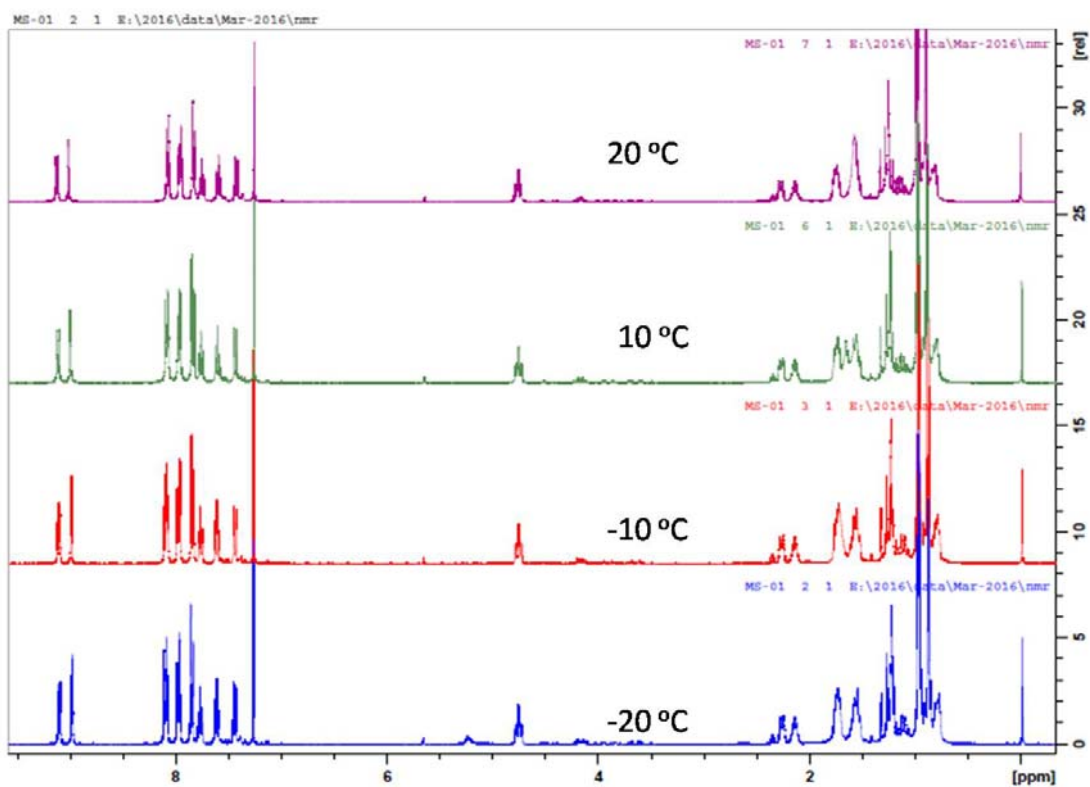
^1H NMR spectrum of (1R,2S,5R)-2-isopropyl-5-methylcyclohexyl (1-nitrodinaphtho[2,1-b:1',2'-d]furan-2-yl) carbonate (**93**)



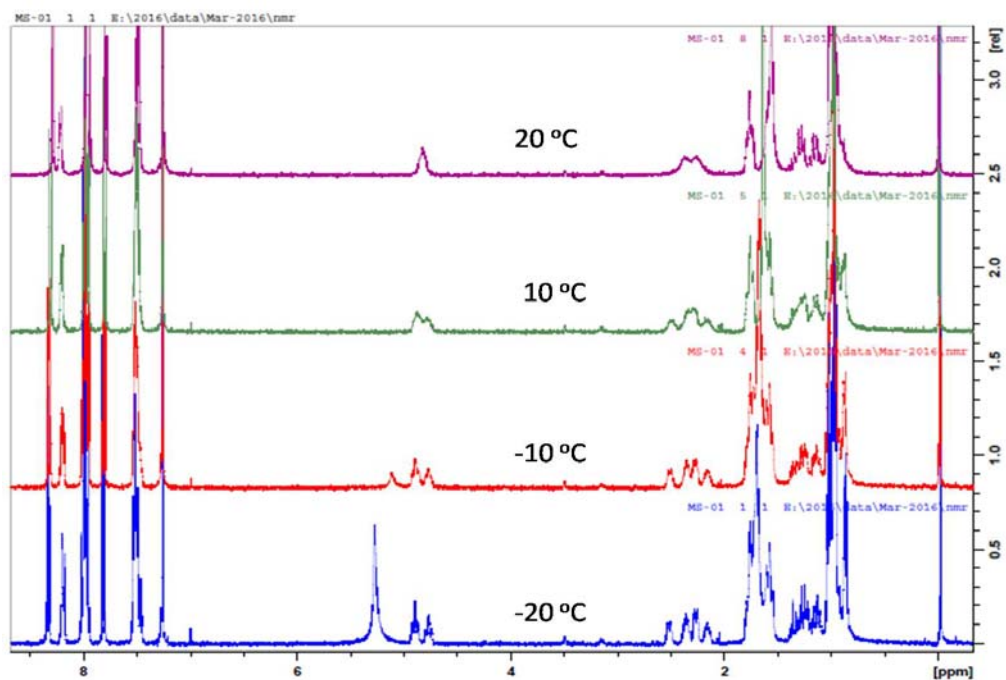
¹³C NMR spectrum of 93



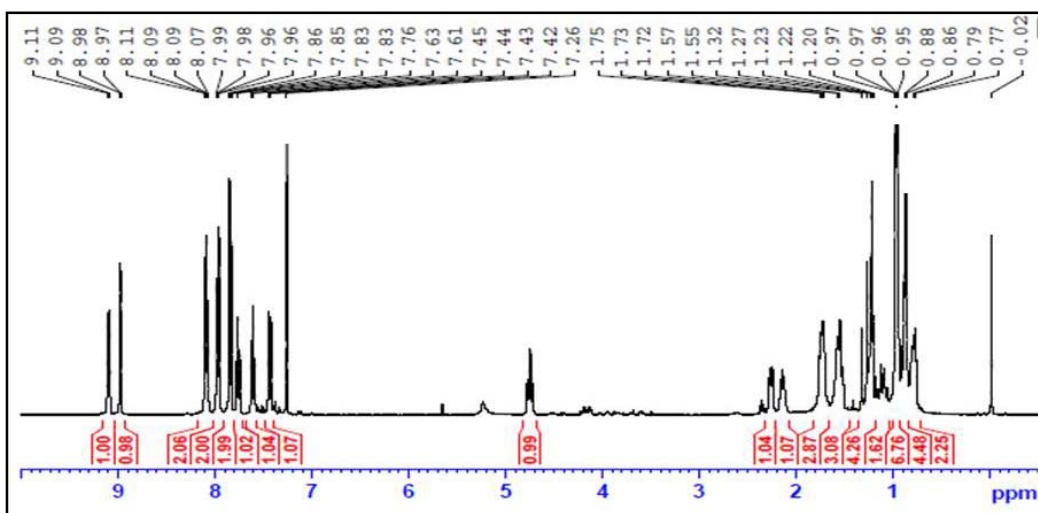
HRMS of compound 93



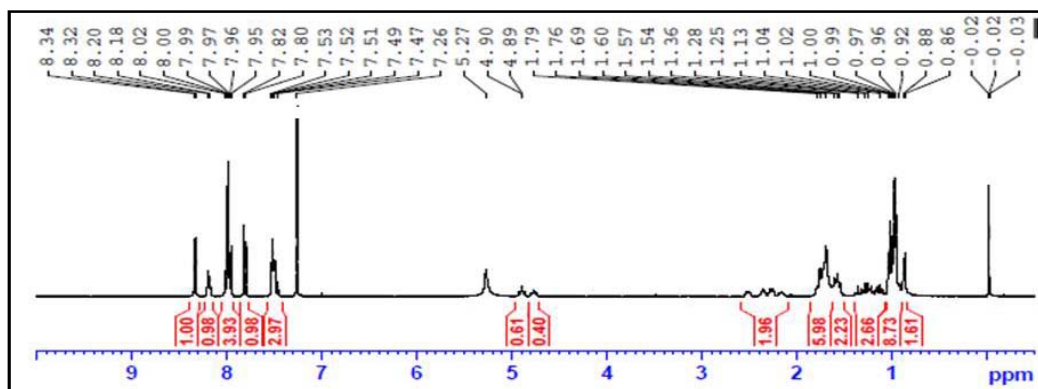
Low temperature analysis of compound 87 in CDCl₃ on 500 MHz



Low temperature analysis of compound 87 in CDCl₃ on 500 MHz



¹H NMR spectrum of compound 87 at -20 °C.



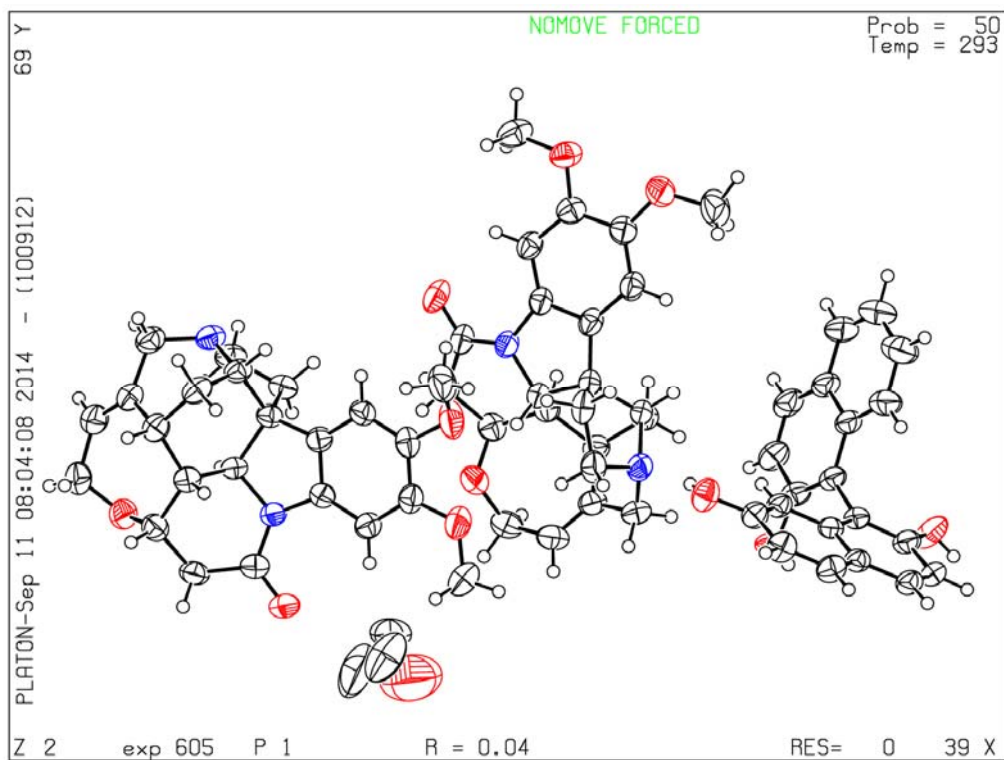
¹H NMR spectrum of compound 93 at -20 °C.

3.6 X-ray Crystal Data

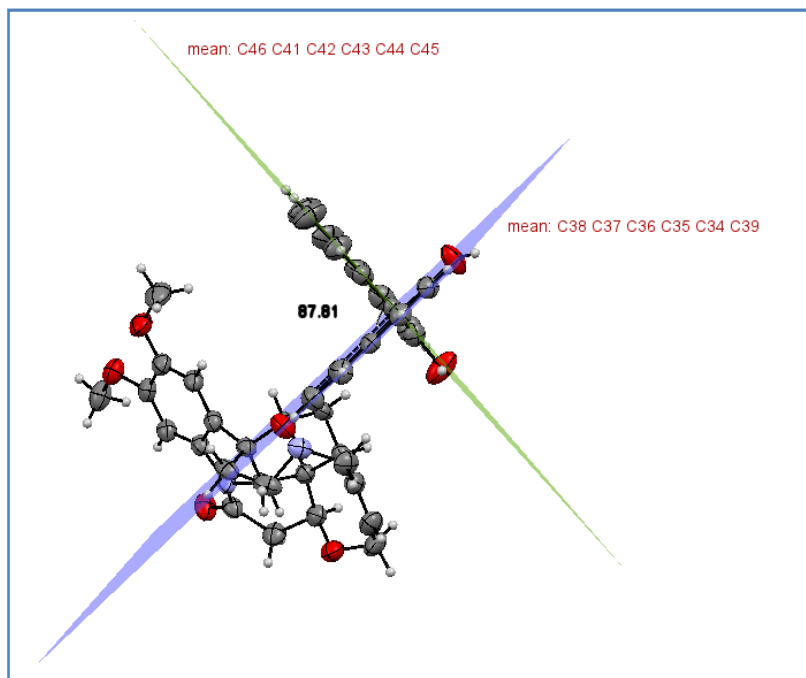
Crystallographic data for the structures of compounds have been deposited with the Cambridge Crystallographic Data Centre. Copies of the data can be obtained from <http://www.ccdc.cam.ac.uk/conts/retrieving.html> or from the Cambridge Crystallographic Data Centre, 12 Union Road, Cambridge CD21EZ, UK (fax: +44-1223-336-033; e-mail: deposit@ccdc.cam.ac.uk)

1. For the complex of (*S_a*)-44 and (*S*)-Brucine (CCDC 1023827):
2. For the complex of (*R_a*)-41 and (*S*)-Proline (CCDC 948082):
3. For compound (*S_a*)-76 (CCDC 1453552):
4. For compound (*S_a*,*S*)-78 (CCDC 1041059):
5. For compound (*M*)-75 (CCDC 948083):
6. For Compound 81 (CCDC No. 999893):
7. For compound 7,12,17-trioxa[11]helicene (78) (CCDC No. 999892):
8. For compound 87 (CCDC No. 1019988):

1. For the complex of (*S_a*)-**44** and (*S*)-Brucine (CCDC 1023827):



ORTEP diagram of the salt of (*S_a*)-**44**•(*S*)-Brucine with atom numbering scheme (50% probability factor for the thermal ellipsoids).

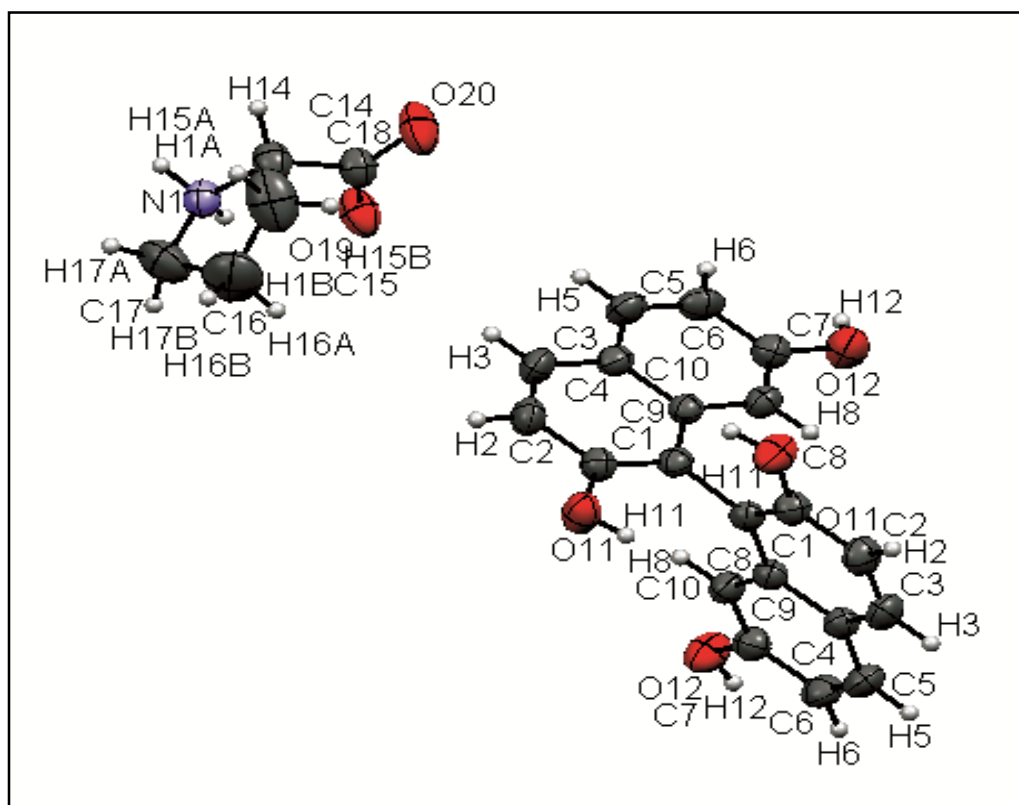


The planes passing through the molecule from the carbons C-46-C41-C42-C43-C44-C55 and C38-C37-C36-C35-C34-C39 showing the twist and the angle between the two planes are 87.81

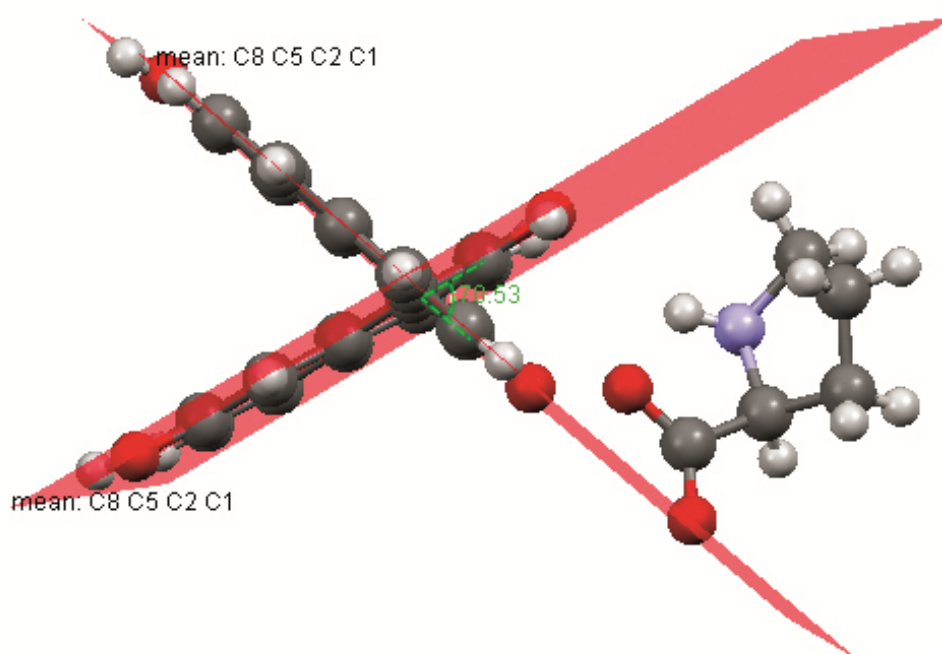
Crystal data and structure refinement for compound (S_a)-44•(S)-Brucine

Empirical formula	C ₆₇ H ₆₆ N ₄ O ₁₂
Formula weight	1119.24
Temperature/K	293(2)
Crystal system	triclinic
Space group	P1
a/Å	9.0356(2)
b/Å	10.3472(3)
c/Å	16.0067(5)
α/°	97.804(3)
β/°	104.923(2)
γ/°	100.186(2)
Volume/Å ³	1397.13(7)
Z	1
ρ _{calc} /g/cm ³	1.330
μ/mm ⁻¹	0.745
F(000)	592.0
Radiation	CuKα (λ = 1.54184)
2θ range for data collection/°	8.84 to 146.1
Index ranges	-9 ≤ h ≤ 11, -12 ≤ k ≤ 12, -19 ≤ l ≤ 19
Reflections collected	14244
Independent reflections	7223 [R _{int} = 0.0340, R _{sigma} = 0.0333]
Data/restraints/parameters	7223/3/778
Goodness-of-fit on F ²	1.036
Final R indexes [I ≥ 2σ (I)]	R ₁ = 0.0438, wR ₂ = 0.1189
Final R indexes [all data]	R ₁ = 0.0446, wR ₂ = 0.1200
Largest diff. peak/hole / e Å ⁻³	0.20/-0.21
Flack parameter	-0.06(15)

2. For the complex of (*R_a*)-41 and (*S*)-Proline (CCDC 948082):



ORTEP diagram of the salt of (*R_a*)-41•(*S*)-Proline with atom numbering scheme (50% probability factor for the thermal ellipsoids).

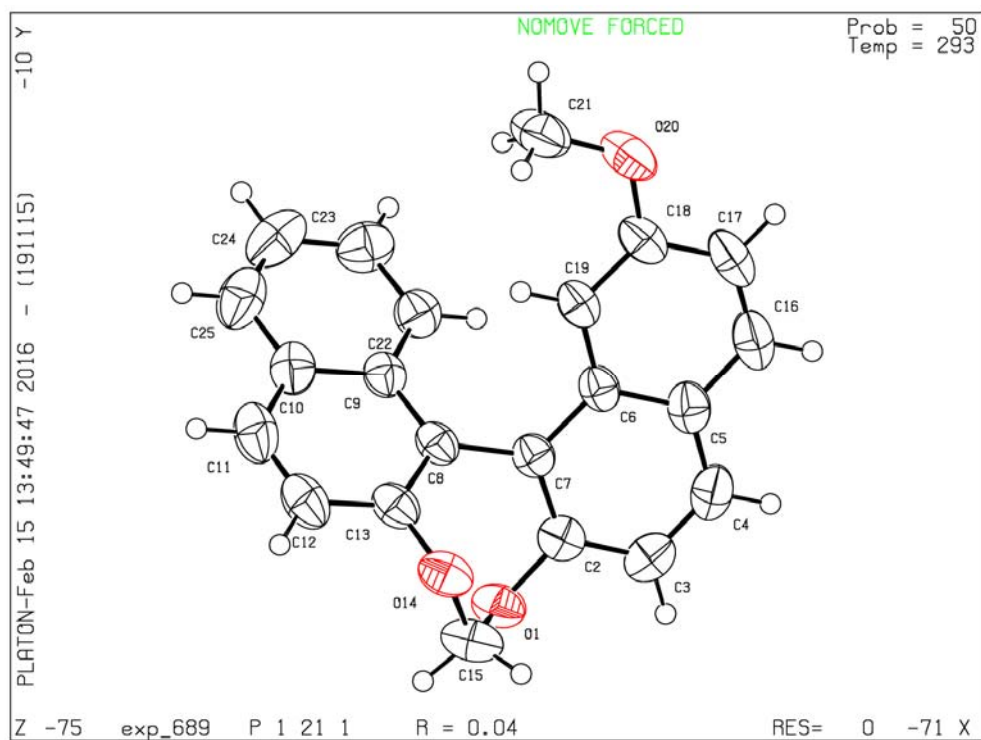


The planes passing through the molecule from the carbons C-8-C5-C2-C1 and C8-C5-C2-C1 showing the twist and the angle between the two planes are 70.53°.

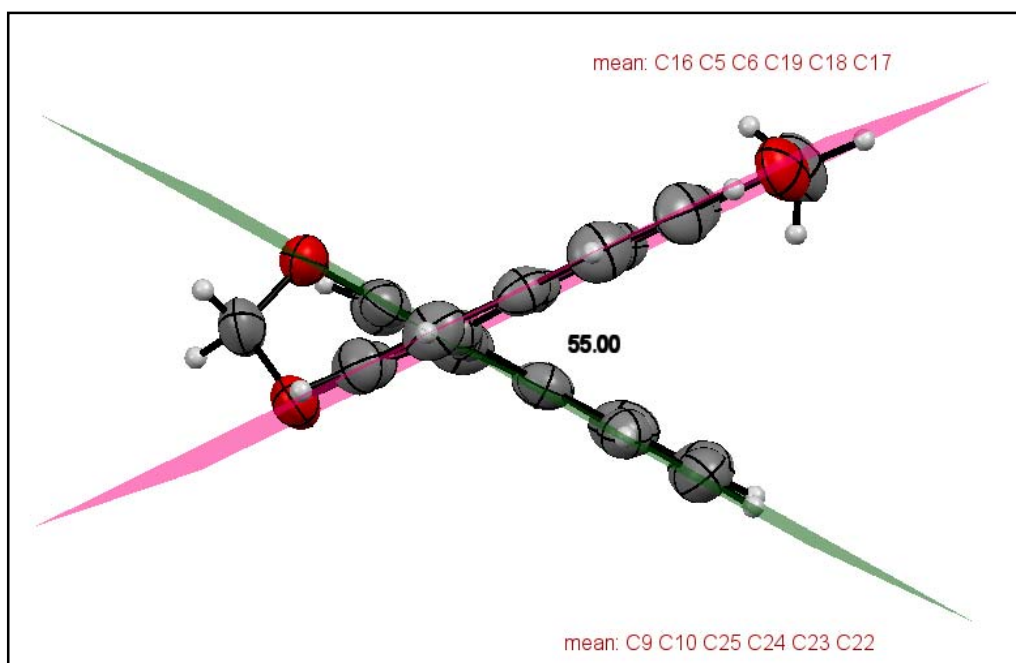
Crystal data and structure refinement for (*R_a*)-41 and (*S*)-Proline

Empirical formula	C ₁₅ H ₁₄ O ₅ N _{0.25}
Formula weight	277.76
Temperature/K	293(2)
Crystal system	orthorhombic
Space group	P2 ₁ 2 ₁ 2
a/Å	10.1763(2)
b/Å	12.9527(4)
c/Å	10.5700(3)
α/°	90.00
β/°	90.00
γ/°	90.00
Volume/Å ³	1393.24(7)
Z	4
ρ _{calc} /mg/mm ³	1.324
μ/mm ⁻¹	0.839
F(000)	583.0
Crystal size/mm ³	0.3 × 0.25 × 0.23
2Θ range for data collection	8.36 to 143.14°
Index ranges	-5 ≤ h ≤ 12, -14 ≤ k ≤ 15, -10 ≤ l ≤ 12
Reflections collected	3415
Independent reflections	2329[R(int) = 0.0194]
Data/restraints/parameters	2329/0/184
Goodness-of-fit on F ²	1.056
Final R indexes [I ≥ 2σ (I)]	R ₁ = 0.0496, wR ₂ = 0.1396
Final R indexes [all data]	R ₁ = 0.0526, wR ₂ = 0.1440
Largest diff. peak/hole / e Å ⁻³	0.23/-0.21
Flack parameter	0.3(3)

3. For compound (*S_a*)-**76** (CCDC 1453552):



ORTEP diagram of (*S_a*)-**76**. Hydrogens are omitted for clarity with atom numbering scheme (50% probability factor for the thermal ellipsoids).

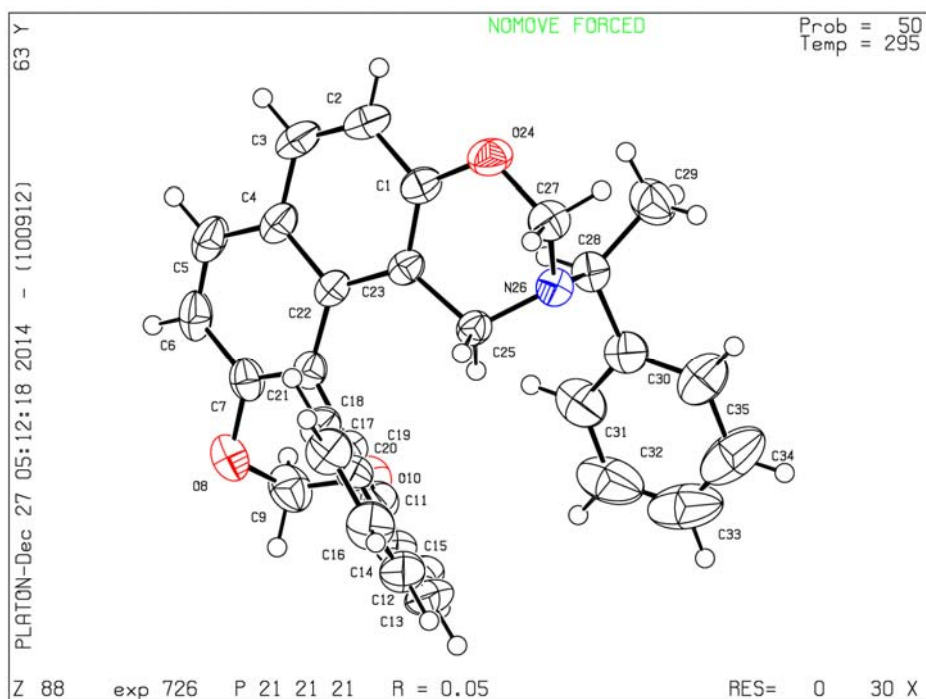


The planes passing through the molecule from the carbons C-16-C5-C6-C19-C18-C17 and C9-C10-C25-C24-C23-C22 showing the twist and the angle between the two planes are 55.0

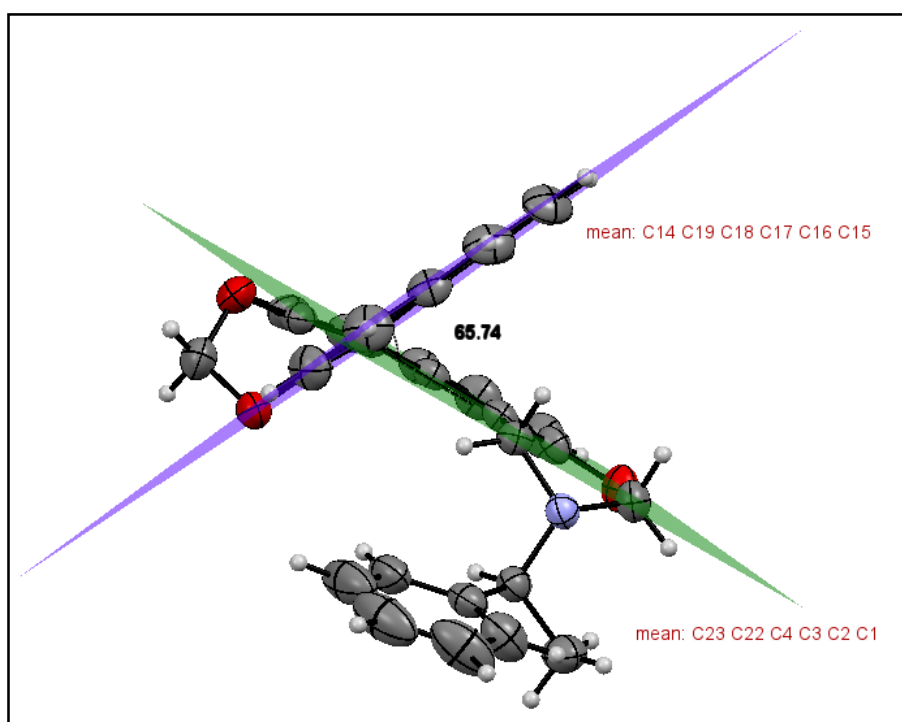
Crystal data and structure refinement for compound (S_a)-76.

Empirical formula	C ₂₃ H ₁₇ O ₂
Formula weight	328.35
Temperature/K	293
Crystal system	monoclinic
Space group	P2 ₁
a/Å	9.9608(3)
b/Å	9.4348(3)
c/Å	10.0343(3)
α/°	90
β/°	113.748(4)
γ/°	90
Volume/Å ³	863.16(5)
Z	2
ρ _{calc} /g/cm ³	1.2633
μ/mm ⁻¹	0.672
F(000)	344.0
2θ range for data collection/°	9.62 to 146.2
Index ranges	-12 ≤ h ≤ 12, -11 ≤ k ≤ 9, -12 ≤ l ≤ 12
Reflections collected	9817
Independent reflections	2967 [R _{int} = 0.0232, R _{sigma} = 0.0208]
Data/restraints/parameters	2967/0/226
Goodness-of-fit on F ²	0.637
Final R indexes [I ≥ 2σ (I)]	R ₁ = 0.0366
Final R indexes [all data]	R ₁ = 0.0391, wR ₂ = 0.1175
Largest diff. peak/hole / e Å ⁻³	0.16/-0.15
Flack parameter	0.1(2)

4. For compound (*S_a*,*S*)-78 (CCDC 1041059):



ORTEP diagram of (*S_a*,*S*)-78. Hydrogens are omitted for clarity with atom numbering scheme (50% probability factor for the thermal ellipsoids).

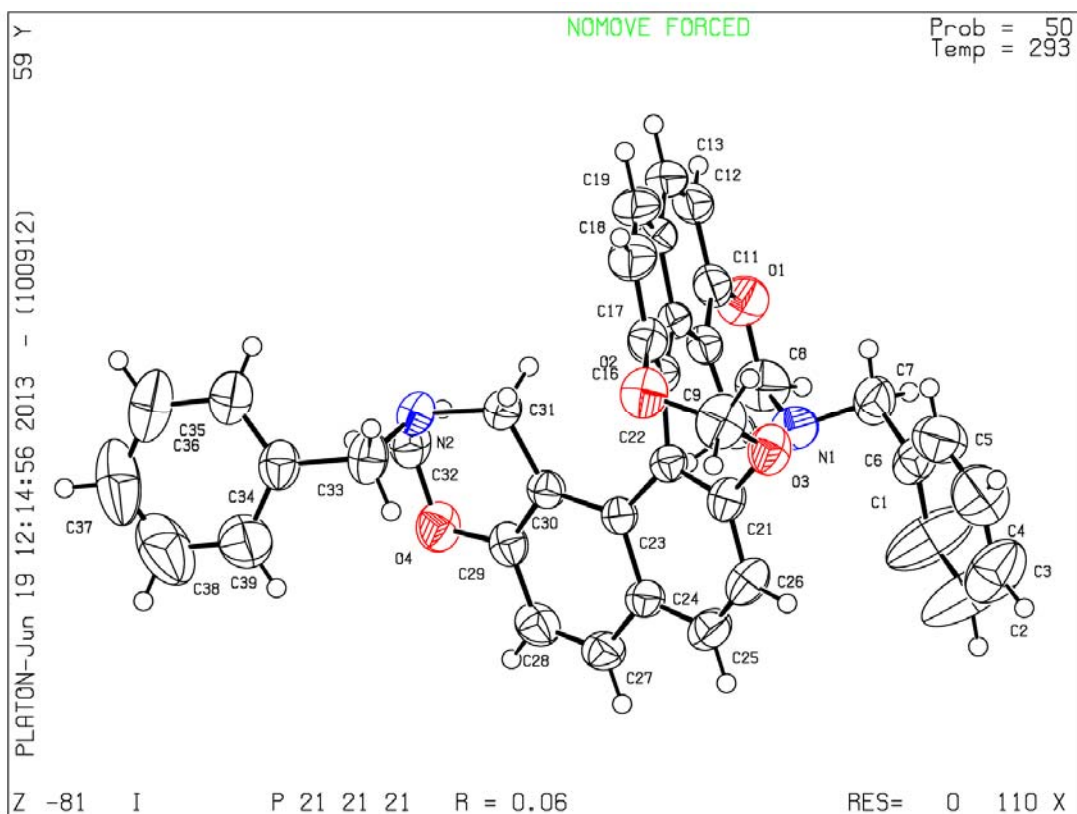


The planes passing through the molecule from the carbons C-14-C19-C18-C17-C16-C15 and C23-C22-C4-C3-C2-C1 showing the twist and the angle between the two planes are 65.74

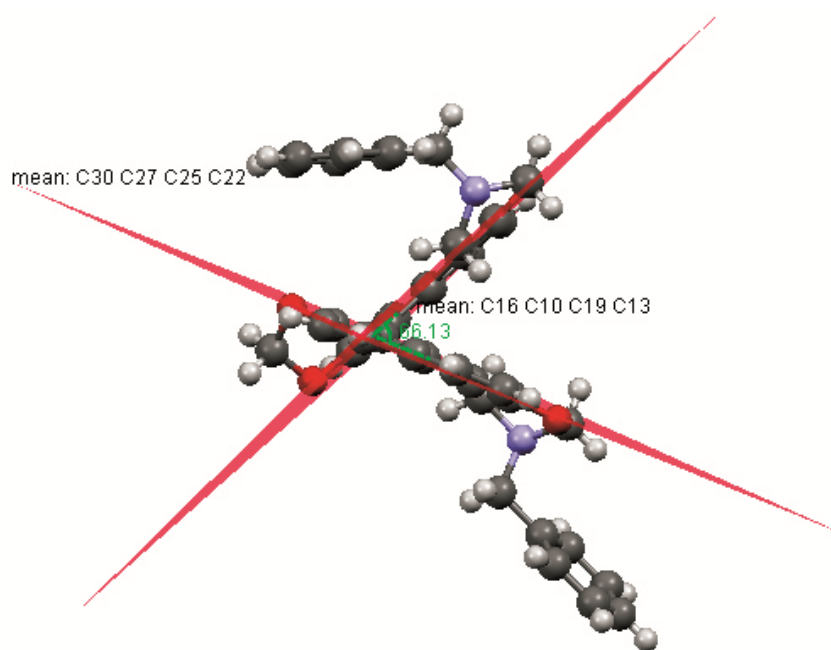
Crystal data and structure refinement for compound (S_a,S)-78.

Empirical formula	C ₃₂ H ₂₄ O ₃ N _{0.25}
Formula weight	459.52
Temperature/K	295
Crystal system	orthorhombic
Space group	P2 ₁ 2 ₁ 2 ₁
a/Å	9.0291(3)
b/Å	12.1317(4)
c/Å	21.5315(9)
α/°	90
β/°	90
γ/°	90
Volume/Å ³	2358.53(15)
Z	4
ρ _{calc} /g/cm ³	1.2941
μ/mm ⁻¹	0.659
F(000)	968.0
Radiation	(λ = 1.54184)
2θ range for data collection/°	8.22 to 146.82
Index ranges	-11 ≤ h ≤ 6, -14 ≤ k ≤ 15, -25 ≤ l ≤ 26
Reflections collected	8159
Independent reflections	4731 [R _{int} = 0.0333, R _{sigma} = 0.0411]
Data/restraints/parameters	4731/0/332
Goodness-of-fit on F ²	0.807
Final R indexes [I ≥ 2σ (I)]	R ₁ = 0.0467
Final R indexes [all data]	R ₁ = 0.0520, wR ₂ = 0.1346
Largest diff. peak/hole / e Å ⁻³	0.17/-0.28
Flack parameter	-0.1(2)

5. For compound (*M*)-75 (CCDC 948083):



ORTEP diagram of (*M*)-75. Hydrogens are omitted for clarity with atom numbering scheme (50% probability factor for the thermal ellipsoids).

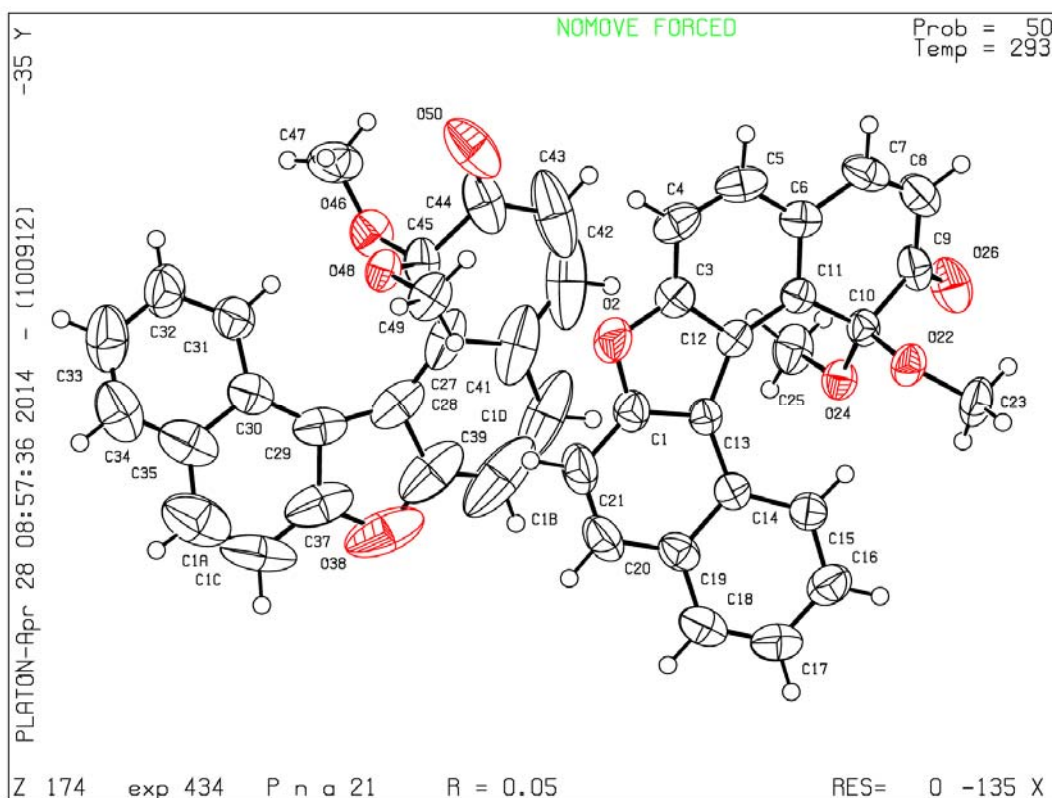


The planes passing through the molecule from the carbons C-30-C27-C25-C22 and C16-C10-C19-C13 showing the twist and the angle between the two planes are 66.13°.

Crystal data and structure refinement for (M)-75

Empirical formula	C ₃₉ H ₃₄ N ₂ O ₄
Formula weight	594.68
Temperature/K	293(2)
Crystal system	orthorhombic
Space group	P2 ₁ 2 ₁ 2 ₁
a/Å	9.2249(3)
b/Å	16.6146(4)
c/Å	20.0890(6)
α/°	90.00
β/°	90.00
γ/°	90.00
Volume/Å ³	3079.00(15)
Z	4
ρ _{calc} /mg/mm ³	1.283
m/mm ⁻¹	0.661
F(000)	1256.0
Crystal size/mm ³	0.26 × 0.2 × 0.18
2θ range for data collection	6.9 to 143.66°
Index ranges	-11 ≤ h ≤ 10, -12 ≤ k ≤ 20, -21 ≤ l ≤ 24
Reflections collected	7768
Independent reflections	5087[R(int) = 0.0353]
Data/restraints/parameters	5087/0/407
Goodness-of-fit on F ²	1.040
Final R indexes [I ≥ 2σ (I)]	R ₁ = 0.0568, wR ₂ = 0.1514
Final R indexes [all data]	R ₁ = 0.0627, wR ₂ = 0.1595
Largest diff. peak/hole / e Å ⁻³	0.24/-0.36
Flack parameter	0.0(3)

1. For Compound **81**(CCDC No. 999893):



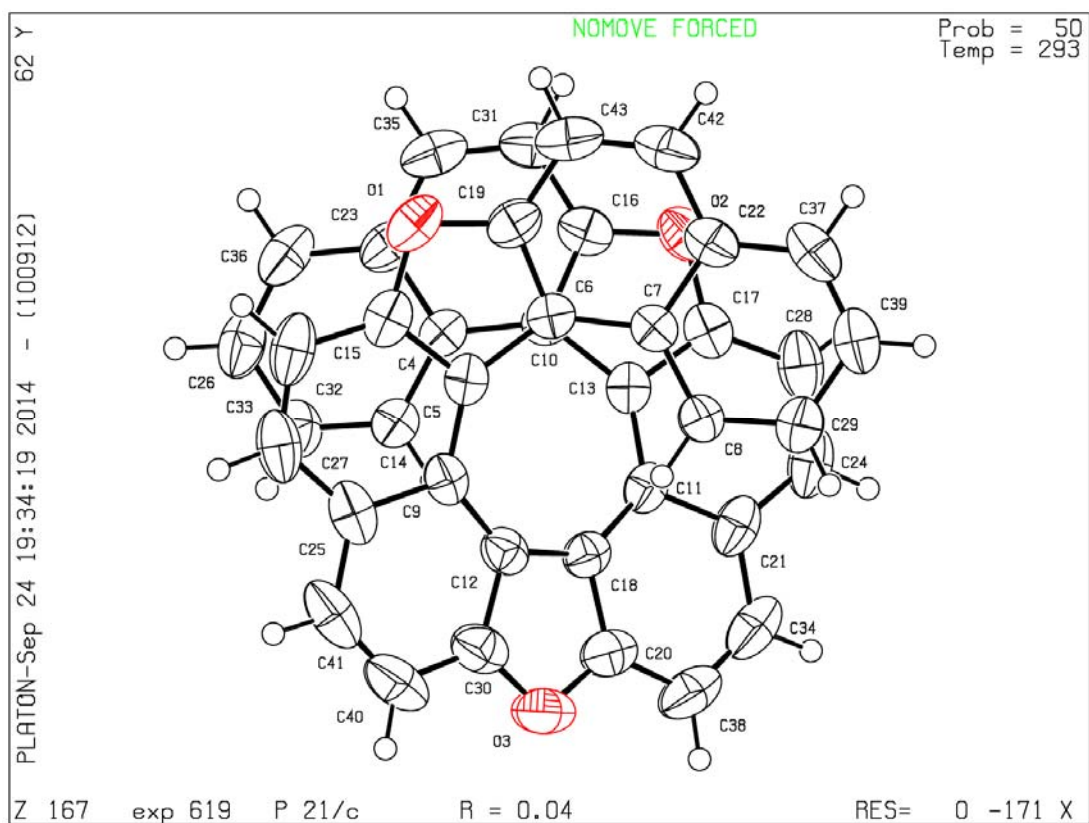
ORTEP diagram of **81** with atom numbering scheme 50% probability factor for the thermal ellipsoids.

Crystal data and structure refinement for compound 81

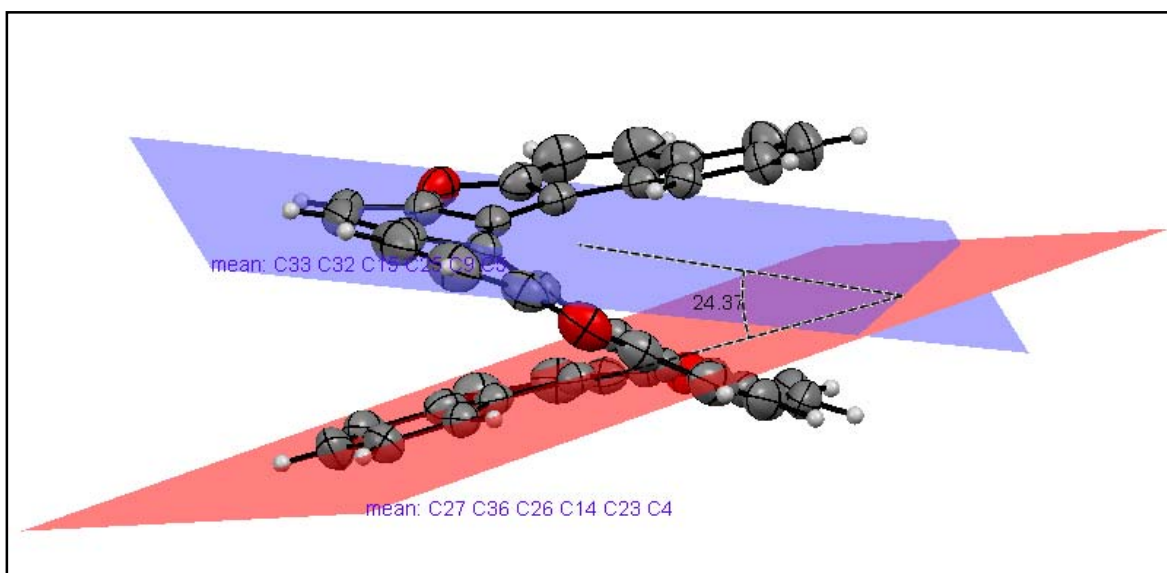
Empirical formula	C ₄₄ H ₃₃ O ₆
Formula weight	657.70
Temperature/K	293(2)
Crystal system	Orthorhombic
Space group	Pna2 ₁
a/Å	23.0883(10)
b/Å	8.2485(4)
c/Å	17.6035(8)
α/°	90.00
β/°	90.00
γ/°	90.00
Volume/Å ³	3352.5(3)
Z	4
ρ _{calc} /mm ³	1.303
μ/mm ⁻¹	0.086
F(000)	1380.0
2θ range for data collection	6.5 to 58.06°

Index ranges	-29 ≤ h ≤ 30, -11 ≤ k ≤ 10, -23 ≤ l ≤ 23
Reflections collected	19835
Independent reflections	7464[R(int) = 0.0318]
Data/restraints/parameters	7464/1/455
Goodness-of-fit on F ²	1.056
Final R indexes [I ≥ 2σ (I)]	R ₁ = 0.0856, wR ₂ = 0.2314
Final R indexes [all data]	R ₁ = 0.1102, wR ₂ = 0.2554
Largest diff. peak/hole / e Å ⁻³	0.82/-0.26
Flack parameter	-0.3(18)

2. For compound 7,12,17-trioxa[11]helicene (**78**) (CCDC No. 999892):



ORTEP diagram of **78** with atom numbering scheme 50% probability factor for the thermal ellipsoids.

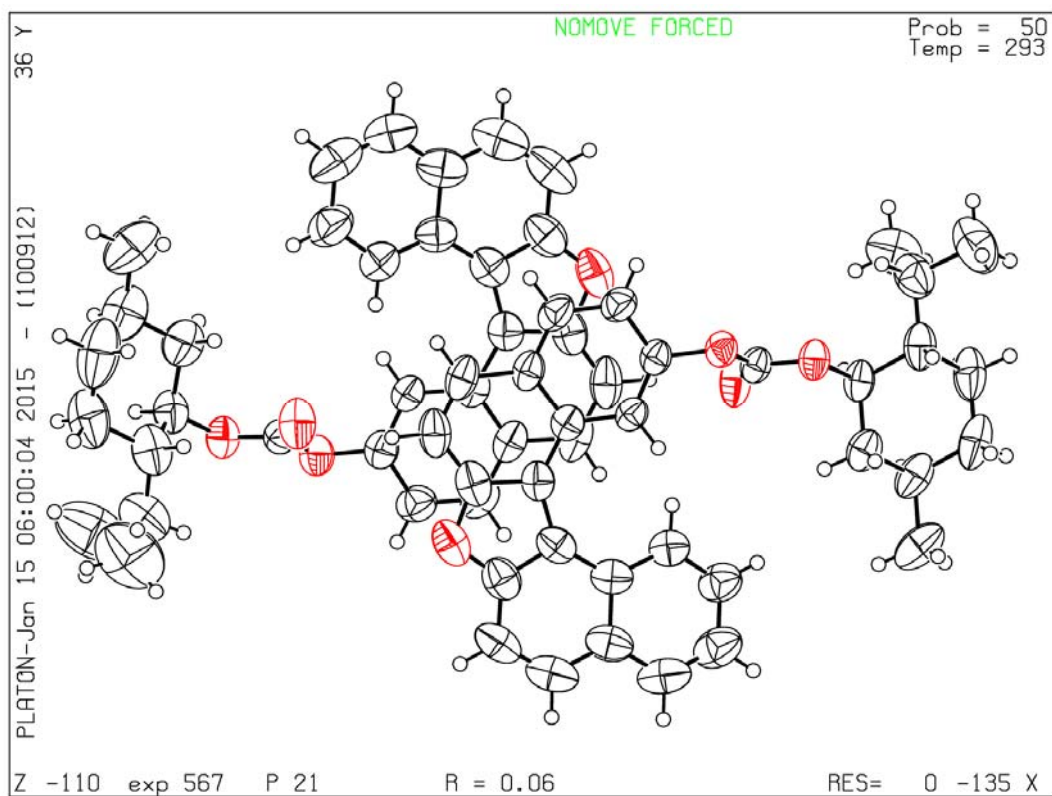


Interplanar angle of **78**

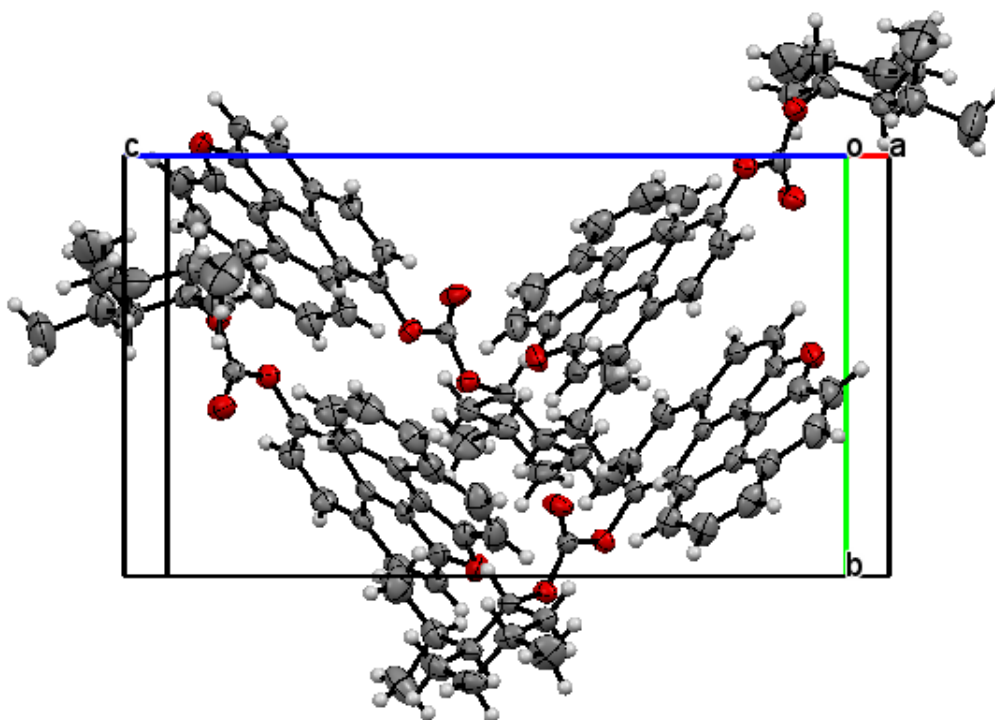
Crystal data and structure refinement for 7,12,17-trioxa[11]helicene(78):

Empirical formula	C ₄₀ H ₂₀ O ₃
Formula weight	548.56
Temperature/K	293
Crystal system	monoclinic
Space group	P2 ₁ /c
a/Å	7.63737(19)
b/Å	22.5914(7)
c/Å	15.1095(4)
α/°	90
β/°	99.906(3)
γ/°	90
Volume/Å ³	2568.11(12)
Z	4
ρ _{calc} /cm ³	1.4188
μ/mm ⁻¹	0.704
F(000)	1136.0
Crystal size/mm ³	0.29 × 0.26 × 0.22
Radiation	Cu Kα (λ = 1.54184)
2θ range for data collection/°	7.12 to 150.94
Index ranges	-8 ≤ h ≤ 9, -28 ≤ k ≤ 27, -18 ≤ l ≤ 11
Reflections collected	12179
Independent reflections	5333 [R _{int} = 0.0203, R _{sigma} = 0.0261]
Data/restraints/parameters	5333/0/396
Goodness-of-fit on F ²	1.052
Final R indexes [I ≥ 2σ (I)]	R ₁ = 0.0427, wR ₂ = 0.1124
Final R indexes [all data]	R ₁ = 0.0522, wR ₂ = 0.1209
Largest diff. peak/hole / e Å ⁻³	0.22/-0.20

3. For compound **87** (CCDC No. 1019988):



ORTEP diagram of **87** with atom numbering scheme 50% probability factor for the thermal ellipsoids.



Four molecules arranged in unit cell.

Crystal data and structure refinement for 87

Empirical formula	C ₃₁ H ₃₀ O ₄
Formula weight	466.55
Temperature/K	293(2)
Crystal system	monoclinic
Space group	P2 ₁
a/Å	14.2395(8)
b/Å	10.1525(4)
c/Å	17.4708(8)
α/°	90.00
β/°	94.248(5)
γ/°	90.00
Volume/Å ³	2518.8(2)
Z	4
ρ _{calc} /cm ³	1.230
μ/mm ⁻¹	0.639
F(000)	992.0
Radiation	CuKα (λ = 1.54184)
2θ range for data collection/°	6.22 to 146.74
Index ranges	-17 ≤ h ≤ 16, -8 ≤ k ≤ 12, -21 ≤ l ≤ 21
Reflections collected	15926
Independent reflections	10148 [R _{int} = 0.0339, R _{sigma} = 0.0386]
Data/restraints/parameters	10148/1/638
Goodness-of-fit on F ²	1.019
Final R indexes [I ≥ 2σ (I)]	R ₁ = 0.0554, wR ₂ = 0.1596
Final R indexes [all data]	R ₁ = 0.0741, wR ₂ = 0.1728
Largest diff. peak/hole / e Å ⁻³	0.29/-0.17
Flack parameter	0.2(3)

3.7 References

1. de Koning, C. B.; Rousseau, A. L.; van Otterlo, W. A. L. *Tetrahedron* **2003**, *59*, 7.
2. Bringmann, G.; Gulder, T.; Gulder, T. A. M.; Breuning, M. *Chem. Rev.* **2011**, *111*, 563.
3. Band, V.; Hoffer, A. P.; Band, H.; Rhinehardt, A. E.; Knapp, R. C.; Matlin, S. A.; Anderson, D. J. *Gynecol. Oncol.* **1989**, *32*, 273.
4. Gorst-Allman, D. P.; Stern, P. S.; Rabie, C. J. *J. Chem. Soc., Perkin Trans.* **1980**, 2474.
5. Auffray, Y.; Boutibonnes, P. *Mutat. Res., Genet. Toxicol.* **1986**, *171*, 79.
6. Wu, F.C. *Baillieres Clin. Obstet. Gynaecol.* **1996**, *10*, 1.
7. Manfredi, K. P.; Blunt, J. W.; Cardellina, J. H., II; McMahon, J. B.; Pannell, L. L.; Cragg, G. M.; Boyd, M. R. *J. Med. Chem.* **1991**, *34*, 3402.
8. Xu M.; Bruhn, T.; Hertlein, B.; Brun, R.; Stich, A.; Wu, J.; Bringmann, G. *Chem. Eur. J.*, **2010**, *16*, 4206.
9. (a) Noyori, R.; Takaya, H. *Acc. Chem. Res.*, **1990**, *23*, 345-350; (b) Brunel, J. M. *Chem. Rev.*, **2005**, *105*, 857.
10. Ohta, T.; Takaya, H.; Kitamura, M.; Nagai, K.; Noyori, R. *J. Org. Chem.*, **1987**, *52*, 3176.
11. Takaishi, K.; Kawamoto, M.; Tsubaki, K. *Org. Lett.*, **2010**, *12*, 1832.
12. Feringa, B. L.; Koumura, N.; Van Delden, R. A.; Ter Wiel, M. K. *J. Appl. Phys. A*, **2002**, *75*, 301.
13. Bao, X.; Snurr, R. Q.; Broadbelt L. J. *Langmuir*, **2009**, *25*, 10730.
14. Von Richter, V. *Chem. Ber.*, **1873**, *6*, 1252.
15. (a) Taylor, W. I.; Battersby, A.R. *Oxidative Coupling of Phenols*, **1967**, Marcel Dekker, New York, New York; (b) Feringa, B.; Wynberg, H. *Tetrahedron Lett.*, **1977**, 4447.
16. Doussot, J.; Guy, A.; Ferroud, C. *Tetrahedron Lett.*, **2000**, *41*, 2545.
17. Pummerer, R.; Rieche, A.; Prell, E. *Chem. Ber.*, **1926**, *59*, 2159
18. See: **9b**.
19. (a) Blaser, H.-U. *Chem. Rev.* **1992**, *92*, 935; (b) Periasamy, M. *Aldrichim. Acta.* **2002**, *35*, 89-101; (c) Brunel, J.M. *Chem. Rev.* **2005**, *105*, 857.
20. (a) Feringa, B. and Wynberg, H., *J. Org. Chem.* **1981**, *46*, 2547; (b) Toda, F.; Tanaka, K. and Iwata, S., *J. Org. Chem.* **1989**, *54*, 3007; (c) Hovorka, M.; Scigel, R.; Gunterova, J.; Tichy, M. and Zavada, J., *Tetrahedron* **1992**, *48*, 9503; (d)

-
- Doussot, J.; Guy, A. and Ferroud, C., *Tetrahedron Lett.* **2000**, *41*, 2545; (e) Sharma, V. B.; Jain, S. L. and Sain, B., *Tetrahedron Lett.* **2003**, *44*, 2655; (f) Bhor, M.; Nandurkar, N.; Bhanushali, M. and Bhanage, B., *Ultrasonics Sonochemistry* **2008**, *15*, 195; (g) Noji, M.; Nakajima, M. and Koga, K., *Tetrahedron Lett.* **1994**, 7983.
21. Periasamy, M.; Bhanu Prasad, A.S.; Bhaskar Kanth, J.V.; Kishan Reddy, Ch. *Tetrahedron: Asymmetry* **1995**, *6*, 341.
22. Hu, X.; Shan, Z.; Chang, Q. *Tetrahedron: Asymmetry* **2012**, *23*, 1327.
23. Noyori, R.; Tomino, I.; Tanimoto, Y. *J. Am. Chem. Soc.* **1979**, *101*, 3129.
24. Yamamoto, H.; Yanagisawa, A.; Ishihara, K.; Saito, S. *Pure Appl. Chem.* **1998**, *70*, 1507.
25. Roshini, C.; Franzini, L.; Raffaeli, A.; Salvadori, P. *Synthesis* **1992**, 503.
26. Qian, C.; Zhu, C.; Huang, T. *J. Chem. Soc., Perkin Trans. 1* **1998**, 2131.
27. Chen, Y.; Yekta, S.; Yudin, A. K. *Chem. Rev.* **2003**, *103*, 3155.
28. Natural products. Marisa C. Kozlowski, Barbara J. Morgan and Elizabeth C. Linton *Chem. Soc. Rev.*, **2009**, *38*, 3193.
29. Kozlowski, M. C.; Morgan, B. J.; Linton, E. C. *Chem. Soc. Rev.*, **2009**, *38*, 3193.
30. Feringa, B.; Wynberg, H. *Bioorg. Chem.*, **1978**, *7*, 397.
31. Brussee, J.; Groenendijk, J. L. G.; te Koppele, J. M.; Jansen, A. C. A. *Tetrahedron*, **1985**, *41*, 3313.
32. Yamamoto, K.; Fukushima, H.; Nakazaki, M. *Chem. Commun.*, **1984**, 1490.
33. Smrcina, M.; Lorenc, M.; Hanus V.; Sedmera, P.; Kocovsky, P.; *J. Org. Chem.*, **1992**, *57*, 1917.
34. Nakajima, M.; Kanayama, K.; Miyoshi, I.; Hashimoto, S.; *Tetrahedron Lett.*, **1995**, *36*, 9519.
35. Li, X.; Hewgley, B.; Mulrooney, C. A.; Yang, J.; Kozlowski, M. C. *J. Org. Chem.* **2003**, *68*, 5500.
36. Tada, M.; Taniike, T.; Kantam, L. M.; Iwasawa, Y. *Chem. Commun.* **2004**, 2542.
37. Egami, H.; Katsuki, T. *J. Am. Chem. Soc.*, **2009**, *131*, 6082.
38. Takizawa, S.; Kodera, J.; Yoshida, Y.; Sako, M.; Breukers, S.; Enders D.; Sasai, H. *Tetrahedron*, **2014**, *70*, 1786.
39. (a) Hovorka, M.; Guñterova', J.; Za'vada, J. *Tetrahedron Lett.* **1990**, *31*, 413; (b) Hovorka, M.; Š c' igel, R.; Guñterova', J.; Tichy', M.; Za'vada, J. *Tetrahedron*
-

-
- 1992**, 48, 9503; (c) Smrc̣ina, M.; Lorenc, M.; Hanuṣ, V.; Sedmera, P.; Koc̣ovsky', P. *J. Org. Chem.* **1992**, 57, 1917; (d) Smrc̣ina, M.; Pola'kova', J.; Vyskoc̣il, Ṣ.; Koc̣ovsky, P. *J. Org. Chem.* **1993**, 58, 4534; (e) Smrc̣ina, M.; Vyskoc̣il, Ṣ.; Ma'ca, B.; Pola'ṣek, M.; Claxton, T. A.; Abbott, A. P.; Koc̣ovsky', P. *J. Org. Chem.* **1994**, 59, 2156.
40. (a) Li, X.; Yang, J.; Kozlowski, M. C. *Org. Lett.* **2001**, 3, 1137. (b) Li, X.; Hewgley, J. B.; Mulrooney, C. A.; Yang, J.; Kozlowski, M. C. *J. Org. Chem.* **2003**, 68, 5500.
41. (a) Habaue, S.; Seko, T.; Okamoto, Y. *Macromolecules* **2002**, 35, 2437. (b) Habaue, S.; Seko, T.; Okamoto, Y. *Macromolecules* **2003**, 36, 2604. (c) Habaue, S.; Seko, T.; Isonaga, M.; Ajiro, H.; Okamoto, Y. *Polym. J.* **2003**, 35, 592. (d) Habaue, S.; Seko, T.; Okamoto, Y. *Polymer* **2003**, 44, 7377. (e) Habaue, S.; Ajiro, H.; Yoshii, Y.; Hirasa, T. *J. Polym. Sci. Part A: Polym. Chem.* **2004**, 42, 4528.
42. a) Razakantoanina, V.; Phung, N. K. P.; Jaureguiberry, G. *Prasitol. Res.*, **2000**, 86, 665; b) Wang, X.; Wang, J.; Wong, S. C. H.; Chow, L. S. N.; Nicholls, J. M.; Wong, Y. C.; Liu, Y.; Kwong, D. L. W.; Sham, J. S. T.; Tsao, S. W. *Life Sciences* **2000**, 67, 2663; c) Laughton, M. J.; Halliwell, B.; Evans, P. J.; Robin, J.; Hoult, S. *Biochem. Pharm.*, **1989**, 38, 2859.
43. Hallock, Y. F.; Manfredi, K. P.; Dai, J.-R.; Cardellina, J. H.; Gulakowski, R. J.; McMahon, J. B.; Schaffer, M.; Stahl, M.; Gulden, K.-P.; Bringmann, G.; Francois, G.; Boyd, M. R. *J. Nat. Prod.*, **1997**, 60, 677.
44. Bringmann G.; Holenz, J.; Wiesen, B.; Nugroho, B. W.; Proksch, P. *J. Nat. Prod.*, **1997**, 60, 342.
45. (a) Wang, Z.-J.; Deng, G.-D.; Li, Y.; He, Y.-M.; Tang, W.-J.; Fan, Q.-H. *Org. Lett.*, **2007**, 9, 1243; (b) Arai, N.; Suzuki, K.; Sugizaki, S.; Sorimachi, H.; Ohkuma, T.; *Angew. Chem. Int. Ed.*, **2008**, 47, 1770; (c) Berthod, M.; Mignani, G.; Woodward, G.; Lemaire, M. *Chem. Rev.*, **2005**, 105, 1801.
46. Ma, Q.-Z; Ma, M.-S; Tian, H.-Y; Ye, X.-X; Xiao, H.-P; Chen, L.-H.; Lei, X.-X. *Org. Lett.* **2012**, 14, 5813
47. Gingras, M.; Goretta, S.; Tasciotti, C.; Mathieu, S.; Smet, M.; Maes, W.; Chabre, Y. M.; Dehaen, W.; Giasson, R.; Raimundo, J. M.; Henry, C. R.; Barth, C. *Org. Lett.* **2009**, 11, 3846.
-

-
48. Nakano, K.; Hidehira, Y.; Takahashi, K.; Hiyama, T.; Nozaki, K. *Angew. Chem.* **2005**, *117*, 7298.
49. Nakanishi, K.; Sasamori, T.; Kuramochi, K.; Tokitoh, N.; Kawabata, T.; Tsubaki, K. *J. Org. Chem.* **2014**, *79*, 2625.
50. Nakanishi, K.; Fukatsu, D.; Takaishi, K.; Tsuji, T.; Uenaka, K.; Kuramochi, K.; Kawabata, T.; Tsubaki, K. *J. Am. Chem. Soc.* **2014**, *136*, 7101.
51. See reference 11.
52. Bao, X.; Snurr, R. Q.; Broadbelt, L. J. *Langmuir*, **2009**, *25*, 10730.
53. (a) Sue, D.; Takaishi, K.; Harada, T.; Kuroda, R.; Kawabata, T.; Tsubaki, K. *J. Org. Chem.* **2009**, *74*, 3940; (b) Tsubaki, K.; Takaishi, K.; Sue, D.; Kawabata, T. *J. Org. Chem.* **2007**, *72*, 4238.
54. (a) Wagnière, G. H. On Chirality and the Universal Asymmetry. *Wiley VCH: Verlag Helvetica Chimica Acta, Zürich* **2007**; (b) Busch, K. W. and Busch, M. A. Chiral Analysis. *Elsevier B.V., Amsterdam* **2006**.
55. Morris, D. G. Stereochemistry. *The Royal Society of Chemistry: Thomas Graham House, Cambridge* **2001**.
56. (a) Atkins, P. W. Physical Chemistry. 4th Ed. *Oxford University Press, Oxford* **1990**; (b) Silbey, R. J. and Alberty, R. A. Physical Chemistry. 3rd Ed. *John Wiley & Sons, Inc. USA* **2001**; (c) Berry, R. S.; Rice, S. A. and Ross, J. Physical Chemistry. 2nd Ed. *Oxford University Press, Oxford* **2000**.
57. For recent reviews on atropisomeric compounds see: (a) Bringmann, G.; Menche, D. *Acc. Chem. Res.* **2001**, *34*, 615; (b) Kocovsky, P.; Vyskocil, S.; Smrcina, M. *Chem. Rev.* **2003**, *103*, 3213; (c) Clayden, J.; Moran, W.J.; Edwards, P.J.; LaPlante, S.R. *Angew. Chem. Int. Ed.* **2009**, *48*, 6398; (d) Zask, A.; Murphy, J.; Ellestad, G.A. *Chirality* **2013**, *25*, 265.
58. Helical molecules: (a) Meurer, K.P.; Vögtle, F. *Top. Curr. Chem.* **1985**, *127*, 1; (b) Grimme, S.; Harren, J.; Sobanski, A.; Vögtle, F. *Eur. J. Org. Chem.* **1998**, 1491; (c) Rajca, A.; Miyasaki, M. in *Functional Organic Materials*, Muller, T.J.J.; Bunz, U.H.F. (Eds.) *Wiley-VCH, Weinheim*, 2007, pp 543-577; (d) Katz, T.J. *Angew. Chem. Int. Ed.* **2000**, *39*, 1921; (e) Urbano, A. *Angew. Chem. Int. Ed.* **2003**, *42*, 3986; (f) Collins, S.K.; Vachon, M.P. *Org. Biomol. Chem.* **2006**, *4*, 2518; (g) Rajca, A.; Rajca, S.; Pink, M.; Miyasaki, M. *Synlett*, **2007**, 1799; (i) Shen, Y.; Chen, C.-F. *Chem. Rev.* **2012**, *112*, 1463.
-

-
59. Allenes: (a) Ma, S. *Chem. Rev.* **2005**, *105*, 2829; (b) Lo, V.K.-Y.; Wong M.-K.; Che, C.-M. *Org. Lett.* **2008**, *10*, 517; (c) Ogasawara, M. *Tetrahedron: Asymmetry* **2009**, *20*, 259; (d) Trost, B.M.; Maruniak, A. *Angew. Chem. Int. Ed.* **2013**, *52*, 6262.
60. (a) Periasamy, M. *Aldrichim. Acta* **2002**, *35*, 89; (b) Brunel, J.M. *Chem. Rev.* **2005**, *105*, 857.
61. (a) Feringa, B.; Wynberg, H. *Bioorg. Chem.* **1978**, *7*, 397; (b) Reeder, J.; Castro, P.P.; Knobler, C.B.; Martinborough, E.; Owens, L.; Diederich, F. *J. Org. Chem.* **1994**, *59*, 3151.
62. Bandyopadhyaya, A.K.; Sangeetha, N.M.; Maitra, U. *J. Org. Chem.* **2000**, *65*, 8239.
63. (a) Hovorka, M.; Günterová, J.; Závada, J. *Tetrahedron Lett.* **1990**, *31*, 413; (b) Smrčina, M.; Lorenc, M.; Hanuš, V. Sedmera, P.; Kocovský, P. *J. Org. Chem.* **1992**, *57*, 1917; (c) Temma, T.; Habaue, S. *Tetrahedron Lett.* **2005**, *46*, 5655; (d) Grandbois, A.; Mayer, M.-E.; Bedard, M.; Collins, S.K.; Michel, T. *Chem.-Eur. J.* **2009**, *15*, 9655; (e) Habaue, S.; Temma, T.; Sugiyama, Y.; Yan, P. *Tetrahedron Lett.* **2007**, *48*, 8595; (f) Egami, H.; Matsumoto, K.; Oguma, T.; Kunisu, T.; Katsuki, T. *J. Am. Chem. Soc.* **2010**, *132*, 13633; (g) Holtz-Mulholland, M.; de Léséleuc, M.; Collins, S.K. *Chem. Commun.* **2013**, *49*, 1835.
64. (a) Feringa, B.; Wynberg, H. *Tetrahedron Lett.* **1997**, *50*, 4447; (b) Brussee, J.; Groenendijk, J.L.G.; te Koppele, J.M.; Jansen, A.C.A. *Tetrahedron* **1985**, *41*, 3313.
65. (a) Bell, F.; Waring, D. H. *J. Chem. Soc.* **1949**, 267; (b) Zhang, S.; Wang, Y.; Song, Z.; Nakajima, K.; Takahashi, T. *Chem. Lett.* **2013**, *42*, 697.
66. (a) Yamamoto, K.; Fukushima, H.; Okamoto, Y.; Hatada, K.; Nakazaki, M. *J. Chem. Soc., Chem. Commun.* **1984**, 1111; (b) Yamamoto, K.; Fukushima, H.; Nakazaki, M. *J. Chem. Soc., Chem. Commun.* **1984**, 1490; (c) Yamamoto, K.; Noda, K.; Okamoto, Y. *J. Chem. Soc., Chem. Commun.* **1985**, 1065; (d) Yamamoto, K.; Fukushima, H.; Yumioka, H.; Nakazaki, M. *Bull. Chem. Soc. Jpn.* **1985**, *58*, 3633; (e) Toda, F.; Tanaka, K. *Tetrahedron Lett.* **1988**, *29*, 1807; (f) Toda, F.; Tanaka, K.; Nassimbeni, L.; Niven, M. *Chem. Lett.* **1988**, *8*, 1371; (g) Yamamura, K.; Ono, S.; Ogoshi, H.; Masuda, H.; Kuroda, Y. *Synlett* **1989**, 18; (h) Smrcina, M.; Polakova, J.; Vyskocil, S.; Kocovsky, P. *J. Org. Chem.* **1993**, *58*,
-

-
- 4534; (i) Osa, T.; Kashiwagi, Y.; Yanagisawa, Y.; Bobbitt, J. M. *J. Chem. Soc., Chem. Commun.* **1994**, 2535; (j) Koike, N.; Hattori, T.; Miyano, S. *Tetrahedron: Asymmetry* **1994**, *5*, 1899; (k) Dore, A.; Fabbri, D.; Gladiali, S.; Valle, G. *Tetrahedron: Asymmetry* **1995**, *6*, 779; (l) Lin, Y.; Chien, L. C. *Tetrahedron: Asymmetry* **1998**, *9*, 63; (m) Nakano, K.; Hidehira, Y.; Takahashi, K.; Hiyama, T.; Nozaki, K. *Angew. Chem., Int. Ed.* **2005**, *44*, 7136; (n) Aydin, J.; Kumar, K. S.; Sayah, M. J.; Wallner, O. A.; Szabo, K. *J. Org. Chem.* **2007**, *72*, 4689; (o) Hu, G.; Holmes, D.; Gendhar, B. F.; Wulff, W. D. *J. Am. Chem. Soc.* **2009**, *131*, 14355.
67. (a) Fu, J.-M.; Snieckus, V. *Can. J. Chem.* **2000**, *78*, 905; (b) Karikomi, M.; Yamada, M.; Ogawa, Y.; Houjou, H.; Seki, K.; Hiratani, K.; Haga, K.; Uyehara, T. *Tetrahedron Lett.* **2005**, *46*, 5867.
68. Salim, M.; Akutsu, A.; Kimura, T.; Minabe, M.; Karikomi, M. *Tetrahedron Lett.* **2011**, *52*, 4518.
69. (a) Talele, H. R.; Gohil, M. J.; Bedekar, A. V. *Bull. Chem. Soc. Jpn.* **2009**, *82*, 1182; (b) Talele, H. R.; Chaudhary, A. R.; Patel, P. R.; Bedekar, A. V. *ARKIVOC* **2011**, *ix*, 15.
70. (a) Chaudhary, A. R.; Bedekar, A. V. *Synth. Commun.* **2012**, *42*, 1778; (b) Saiyed, A. S.; Bedekar, A. V. *Tetrahedron Lett.* **2010**, *51*, 6227; (c) Saiyed, A. S.; Patel, K. N.; Kamath, B. V.; Bedekar, A. V. *Tetrahedron Lett.* **2012**, *53*, 4692.
71. (a) Burke, W.J.; Nasutavicus, W.A.; Weatherbee, C. *J. Org. Chem.* **1964**, *29*, 407; (b) Talele, H.R.; Sahoo, S.; Bedekar, A.V. *Org. Lett.* **2012**, *14*, 3166.
72. (a) Jacques, J.; Fouquey, C.; Viterbo, R. *Tetrahedron Lett.* **1971**, 4617; (b) Jacques, J.; Fouquey, C. *Org. Synth.* **1988**, *67*, 13; (c) Gong, B.; Chen, W.; Hu, B. *J. Org. Chem.* **1991**, *56*, 423; (d) Brunel, J. M.; Buono, G. *J. Org. Chem.* **1993**, *58*, 7313.
73. Kazlauskas, R. J. *J. Am. Chem. Soc.* **1989**, *111*, 4953.
74. See reference 21
75. See reference 22
76. (a) Kanoh, S.; Muramoto, H.; Kobayashi, N.; Motoi, M.; Suda, H. *Bull. Chem. Soc. Jpn.*, **1987**, *60*, 3659; (b) Holzwarth, R.; Bartsch, R.; Cherkaoui, Z.; Solladié, G. *Eur. J. Org. Chem.* **2005**, 3536.
77. Bialońska, A.; Ciunik, Z. *Cryst. Eng. Comm.* **2004**, *6*, 276.
-

-
78. Details of crystallographic analysis of (*R*_a)-**44**•(*S*)-proline salt has been deposited with the Cambridge Crystallographic Data Centre (CCDC 948082). Detail discussion of the crystallographic analysis will be separately presented elsewhere.
79. De Lucchi, O.; Fabbri, D.; Delogu, G.; *J. Org. Chem.* **1995**, *60*, 6599.
80. Aree-phong, J.; Ruangsupapichart, N.; Thongpanchang, T. *Tetrahedron Lett.* **2004**, *45*, 3067.
81. Newman, M.S.; Lednicer, D. *J. Am. Chem. Soc.* **1956**, *78*, 4765.
82. See reference 58.
83. See reference 80.
84. Shyam Sundar, M.; Talele, H.R.; Mande, H.M.; Bedekar, A.V.; Tovar, R.C.; Muller G. *Tetrahedron Lett.* **2014**, *55*, 1760-1764.
85. Jierry, L.; Harthong, S.; Aronica, C.; Mulatier, J.-C.; Guy, L.; Guy, S. *Org. Lett.* **2012**, *14*, 288.
86. Blackemore, P.R.; Kilner, C.; Milicevic, S.D. *J. Org. Chem.* **2006**, *71*, 8212.
87. Jierry, L.; Harthong, S.; Aronica, C.; Mulatier, J.-C.; Guy, L.; Guy, S. *Org. Lett.* **2012**, *14*, 288.
88. Krykunov, M.; Kundrat, M.D.; Autschbach, J. *J. Chem. Phys.* **2006**, *125*, 194110.
89. Guy, S.; Guy, L.; Bensalah-Ledoux, A.; Pereira, A.; Grenard, V.; Cosso, O.; Vautey, T. *J. Mater. Chem.* **2009**, *19*, 7093.
90. Tetreau, C.; Lavalette, D.; Cabaret, D.; Geraghty, N.; Welvert, Z. *J. Phys. Chem.* **1983**, *87*, 3234.
91. Details of crystallographic analysis of (*M*)-**75** have been deposited with the Cambridge Crystallographic Data Centre (CCDC 948083).
92. Talele, H.R.; Bedekar, A.V. *Org. Biomol. Chem.* **2012**, *10*, 8579.
93. *Circularly Polarized Luminescence Spectroscopy and Emission-Detected Circular Dichroism*; Riehl, J.P.; Muller, G. In *Comprehensive Chiroptical Spectroscopy*, First Edition, Ed. Berova, N.; Polavarapu, P.L.; Nakanishi, K.; Woody, R.W. John Wiley & Sons, Inc.: Hoboken, New Jersey, **2012**, Vol. *1*: Instrumentation, Methodologies, and Theoretical Simulations, Chapter 3, pp. 65-90, and references therein.
94. Solntsev, K.M.; Gould, E.-A.; Pan, G.; Muller, G.; Bommireddy, S.; Huppert, D.; Tolbert, L.M. *Isr. J. Chem.*, **2009**, *49*, 227.

-
95. *Circularly Polarized Luminescence Spectroscopy from Lanthanide Systems*; Riehl J.P.; Muller, G. In *Handbook on the Physics and Chemistry of Rare Earths*, ed. Gschneidner Jr. K.A.; Bünzli, G.; Pecharsky, V.K. North-Holland Publishing Company: Amsterdam, **2005**, Vol. 34, Chapter 220, pp.289-357, and references therein.
96. Field, J.E.; Muller, G.; Riehl, J.P.; Venkataraman, D. *J. Am. Chem. Soc.*, **2003**, *125*, 11808.
97. Yang, L.; von Zelewski, A.; Nguyen, H.P.; Muller, G.; Labat, G.H.; Stoeckli-Evans, H. *Inorg. Chim. Acta*, **2009**, *362*, 3853.
98. (a) see reference 58b; (b) Urbano, A. *Angew. Chem. Int. Ed.* **2003**, *42*, 3986; (c) Collins, S.K.; Vachon, M.P. *Org. Biomol. Chem.* **2006**, *4*, 2518; (d) Rajca, A.; Miyasaki, M. in *Functional Organic Materials* (Eds. Muller, T.J.J.; Bunz, U.H.F.), Wiley-VCH, Weinheim, 2007, p. 547; (e) Shen, Y.; Chen, C.-F. *Chem. Rev.* **2012**, *112*, 1463; (f) Gingras, M. *Chem. Soc. Rev.* **2013**, *42*, 968; (g) Gingras, M.; Félix, G.; Peresutti, R. *Chem. Soc. Rev.* **2013**, *42*, 1007; (h) Gingras, M. *Chem. Soc. Rev.* **2013**, *42*, 1051.
99. Bunz, U.H.F. *Angew. Chem., Int. Ed.* **2010**, *49*, 5037.
100. Tsuji, H.; Mitsui, C.; Ilies, L.; Sato, Y.; Nakamura, E. *J. Am. Chem. Soc.* **2007**, *129*, 11902.
101. (a) Mitsui, C.; Soeda, J.; Miwa, K.; Tsuji, H.; Takeya, J.; Nakamura, E. *J. Am. Chem. Soc.* **2012**, *134*, 5448; (b) Nakano, M.; Niimi, K.; Miyazaki, E.; Osaka, I.; Takimiya, K. *J. Org. Chem.* **2012**, *77*, 8099.
102. (a) Nakanishi, K.; Sasamori, T.; Kuramochi, K.; Tokitoh, N.; Kawabata, T.; Tsubaki, K. *J. Org. Chem.* **2014**, *79*, 2625; (b) Nakanishi, K.; Fukatsu, D.; Takaishi, K.; Tsuji, T.; Uenaka, K.; Kuramochi, K.; Kawabata, T.; Tsubaki, K. *J. Am. Chem. Soc.* **2014**, *136*, 7101.
103. (a) Högberg, H.-E. *Act. Chem. Scand.* **1973**, *27*, 2591; (b) Berg, J.-E.; Erdtman, H.; Högberg, H.-E.; Karlsson, B.; Pilotti, A.-M.; Söderholm, A.-C. *Tetrahedron Lett.* **1977**, *18*, 1831; (c) Lipshutz, B.H.; Kayser, F.; Maullin, N. *Tetrahedron Lett.* **1994**, *35*, 815; (d) Areephong, J.; Ruangsupapichart, N.; Thongpanchang, T. *Tetrahedron Lett.* **2004**, *45*, 3067; (e) see reference 66m; (f) Schneider, J.-F.; Nieger, M.; Nättinen, K.; Dötz, K.H. *Synthesis* **2005**, 1109; (g) Campeau, L.C.; Parisien, M.; Jean, A.; Fagnou, K. *J. Am. Chem. Soc.* **2006**, *128*, 581; (h) Tanaka, K.; Fukawa,
-

-
- N.; Suda, T.; Noguchi, K. *Angew. Chem., Int. Ed.* **2009**, *48*, 5470; (i) Irie, R.; Tanoue, A.; Urakawa, S.; Imahori, T.; Igawa, K.; Matsumoto, T.; Tomooka, K.; Kikuta, S.; Uchida, T.; Katsuki, T. *Chem. Lett.* **2011**, *40*, 1343; (j) Salim, M.; Akutsu, A.; Kimura, T.; Minabe, M.; Karikomi, M. *Tetrahedron Lett.* **2011**, *52*, 4518; (k) Goel, A.; Verma, D.; Pratap, R.; Taneja, G.; Hemberger, Y.; Knauer, M.; Raghunandan, R.; Maulik, P.R.; Ram, V.J.; Bringmann, G. *Eur. J. Org. Chem.* **2011**, 2940; (l) Requet, A.; Souibgui, A.; Pieters, G.; Ferhi, S.; Letaieff, A.; Carlin-Sinclair, A.; Marque, S.; Marrot, J.; Hassine, B.B.; Gaucher, A.; Prim, D. *Tetrahedron Lett.* **2013**, *54*, 4721; (m) Matsuno, T.; Koyama, Y.; Hiroto, S.; Kumar, J.; Kawai, T.; Shinokubo, H. *Chem. Commun.* **2015**, *51*, 4607; (n) Hasan, M.; Pandey, A.D.; Khose, V.N.; Mirgane, N.A.; Karnik, A.V. *Eur. J. Org. Chem.* **2015**, 3702.
104. Crystallographic data for the structures of compounds **81** (CCDC No. 999893) and **78** (CCDC No. 999892) have been deposited with the Cambridge Crystallographic Data Centre.
105. Hovorka, M.; Günterová, J.; Závada, J. *Tetrahedron Lett.* **1990**, *31*, 413.
106. Mori, K.; Murase, T.; Fujita, M. *Angew. Chem., Int. Ed.* **2015**, *54*, 6847.
107. (a) Martin, R.H.; Flammang-Barbieux, M.; Cosyn, J.P.; Gelbcke, M. *Tetrahedron Lett.* **1968**, *31*, 3507; (b) Martin, R.H.; Marchant, M.J. *Tetrahedron* **1974**, *30*, 343; (c) Pérez-García, L.; Amabilino, D.B. *Chem. Soc. Rev.* **2002**, *31*, 342; (d) Stöhr, M.; Boz, S.; Schär, M.; Nguyen, M.-T.; Pignedoli, C.A.; Passerone, D.; Bernd Schweizer, W.; Thilgen, C.; Jung, T.A.; Diederich, F. *Angew. Chem., Int. Ed.* **2011**, *50*, 9982.
108. Bas, G.L.; Navaza, A.; Knossow, D.R.C.M. *Cryst. Struct. Commun.* **1976**, *5*, 713.
109. Allen, F.H.; Kennard, O.; Watson, D.G.; Brammer, L.; Orpen, A.G.; Taylor, R. *J. Chem. Soc. Perkin Trans. 2* **1987**, S1.
110. Nakanishi, K.; Fukatsu, D.; Takaishi, K.; Tsuji, T.; Uenaka, K.; Kuramochi, K.; Kawabata, T.; Tsubaki, K. *J. Am. Chem. Soc.* **2014**, *136*, 7101.
111. Upadhyay, G.M.; Talele, H.R.; Sahoo, S.; Bedekar, A.V. *Tetrahedron Lett.* **2014**, *55*, 5394.
- Braiek, M.B.; Aloui, F.; Moussa, S.; Tounsi, M.; Marrot, J.; Hassine, B.B. *Tetrahedron Lett.* **2013**, *54*, 5421.
-

-
112. Maiorana, S.; Papagni, A.; Licandro, E.; Annunziata, R.; Paravidino, P.; Perdicchia, D.; Giannini, C.; Bencini, M.; Clays, K.; Persoons, A. *Tetrahedron* **2003**, *59*, 6481.
113. (a) For recent review, see: Dumitrascu, F.; Dumitrescu, D., G.; Aron, I. *ARKIVOC* **2010**, *1*, 1; (b) Rajca, A.; Pink, M.; Xiao, S.; Miyasaka, M.; Rajca, S.; Das, K.; Plessel, K. *J. Org. Chem.* **2009**, *74*, 7504; (c) Miyasaka, M.; Pink, M.; Rajca, S.; Rajca, A. *Angew. Chem., Int. Ed.* **2009**, *48*, 5954; (d) see reference 103h; (e) Graule, S.; Rudolph, M.; Vanthuyne, N.; Autschbach, J.; Roussel, Ch.; Crassous, J.; Reau, R. *J. Am. Chem. Soc.* **2009**, *131*, 3183; (f) Li, Ch.; Shi, J.; Xu, L.; Wang, Y.; Cheng, Y.; Wang, H. *J. Org. Chem.* **2009**, *74*, 408; (g) Sato, K.; Katayama, Y.; Yamagishi, T.; Arai, S. *J. Heterocycl. Chem.* **2006**, *43*, 177; (h) See reference 48.
114. (a) Aloui, F.; Abed, R. E.; Marinetti, A.; Hassine, B. B. *Tetrahedron Lett.* **2008**, *49*, 4092; (b) Waghray, D.; Zhang, J.; Jacobs, J.; Nulens, W.; Basari-c, N.; Van Meervelt, L.; Dehaen, W. *J. Org. Chem.* **2012**, *77*, 10176; (c) Jierry, L.; Harthong, S.; Aronica, C.; Mulatier, J.-C.; Guy, L.; Guy, S. *Org. Lett.* **2012**, *14*, 288; (d) Hatakeyama, T.; Hashimoto, S.; Oba, T.; Nakamura, M. *J. Am. Chem. Soc.* **2012**, *134*, 19600; (e) Zheng, Y.-H.; Lu, H.-Y.; Li, M.; Chen, C.-F. *Eur. J. Org. Chem.* **2013**, 3059; (f) Nakai, Y.; Mori, T.; Sato, K.; Inoue, Y. *J. Phys. Chem. A* **2013**, *117*, 5082; (g) Li, M.; Lv, X.-L.; Wen, L.-R.; Hu, Z.-Q. *Org. Lett.* **2013**, *15*, 1262; (h) Weimar, M.; Correa de Costa, R.; Lee, F.-H.; Fuchter, M. *J. Org. Lett.* **2013**, *15*, 1706.
115. Sadorn, K.; Sinananwanich, W.; Areephong, J.; Nerungsi, C.; Wongma, C.; Pakawatchai, C.; Thongpanchang, T. *Tetrahedron Lett.* **2008**, *49*, 4519.
116. Details of crystallographic analysis of **92** have been deposited with the Cambridge Crystallographic Data Centre (CCDC 1019988).
-